Distribution Agreement

In presenting this thesis or dissertation as a partial fulfillment of the requirements for an advanced degree from Emory University, I hereby grant to Emory University and its agents the non-exclusive license to archive, make accessible, and display my thesis or dissertation in whole or in part in all forms of media, now or hereafter known, including display on the world wide web. I understand that I may select some access restrictions as part of the online submission of this thesis or dissertation. I retain all ownership rights to the copyright of the thesis or dissertation. I also retain the right to use in future works (such as articles or books) all or part of this thesis or dissertation.

Signature:

_____ _____

Kathryn R. Williams Date

Neuronal Function of hnRNP-Q1: Identification of a Novel Mechanism for *Gap-43* mRNA Translation Regulation

By

Kathryn R. Williams
Doctor of Philosophy

Graduate Division of Biological and Biomedical Science
Biochemistry, Cell and Developmental Biology

_____
Gary J. Bassell, Ph.D.
Advisor

_____
Anita H. Corbett, Ph.D.
Committee Member

_____
Yue Feng, Ph.D.
Committee Member

_____
Lian Li, Ph.D.
Committee Member

_____
James Q. Zheng, Ph.D.
Committee Member

Accepted:

_____
Lisa A. Tedesco, Ph.D.
Dean of the James T. Laney School of Graduate Studies

_____
Date

Neuronal Function of hnRNP-Q1: Identification of a Novel Mechanism for *Gap-43* mRNA Translation Regulation

By

Kathryn R. Williams
B.S., University of Michigan, 2007

Advisor: Gary J. Bassell, Ph.D.

An abstract of
A dissertation submitted to the Faculty of the
James T. Laney School of Graduate Studies of Emory University
in partial fulfillment of the requirements for the degree of
Doctor of Philosophy

in the Graduate Division of Biological and Biomedical Science
Biochemistry, Cell and Developmental Biology
2016

Abstract

Neuronal Function of hnRNP-Q1: Identification of a Novel Mechanism for *Gap-43* mRNA Translation Regulation

By: Kathryn R. Williams

Post-transcriptional regulation of gene expression by mRNA binding proteins is critical for neuronal development and function. hnRNP-Q1 is an mRNA binding protein that was identified as a splicing factor but recent findings demonstrate that hnRNP-Q1 performs critical post-transcriptional regulatory mechanisms in the cytoplasm as well. hnRNP-Q1 has been implicated in mRNA localization, translation and decay modulation. Given that hnRNP-Q1 is highly expressed in brain tissue, we hypothesized that hnRNP-Q1 post-transcriptionally represses the expression of specific mRNAs as a means to alter neuron morphology and consequently, function. Here we have identified *Growth associated protein 43* (*Gap-43*) mRNA as a novel target of hnRNP-Q1 and demonstrate that hnRNP-Q1 inhibits *Gap-43* mRNA translation and consequently GAP-43 function. GAP-43 is an important neuronal protein that regulates actin dynamics in growth cones and facilitates axonal growth. Previous studies have identified factors that regulate *Gap-43* mRNA stability and localization, but it remains unclear whether *Gap-43* mRNA translation is also regulated. Our results reveal that hnRNP-Q1 knockdown increased nascent axon length, total neurite length and neurite number in *M. musculus* embryonic cortical neurons and enhanced Neuro2a cell process extension; phenotypes that were rescued by GAP-43 knockdown. Additionally, we have identified a G-Quadruplex structure in the 5'-UTR of *Gap-43* mRNA that directly interacts with hnRNP-Q1 as a means to inhibit *Gap-43* mRNA translation. These findings reveal a novel mechanism for regulating GAP-43 expression and function, demonstrate that hnRNP-Q1 is a novel G-Quadruplex binding protein and suggest a potential conserved mechanism for hnRNP-Q1-mediated translation inhibition. hnRNP-Q1-mediated inhibition of *Gap-43* mRNA translation and potentially additional mRNAs by a similar mechanism may be critical for proper neuronal development, function and regeneration.

Neuronal Function of hnRNP-Q1: Identification of a Novel Mechanism for *Gap-43* mRNA Translation Regulation

By

Kathryn R. Williams
B.S., University of Michigan, 2007

Advisor: Gary J. Bassell, Ph.D.

A dissertation submitted to the Faculty of the
James T. Laney School of Graduate Studies of Emory University
in partial fulfillment of the requirements for the degree of
Doctor of Philosophy

in the Graduate Division of Biological and Biomedical Science
Biochemistry, Cell and Developmental Biology
2016

Acknowledgements

I am so grateful for my experience in the Biochemistry, Cell and Developmental Biology Program at Emory University. The program has provided me numerous opportunities to grow as a scientist and the dedication of the faculty to constantly strengthen the curriculum has prepared me for the next stage of my career. I am especially thankful for my advisor Dr. Gary Bassell. His guidance was crucial to my success as a graduate student but he ultimately let me direct the path of my studies. This process has allowed me to develop into a productive independent scientist. Additionally, his enthusiasm for science is contagious, which created a wonderful training environment in his lab. Several past and present Bassell lab members have contributed to my training. I specifically want to thank Nina Gross, Sharon Swanger, Wilfried Rossoll and Lei Xing for being great mentors, Paul Donlin-Asp for experimental support and Tawana Randall for administrative support. I am also appreciative of my committee members who have provided critical feedback and suggested several experiments to strengthen my conclusions. Furthermore, I am grateful for my collaborators Dr. Rita Mihailescu, Dr. Snezana Stefanovic, Damian McAninch, Dr. Yue Feng, Megan Allen, Dr. Wenqi Li, Dr. Anita Corbett and Dr. Callie Wigington who have greatly contributed to my training and research. Overall, the training that I have received at Emory University has been exceptional and I am thankful for all the opportunities that have allowed me to learn and grow as a scientist.

I would also like to thank my friends and family for their support during my studies. My mom and dad, Leta and Ed Williams, have always encouraged me to follow my dreams and provided me with the support to turn my dreams into reality. My siblings, Matt Williams and Heather Keister, and my brother-in-law, Andrew Keister, have also always been supportive and are ready with a good joke whenever you need a laugh. Additionally, I am truly grateful for my fiancé, Joe Moss, who has been my rock for the past two and a half years. He has provided encouragement through the difficult times that science is often known for and helped me celebrate during the exciting times. I am also appreciative for the support from my future in-laws, Anna Moss, Joe Moss, Alex Flowe, Michael Flowe and Ryan Flowe. Additionally, I was lucky to make several new friends during my graduate studies including Sara Stahley, Tara Wabbersen, Paul Donlin-Asp and Megan Allen. Their friendship has meant a lot during my time as a graduate student. I am so excited to be moving on to the next stage of my career and I am so grateful for everyone who has supported me along the way.

Table of Contents

Figures and Tables

Chapter 1

General Introduction

Portions of this chapter were adapted from the following publication and manuscript:

Wigington, C.P.*, Williams, K.R.*, Meers, M.P., Bassell, G.J., Corbett, A.H. (2013) Poly(A) RNA binding proteins and polyadenosine RNA: new members and novel functions. Wiley Interdiscip Rev RNA. 5(5): 601-22. PMID: 24789627. * indicates equal contribution

Williams, K.R., Stefanovic, S., McAninch, D.S., Xing, L., Allen, M., Li, W., Feng, Y., Mihailescu, M.R., Bassell, G.J. (2015) hnRNP-Q1 Represses Nascent Axon Growth in Cortical Neurons by Inhibiting *Gap-43* mRNA Translation. *Mol Biol Cell*. Revision Under Review.

1.1: mRNA Binding Proteins

Messenger RNAs (mRNAs) are templates that allow the information stored in our genomes to be encoded into protein. However, considering mRNAs as solely an intermediate step between DNA and protein vastly underestimates the role of these molecules. mRNAs are covered with mRNA binding proteins (mRBPs) from the time of transcription until they are degraded[1]. mRBPs and cis-regulatory sequences present in the mRNAs regulate the mRNA lifecycle and tightly control the expression and localization of the proteins that they encode[1]. mRNAs and mRBPs play an important role in the regulation of gene expression and dysregulation has been implicated in disease[2, 3].

1.1.1: mRNA Binding Proteins Control mRNA Processing and Post-Transcriptional Regulation

mRNAs undergo a number of processing and post-transcriptional regulatory steps throughout their lifecycle including 5'-end capping, editing, pre-mRNA splicing, 3'-end processing, nuclear export, localization, translation and degradation[4]. These steps are precisely regulated by a multitude of mRBPs in order to ensure proper spatial and temporal gene expression. The contribution of mRBPs begins before the mRNA has been fully transcribed[5]. Co-transcriptional mRNA processing occurs due to recruitment of mRNA processing factors by the C-terminial domain (CTD) of actively transcribing RNA polymerase II (RNA Pol II), which contains repeats of the peptide YSPTSPS[5]. The first mRNA processing event happens shortly after transcription initiation. Guanine 7-methyltransferase and the mRNA capping enzyme are recruited by the RNA Pol II CTD to covalently attach a 7 methylguanosine (m^7G) cap to the 5'-end of the mRNA[6, 7]. The m^7G

cap is then quickly bound by the nuclear cap binding heterodimer CBP-80/CBP-20 (nCBC) to protect the molecule from degradation and to serve as the initial checkpoint of gene expression[8, 9].

Another co-transcriptional mRNA processing event is editing[5]. A common edit is converting an adenosine base to inosine, which is carried out by adenosine deaminase double-stranded RNA enzymes (ADAR)[10]. ADAR requires double-stranded RNA to perform the editing reaction, which necessitates the RNA folding into a hairpin structure[10]. Inosine effectively acts like guanosine, which can alter the splicing, RNA secondary structure, codon usage, etc. of the mRNA.

Removing non-coding sequences from coding sequences or precursor mRNA (pre-mRNA) splicing also occurs co-trascriptionally[5]. The spliceosome is composed of four different small nuclear ribonucleoproteins (snRNPs, U1, U2, U5 and U4/U6), which each contain one or two small nuclear RNAs (snRNAs) and various Sm and other proteins[11]. Splicing is multi-step process that is influenced by the RNA Pol II CTD[5, 12]. U1 and U2 recognize the 5' splice site and the branch point near the 3' splice site, respectively, which is followed by binding of the U5-U4/U6 complex[11]. U1 and U4 are then removed and the U2-U5-U6 complex with the assistance of multiple enzymes perform two consecutive transesterification reactions to remove the non-coding intron sequence[11]. This process includes the involvement of several supplementary factors including proteins to assemble the snRNPs, like survival of motor neuron protein (SMN)[13], and proteins to regulate alternative splicing, which allows multiple different mRNA transcripts to be made from a single gene, like the well-characterized proteins TAR DNA-Binding Protein 43 (TDP-43)[14] and Muscleblind-Like Splicing Regulator 1 (MBNL1)[15]. Additionally, exon junction complexes

(EJCs) are composed of 4 proteins (MLN51, Magoh, Y14 and eIF4AIII) and are deposited upstream of the exon-exon junction after splicing to serve as a mark of successful splicing[9, 16].

The final co-transcriptional mRNA processing event is 3'-end processing and includes three steps: cleavage, polyadenylation and transcription termination[5]. Cleavage occurs downstream of the consensus sequence AAUAAA and is mediated by a multi-subunit protein complex that is comprised in part by the cleavage stimulation factor (CstF) and the cleavage and polyadenylation specificity factor (CPSF)[17]. CPSF is recruited by a transcription factor and is transferred to the RNA Pol II CTD upon transcription initiation[18] suggesting that the RNA Pol II CTD also affects 3'-end processing. After cleavage, polyA polymerase (PAP) then adds adenosine residues to the upstream cleavage product in a slow, or distributive, manner[19]. Upon addition of the first 11 adenosine residues, the nuclear polyA binding protein (PABPN1) binds to the nascent polyA tail and stimulates PAP activity leading to processive polyadenylation[20, 21]. Additional PABPN1 molecules continue to bind the growing polyA tail and have been hypothesized to serve as a molecular ruler to signal to PAP when the polyA tail has reached a length of 200-300 adenosine bases[22]. The polyA tail and PABPN1 function to protect the newly transcribed mRNA from degradation and to signal that transcription was completed successfully[9]. The downstream cleavage product is degraded by the 5'-to-3' RNA exonuclease 2 (XRN2), a process that promotes transcription termination[23].

After the mRNA has been transcribed, the transcript must be exported to the cytoplasm. Although this process occurs post-transcriptionally, the factors required for nuclear export are deposited on the mRNA co-transcriptionally[24]. The transcription-export complex (TREX), which is composed of the THO sub-complex, containing Uap56 and

Aly/REF, and specific SR proteins are recruited to the mRNA co-transcriptionally[24]. TREX is recruited by the RNA Pol II CTD[25] and the SR proteins are deposited as a result of splicing[26]. TREX and the SR proteins function as adaptors and recruit the nuclear export receptor heterodimer Tap-p15, which directs remodeling of the mRNP and export through the nuclear pore complex[24]. After export, the export adaptors and receptors are removed from the mRNA transcript to prevent reentry into the nucleus[24].

Upon entering the cytoplasm, mRNAs may be localized to specific sub-cellular regions in order to spatially regulate gene expression. This importance of mRNA localization is highlighted in polarized cells like neurons, which require differential gene expression in order create and maintain their polarity[27]. This process requires trans-regulatory mRNA binding proteins that link the mRNA transcript to an adaptor protein or directly to a molecular motor (Kinesin for plus-end movement on microtubules, Dynein for minus-end movement on microtubules and Myosin for movement on actin)[27]. Insulin-like growth factor 2 mRNA binding protein 1/Zipcode binding protein 1 (IMP1/ZBP1) and Fragile X Mental Retardation Protein (FMRP) are two well-characterized trans-regulatory factors. IMP1/ZBP1, specifically the third and fourth K Homology (KH) domains of the protein, binds to a cis-regulatory sequence in the 3'-UTR of *β-Actin* mRNA termed the "zipcode sequence" which contains repeats of the hexanucleotide sequence ACACCC[28-30]. A second zipcode sequence is present in the 3'-UTR of *β-Actin* mRNA but binds IMP1/ZBP1 with much lower affinity suggesting a redundant mechanism[28]. IMP1/ZBP1 transports *β-Actin* mRNA to the leading edge of motile fibroblasts and to the growth cones of developing neurons by binding the kinesin KIF11[27, 31]. The localized *β-Actin* mRNA can then undergo local translation, which will be discussed in detail below. Additionally, trans-regulatory mRNA binding proteins may

preferentially bind specific cis-regulatory secondary structures instead of cis-regulatory sequences. FMRP, specifically the arginine- and glycine-rich domain (RGG box), binds to G-Quadruplex structures (GQs) in several of its mRNA targets including *Psd-95* mRNA[32-36]. GQs are comprised of stacked DNA or RNA G-Quartets and will be discussed in more detail in Chapter 5. The FMRP binding site in the 3'-UTR of *Psd-95* mRNA is G-rich and folds into two tandem G-Quadruplex structures that have dual conformations and is necessary and sufficient for *Psd-95* mRNA localization[36, 37]. The *Psd-95* mRNA-FMRP complex is transported to dendrites by the kinesin KIF5 or KIF3C but FMRP is not required for this process suggesting a redundancy in this pathway[38-40]. Localized *Psd-95* mRNA can then undergo local translation, which again will be discussed in detail below.

After completing the many mRNA processing events described above, the transcript is finally ready to be translated into protein. The pioneer round of mRNA translation is initiated by the nCBC binding PABPC1 that has displaced PABPN1 on the polyA tail through the eukaryotic initiation factor 4G (eIF4G) to create a closed loop structure[41, 42]. Additional factors also bind the 5' cap including eIF4A, eIF4B and the CBP80-CBP20-dependent translation initiation factor (CTIF)[43]. The 43S pre-initiation complex, which includes the 40S subunit of the ribosome, eIF1, eIF1A, eIF3, eIF5 and eIF2-GTP with Met-$tRNA_i$, is then loaded onto the mRNA transcript near the 5' cap and begins to scan for the start codon[43]. Upon start codon recognition, eIF1 dissociates from the complex and the phosphate from eIF2-GTP hydrolysis is released[43]. eIF5B-GTP then promotes 60S ribosomal subunit recruitment resulting in eIF5B-GDP and eIF1A release from the 80S initiation complex[43]. Eukaryotic elongation factor 1A (eEF1A) then delivers the appropriate aminoacyl-tRNA to the A-site of the ribosome and peptide bond formation is catalyzed by

the ribosome[44]. The ribosome translocates three nucleotide bases downstream which moves the peptidyl tRNA to the P-site, releases the empty tRNA from the E-site and frees up the A-site for the next aminoacyl-tRNA to bind[44]. Peptide chain elongation occurs until a stop codon is positioned in the A-site[45]. The stop codon is recognized by the eukaryotic release factor 1 (eRF1) and forms a complex with eRF3-GTP[45]. This complex cleaves the bond between the peptide chain and tRNA, which releases the peptide chain and allows the ribosome to participate in another round of translation[45]. After the pioneer round of translation, nCBP is replaced by eIF4E, the exon junction complex is removed from the transcript and any remaining PABPN1 is replaced by PABPC1[46]. In addition to the canonical translation mechanism, multiple proteins contribute to either enhance or repress this process and two well-characterized mechanisms are discussed below.

As discussed earlier, mRNAs may be localized to specific sub-cellular regions, which establishes that the mRNAs may be locally translated within these compartments. This mechanism allows proteins to be synthesized where they are required in response to specific signals. IMP1/ZBP1 holds *β-Actin* mRNA in a translationally silent state during transport demonstrating that IMP1/ZBP1 is a translational repressor[47]. Specifically, the *β-Actin* mRNA-IMP1/ZBP1 complex and ribosomes are transported in the same mRNP granule but IMP1/ZBP1 is suggested to repress translation by preventing 60S ribosomal subunit recruitment[47, 48]. Upon arrival at the leading edge of motile fibroblasts or to the growth cones of developing neurons, *β-Actin* mRNA translation may be induced. In response to a growth or guidance cues, like brain derived neurotrophic factor (BDNF) or netrin-1, Src kinase is activated and phosphorylates IMP1/ZBP1[47, 49, 50]. Phospohorylated IMP1/ZBP1 releases *β-Actin* mRNA allowing it to undergo local translation[47]. Newly synthesized β-Actin protein

can then be assembled into actin filaments enabling the fibroblast and growth cone to steer towards the growth or guidance cue[49, 50]. FMRP also functions as a translational repressor and inhibits *Psd-95* mRNA translation until the mRNA is appropriately localized. Specifically, phosphorylated FMRP recruits the RNA induced silencing complex (RISC) facilitating microRNA 125a (miRNA-125a) binding, which has been suggested to block translation by stalling actively translating ribosomes[51, 52]. In response to the activation of group 1 metabotropic glutamate receptors, protein phosphatase 2a (PP2a) is activated and deposphorylates FMRP causing the RISC complex to dissociate from *Psd-95* mRNA[52, 53]. This process relieves the translation inhibition and allows *Psd-95* mRNA to be locally translated[52, 54]. Newly synthesized PSD-95 protein can then be incorporated into the post-synaptic density where it functions to control AMPA receptor content and synaptic strength. FMRP can also function to enhance translation of *Kv4.2* mRNA demonstrating the complexity of FMRP translation regulation[55]. There are several additional mechanisms of translation regulation including cytoplasmic polyadenylation in which the length of mRNA polyA tails are regulated by the cytoplasmic polyadenylation element binding protein (CPEB)-cytoplasmic poly(A) polymerase (Gld2)-deadenylase (PARN) complex as a means to modulate translation[56].

The final stage of the mRNA lifecycle is mRNA degradation, a process that is regulated at multiple steps along the mRNA biogenesis pathway. The fidelity of mRNA processing is ensured by both nuclear (exosome and 5'-3' exoribonucleases) and cytoplasmic (non-sense mediated decay (NMD)) quality control mechanisms and mRNA stability can be regulated by trans-acting mRBPs[9]. The exosome is composed of a catalytically inactive core, and three RNases; RRP6 and DIS3L, which are 3′–5′ exoRNases, and RRP44/DIS3, which is

both an endoRNase and a 3′–5′ exoRNase[9]. The exosome is recruited to all mRNAs co-transcriptionally where it is poised to detect mRNA processing errors[57]. In addition to the exosome, the nucleus also contains two 5'-3' expribonucleases called XRN2 (discussed earlier in 3'-end processing) and DXO[58, 59]. The accumulation of mRNA binding proteins on the mRNA during processing is the first line of defense against nascent mRNA degradation because bound mRNA binding proteins protect against the exosome[60]. Multiple nuclear processing events are also individually inspected to verify fidelity including 5'-end capping, splicing and 3'-end processing. XRN2, with the aid of the decapping enzymes EDC3, DCP1a and DCP2, and DOX, which possesses both decapping and exonuclease activities, have both been suggested to detect mRNA targets with defective 5'-end caps and degrade them[58, 61]. The exosome and XRN2 have also both been implicated in degrading splicing-defective mRNAs[62, 63]. However, the mechanism of detecting splicing-defective mRNAs and generating the 5'-end for XRN2 function has not been fully elucidated. 3'-end processing integrity is evaluated by multiple mechanisms. mRNA transcripts without proper polyA tails are degraded by the exosome and XRN2[62, 64, 65]. Additionally, the exosome subunit Rrp6 interacts with the canonical polyA polymerase Pap1 and the non-canonical polyA polymerase Trf4 and counteracts Trf4 polyA tail elongation[66, 67]. Rrp6 also regulates polyA tail binding proteins; specifically Rrp6 interacts with Nab2 (ZC3H14 *S. cerevisiae* homolog) to displace it from the polyA tail, which induces mRNA degradation[67]. However, the polyA tail binding protein Pab2 (PABPN1 *S. cerevisiae* homolog) signals for the mRNA transcript to be degraded by the exosome, which demonstrates the opposing roles of the two nuclear Pabs[68-70]. After an mRNA is exported from the nucleus, the cytoplasmic quality control mechanism nonsense mediated decay (NMD) detects mRNAs with pre-mature termination

codons (PTCs)[9]. This process involves an interaction between the RNA helicase and kinase complex UPF1-SMG1 and a stalled ribosome positioned over stop codon through the eukaryotic release factors eRF1 and eFR3[71, 72]. SMG1 phosphorylates UPF1 when an EJC with bound UPF2 and UPF 3 is detected downstream of the stalled ribosome[72, 73]. SMG5, SMG6 and/or SMG7 then bind to phosphorylated UPF1 leading to mRNA transcript degradation[74-77]. In addition to degrading mis-processed mRNA transcripts, properly processed mRNAs are also degraded after translation has occurred and many trans-regulatory mRNA binding proteins regulate this process. mRNA decay is a multi-step process that is typically initiated by poly(A) tail shortening to a length of 10-15 nucleotides[78]. Deadenylation leads to 3'-5' decay by the exosome and facilitates decapping by the Dcp1-Dcp2 complex followed by 5'-3' decay by exoribonucleases, like XRN1[79]. Two well-characterized modulators of mRNA stability are HuD, a neuronal ELAV family mRBP, and KSRP, a KH-type splicing regulatory protein (discussed in more detail in Chapter 2). HuD binds to an AU-rich element (ARE) in the 3'-UTR of *Gap-43* mRNA, which increases *Gap-43* mRNA stability by preventing deadenylation[80, 81]. Conversely, KSRP competes with HuD for binding to the *Gap-43* ARE sequence and induces mRNA degradation by an unknown mechanism[82].

In summary, mRNA processing and post-transcriptional regulation are a complex set of events that ultimately leads to the synthesis of proteins as depicted in Figure 1-1. The entire process is precisely coordinated with trans-regulatory mRNA binding proteins controlling multiple mRNA processing and post-transcriptional regulatory events. For example, the canonical polyA tail binding proteins have recently been demonstrated to perform multiple additional functions. In addition to regulating polyA tail length, PABPN1

also plays a role in alternative polyadenylation site selection, nuclear export, nuclear mRNA decay, regulating long non-coding RNAs and the pioneer round of translation[83]. Also, in addition to its role in mRNA translation and decay, PABPC1 also affects L1 mRNP nuclear import, mRNA local translation, miRNA-mediated translation repression and decay and NMD[83]. This cross-talk along with multiple surveillance pathways ensures fidelity of gene expression. Furthermore, the importance of post-transcriptional regulation is clear due to the many diseases caused by the dysregulation of these processing and post-transcriptional regulatory events, which will be discussed in the next section.

1.1.2: mRNA Binding Protein Dysregulation and Disease

Numerous diseases are caused by dysregulated mRNA processing and post-transcriptional regulatory events and a select few of these will be discussed in detail to demonstrate the importance of post-transcriptional regulation. A more extensive list of these types of diseases is displayed in Table 1-1 and the disease mechanisms discussed below are depicted in Figure 1-1 E-J. Additionally, several of the diseases discussed below specifically affect the nervous system so a brief overview of neuronal development will be described before proceeding to the disease mechanisms.

Neurons are polar cells that generally have a single axon that transmits electrical and chemical signals and multiple dendrites that receive and process signals. The axon of one neuron forms synapses, or physical connections, with the dendrites of several other neurons, which then form synapses with several additional neurons and so on until the neuronal circuitry is complete. Neuronal development and circuit establishment is a complex set of processes that require multiple intracellular and extracellular signals. Neural progenitor cells

asymmetrically divide and induce specific transcriptional programs to give rise to the multiple cell types of the nervous system including neurons. For example, neurons of the cerebral cortex, or cortical neurons, are specified by a mechanism involving the transcription factors Pax6, Ngn1 and Ngn2[84]. The post-mitotic neuronal cells then migrate to the appropriate location through the help of guidance cues. For example, the layer of the cortex that the cortical neurons will occupy depends on time that the neuron became post-mitotic: early neurons in the deep layers and late neurons in the outer layers[84]. The neurons then extend neuritic processes and one is specified to become the axon in a process that potentially involves GAP-43 (discussed in more detail in Chapters 2 and 5). Axonal and dendritic growth is directed by guidance cues and physical interactions with other cells of the nervous system. For example, the secreted guidance cue netrin-1 has been demonstrated to attract cultured cortical axons[85, 86] and the secreted guidance cue semaphorin 3A has been demonstrated to repel cultured cortical axons[87, 88]. Upon reaching their targets, the axon innervates a downstream neuron by forming a synapse and the dendrites branch and become innervated by upstream axons. For example, netrin-1 and its receptor DCC have been demonstrated to promote synaptogenesis in cultured cortical neurons[89]. After the neuronal circuitry is established, individual synapses are modified in response to activity, called synaptic plasticity, which ultimately affects neuronal function. This brief outline demonstrates that several complex and interconnected steps are required for proper neuronal development.

The motor neuron disease spinal muscular atrophy (SMA) is caused by a deficiency in the splicing factor SMN. SMA is an autosomal recessive disease that is the leading genetic cause of infant mortality with an incidence rate of 1:6000 live births[90]. *H. sapiens* have two

SMN encoding genes (*SMN1* and *SMN2*) that are identical expect for a point mutation in *SMN2* that leads to exclusion of exon 7 by alternative splicing[90]. Only ~10% of *SMN2* mRNA transcripts produce full-length SMN protein and the remaining ~90% produce a truncated protein that is rapidly degraded[90]. *SMN1* is deleted or mutated in the majority of SMA cases and the number of copies of the *SMN2* gene, and accordingly the amount of full-length SMN protein, dictates the severity of the disease[90]. As mentioned previously, SMN is involved in snRNP assembly, specifically SMN and members of the SMN complex (GEMINs and UNRIP) assemble the Sm proteins onto the snRNA[13]. The SMN-Sm-snRNA complex is then imported into the nucleus where the snRNP undergoes further processing[13]. Altered splicing of mRNA transcripts that are specifically required for motor neuron function has been hypothesized to cause SMA and splicing defects have been observed in an SMA mouse model[91-93]. However, novel functions of SMN have been identified, which suggests that additional mechanisms contribute to the motor neuron-specific pathology of SMA. SMN is localized to the axons of primary cultured motor neurons and is actively transported in a bi-directional manner[94-97]. However, Sm proteins are not localized to axons suggesting that axonal SMN is performing a novel function[98-100]. In support of this, SMN has been demonstrated to interact with a growing list of mRBPs including IMP1/ZBP1, FMRP, HuD, KSRP and hnRNP-Q (discussed in detail below)[99, 101-104] and the localization of specific mRNAs, including *β-Actin* and *GAP-43*, to axons is dysregulated in SMA models[105]. These recent findings suggest that SMN plays a role in assembling mRNP granules and that motor neurons are specifically affected due to their long axon lengths[106]. Therefore, a deficiency in SMN protein levels would prevent mRNPs and their mRNA cargoes from being packaged and delivered to axons, which are critical for axonal maintenance.

Myotonic dystrophy (DM) is a disease that leads to myotonia and muscle wasting and is caused in part by the loss of MBNL1 function[107]. DM is an autosomal dominant disease that has two types, DM1 and DM2, with prevalence rates of 1:20,000 and 1:8,000, respectively[108, 109]. DM1 is a more severe with an earlier onset while DM2 is less severe and develops later in life. DM1 is caused by expanded CTG repeats in the 3'-UTR of the myotonic dystrophy protein kinase gene (*DMPK*) and DM2 is caused by expanded CCTG repeats in an intron of the zinc finger protein 9 gene (*ZNF9*)[107]. These repeats minimally affect *DMPK* and *ZNF9* mRNAs due to their presence in non-coding regions, instead they lead to the formation of toxic aggregates in the nucleus that bind mRNA processing factors[107]. The alternative splicing factor MBNL1 is sequestered in these aggregates and the loss of MBNL1 function is a major component of DM pathology[107]. MBNL1 normally interacts with CHHG sequences in mRNA transcripts, where H = A, U or C, to either activate or repress exon inclusion[110]. Binding near a 3' splice site generally represses splicing leading to exclusion of the downstream exon and binding near a 5' splice site generally activates splicing of the exon leading to inclusion of the upstream exon[111]. Several mRNAs have been demonstrated to be aberrantly spliced in DM1 while less is known about altered splicing in DM2[107]. Although MBNL1 is not the only splicing regulator affected in DM1 and DM2, the mis-regulated splicing is likely at least partially due to loss of MBNL1 function. Additionally, many mRNAs that are incorrectly spliced in DM1 play a critical role in muscle function, which explains the muscle pathology of the disease[107]. However, DM1 can also present with central nervous system symptoms including cognitive impairment, developmental delays and psychiatric disorders like attention deficit and anxiety[109]. These neuronal phenotypes may be explained by splicing deficiencies but novel roles for MBNL1 in mRNA stability[112], miRNA

processing[113] and mRNA localization[114] may also contribute. Therefore, it is likely that MBNL1 regulates multiple mRNA processing events leading to gross alterations in gene expression in both muscle tissue and neurons. In support of this, MBNL1 binding sites are enriched in the 3'-UTRs of mRNA transcripts and this region has been demonstrated to play a pivotal role in post-transcriptional regulation including mRNA transport and decay[114].

The motor neuron disease amyotrophic lateral sclerosis (ALS) is caused in part by mutations in TDP-43[115]. ALS is an adult-onset disease that is typically fatal within 1-5 years after diagnosis and has a prevalence of 1:20,000 people each year[115]. Only ~10% of ALS cases are inherited or familial (fALS), usually dominantly, while the remaining ~90% are sporadic cases[115]. The splicing factor TDP-43 is encoded by the *Tar DNA Binding Protein* (*TARBP*) gene, which is mutated in ~5% of fALS cases[115]. The vast majority of these mutations affect residues in the glycine-rich C-terminal domain of the protein[14]. This region of TDP-43 also contains a putative prion-like domain and cytoplasmic protein aggregates in motor neurons and the central nervous system are a hallmark of the disease[14]. These aggregates contain TDP-43, ubiquitin and other mRNA binding proteins[116], which leads to the question of whether TDP-43-meidated ALS is due to the loss of TDP-43 function by sequestration in cytoplasmic aggregates or the gain of an additional toxic TDP-43 function in the cytoplasm. TDP-43 is normally enriched in the nucleus and functions to regulate transcription, alternative splicing and potentially miRNA processing.[14] TDP-43 binds it TG-rich DNA sequences leading to transcription repression or binds to UG-rich mRNA sequences leading to alternative splicing (i.e. exon 9 skipping of the cystic fibrosis transmembrane receptor)[14]. TDP-43 also associates with enzymes that process miRNAs, including Drosha, Argonaute2 and DDX17, suggesting that TDP-43 plays a role in miRNA

processing[14]. To determine if TDP-43-mediated ALS is due to the loss of these nuclear functions or a toxic gain of cytoplasmic functions, TDP-43 overexpression and knockdown experiments were performed. Overexpressing TDP-43 dramatically reduced axon outgrowth and complexity suggesting that cytoplasmic TDP-43 negatively regulates axon growth[117]. Additionally, TDP-43 co-localizes with mRBPs, including FMRP, IMP1/ZBP1 and HuD, in motor neuron axons and sequesters HuD in the cytoplasmic aggregates[117]. These results suggest that cytoplasmic TDP-43 negatively regulates axon growth by affecting mRBP function potentially by sequestering them is cytoplasmic aggregates. In support of the toxic gain of function hypothesis, overexpression of TDP-43 also mimics features of TDP-43-mediated ALS, including the sequestration of mRBPs in cytoplasmic aggregates[118]. However, knockdown of TDP-43 has also been shown to mimic features of the disease[119] suggesting that toxic gain of function and the loss of function hypotheses are not mutually exclusive and both could contribute to TDP-43-mediated ALS pathology. Additionally, recent findings demonstrate that TDP-43 interacts with PABPN1 and that PABPN1 overexpression rescues many aspects of TDP-43-mediated ALS[120] suggesting that TDP-43 may participate in additional mRNA processing and post-transcriptional regulatory events and underscoring that the pathological mechanism of ALS is complex.

Oculopharyngeal muscular dystrophy (OPMD) is a disease that leads to drooping eyelids (ptosis) and difficulty swallowing (dysphagia) and is caused a polyalanine expansion in the N-terminus of PABPN1[121]. OPMD is an adult-onset, autosomal dominant disease that has a prevalence of 1:100,000 in western countries[121]. PABPN1 contains a stretch of 10 alanine residues at the N-terminus of the protein and this stretch is expanded to 12-17 alanines in OPMD[122]. OPMD specifically affects skeletal muscle especially the levator

palpebrae superioris and pharyngeal muscles and a hallmark of the disease is nuclear aggregates containing PABPN1, polyA RNA and potentially additional mRBPs[122]. Therefore, major questions driving the field are whether OPMD is caused by a loss of PABPN1 function or a toxic gain of function and why specific skeletal muscles are most affected. As described previously, the canonical role of PABPN1 is to regulate polyA tail length but additional PABPN1 functions have also been identified including alternative polyadenylation site selection, nuclear export, nuclear mRNA decay, regulating long non-coding RNAs and participating in the pioneer round of translation[83]. Evidence for the loss of function mechanism include impaired myogenesis *in vitro*, shortened polyA tails, nuclear accumulation of polyA RNA upon PABPN1 knockdown[123] and altered polyadenylation site selection in a mouse model of OPMD[124, 125]. Evidence for the gain of function mechanism include the ability of anti-aggregation drugs to rescue the pathology of an OPMD mouse model and the speculation that the nuclear aggregates sequester wildtype PABPN1 and additional mRBPs[122]. Therefore, similar to TDP-43-mediated ALS, the loss of function and gain of function hypotheses appear to not be mutually exclusive and it is likely that both contribute to OPMD pathology. Additionally, how altering the ubiquitous functions of PABPN1 leads to a skeletal muscle-specific disease is also a work in progress. The current model is that skeletal muscles have a much lower level of PABPN1 than other tissues, which makes them vulnerable to alterations in PABPN1 expression[126]. The low level of PABPN1 in skeletal muscle is sufficient for normal muscle function but when the function of PABPN1 is perturbed by OPMD, normal muscle function cannot be maintained[126]. In support of this, PABPN1 expression is upregulated during muscle regeneration suggesting that PABPN1 function is critical for skeletal muscle homeostasis[126].

Zinc finger CCCH-type containing protein 14 (ZC3H14) is the *H. sapiens* homolog of the *S. cerevisiae* polyA binding protein Nab2p and mutated ZC3H14 leads to a rare form of non-syndromic intellectual disability (ID)[127]. This form of ID is autosomal recessive and has only been identified in single family from Iran[127]. These patients have a premature stop codon in the ZC3H14 gene, which leads to loss of ZC3H14 protein[127]. Studies from *S. cerevisiae* suggest that ZC3H14 likely regulates polyA tail length by repressing polyadenylation and facilities mRNP export from the nucleus[128]. However, these ubiquitous functions do not explain the brain-specific symptoms of the patients. Studies in *D. melanogaster* demonstrate that ZC3H14 knockout mimics features of ID and these phenotypes can be rescued by expressing ZC3H14 only in neurons[127]. These results suggest that ZC3H14 may be performing novel functions, potentially additional mRNA processing events, which are specifically required for proper neuronal development and function.

Fragile X syndrome (FXS) is the most common genetic cause of ID and autism and is caused by a deficiency in the translation regulator FMRP[129]. FXS is an x-linked disease with an incidence of 1:2,500-5,000 in males and 1:4,000-6,000 in females[129]. The FMR1 gene encodes FMRP and most patients have an expansion of the CGG trinucleotide repeat in the 5'-UTR region of the gene[129]. There are normally 5-45 CGG repeats in the FMR1 gene and patients with FXS have more than 200 repeats[129]. This large stretch of GC residues leads to hypermethylation of the cytosine residues, which inhibits transcription of the gene leading to a deficiency in FMRP[129]. As described previously, FMRP represses local translation of specific mRNA transcripts by stalling ribosomes[51, 52, 54], which suggests that FXS symptoms are caused by excess protein synthesis. This paradigm is supported by increased translation in brain slices from FMRP knockout mice by ^{14}C-leucine incorporation[130]. Therefore,

identifying the mRNA targets regulated by FMRP is key to understanding how FMRP deficiency causes the gross neurological defects in FXS that lead to ID and autism. High throughput FMRP interaction studies have identified anywhere from a few hundred to a few thousand FMRP mRNA targets (summarized in[131]). Many FMRP targets encode proteins that are components of the postsynaptic density (PSD)[130], the electron dense region under the postsynaptic membrane that contains scaffolding proteins, receptors and signaling molecules. These targets include N-methyl-D-aspartate receptor (NMDA) subunits NR1, NR2A, NR3A, the metabotropic glutamate receptor 5 (mGluR5) interacting proteins Homer1 (scaffold protein), PIKE (GTPase) and p110β (PI3 Kinase catalytic subunit) and the scaffolding proteins PSD-93, PSD-95, SAPAP1-4 and Shank1-3[130]. NMDARs and mGluR5 modulate synaptic plasticity by activating the MEK/ERK and PI3K/Akt/mTORC1 pathways, which leads to increased translation[132]. Additionally, excess mGluR5 signaling has been observed in FXS models and pharmacologic reduction of mGluR5 signaling rescues FXS phenotypes[130, 133]. Therefore, increased translation is likely amplified in FXS due to loss of the translational repressor FMRP and to the downstream activation of translation by the MEK/ERK and PI3K/Akt/mTORC1 pathways. mRNA targets that are dysregulated in FXS and how their altered expression contributes to the neurological defects that cause ID and autism is still a work in progress. However, some FMRP targets have been identified that likely contribute to FXS pathology. As described previously, FMRP regulates the local translation of *Psd-95* mRNA[52, 54] which encodes a scaffolding protein that is critical for PSD function, and consequently synaptic and neuronal function[134]. FMRP also represses the translation of the calcium/calmodulin-dependent kinase IIα (CamKIIα)[38], the AMPA receptor subunit GluR1/2[38] and the amyloid precursor protein (APP)[135], which are proteins that play a vital

role in neuron function. Additionally, FMRP enhances the translation of the potassium channel Kv4.2, which may explain the hypersensitivity and susceptibility to epileptic seizures in FXS patients[55].

This incomplete list of diseases that are caused by altered post-transcriptional regulation highlights the importance of this process and demonstrates the complex cross-talk that occurs between the many mRNA processing and post-transcriptional regulatory events. Understanding the mechanisms of these events and the proteins that regulate them will progress our knowledge of the pathomechanisms of these diseases and will likely help identify novel treatments.

1.2: The hnRNP Family of Proteins

The heterogenous ribonucleoprotein (hnRNP) family of proteins was identified as a novel mRBP complex. However, structural and functional analysis of the individual proteins reveals that they are actually a group of highly divergent proteins that participate in mRNA processing and post-transcriptional regulatory events (Table 1-2). Additionally, the manner in which these proteins were identified illustrates the diverse mechanisms required for mRNA biogenesis.

1.2.1: Identification of hnRNP Proteins

The hnRNP proteins were identified as being able to bind mRNA but were not stably associated with other known mRBP complexes (i.e. snRNPs)[136, 137]. The first characterization of hnRNP proteins was by sucrose gradient isolation of mRBP granules, which identified the core hnRNP proteins, hnRNP-A/B and hnRNP-C[136, 137]. UV crosslinking and

immunoprecipitation increased the detection of hnRNP proteins and identified a total of 20 proteins that were named hnRNP-A to -U[136, 137]. Additional proteins that bind less stably to mRNA have since been identified and were named minor hnRNP proteins[138]. Despite their common ability to bind mRNA and their presence in the same mRNP granule, these proteins are structurally and functionally diverse, as discussed below.

1.2.2: Diverse hnRNP Protein Structure

The hnRNPs are modular proteins that usually contain multiple protein domains, which recognize diverse mRNA sequences and structures (Table 1-2). The most common RNA binding domain present in hnRNP proteins is the RNA recognition motif (RRM)[137]. RRMs contain α-helices and β-sheets in the following configuration β_1-α_1-β_2-β_3-α_2-β_4 and consensus sequences for RNA binding, called RNP-1 and RNP-2, are present in the β_3 and β_1 regions, respectively[137]. RNP-1 and -2 bind to single-stranded nucleic acids without sequence specificity[137]. Additional regions of the RRM, including residues in the β_2 and β_4 sheets, can confer sequence specificity for binding, which allows RRMs to bind RNA in a sequence-independent and sequence-dependent manner[137]. Some hnRNPs contain atypical RRM domains, which have an altered structure as compared to canonical RRMs and consequently bind RNA by an alternative mechanism[137]. The next most prevalent hnRNP RNA binding domain is the arginine- and glycine-rich domain (RGG box)[137]. RGG boxes contain RGG or RG repeats separated by spacers of different amino acids. RGG boxes are predicted to have low complexity, which has hindered structural studies of this protein domain[139]. However, circular dichroic and infrared spectroscopy analysis revealed that the nucleolin C-terminal RGG box contains repeated β-turn motifs[139]. Additionally, circular dichroism and nuclear

magnetic resonance (NMR) analysis of the FMRP RGG box revealed that the arginines of the RGG repeats bind RNA while the glycines serve as a flexible hinge[139]. RGG boxes have been demonstrated to interact with GQ structures (discussed in detail in Chapter 5) in RNA suggesting that this domain binds RNA in a sequence-specific manner[139]. The final RNA binding domain present in hnRNP proteins is the KH domain. KH domains contain α-helices and β-sheets in the following configuration β_1-α_1-α_2-β_2-β'-α' which creates a nucleic acid binding cleft[137]. KH domains bind to 4 nucleotides in a sequence-specific manner but there is not a single consensus sequence for binding[137, 140]. Several KH binding sequences are A- and C- rich suggesting a conserved mechanism for RNA recognition[140]. The presence of multiple different RNA binding domains in hnRNP proteins suggests that these proteins interact with RNA by a variety of mechanisms and therefore, likely perform diverse functions for mRNA biogenesis.

1.2.3: Diverse hnRNP Protein Function

The hnRNP proteins were originally characterized as splicing factors due to the method used to identify them[136]. However, several of these proteins have more recently been demonstrated to play important post-transcriptional regulatory roles in the cytoplasm as well[136]. These findings demonstrate that the hnRNP proteins are critical trans-regulatory factors which together participate in nearly every step of mRNA biogenesis[136]. The hnRNP proteins have been grouped into sub-families based on homology and their function in both the nucleus and cytoplasm will be discussed according to this grouping[141]. However, little is known about hnRNP-N, -S and -T so they will not be discussed below.

hnRNP-A, B and -D belong to the hnRNP-A/B/D sub-family, which consists of seven paralogs: hnRNP-A0, -A1, -A2, -A3, -A/B, -D and -D-like[141]. The hnRNP-A/B/D sub-family has been extensively studied, which revealed that it participates in several mRNA processing and post-transcriptional regulatory events including pre-mRNA splicing and mRNA editing, packaging, nuclear export, localization, translation and stability. hnRNP-A/B interacts with Apobec-1, the catalytic component of the editosome, suggesting that it plays a role in mRNA editing[137]. hnRNP-A1 and -A2 regulate alternative splicing by binding to or near an exon leading to exclusion of that exon[137, 142]. The highly abundant hnRNP-A2 protein also participates in packaging nuclear mRNPs in a non-sequence-specific manner.[137] Overexpressing hnRNP-A1 but not a mutant lacking the M9 nuclear export signal inhibits mRNA nuclear export indicating that the hnRNP-A1/mRNA export pathway is saturable and that hnRNP-A1 likely plays a role in this process[143]. Additionally, phosphorylation of hnRNP-A1 promotes nuclear export of *XL* and *XIAP* mRNAs[144]. The role of hnRNP-A2 in mRNA localization has been well-characterized. hnRNP-A2 binds to a 21 nucleotide cis-regulatory element in *myelin basic protein* (*MBP*) mRNA called the A2 response element (A2RE) and transports the mRNA to oligodendrocyte processes[137]. hnRNP-A2 also transports additional mRNAs by binding to their A2RE-like elements[137] and hnRNP-A1, -A/B and -A3 have been speculated to form a complex with hnRNP-A2 on A2REs during mRNA localization. hnRNP-A1, -A2 and -D are also involved in translation regulation[145]. hnRNP-A1 can function to either enhance or repress internal ribosome entry site (IRES) translation by binding to the 5'-UTRs of specific genes[142]. hnRNP-A2 has been suggested to repress translation (discussed in more detail in the hnRNP-E/J/K paragraph)[146, 147] and hnRNP-D has been implicated in promoting IRES translation[148, 149]. And finally, hnRNP-A1, -A2 and -D

regulate mRNA stability. hnRNP-A1 destabilizes *cIAP1* mRNA by binding to a 3'-UTR ARE[150], hnRNP-A2 stabilizes *C-P4H-α I* mRNA by binding to a stretch of Us in the 3'-UTR[151] and hnRNP-D has been suggested to both stabilize and destabilize specific mRNAs by binding to AREs[152]. The hnRNP-A/B/D sub-family members hnRNP-A0 and -D-like have not been studied in detail.

The hnRNP-C sub-family has three paralogs: hnRNP-C, RALY and RALY-like[141]. hnRNP-C was the first hnRNP protein identified and it has since been demonstrated to play a role in pre-mRNA splicing and mRNA packaging, translation and stability. hnRNP-C regulates alternative splicing and can promote exon inclusion or exclusion depending on the position of the binding site[153]. The best-characterized role of hnRNP-C is in mRNA packaging. hnRNP-C has two isoforms, hnRNP-C1 and -C2, that form a heterotetramer containing 3 hnRNP-C1 proteins and 1 hnRNP-C2 protein[153]. The hnRNP-C heterotetramer along with members of the hnRNP-A/B/D sub-family form the 40S hnRNP complex that assembles on all mRNAs and facilitates packaging[153]. hnRNP-C has also been demonstrated to enhance IRES translation[154, 155] and stabilize *uPAR* mRNA by binding to the 3'-UTR[156]. The hnRNP-C sub-family members RALY and RALY-like have not been studied in detail.

hnRNP-E, -J and -K belong to the hnRNP-E/J/K sub-family, which has six paralogs: hnRNP-E1, -E2, -E3, -E4, -J and -K[141]. The hnRNP- E/J/K sub-family proteins are also known as polyC binding proteins (PCBP) and they regulate pre-mRNA splicing and mRNA 3'-end processing, translation and stability. hnRNP-E1 interacts with the splicing factor sc-35 and hnRNP-E1 and -E3 have been demonstrated to regulate splicing *in vitro*[157] and of *Tau* mRNA[158], respectively. hnRNP-K also interacts with splicing factors (9G8 and SRp20) and can enhance or silence splicing leading to exon inclusion or exclusion, respectively[159, 160].

hnRNP-K contributes to the co-transcriptional recruitment of XRN2 suggesting that it is involved in 3'-end processing[161]. hnRNP-E1 and -E2 can enhance IRES translation potentially by unfolding secondary structure in the mRNA[137]. hnRNP-E1 has also been demonstrated to repress translation[162]. hnRNP-E1 is recruited into granules containing hnRNP-A2 and A2RE mRNA, like *MBP* mRNA, and functions to inhibit translation of the A2RE mRNA during granule transport[137]. hnRNP-K also represses *MBP* mRNA translation suggesting that hnRNP-A2, -E1 and -K work cooperatively to regulate the local translation of *MBP* mRNA[163]. hnRNP-E1, -E2 and -K also jointly regulate *15-lipoxygenase* (*LOX*) mRNA translation[160]. hnRNP-E1, -E2 and -K inhibit *LOX* mRNA translation by binding to the differentiation control element (DICE) in the 3'-UTR[160]. Binding of the hnRNP-E1/-E2/-K complex blocks 60S ribosomal subunit recruitment and c-Src phosphorylation of hnRNP-K leads to complex disassembly and translation activation[160]. hnRNP-K also inhibits androgen receptor translation[164]. hnRNP-E1 and -E2 enhance mRNA stability by interacting with PABPC1[137] and hnRNP-E1, -E2, -E4 and -K have all been suggested to destabilize mRNA by binding to CU-rich elements[165-167]. hnRNP-E1 and -K are also components of the complex that stabilizes *renin* mRNA by binding the 3'-UTR[160]. The hnRNP-E/J/K sub-family member hnRNP-J has not been studied in detail.

hnRNP-F and -H belong to the hnRNP-F/H sub-family, which has five paralogs: hnRNP-F, -H1, -H2, -H3 and GRSF1[141]. The hnRNP- F/H sub-family generally binds G-rich sequences (GRSs) and these proteins regulate pre-mRNA splicing and mRNA 3'-end processing, translation and stability. The best-characterize role of hnRNP-F, -H1 and -H2 is in alternative splicing. hnRNP-F, -H1 and -H2 generally bind splicing silencers at or near an exon, which leads to exon exclusion[137, 168]. hnRNP-H1 can also self-associate to form RNA

loops to sequester silenced exons and bring distal splice sites closer together[169, 170]. This mechanism has also been described for hnRNP-A1 and hnRNP-H1 and -A1 can cooperatively modulate alternative splicing by forming homomeric or heteromeric complexes[142, 169, 170]. hnRNP-F and -H1 can also enhance splicing as shown with *c-Src* mRNA[171]. hnRNP-F and -H1 also regulate 3'-end processing. hnRNP-F blocks CstF recruitment while hnRNP-H1 and -H2 bind to GRSs downstream of the polyadenylation signal and promote 3'-end processing[172-174]. hnRNP-F can regulate polyadenylation site selection by blocking CstF recruitment to polyadenylation signals[175]. hnRNP-F has also been identified as a component of *MBP* transport mRNP granules and it represses MBP expression suggesting that multiple hnRNP protein regulate the local translation of MBP[176, 177]. hnRNP-F plays a role in ARE-mediated mRNA destabilization. The hnRNP-F/H sub-family member hnRNP-H3 has not been studied in detail and GRSF1 is a mitochondrial mRBP.

The hnRNP-G sub-family has two paralogs: hnRNP-G and –GT[141]. hnRNP-G, also called RNA binding motif protein, X-linked (RBMX), is ubiquitously expressed while its Y chromosome equivalent RNA binding motif protein, Y-linked (RBMY) and the paralog hnRNP-GT are primary expressed in testes[137]. hnRNP-G, -GT and RBMY are highly homologous to SR proteins and modulate alternative splicing[137]. These proteins can function cooperatively or antagonistically to the splicing factor Tra2β to facilitate exon inclusion or exclusion[137]. Additionally, the *SMN2* gene contains a mutated exonic splicing enhancer sequence that leads to exclusion of exon 7[178, 179]. hnRNP-G binds exon 7 and facilitates splicing with Tra2β leading to exon 7 inclusion suggesting that hnRNP-G may be a potential target for SMA treatments[178, 179]. Future studies may address whether hnRNP-G sub-family members regulate additional mRNA processing and post-transcriptional regulatory events.

hnRNP-I and -L belong to the hnRNP-I/L sub-family, which consists of five paralogs: hnRNP-I1, -I2, -L, -L-like and ROD1[141]. hnRNP-I1, also called polypyrimidine-tract-binding protein (PTB), is ubiquitously expressed while the paralogs hnRNP-I2, also called neural PTB (nPTB), and ROD1 are enriched in brain, muscle and testis tissues and haematopoietic cells, respectively[180]. hnRNP-L is also ubiquitously expressed and the paralog hnRNP-L-like is enriched in lymphoid cells, activated T-cells and testes[181]. The hnRNP- I sub-family members bind polypyrimidine-tracts (PTs) while hnRNP-L sub-family members bind CA-rich sequences[137]. These proteins regulate pre-mRNA splicing and mRNA 3'-end processing, nuclear export, localization, translation and stability. The best-characterized role of hnRNP-I1, -I2, -L and –L-like is in alternative splicing. hnRNP-I1 is an established splicing repressor[180, 182]. It binds to PTs at or near an exon and prevents exon inclusion[180, 182]. Two mechanisms for hnRNP-I1 splicing suppression are 1.) competing with splicing factors (i.e. U2AF or U2 snRNP) for binding to regulatory sequences and 2.) creating RNA loops, like hnRNP-A1 and –H1, to sequester exons or the branch point adenosine[180, 182]. hnRNP-I1 may also require the co-repressors Raver1 and Raver2 for efficient splicing suppression[182]. hnRNP-I2 also regulates alternative splicing but demonstrates key differences as compared to hnRNP-I1. hnRNP-I2 has higher mRNA binding affinity, lower splicing activity and can recruit additional splicing factors[180]. These differences allow hnRNP-I2 to carry out a neuronal splicing program[180]. hnRNP-L and –L-like repress splicing by various mechanisms including blocking U2AF binding[183, 184] and RNA looping[181], like hnRNP-I1, and also interacting with hnRNP-A1 to block U1 snRNP from associating with U6 snRNP[185]. hnRNP-I1 also modulates polyadenylation site selection with binding of PTs upstream of the polyadenylation signal promoting 3'-end processing and binding of PTs downstream of the

polyadenylation signal decreasing cleavage[182]. hnRNP-L has also been suggested to regulate polyadenylation site selection by alternative splicing[186]. Additionally, hnRNP-I1 and -L are involved in nuclear export[182, 187]. hnRNP-I1 localizes *Vg1* mRNA in *X. laevis* by binding to the 3'-UTR and *α-Actin* mRNA to neuronal processes[180]. hnRNP-I1 and -L are well-characterized IRES translation enhancers and modulate the translation of both viral and endogenous host mRNA transcripts[137, 180, 182, 188]. hnRNP-I1, -I2 and -L can also increase mRNA stability by binding to PTs or CA repeats in 3'-UTRs[180, 189]. The hnRNP-I/L sub-family member ROD1 has not been studied in detail but it has been show to interact with UPF1 and be involved in NMD[190].

hnRNP-M, -P and –U each belong to their own sub-family which have two (hnRNP-M, MYEF2), one (hnRNP-P2), three (hnRNP-U, -U-like 1 and -U-like 2) paralogs, respectively[141]. hnRNP-M is involved in pre-mRNA splicing and mRNA localization. hnRNP-M affects 5' and 3' splice site selection by interacting with CDC5L/PLRG1[191], functions antagonistically to hnRNP-A1 and -L to promote exon 7 exclusion of *CEACAM1-L* mRNA[192] and promotes exon 7 inclusion in *SMN2* mRNA by recruiting U2AF[193]. Also, the *D. melanogaster* homolog of hnRNP-M, Rumpelstiltskin, localizes *nanos* mRNA by binding to the 3'-UTR[194]. The hnRNP-M sub-family member MYEF2 has not been studied in detail. hnRNP-P2 was initially identified in sarcomas as a fusion protein with different transcription factors due to a chromosomal translocation events[195]. The protein was originally named fused in sarcoma/translocated in sarcoma (FUS/TLS) and hnRNP-P2 was confirmed to be FUS/TLS by mass spectrometry[196]. FUS/TLS is now considered a member of the TET protein family and participates in pre-mRNA splicing and mRNA localization[14, 197]. hnRNP-U is involved in pre-mRNA splicing and mRNA stability. hnRNP-U affects splicing globally

by regulating U2 snRNP maturation[198] and functions antagonistically to hnRNP-L to promote the inclusion of 4 exons in *caspase-9* mRNA[199]. hnRNP-U also stabilizes mRNAs potentially by binding 3'-UTR sequences[200]. The hnRNP-U sub-family members hnRNP-U-like 1 and -U-like 2 have not been studied in detail.

hnRNP-Q and -R belong to the hnRNP-Q/R sub-family, which consists of two paralogs: hnRNP-Q and hnRNP-R. hnRNP-Q regulates mRNA editing, splicing, localization, translation and stability, which will be discusses extensively below. hnRNP-R is highly homologous to hnRNP-Q (Figure 1-2 A) and has been demonstrated to regulate mRNA localization, stability and potentially splicing (as discussed in the hnRNP-Q section). hnRNP-R localizes *β-Actin* mRNA to the axons of motor neurons by binding the 3'-UTR suggesting a redundant role to IMP1/ZBP1-mediated *β-Actin* mRNA localization[201]. hnRNP-R also interacts with SMN suggesting that hnRNP-R-mediated *β-Actin* mRNA localization may be disrupted in SMA[105, 202]. hnRNP-R is also involved in *serotonin N-acetyltransferase* and *c-fos* mRNA destabilization by binding the 3'-UTR and an ARE, respectively[203, 204]. Future studies may address whether hnRNP-R regulates additional mRNA processing and post-transcriptional regulatory events.

The hnRNP proteins are clearly a diverse family of proteins that perform their functions by divergent mechanisms. Most hnRNP proteins participate in several mRNA processing and post-transcriptional regulatory events demonstrating the muli-functional nature of these proteins and the cross-talk that occurs during mRNA biogenesis.

1.3: hnRNP-Q

hnRNP-Q (also called Glycine, Arginine, Tyrosine-rich-RNA Binding Protein (GRY-RBP)[205, 206], NS1-associated protein 1 (NSAP1)[207] and synaptotagmin-binding, cytoplasmic RNA-interacting protein (SYNCRIP)[208]) is alternatively spliced to produce proteins with divergent functions. *H. sapiens* express three hnRNP-Q isoforms: -Q1, -Q2 and -Q3 while *M. musculus* express two: -Q1 and -Q3 (both have 99% sequence identity to *H. sapiens* hnRNP-Q1 and -Q3, respectively). All hnRNP-Q isoforms contain two different RNA binding domains, three RRMs and a single RGG box, and an N-terminal acid region[209] (Figure 1-2 A). However, hnRNP-Q1 has a single predicted nuclear localization sequence (NLS) while hnRNP-Q2 and -Q3 have two[209] (Figure 1-2 A). hnRNP-Q2 and -Q3 are predominantly localized to the nucleus which correlates with the presence of an additional NLS (Figure 1-2 B). Conversely, hnRNP-Q1 is mostly cytoplasmic (Figure 1-2 B) but all hnRNP-Q isoforms likely shuttle between the nucleus and cytoplasm to participate in multiple mRNA processing and post-transcriptional regulatory events. hnRNP-Q1 is also localized to the neurites and growth cones of cortical neurons suggesting that it may function locally in axons and dendrites (Figure 1-2 C, D). Additional differences between the isoforms include a truncation in RRM 2 in hnRNP-Q2 and an alternative C-terminal region in hnRNP-Q1[209] (Figure 1-2 A).

The nuclear isoforms of hnRNP-Q have been understudied but have been implicated in mRNA editing and pre-mRNA splicing. The C-terminal domain of hnRNP-Q3 interacts with Apobec-1, the catalytic component of the editosome which performs C to U editing of the *apolipoporotein B* (*ApoB*) mRNA[205, 206, 210]. hnRNP-Q3 also binds to the editosome component Apobec-1 complementation factor (ACF) and *ApoB* mRNA[206]. *In vitro* binding and knockdown assays suggest that hnRNP-Q3 sequesters ACF from binding *ApoB* mRNA to inhibit editing[205, 206]. hnRNP-Q2 also contains an N-terminal acidic domain suggesting that

it may be involved in mRNA editing as well[208]. hnRNP-Q2 and -Q3 have also implicated in pre-mRNA splicing. All hnRNP-Q isoforms interact with SMN and immunodepleting all hnRNP-Q isoforms and hnRNP-R inhibits *in vitro* splicing reactions[208]. These early studies demonstrate that hnRNP-Q2 and -Q3 likely play in important role in nuclear mRNA processing but future studies may address specific mechanisms and determine whether they regulate additional mRNA processing and post-transcriptional regulatory events. However, the cytoplasmic isoform hnRNP-Q1 regulates nearly every step of mRNA biogenesis suggesting that is a master post-transcriptional regulator similar to hnRNP-A1, -A2, -F, -I1 and -L. These findings suggest that hnRNP-Q2 and -Q3 may perform redundant functions to hnRNP-Q1 or that the lack of a second NLS and/or the addition of a unique C-terminal region in hnRNP-Q1 confer additional RNA processing and post-transcriptional regulatory functions.

1.3.1: hnRNP-Q1 Nuclear mRNA Processing and Post-Transcriptional Regulatory Functions

Although hnRNP-Q1 is predominantly nuclear, it likely undergoes nucleocytoplasmic shuttling. In support of this, hnRNP-Q1 functions in the nucleus to regulate mRNA editing and pre- mRNA splicing (Figure 1-3 Ai, Aii). hnRNP-Q3 was originally identified to inhibit ApoB mRNA editing, but hnRNP-Q1, like -Q2, also contains an N-terminal acidic domain suggesting that it may also be involved in this process[209]. Additionally, hnRNP-Q1 facilitates Apobec-1 binding target mRNAs suggesting that hnRNP-Q1 plays a key role in mRNA editing[211]. hnRNP-Q1 also regulates pre-mRNA splicing. hnRNP-Q1 was first implicated in splicing when immunodepleting all hnRNP-Q isoforms and hnRNP-R inhibited *in vitro* splicing reactions[209]. hnRNP-Q1 was subsequently shown to promote exon 7 inclusion in

SMN2 by activating a 3' splice site[212]. Interestingly, hnRNP-Q2 and -Q3 antagonized hnRNP-Q1 splicing activity leading to exon 7 exclusion[212]. However, depleting all three hnRNP-Q isoforms enhanced exon 7 inclusion suggesting that the hnRNP-Q proteins differentially regulate splicing and the levels of the different hnRNP-Q isoforms can fine-tune *SMN2* alternative splicing[212]. In support of a role for hnRNP-Q1 in splicing, the *C. elegans* homolog of hnRNP-Q and -R, HRP2, regulates alternative splicing by binding to UCUAUC elements[213].

1.3.2: hnRNP-Q1 Cytoplasmic mRNA Processing and Post-transcriptional Regulatory Functions

In the cytoplasm, hnRNP-Q1 regulates mRNA localization, translation and stability (Figure 1-3 B-D). hnRNP-Q1 was proposed to be involved in mRNA localization when it was identified as a component of transport mRNP granules[101, 214]. A KIF5 mRNP granule that was purified from *M. musculus* brain lysates was found to contain hnRNP-Q1, *CaMKIIα* and *Arc* mRNAs and 41 additional proteins including FUS/TLS, hnRNP-U and FMRP[101]. In support of this, punctate fluorescently-tagged hnRNP-Q1 is localized to the dendrites of rat hippocampal neurons and some of these granules are bi-directionally transported at ~0.05 μm/sec[214]. The hnRNP-Q1 granules also contained staufen1, a well-characterized regulator of mRNA localization, and *inositol 1,4,5-trisphosphate receptor type 1* (*ITPR1*) mRNA[214]. hnRNP-Q1 also regulates the localization of *Cdc-42*, *N-Wasp*, *Arp2*, and *Arpc1a* mRNAs, which encode actin regulators[215]. hnRNP-Q1 knockdown depleted these mRNAs from the neurites of differentiated Nuero2a (N2a) cells[215]. Additionally, the *D. melanogaster* homolog of hnRNP-Q, Syncrip, is required for proper localization of *gurken* and *oskar* mRNAs during

oogenesis[216]. Syncrip loss of function led to mRNA and protein mislocalization suggesting that Syncrip may also regulate the local translation of *gurken* and *oskar* mRNAs[216].

hnRNP-Q1 has also been demonstrated to regulate both cap-dependent and cap-independent translation. hnRNP-Q1 represses the cap-dependent translation of *RhoA* and *YB-1* mRNAs as shown by luciferase and cell-free translation assays, respectively[217, 218]. The binding sites for hnRNP-Q1 were identified to be in the 3'-UTR of both *RhoA* and *YB-1* mRNAs suggesting that hnRNP-Q1 represses the translation of a sub-set of mRNAs that likely contain similar hnRNP-Q1 binding sites[217, 218]. Conversely, hnRNP-Q1 has been proposed to repress the translation of all mRNAs by competing with PABPC1 for binding polyA tails[219]. In this model, hnRNP-Q1 represses translation by inhibiting eIF4F complex recruitment to the mRNA and consequently 48S and 80S initiation complex formation and ultimately cap-dependent translation[219]. hnRNP-Q1-mediated translational repression was dependent on both the poly(A) tail and PABPC1 and the fold change of hnRNP-Q1-mediated translational inhibition increased with the length of the poly(A) tail[219]. Additionally, when PABPC1 was sequestered by the repressor poly(A) binding protein interacting protein 2 (Paip2), hnRNP-Q1 did not affect translation and depleting hnRNP-Q via shRNA sequences targeting all isoforms of hnRNP-Q lead to increased global translation as detected by ^{35}S-methionine/cysteine incorporation[219]. This mechanism is consistent with a previous study that demonstrated that hnRNP-Q1 preferentially binds polyA RNA and DNA[208]. However, the hnRNP-Q1 binding sites in *RhoA* and *YB-1* mRNAs are non-A-rich sequences suggesting that hnRNP-Q1 can bind different sequences and inhibit cap-dependent translation by multiple mechanisms[217, 218]. hnRNP-Q1 also enhances the cap-independent translation of *Hepatitis C Virus (HCV)* RNA[220] and *Binding Immunoglobulin Protein* (*BiP*)[221],

arylalkylamine N-acetyltransferase (*AANAT*)[222], *Nuclear Receptor Sub-family 1, Group D, Member 1* (*NR1D1* or *Rev-erb α*)[223], *Period 1* (*Per1*)[224] and *Tumor Protein 53* (*p53*)[225] mRNAs. Interestingly, hnRNP-Q1 enhances the IRES translation of *HCV* RNA and *AANAT* mRNA by binding to A-rich sequences in their 5'-UTRs[220, 222]. Additionally, hnRNP-Q1 interacts with BC200, a non-coding RNA that inhibits translation by blocking the helicase activity of eIF4A[226]. PABPC1 blocks BC200-mediated translation inhibition *in vitro* and *in vivo*[227]. hnRNP-Q1 RRMs 1 and 2 bind to an A-rich region of BC200 suggesting that BC200 may contribute to hnRNP-Q1-mediated translation inhibition[226]. These findings also indicate that hnRNP-Q1 interacts with polyA RNA with its RRM domains. hnRNP-Q1 is also a component of the Interferon-γ-Activated Inhibitor of Translation (GAIT) complex which contains IFN-γ, glutamyl-prolyl tRNA synthetase (EPRS), ribosomal protein L13a and glyceraldehyde-3-phosphate dehydrogenase (GAPDH)[228]. The GAIT complex assembles on the 3'-UTRs of inflammatory mRNAs to suppress their translation[228]. Additionally, the roles for hnRNP-Q1 in mRNA localization and translation regulation suggest that hnRNP-Q1 modulates local translation but this mechanism has yet to be tested.

hnRNP-Q1 also positively and negatively regulates mRNA stability. hnRNP-Q1 is involved in stabilizing *c-Fos* and *c-Myc* mRNAs[229, 230]. These mRNAs both contain coding region instability determinants (CRDs) that destabilize the mRNAs unless they are bound specific proteins[229, 230]. The *c-Fos* mRNA CRD is bound by a complex of proteins that includes Unr, PABPC1, PAIP1, hnRNP-D and hnRNP-Q1[229]. This complex stabilizes *c-Fos* mRNA by preventing deadenylation[229]. The *c-Myc* mRNA CRD is bound by a different complex of proteins that protects the mRNA from degradation[230]. This complex includes IMP1/ZBP1, hnRNP-U, hnRNP-Q1, YB-1 and DHX9[230]. hnRNP-Q1 also stabilizes *NADPH*

oxidase 2 (*Nox2*) mRNA by binding to the 3'-UTR[231]. However, hnRNP-Q1 also destabilizes mRNAs by enhancing translation-coupled mRNA decay[204, 232]. hnRNP-Q1 enhances the translation of *Period 3* (*Per3*) mRNA alone and *AANAT* mRNA with hnRNP-R and -L, which accelerates the decay of these mRNAs[204, 232].

1.3.3: Additional Functions and Regulation of hnRNP-Q1

hnRNP-Q1 clearly plays an important role in several mRNA processing and post-transcriptional regulatory events and altered hnRNP-Q1 function may affect colon cancer and SMA pathogenesis[212, 233]. Additionally, hnRNP-Q1 is highly expressed in brain tissue suggesting that it may also be involved in neuronal development and function[202, 208, 214, 218]. In support of this, hnRNP-Q1-mediated repression of *RhoA* mRNA translation has previously been demonstrated to affect hippocampal neuron morphology[218] and disrupted hnRNP-Q1-mediated localization of *Cdc-42* and associated mRNAs has previously been demonstrated to affect cortical neuron morphology[215] (discussed in detail in Chapter 3). Additionally, the *D. melanogaster* homolog of hnRNP-Q, Syncrip, is localized to the post-synaptic compartment of the neuromuscular junction where it modulates synaptic transmission by repressing BMP expression and consequently, retrograde BMP signaling from the muscle to the motor neuron[234]. hnRNP-Q1 has also been demonstrated to have non-mRNA processing and post-transcriptional regulatory functions. hnRNP-Q1 participates in insulin receptor internalization suggesting that it may be involved in insulin signaling[235]. Additionally, hnRNP-Q1 plays a role in HCV RNA replication suggesting that hnRNP-Q1 plays multiple roles during HCV infection[236].

Regulation of hnRNP-Q1 is vastly understudied. hnRNP-Q1 is tyrosine phosphorylated by the insulin receptor[235, 237, 238] and dephosphorylated by SH2 domain-containing phosphatase 2 (SHP2)[239]. However, little else is known about how phosphorylation alters hnRNP-Q1 function. hnRNP-Q1 is methylated by PRMT1, which stimulates the association between hnRNP-Q1 and the insulin receptor[235]. hnRNP-Q3 is also methylated by PRMT1 in the RGG box domain and this modification is required for nuclear localization[240]. Future studies may address whether hnRNP-Q1 phosphorylation and/or methylation affect its roles in mRNA processing and post-transcriptional regulation. hnRNP-Q1 has also been demonstrated to be localized to processing bodies (P-bodies) which are cytoplasmic foci that contain translationally repressed mRNPs, miRNA components and mRNA degradation enzymes[241, 242]. hnRNP-Q3 has also been suggested to localize to stress granules upon cellular stress suggesting that hnRNP-Q2 may also be recruited[243]. The localization of hnRNP-Q1 to P-bodies and stress granules may affect its multiple mRNA processing functions.

1.4: Dissertation Hypothesis and Objectives

Given the clear role of hnRNP-Q1 in cytoplasmic mRNA processing and post-transcriptional regulatory events and high expression in brain tissue, the focus of this thesis research was to investigate the neuronal function of hnRNP-Q1. We hypothesized that hnRNP-Q1 post-transcriptionally regulates the expression of specific mRNAs as a means to alter neuron morphology and consequently, function. In this dissertation, we begin addressing this hypothesis. Our objective was to identify a novel mRNA target that is post-transcriptionally regulated by hnRNP-Q1 in order to affect neuronal morphology and

consequently, function. In Chapter 2, we characterized *growth associated protein 43* (*Gap-43*) as a novel hnRNP-Q1 mRNA target and demonstrated that hnRNP-Q1 repressed GAP-43 expression in neuronal cells. Chapter 3 is focused on the neuronal phenotypes that are affected by hnRNP-Q1-mediated GAP-43 expression regulation and Chapter 4 begins addressing the mechanism of this regulation. In Chapter 5, we will discuss the future directions of this research including addressing whether this mechanism occurs locally within axonal growth cones in order to synthesize new GAP-43 protein immediately in response to axon guidance signals.

1.5: Materials and Methods

Plasmids

Full-length *H. sapien* cDNA of hnRNP-Q1, hnRNP-Q3 and hnRNP-R was obtained by RT-PCR from total RNA extracted from HEK 293 cells. The cDNA was inserted into the pEGFP-C1 vector to generate the pEGFP-C1/human hnRNP-Q1, pEGFP-C1/human hnRNP-Q3 and pEGFP-C1/human hnRNP-R constructs.

Cell Culture and Transfection

Timed pregnant C57BL/6J mice were delivered from Charles River and primary cortical neurons were cultured from the embryos at E16.5. Cortices were dissected from the embryos, trypsinized (0.25%, EDTA-free, Life Technologies) at 37° C, rinsed with warm HBSS containing 10 mM HEPES (HBSS/HEPES, Fisher Scientific) and dissociated in MEM (Cellgro/Corning, Manassas, VA) containing FBS (MEM/FBS, Sigma- Aldrich). Primary cortical neurons were transfected with the Amaxa nucleofector II device (Lonza, Allendale,

NJ) and the mouse neuron nucleofector kit (Lonza) according to the manufacturer's protocol. The neurons were washed with warm HBSS/HEPES immediately following the dissection. 2.5 μg of each construct was transfected into 5 million cells followed by recovery in RPMI (Life Technologies) containing 10% horse serum (Gibco/Life Technologies) at 37° C. Cells were plated in MEM/FBS on coverslips previously coated with 1mg/ml poly-L-lysine (Sigma-Aldrich) in Borate Buffer for 72 hours followed by three 1 hour washes with sterile H^2O. Two hours after plating, the neurons were co-cultured with glia in Neurobasal medium (Gibco/Life Technologies) with 1x Glutamax (Gibco/Life Technologies) and 1x B-27 (Gibco/Life Technologies) at 5% CO_2 and 37° C and fixed 28.5 hours later for immunofluorescence.

Antibodies and Immunofluorescence

The following antibodies were used for immunofluorescence: α-Tubulin (1:1000, Sigma), 488 Phalloidin (1:1,000, Life Technologies), Goat anti-Rabbit Cy3 (1:500, Jackson Immuno Research Laboratories, Inc., West Grove, PA), Donkey anti-Mouse Cy5 (1:500, Jackson Immuno Research Laboratories, Inc.). Additionally, an hnRNP-Q1 specific antibody was produced by immunizing rabbits with a KLH-conjugated peptide corresponding to the C-terminal region of hnRNP-Q1 (KGVEAGPDLLQ, through Anaspec, Freemont, CA). The antibody was affinity purified by the company and delivered at a concentration of 0.076mg/ml. The hnRNP-Q1 antibody was tested by immunoblotting at 1:300 similar to Xing et al. 2012 (Supplemental Figure 1-1 A, B) and used for immunofluorescence at 1:100. Immunofluorescence was performed following the standard protocol. Cells were fixed with 4% paraformaldehyde (Sigma-Aldrich) in 1x PBS for 10 minutes, washed with 1x PBS,

permeabilized with 0.2% Triton X-100 in 1x PBS and washed with Tris-Glycine buffer (200 mM Tris-HCl, pH 7.5, 100 mM Glycine). Cells were blocked and incubated with primary and secondary antibodies in 5% BSA in 1x PBS with 0.1% Tween 20 at room temperature for 1 hour, 1 hour and 30 minutes, respectively. Coverslips were mounted with prolong gold anti-fade reagent with 4′,6-diamidino-2-phenylindole (DAPI, Life Technologies).

Fluorescence Microscopy

Cells were visualized with a 60x Plan-Neofluar objective (Nikon, Melville, NY) on a Nikon Eclipse inverted microscope. Images were acquired with a cooled CCD camera (Photometrics, Tucson, AZ) and Nikon Elements software. Exposure times were kept constant and below saturation for quantitative analysis. Images were deconvolved using AutoQuant X (Media Cybernetics, Bethesda, MD). Immunofluorescence images were prepared by creating easy 3D images with constant look-up table values across all conditions in Imaris (Bitplane, Concord, MA).

1.6: Figures

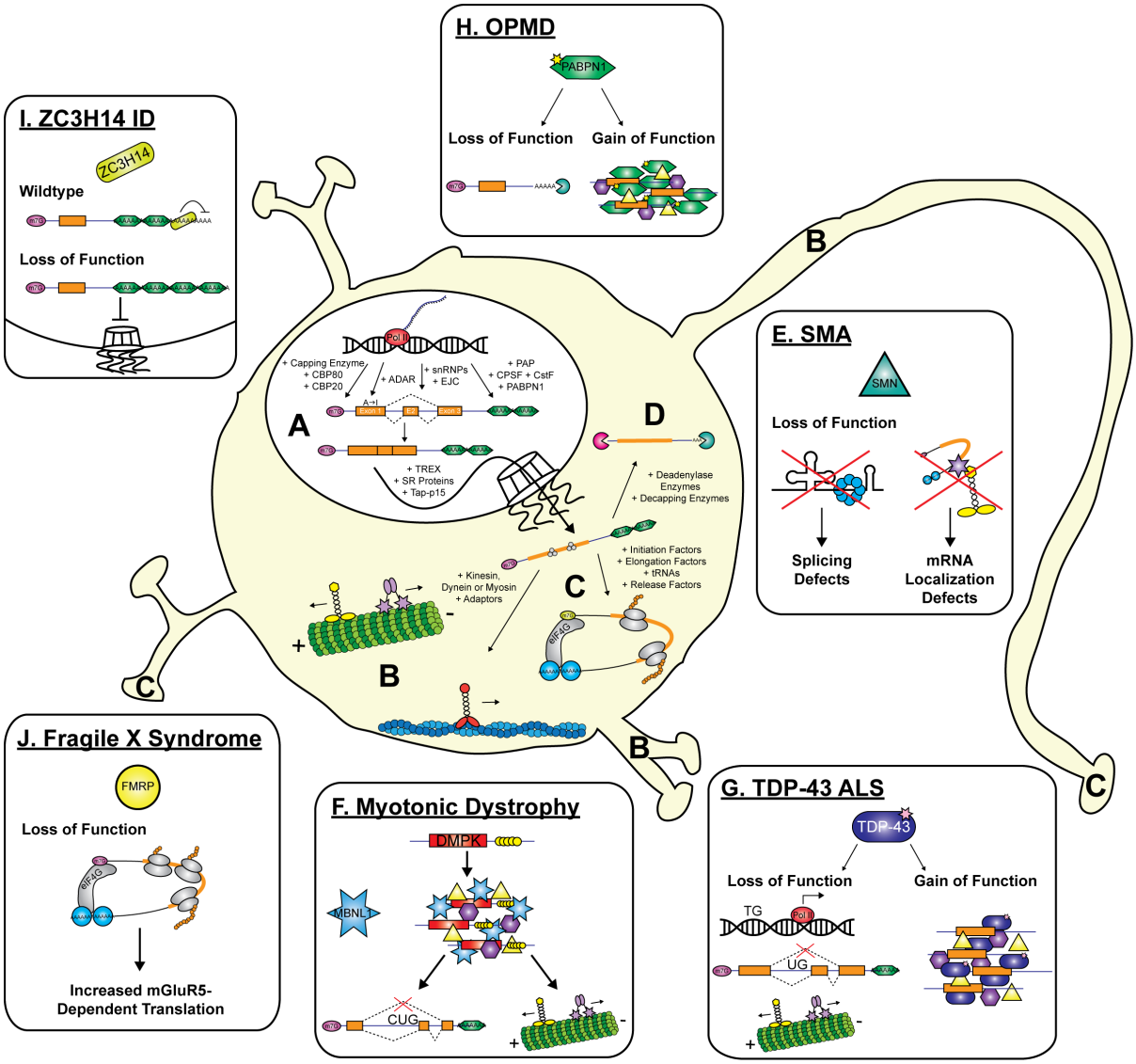

Figure 1-1: mRNA Processing and Post-Transcriptional Regulation and mRNA Binding Proteins and their Dysregulation in Disease. Figure adapted from Lagier-Tourenne et al. 2010. (A) The mRNA capping enzyme is recruited to the mRNA co-transcriptionally and covalently attaches a m^7G cap to the 5'-end of the mRNA. The 5'-cap is then bound by the nuclear cap binding complex CBP-80/CBP-20 (nCBC, dark pink oval). The RNA editing enzyme ADAR performs adenosine to inosine editing and the spliceosome removes non-coding mRNA sequences co-transcriptionally. 3'-end processing involves cleavage by CstF

and CPSF and polyadenylation by PAP. The polyA tail is then bound by PABPN1 (green hexagon). After transcription, the mRNA is exported from the nucleus through a concerted effort from the TREX complex, SR proteins and Tap-p15. (B) Upon entering the cytoplasm, mRNAs can be localized to specific sub-cellular regions including axons and dendrites of neurons. mRNAs are trafficked on microtubules (green circles) with the molecular motors kinesin (yellow) and dynein (light purple) or on actin (blue circles) with the molecular motor myosin (red). (C) mRNAs can then undergo translation or local translation in the axons and dendrites of neurons. eIF4G (grey oblong shape) initiates closed loop formation between the 5'- and 3'-ends of the mRNA by interacting with the nuclear or cytoplasmic cap binding protein (eIF4E, yellow oval) and the nuclear or cytoplasmic polyA tail binding protein (PABPN1 or PABPC1 (light blue circle)). The closed loop structure facilitates translation and the EJCs (small grey cirlces) are removed during the pioneer round of translation. (D) mRNAs are degraded after deadenylation by the exosome (teal pacman) and after decapping by the exoribonuclease XRN2 (pink pacman). (E) Spinal muscular atrophy is caused by a SMN protein (teal triangle) deficiency. SMA motor neuron pathogenesis may be due to disrupted snRNP assembly and splicing defects and/or disrupted mRNP assembly and mRNA localization defects. (F) Myotonic Dystrophy Type 1 (DM1) is partially caused by a loss of MBNL (light blue star) function due to sequestration on the CUG expanded (yellow circles) *DMPK* mRNA. Disrupted MBNL-mediated pre-mRNA splicing and mRNA localization likely contribute to both the muscle and neuronal pathogenesis observed in DM1. (G) TDP-43-mediated amyotrophic lateral sclerosis may result from a loss of TDP-43 (dark blue oval) function in transcription, splicing and localization and/or a toxic gain of function of mutated TDP-43 to sequester mRBPs in cytoplasmic aggregates. (H) Oculopharyngeal

muscular dystrophy may result from a loss of PABPN1 function in mRNA polyadenylation and/or a toxic gain of function of alanine-expanded PABPN1 to sequester mRBPs in nuclear aggregates. (I) ZC3H14-mediated intellectual disability is caused by a loss of ZC3H14 (lime oval) function. ZC3H14 has been demonstrated to control poly(A) tail length antagonistically to PABPN1 leading to mRNAs being retained in the nucleus. (J) Fragile X syndrome is caused by a deficiency in FMRP (yellow circle), which leads to enhanced translation of FMRP mRNA targets and excess mGluR5-dependent translation.

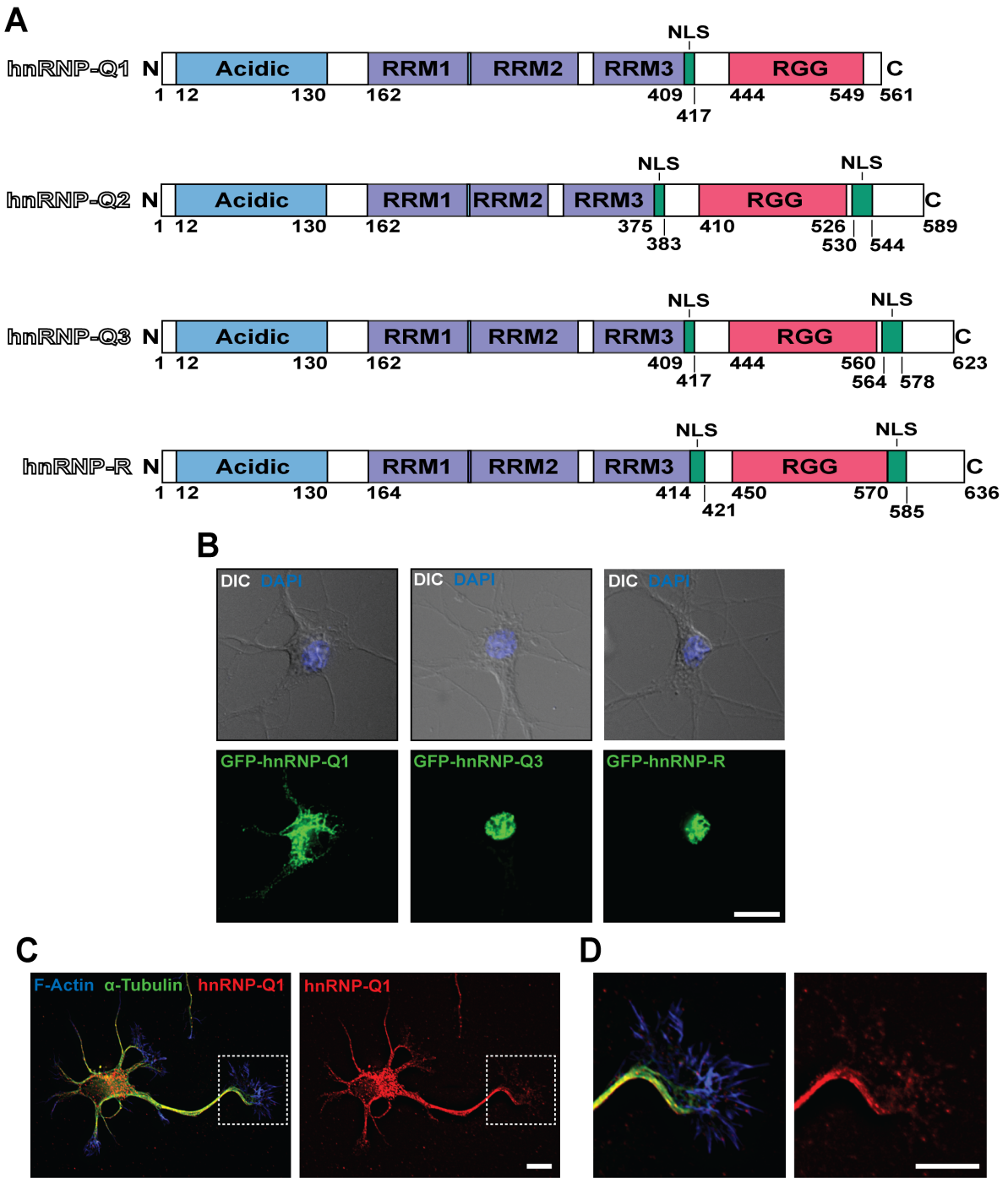

Figure 1-2: hnRNP-Q/R Sub-Family Protein Domains and Localization. (A) The domain structures of *H. sapiens* hnRNP-Q isoforms and hnRNP-R. Abbreviations: RNA recognition motif (RRM), nuclear localization sequence (NLS) and arginine- and glycine-rich domain (RGG box). (B) GFP-tagged hnRNP-Q1, -Q3 and -R were overexpressed in hippocampal

neurons for 96 hours. (C) Cultured cortical neurons were fixed after 28.5 hours in vitro and processed for immunofluorescence with hnRNP-Q1 and α-Tubulin antibodies. F-actin was detected with fluorescent conjugated phalloidin. (D) Enlarged views of the growth cone (white box in (C)). Scale bars = 10 μm.

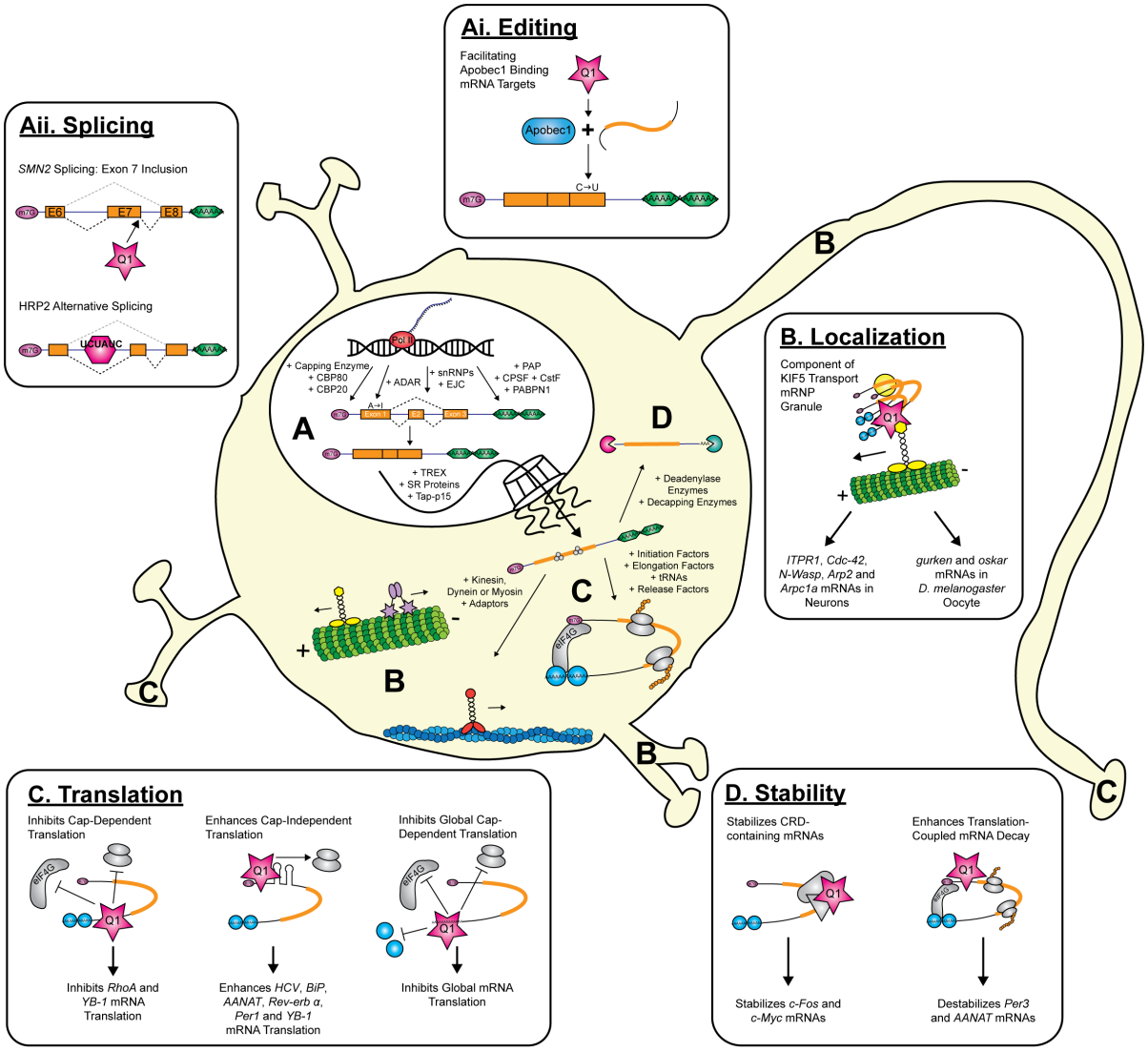

Figure 1-3: hnRNP-Q1 mRNA Processing and Post-Transcriptional Regulatory Functions. Figure adapted from Lagier-Tourenne et al. 2010. (Center) General mRNA processing and post-transcriptional regulatory events as described in Figure 1-1. (Ai) hnRNP-Q1 (pink star) facilitates Apobec-1 binding to its mRNA targets suggesting that it enhances editosome-mediated cytosine to uracil editing. (Aii) hnRNP-Q1 promotes exon 7 inclusion in *SMN2* mRNA by activating a 3' splice site and the *C. elegans* homolog of hnRNP-Q and -R, HRP2 (pink hexagon), regulates alternative splicing by binding to UCUAUC elements. (B) hnRNP-Q1 is a component of a KIF5 transport mRNP granule and is suggested to regulate to

the localization of *ITPR1*, *Cdc-42*, *N-Wasp*, *Arp2*, and *Arpc1a* mRNAs to the neurites of cultured neurons. The *D. melanogaster* homolog of hnRNP-Q, Syncrip, regulates the localization of *gurken* and *oskar* mRNAs during oogenesis. (C) hnRNP-Q1 inhibits the cap-dependent translation of *RhoA* and *YB-1* mRNAs and enhances the cap-independent translation of *HCV*, *BiP*, *AANAT*, *Rev-erb α*, *Per1* and *p53* mRNAs. hnRNP-Q1 has also been suggested to inhibit the cap-dependent translation of all mRNAs by competing with PABPC1 for binding polyA tails. hnRNP-Q1 may also regulate translation locally. (D) hnRNP-Q1 is a component of the protein complexes that bind the CRD of *c-Fos* and *c-Myc* mRNAs to stabilize them. hnRNP-Q1 also promotes the translation-coupled mRNA decay of *Per3* and *AANAT* mRNAs.

1.7: Supplemental Figures

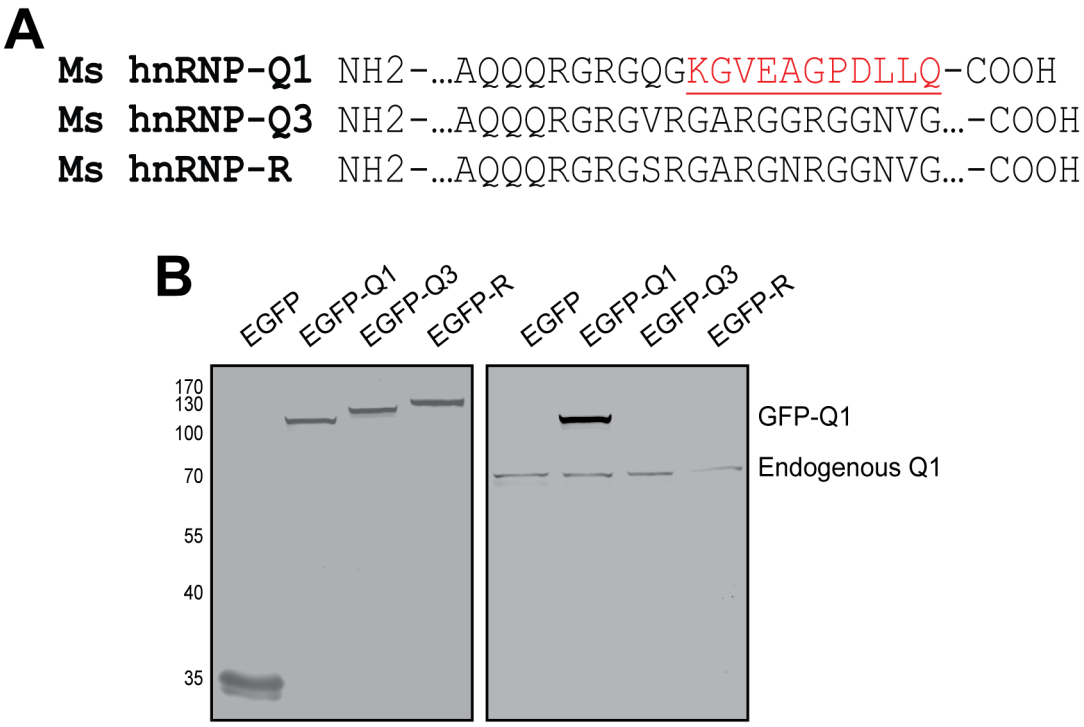

Supplemental Figure 1-1: hnRNP-Q1 Antibody Specificity. (A) An hnRNP-Q1 specific antibody was produced by immunizing rabbits with a KLH-conjugated peptide corresponding to the C-terminal region of hnRNP-Q1 (KGVEAGPDLLQ) that is not present in hnRNP-Q3 and -R. (B) EGFP and EGFP-tagged hnRNP-Q1 and the homologous proteins hnRNP-Q3 and hnRNP-R were overexpressed in N2a cells for ~16 hours and lysates were immunoblotted for GFP and hnRNP- Q1.

1.8: Tables

RNA Binding Protein	Mutation and/or Alternations	Disease	Disease Symptoms	mRNA Processing Functions	Disease Mechanism
eIF4E	Upregulation and Increased Phosphorylation	Breast Cancer, Glioma, Prostate Cancer, etc.	Promotes Metastasis and Tumor Progression	Translation	Excess Translation
FMRP	CGG Expansion in the *FMR1* Gene	Fragile X Syndrome	Intellectual Disability, Attention Deficit, Autistic Behavior and Hypersensitivity	Translation	Gene Silencing due to Methylation, Excess Translation due to loss of FMRP Function and Enhanced mGluR5 Signaling
HuR	Upregulation	Breast Cancer, Lung Cancer, Ovarian Caner, etc.	Reduced Survival	Translation and Stability	Promotes Angiogenesis
MBNL1/CUGBP1	CUG Expanded *DMPK* mRNA	Myotonic Dystrophy Type 1	Early to Adult-onset, Muscle Weakness/Wasting, Myotonia, Cognitive Impairment with Early Onset	MBNL1: Splicing, Localization and Stability, CUGBP1: Splicing, Translation and Stability	Loss of MBNL1 Function due to Sequestration and Gain of CUGBP1 Function due to Hyperphosphorylation
MBNL1/CUGBP1	CCUG Expanded *ZNF9* mRNA	Myotonic Dystrophy Type 2	Adult-onset, Mild Muscle Weakness/Wasting, Myotonia	MBNL1: Splicing, Localization and Stability, CUGBP1: Splicing, Translation and Stability	Differences from Myotonic Dystrophy Type 1 disease mechanism are unknown
PABPN1	N-terminal polyalanine expansion	Oculopharyngeal Muscular Dystrophy	Adult-onset, Ptosis, Dysphagia	PolyA Tail Length and 3'-end Processing	Loss of Function and Toxic Gain of Function Mechanisms Proposed
QKI	Downregulation	Gastric Cancer, Prostate Cancer and Squamous Cell Carcinoma	Reduced Survival	Splicing	Tumor Suppressor/ Anti-proliferaction Factor
	Single Nucleotide Polymorphism Leading to Altered Splicing	Schizophrenia	Higher Susceptibility		Unknown Mechanism
	Deletion	Glioma	Reduced Survival		Tumor Suppressor/ Anti-proliferaction Factor
SMN	*SMN1* gene deletion or mutation	Spinal Muscular Atrophy	Early-onset, Muscle Weakness, Motor Neuron Degeneragtion	Splicing and Localization	Loss of SMN Function
TDP-43	Missense Mutations	Amytrophic Lateral Sclerosis	Adult-onset, Muscle Weakness, Motor Neuron Degeneration	Transcription, Splicing and Localization	Loss of Function and Toxic Gain of Function Mechanisms Proposed
TIA1	Missense Mutation	Welander Distal Myopathy	Distal Muscle Weakness	Splicing and Translation	Altered Splicing due to loss of TIA1 Function?
ZC3H14	Nonsense Mutation	Non-syndromic Intellectual Disability	Intellectual Disability	PolyA Tail Length and Nuclear Export	Unknown Mechanism

Table 1-1: Dysregulated mRNA Processing and Post-Transcriptional Regulation in Disease. mRBPs that are dysregulated in disease are listed along with the type of mutation or

alteration, disease name, disease symptoms, mRNA processing and post-transcriptional regulatory functions of the mRBP implicated and disease mechanism[14, 90, 107, 122, 127, 129, 244-248].

hnRNP Sub-Family	hnRNP Protein	Alternative Name(s)	RNA Binding Domains	Binding Sequences	mRNA Processing Functions	Diseases
hnRNP-A/B/D	hnRNP-A0		2 RRM, 1 RGG			
	hnRNP-A1		2 RRM, 1 RGG	UAGAGU, UAGGG(A/U), UAGRG(A/U), UAGAGA, UAGG, GGGU, UGGGGU and A/U-rich	Splicing, Export, Localization, Translation and Stability	Alzheimer's Disease, Cancer, Crohn's Disease, Multip Sclerosis, OPMD, SMA
	hnRNP-A2	hnRNP-A2/B1	2 RRM, 1 RGG	GCCAAGGAGCC and UUUAGGG repeats	Splicing, Packaging, Localization, Translation and Stability	Alzheimer's Disease, Behçet's Disease, Cancer, Rheumatiod Arthritis
	hnRNP-A3		2 RRM, 1 RGG	GCCAAGGAGCC	Localization	
	hnRNP-A/B		2 RRM, 1 RGG		Editing and Localization	
	hnRNP-D	AUF1	2 RRM, 1 RGG	UUAGG, AUUUA and AU-rich elements	Translation and Stability	Cancer and Inflammatory Skin Disease
	hnRNP-D-like	laAUF1	2 RRM, 1 RGG			
hnRNP-C	hnRNP-C		1 RRM	U-rich	Splicing, Packaging, Translation and Stability	Alzheimer's Disease and Cancer
	RALY		1 RRM			
	RALY-like		1 RRM			
hnRNP-E/J/K	hnRNP-E1	PCBP1	3 KH	UUAGG, C-rich, TTAGGG repeats, CU-rich elements	Splicing, Translation, Stability	Cancer
	hnRNP-E2	PCBP2	3 KH	C-rich	Translation, Stability	Cancer
	hnRNP-E3	PCBP3	3 KH	C-rich	Splicing	Tauopathies
	hnRNP-E4	PCBP4	3 KH	C-rich	Stability	
	hnRNP-J		3 KH, 1 RGG	C-rich		
	hnRNP-K		3 KH, 1 RGG	C-rich	Splicing, 3'-end Processing, Translation, Stability	ALS, Cancer and Spinocerebellar Ataxia 10
hnRNP-F/H	hnRNP-F		3 Atypical RRMs	G-tract, GGGA, G-rich	Splicing, 3'-end Processing, Translation and Stability	
	hnRNP-H1		3 Atypical RRMs, 1 RGG Box	GGGA	Splicing, 3'-end Processing	Cancer and Congenital Myasthenic Syndrome
	hnRNP-H2		3 Atypical RRMs, 1 RGG Box	GGGA, G-rich	Splicing and 3'-end Processing	
	hnRNP-H3		3 Atypical RRMs, 1 RGG Box	GGGA		
	GRSF1		3 Atypical RRMs			

hnRNP Sub-Family	hnRNP Protein	Alternative Name(s)	RNA Binding Domains	Binding Sequences	mRNA Processing Functions	Diseases
hnRNP-G	hnRNP-G	RBMX	1 RRM, 2 RGG	CC(A/C)-rich and AAGU	Splicing	Cancer, Intellectual Disability and SMA
	hnRNP-GT	RBMXL2	1 RRM, 2 RGG		Splicing	
hnRNP-I/L	hnRNP-I1	PTB, PTBP1	4 Atypical RRMs	Polypyrimidine Tracts, UCUUC, UCUU, CUCUCU, CUUCUCUCU	Splicing, 3'-end Processing, Export, Localization, Translation and Stability	Cancer
	hnRNP-I2	nPTB, PTBP2	4 Atypical RRMs	Polypyrimidine Tracts	Splicing and Stability	Cancer
	hnRNP-L		4 Atypical RRMs	CA-repeats	Splicing, 3'-end Processing, Export, Translation and Stability	Cancer
	hnRNP-L-like		4 Atypical RRMs	CA-repeats	Splicing	
	ROD1	PTBP3	4 Atypical RRMs	Polypyrimidine Tracts	Stability (NMD)	
hnRNP-M	hnRNP-M		3 RRMs	G-rich and U-rich	Splicing and Localization	Cancer and SMA
	MYEF2		3 RRMs			
hnRNP-P	hnRNP-P2	FUS/TLS	1 RRM and 2 RGG Boxes	GGUG	Splicing and Localization	ALS, Cancer, Frontotemporal Dimentia
hnRNP-U	hnRNP-U		1 RGG Box		Splicing and Stability	
	hnRNP-U-like 1					
	hnRNP-U-like 2					
hnRNP-Q/R	hnRNP-Q	GRY-RBP, NSAP1, SYNCRIP,	3 RRMs and 1 RGG Box	G-Quadruplex Structures, PolyA	Editing, Splicing, Localization, Translation and Stability	Cancer and SMA
	hnRNP-R		3 RRMs and 1 RGG Box		Localization and Stability	SMA

Table 1-2: hnRNP Proteins. The hnRNP proteins are listed according to their sub-family along with their alternative protein names, RNA binding domains, RNA binding sequences, mRNA processing and post-transcriptional regulatory functions and diseases that they are involved in[137, 138, 141].

Chapter 2

Identification of *Gap-43* mRNA as a Novel hnRNP-Q1 Target

Portions of this chapter were adapted from the following manuscript:

Williams, K.R., Stefanovic, S., McAninch, D.S., Xing, L., Allen, M., Li, W., Feng, Y., Mihailescu, M.R., Bassell, G.J. (2015) hnRNP-Q1 Represses Nascent Axon Growth in Cortical Neurons by Inhibiting *Gap-43* mRNA Translation. *Mol Biol Cell*. Revision Under Review.

2.1: Introduction

The predominantly cytoplasmic localization of hnRNP-Q1 suggests possible functions in mRNA translation, localization and/or decay regulation. Therefore, we sought to identify novel hnRNP-Q1 mRNA targets that are post-transcriptionally regulated in the cytoplasm of neurons. We were particularly interested in mRNA targets that are localized to neurites in order to determine if hnRNP-Q1 modulates local translation. *Growth associated protein 43* (*Gap-43*) mRNA was identified in our lab to associate with hnRNP-Q1 in a candidate RNA immunoprecipitation screen. In support of this, Chen et al. 2012 performed a microarray analysis of hnRNP-Q1 interacting mRNAs and identified 2,250 hnRNP-Q1 target mRNAs including *Gap-43* mRNA[215]. GAP-43 is an important neuronal protein that regulates actin dynamics in growth cones and facilitates axonal growth. This thesis sought to identify a novel post-transcriptional mechanism for how this critical protein is regulated and to provide insight into the function of this mechanism in neuronal development.

2.1.1: Molecular and Systemic Functions of GAP-43

GAP-43 is a neuronal-specific protein that is enriched in axonal growth cones after polarity is established and also accumulates along nascent axons in cultured hippocampal neurons[249]. GAP-43 is a largely unstructured protein due to an abnormal amino acid (AA) composition including several charged residues and few hydrophobic residues[249]. The only identified protein domains in GAP-43 are the membrane binding domain (AA 1-10) and the IQ Domain (AA 38-56)[249]. The membrane binding domain contains two cysteines (C-3 and C-4) that are palmitoylated to facilitate but not maintain GAP-43 membrane binding[249]. Newly synthesized GAP-43 is targeted to the early secretory pathway by palmitoylation and

is sorted into vesicles that are trafficked down the axon to the growth cone plasma membrane[249]. GAP-43 protein can also be synthesized locally in axons[250], which will be discussed below. The IQ domain is a protein-protein interaction domain that contains the serine 41 (S41) phosphorylation residue and interacts with the Ca^{2+} binding protein Calmodulin (CaM)[249].

GAP-43 is a multifunctional protein that interacts with actin, phosphatidylinositol 4,5-bisphosphate (PIP_2) and CaM to modulate actin dynamics and promote axon growth. GAP-43 directly regulates actin polymerization in an S41 phosphorylation-dependent manner. Unphosphorylated GAP-43 functions as an actin capping protein that attenuates actin polymerization[249]. Conversely, protein kinase C (PKC) phosphorylated GAP-43 binds to F-actin with a higher affinity and serves as a lateral stabilizer of actin filaments leading to enhanced actin polymerization[249]. Unphosphorylated GAP-43 can also promote a dynamic actin network by sequestering PIP_2, which inhibits the actin binding proteins profilin (polymerization and actin monomer sequestration), cofilin (depolymerization and severing) and gelsolin (severing and capping)[249]. S41 phosphorylation of GAP-43 by PKC disrupts the interaction between GAP-43 and PIP_2[249]. Additionally, GAP-43 phosphorylation and function can be regulated by CaM. CaM binds the IQ domain of GAP-43 and prevents PKC phosphorylation, PIP_2 interaction and actin association[249]. GAP-43 is sequestered by CaM in resting neurons and increased Ca^{2+} and/or PKC phosphorylation of GAP-43 in activated neurons disrupts this interaction[249]. Phosphorylated GAP-43 then facilitates actin polymerization and axon growth[249]. Additionally, local concentrations of PIP_2 can be sequestered by unphosphorylated GAP-43 and PKC phosphorylation releases GAP-43 to facilitate actin polyermization while PIP_2 promotes the interaction between the actin network

and the plasma membrane to enhance axon growth[249]. GAP-43 regulation of actin cytoskeleton dynamics is summarized in Figure 2-1.

GAP-43 function is required for proper neuronal development and altered GAP-43 expression affects learning, memory formation and neuronal regeneration. GAP-43 heterozygous mice demonstrate impaired contextual memory[251], mice overexpressing non-phosphorylatable GAP-43 have an impaired ability to retain spatial memories[252] and mice overexpressing pseudo-phosphorylated GAP-43 have difficulty unlearning[252]. Conversely, mice overexpressing GAP-43 demonstrate enhanced spatial learning and memory[253]. However, excessive GAP-43 overexpression leads to impaired spatial learning and memory[254]. GAP- 43 also plays an important role in neuron regeneration with increased GAP-43 expression observed[255, 256] and increased GAP-43 protein levels promoting axon sprouting and regeneration after injury and vice versa[257-261]. Additionally, GAP-43 protein levels are reduced in the frontal cortex and in some regions of the hippocampus in post-mortem brain tissue from patients with Alzheimer's disease, schizophrenia and bipolar disorder[262-264] and GAP-43 heterozygous mice demonstrate some autistic-like characteristics[265]. These critical functions of GAP-43 motivate an understanding of how the expression of this protein is regulated.

2.1.2: GAP-43 Expression Regulation

Precise spatial and temporal control of GAP-43 protein levels is achieved through multiple mechanisms and is critical for GAP-43 function. The *Gap-43* gene is transcribed exclusively in neuronal cells due to a repressive element in its promoter region[266] and specific transcription factors[267-269]. *Gap-43* mRNA is localized to the axons and growth cones of

differentiated PC12 cells[270] and IMP1/ZBP1 is required to localize *Gap-43* mRNA to the axons of dorsal root ganglia neurons[271]. The localization of *Gap-43* mRNA to axons suggests that it may be locally translated within axons and growth cones in order to synthesize new GAP-43 protein immediately in response to axon guidance signals. In support of this, GAP-43 knockdown reduces axon length in dorsal root ganglia neurons and this phenotype can only be rescued by GAP-43 that is locally translated in axons[250]. Additionally, IMP1/ZBP1 heterozygous mice have reduced regeneration capabilities suggesting that the localization and local translation of its mRNA targets, including *Gap-43*, are required for efficient regeneration[271]. These findings indicate that *Gap-43* mRNA translation is likely regulated as an additional mechanism to control GAP-43 expression and function but the factors involved have not been identified. *Gap-43* mRNA stability is also positively and negatively regulated. HuD stabilizes *Gap-43* mRNA by binding to an ARE in the 3'-UTR and preventing deadenylation[80, 81]. Spatial learning increases HuD protein levels and post-transcriptionally increases GAP-43 mRNA and protein levels suggesting that *Gap-43* mRNA stabilization by HuD is a mechanism for regulating GAP-43 function[272]. Conversely, KSRP destabilizes *Gap-43* mRNA by competing with HuD for binding the ARE and targeting the mRNA for degradation[82]. These post-transcriptional regulatory mechanisms likely function cooperatively in order to regulate GAP-43 expression and function.

2.1.3: Chapter 2 Hypothesis and Objectives

Given that we identified *Gap-43* mRNA as a candidate hnRNP-Q1 target, we first focused on validating this target. We hypothesized that hnRNP-Q1 post-transcriptionally represses GAP-43 expression in neurons and that endogenous expression profiles would

support an inverse relationship between these proteins. Our results reveal that hnRNP-Q1 modulates total and phosphorylated GAP-43 protein levels without affecting *Gap-43* mRNA levels in neuronal cells. Additionally, endogenous hnRNP-Q1 and GAP-43 demonstrate opposite expression profiles in cultured cortical neurons and enrichment in hippocampal regions. These results suggest that *Gap-43* mRNA is a bona fide target of hnRNP-Q1 and that hnRNP-Q1 like regulates *Gap-43* mRNA translation considering the previously identified functions of hnRNP-Q1.

2.2: Results

Two model systems were used for our experiments, the *M. musculus* neuroblastoma cell line Neuro2a (N2a) and primary *M. musculus* cortical neurons, as a means to assess multiple aspects of hnRNP-Q1-mediated modulation of *Gap-43* expression. N2a cells are an ideal neuronal model system because they are highly amenable to biochemical experiments and can be differentiated into neuron-like cells[273, 274]. Primary cortical neurons were used due to high expression of hnRNP-Q1 in the forebrain[202, 208, 218]. Cultured primary cortical neurons differentiate axons and dendrites and undergo neuronal differentiation[275] and we have used them previously to examine early stages of axon outgrowth[49].

2.2.1: Elevated GAP-43 Expression in hnRNP-Q1 Deficient N2a Cells

We first sought to determine if GAP-43 protein levels were affected by hnRNP-Q1 knockdown. N2a cells were transfected with hnRNP-Q1 siRNAs targeting sequences in the 3' untranslated region (3'-UTR), which are not present in other hnRNP-Q isoforms. Scrambled siRNA was used as a control. Immunoblot analysis of cell lysates 72 hours after transfection

revealed that hnRNP-Q1 can be efficiently depleted (siRNA #1 = 0.31 fold, siRNA #2 = 0.44 fold and siRNA #3 = 0.67 fold, Figure 2-2 A). Interestingly, GAP-43 protein levels were increased according to the degree of hnRNP-Q1 depletion (siRNA #1 = 2.99 fold, siRNA #2 = 2.30 fold and siRNA #3 = 1.72 fold, Figure 2-2 A). The levels of the highly homologous proteins hnRNP-R and hnRNP-Q3 and γ-Actin protein were not significantly affected (Figure 2-2 A). These findings demonstrate that the increased GAP-43 protein levels are specifically due to hnRNP-Q1 knockdown. Similar results were observed with hnRNP-Q1 knockdown by shRNA #1 (Supplemental Figure 2-1 A) and have been demonstrated with both infrared fluorescent and chemiluminescent immunoblot methods (Figure 2-2 A, Supplemental Figure 2-1 A-C). hnRNP-Q1 siRNA #1 was used for the remainder of the experiments because it demonstrated the greatest knockdown. Additionally, overexpressing hnRNP-Q1 in N2a cells for ~16 hours did not significantly affect GAP-43 protein levels suggesting that hnRNP-Q1 is highly expressed and its function is saturated in these cells (1.12 fold, Figure 2-2 B).

To determine if hnRNP-Q1 affects *Gap-43* mRNA levels, quantitative real time-PCR (qRT-PCR) was performed with cDNA reverse transcribed from lysates 72 hours after hnRNP-Q1 #1 or Scrambled siRNA transfection. We found that neither *Gap-43* nor *γ-Actin* mRNA levels were significantly altered upon hnRNP-Q1 knockdown (1.02 fold, 1.05 fold, respectively, Figure 2-2 C) suggesting that hnRNP-Q1 may regulate GAP-43 expression through a translational mechanism. Additionally, the levels of S41 phosphorylated GAP-43 were also measured upon hnRNP-Q1 knockdown due to the important function of this modification. N2a cells were transfected with hnRNP-Q1 #1 or Scrambled siRNA and immunoblotted after 72 hours (Figure 2-2 D). The specificity of the phospho-GAP-43

antibody was assessed by immunoblotting N2a cell lysates with and without phosphatase inhibitor (Supplemental Figure 2-1 D). The levels of phospho-GAP-43 and total GAP-43 are significantly increased upon hnRNP-Q1 knockdown (4.79 fold and 2.65 fold, respectively) but the ratio of phospho-GAP-43/total GAP-43 is not significantly altered (1.77 fold, Figure 2-2 D). These results suggest that the regulation of GAP-43 S41 phosphorylation remains the same upon hnRNP-Q1 knockdown but that there are increased levels of both phosphorylated and unphosphorylated GAP-43, which may affect GAP-43 functions to regulate actin dynamics.

2.2.2: Characterization of Incipient Cortical Neurons

Incipient neurons (28.5 hours *in vitro*) were characterized as a potential model for our studies because GAP-43 is suggested to play an early role in axon outgrowth. Primary cortical neurons were fixed after 28.5 hours in culture and processed for immunofluorescence with GAP-43 and β-III-Tubulin antibodies and fluorescently conjugated phalloidin to detect F-actin (Figure 2-2 A). GAP-43 puncta are present throughout the neuron including in the neurites and growth cones demonstrating that GAP-43 is not solely enriched in the nascent axon at this early stage of neuronal development (Figure 2-2 A). However, a perinuclear enrichment of GAP-43 is visible which is consistent with GAP-43 being targeted to the early secretory pathway by palmitoylation (Figure 2-2 A). The localization of *Gap-43* mRNA was also assessed in incipient cortical neurons by fluorescence *in situ* hybridization (FISH). Cortical neurons were electroporated with Lifeact-GFP immediately after dissection, fixed after 28.5 hours in culture and processed for Stellaris FISH with *Gap-43* cy3 probes and mCherry cy5 probes as a negative control (Figure 2-3 B). *Gap-43* mRNA granules are

enriched in the cell body but an enlarged view of the neurite revealed that there are also numerous *Gap-43* mRNA granules localized to the neurite and growth cone (Figure 2-3 B, C). These findings are consistent with previous reports[270] and the negative control *mCherry* demonstrated background levels of signal (Figure 2-3 B, C).

2.2.3: Elevated GAP-43 Expression in hnRNP-Q1 Deficient Primary Cortical Neurons

Primary cortical neurons were assessed to determine if hnRNP-Q1 depletion increases GAP-43 protein expression at the subcellular level. Neurons were electroporated with hnRNP-Q1 #1 or Scrambled siRNA and Lifeact-GFP immediately following the dissection and fixed after 28.5 hours in culture. siRNA was used instead of shRNA due to higher transfection efficiencies and quicker knockdown times, which is required to assess incipient neuron morphology. The neurons were then processed for immunofluorescence with GAP-43 and hnRNP-Q1 antibodies and transfected cells were selected by GFP signal (Figure 2-4 A, B). Because GAP-43 is enriched in axonal growth cones after polarity is established, we quantified GAP-43 protein levels in both the cell bodies and nascent axons of these incipient neurons. hnRNP-Q1 knockdown increased GAP-43 protein levels on average by 1.36 fold in cell bodies and by 1.56 fold in nascent axons (Figure 2-4 C, D). Plotting hnRNP- Q1 protein levels against GAP-43 protein levels for each cell supports an inverse correlation between hnRNP- Q1 and GAP-43 protein levels (Supplemental Figure 2-2). hnRNP-Q1 knockdown also did not reduce the ratio of GAP-43 protein levels in nascent axon/cell body suggesting that hnRNP-Q1 is not required for GAP-43 protein enrichment in the nascent axon and growth cone (Figure 2-4 E). In fact, the nascent axon/cell body ratio was actually significantly increased upon hnRNP-Q1 knockdown (0.73 to 0.83, 1.14 fold) suggesting that

hnRNP-Q1 negatively regulates GAP-43 levels within the axon (Figure 2-4 E).

2.2.4: Inverse Correlation between the Expression of hnRNP-Q1 and GAP-43

An inverse correlation between hnRNP-Q1 and GAP-43 protein levels should be expected if hnRNP-Q1 negatively regulates GAP-43 protein expression. Thus we investigated the expression profiles of hnRNP-Q1 and GAP-43 in cultured neurons. High-density primary cortical neurons were cultured for 0-21 days, cell lysates were collected every third day and immunoblotted for hnRNP-Q1 and GAP-43. The expression profile from this time course suggests that hnRNP-Q1 and GAP-43 are both developmentally regulated in primary cortical neurons and that these proteins have opposite expression patterns. hnRNP-Q1 protein levels decreased over time while GAP-43 protein levels increased, suggesting that the decreasing levels of hnRNP-Q1 protein may contribute to the increasing levels of GAP-43 protein in primary cortical neurons (Figure 2-5 A). Additionally, GAP-43 and HuD, a positive regulator of GAP-43 expression, have previously been demonstrated to be enriched in Ammon's Horn as compared to the Dentate Gyrus of the hippocampus *in vivo*[276, 277]. Therefore, we assessed whether hnRNP-Q1, a proposed negative regulator of GAP-43 expression, demonstrated the opposite pattern of expression. The two regions of the hippocampus were dissected from P30 wild type mice[278] and the levels of *HuD*, *Gap-43* and *hnRNP-Q1* mRNAs were quantified by qRT-PCR due to an inadequate amounts of tissue for immunoblotting. As expected, *HuD* and *Gap-43* mRNAs were enriched in Ammon's Horn (2.54 fold and 1.65 fold, respectively, Figure 2-5 B). However, *hnRNP-Q1* mRNA was not enriched in the Ammon's Horn and is potentially more enriched in the Dentate Gyrus suggesting that hnRNP-Q1 expression may contribute to GAP-43 protein expression *in vivo*

in the hippocampus (0.72 fold, Figure 2-5 B).

2.3: Discussion

Our results reveal that Gap-43 mRNA is a novel target that is post-transcriptionally regulated by hnRNP-Q1. hnRNP-Q1 knockdown in N2a cells increased GAP-43 protein levels without affecting Gap-43 mRNA levels. However, overexpressing hnRNP-Q1 did not decrease GAP-43 protein levels suggesting that the function of hnRNP-Q1 is saturated and contributes to the precise regulation of GAP-43 expression. S41 phosphorylated GAP-43 protein levels were also increased upon hnRNP-Q1 knockdown but the ratio of phosphorylated/total GAP-43 protein was not significantly altered. These findings indicate that the regulation of GAP-43 phosphorylation is not affected by hnRNP-Q1 knockdown. Specifically PKC expression and consequently function is likely not affected by hnRNP-Q1 knockdown. In support of this, *PKCι* was the only PKC paralog identified as an hnRNP-Q1 mRNA target in the microarray screen and PKCι has not been demonstrated to phosphorylate GAP-43[215]. Although the ratio of phosphorylated/total GAP-43 protein is not affected by hnRNP-Q1 knockdown, the levels of phosphorylated GAP-43 are increased suggesting that actin dynamics may be affected. Additionally, phosphorylation of GAP-43 in growth cones is dynamically regulated and differentially distributed[279]. Therefore, GAP-43 phosphorylation should be assessed in by an immunocytochemical analysis to understand how altered GAP-43 phosphorylation could contribute to altered actin dynamics.

hnRNP-Q1-mediated regulation of GAP-43 expression was also assessed in cortical neurons but this model system was first characterized by immunocytochemical and fluorescence *in situ* hybridization analysis. GAP-43 protein localization is regulated in

developing neurons; GAP-43 is evenly distributed in the processes of unpolarized cells but becomes enriched in the axonal growth cones and depleted from dendritic growth cones upon polarization of hippocampal neurons[280]. These findings suggest that GAP-43 may play a role in axon outgrowth and specification. Therefore, incipient neurons (28.5 hours *in vitro*) were characterized as a potential model for our studies to determine if altering the expression of GAP-43 affects axon outgrowth. Immunocytochemical analysis revealed that these neurons are un-polarized due to the even distribution of GAP-43 signal in the neurites. Additionally, a perinuclear enrichment of GAP-43 signal is observed, which is consistent with GAP-43 being targeted to the early secretory pathway by palmitoylation[249]. The localization of *Gap-43* mRNA was also assessed in incipient cortical neurons. Fluorescence *in situ* hybridization analysis revealed that *Gap-43* mRNA is enriched in the cell body but is also localized to neurites and growth cones. These findings suggest that the local translation of *Gap-43* mRNA may contribute to the neuritic localization of GAP-43 protein and consequently axon outgrowth. The neuritic localization of GAP-43 protein and mRNA in cortical neurons that we observed is consistent with previous reports[270, 280]. Additionally, the expression pattern of GAP-43 protein and mRNA in 28.5 hour *in vitro* primary cortical neurons demonstrates that these neurons are a good model for our studies.

Our results reveal that hnRNP-Q1 also represses GAP-43 expression in incipient cortical neurons. The levels of GAP-43 protein are increased in both cell bodies and nascent axons upon hnRNP-Q1 knockdown. Additionally, the ratio of GAP-43 protein levels in the nascent axon/cell body was not reduced upon hnRNP-Q1 knockdown indicating that hnRNP-Q1 is not required to localize and potentially enrich GAP-43 protein in the growth cone. This ratio is actually reduced upon hnRNP-Q1 knockdown demonstrating that hnRNP-Q1

negatively regulates GAP-43 protein levels within the axon. These findings also suggest that hnRNP-Q1 is not required to localize *Gap-43* mRNA to growth cones but additional studies need to be performed to confirm this result.

The proposed role of hnRNP-Q1 to negatively regulate GAP-43 expression is supported by expression data in cultured cortical neurons and hippocampal tissue. hnRNP-Q1 and GAP-43 protein have opposite expression profiles in a cultured cortical neuron time course suggesting that the decreasing levels of hnRNP-Q1 protein may contribute to the increasing levels of GAP-43 protein. Additionally, the mRNA levels of *HuD*, *Gap-43* and *hnRNP-Q1* were assessed *in vivo* in the hippocampus. *HuD* and *Gap-43* mRNAs were enriched in the Ammon's Horn region of the hippocampus as compared to the Dentate Gyrus, which is consistent with previous reports[276, 277]. Interestingly, *hnRNP-Q1* mRNA was not enriched in Ammon's Horn and was potentially enriched in the Dentate Gyrus. These finding suggest that GAP-43 expression is post-transcriptionally enhanced in Ammon's Horn by HuD and may be post-transcriptionally repressed in the Dentate Gyrus by hnRNP-Q1 *in vivo*.

Our results demonstrate that Gap-43 mRNA is a bona fide target that is post-transcriptionally repressed by hnRNP-Q1. This regulation affects the levels of GAP-43 protein in the nascent axons of primary cortical neurons and also alters the levels of S41 phosphorylated GAP-43 protein in N2a cells. These results strongly suggest that hnRNP-Q1 may affect axon morphology by regulating GAP-43 expression, which will be discussed in Chapter 3.

2.4: Materials and Methods

Plasmids and siRNA

Small interfering RNA (siRNA) targeting the 3'-UTR of mouse *Gap-43* mRNA, the coding region or 3'-UTR of *hnRNP-Q1* mRNA and Scrambled sequences were purchased from Eurofins (Huntsville, AL) and annealed according to the manufacture's directions. Sequences for each siRNA are as follows (including 3' UU overhangs), *hnRNP-Q1 #1* (sense: 5'-GCAGUUUCAGGUGUAAUCAUU-3', antisense: 5'-UGAUUACACCUGAAACUGCUU-3'), *hnRNP-Q1 #2* (sense: 5'-AGCUGGUUAGUCAGGCAUUUU-3', antisense: 5'-AAUGCCUGACUAACCAGCUUU-3'), *hnRNP-Q1 #3* (sense: 5'-GUGUAAGUUUGAGGGCUACUU-3', antisense: 5'-GUAGCCCUCAAACUUACACUU-3'), *hnRNP-Q1* Scrambled (sense: 5'-GGCUUGUAGAGCGUAGAGUUU-3', antisense: 5'- ACUCUACGCUCUACAAGCCUU-3'), *Gap-43* (sense: 5'-GCAGUCAUCUUGGGAAAUUUU-3', antisense: 5'-AAUUUCCCAAGAUGACUGCUU-3') and *Gap-43* Scrambled (sense: 5'-GUUAGUCCGAAUUAGUCGAUU-3', antisense: 5'-UCGACUAAUUCGGACUAACUU-3').

Short hairpin RNA (shRNA) constructs were also generated by inserting the hnRNP-Q1 #1 or Scrambled and GAP-43 or Scrambled siRNA sequences into the pLentilox3.7 vector under the neuronal-specific synapsin promoter using the XhoI and HpaI sites and the following annealed primers: *hnRNP-Q1 #1* (sense: 5'-TGCAGTTTCAGGTGTAATCATTC AAGAGATGATTACACCTGAAACTGCTTTTTT C-3', antisense: 5'-TCGAGAAAAAAG CAGTTTCAGGTGTAATCATCTCTTGAATGATTACACCTGAAACTGCA-3'), *hnRNP-Q1* Scrambled (sense: 5'-TGGCTTGTAGAGCGTAGAGTTTCAAGAGAACTCTACGCT CTACAAGCCTTTTTTC-3', antisense: 5'-TCGAGAAAAAAGGCTTGTAGAGCGTAGA GTTCTCTTGAAACTCTACGCTCTACAAGCCA-3'), *Gap-43* (sense: 5'-TGCAGTCATC

TTGGGAAATTTTCAAGAGAAATTTCCCAAGATGACTGCTTTTTTC-3', antisense: 5'-TCGAGAAAAAAGCAGTCATCTTGGGAAATTTCTCTTGAAAATTTCCCAAGATGACTGCA-3') and *Gap-43* Scrambled (sense: 5'-TGTTAGTCCGAATTAGTCGATTCAAGAGATCGACTAATTCGGACTAACTTTTTTC-3', antisense: 5'-TCGAGAAAAAAGTTAGTCCGAATTAGTCGATCTCTTGAATCGACTAATTCGGACTAACA-3').

The 3xFlag-mCherry-hu hnRNP-Q1 construct was described previously[218]. The 3x-Flag-mCherry, Lifeact-GFP and pLentilox3.7/Synapsin Promoter constructs were generous gifts from Dr. Wilfried Rossoll, Dr. Roland Wedlich-Soldner and Dr. Morgan Sheng, respectively.

Cell Culture and Transfection

Neuro2a cells (N2a, American Type Culture Collection, Manassas, VA) were grown in DMEM (Sigma- Aldrich, St. Louis, MO) with 10% fetal bovine serum (FBS, Sigma-Aldrich, St. Louis, MO), 10 mM HEPES (Fisher Scientific, Pittsburgh, PA), 100 U/ml penicillin, and 100 mg/ml streptomycin (Fisher Scientific) at 5% CO_2 and 37° C. N2a cells were transfected with Lipofectamine 2000 (Life Technologies, Carlsbad, CA) according to the manufacturer's protocol. 100 pmol siRNA was tranfected into cells plated in a 6-well dish and lysed 72 hours later for immunoblotting.

Cortical neurons were cultured as described in the Chapter 1 Materials and Methods section. The neurons were nucleofected with as described in the Chapter 1 Materials and Methods section except with 150pmol of each siRNA and 2.5 μg of Lifeact-GFP.

Antibodies, Immunoblotting and Immunofluorescence

The following antibodies were used for immunoblotting: hnRNP-Q/R (1:1,000, Sigma-Aldrich), GAP- 43 (1:5,000, Abcam, Cambridge, MA), γ-Actin (1:10,000, Santa Cruz, Dallas, TX), α-Tubulin (1:50,000, Sigma-Aldrich), Phospho-GAP-43 (1:100, R&D Systems, Minneapolis, MN), IRDdye 680LT Donkey Anti-Mouse (1:20,000, Li-Cor, Lincoln, NE), IRDye 800CW Donkey Anti-Rabbit (1:20,000, Li-Cor), TrueBlot Anti-Mouse HRP (1:3000, Rockland Immunochemicals Inc., Limerick, PA) and TrueBlot Anti-Rabbit HRP (1:3000, Rockland Immunochemicals Inc.). Immunoblotting was performed following a standard protocol. Lysates were collected in RIPA Buffer (150mM NaCl, 50mM Tris-HCl, pH 8.0, 1% NP-40, 0.5% Deoxycholate and 0.1% Sodium Dodecyl Sulfate) supplemented with 1x protease inhibitor (Roche, Indianapolis, IN), 1x RNase inhibitor (Ambion/Life Technologies) and 1x Phosphatase Inhibitor (Roche) for the phospho-GAP-43 experiments. Unless otherwise noted, Bradford assays were performed and equal amounts of protein were ran on SDS-PAGE gels. Nitrocellulose membranes were blocked with 5% fraction V bovine serum albumin (BSA, Roche) in 1x PBS and primary and secondary antibody incubations were performed in 5% BSA in 1x PBS with 0.1% Tween 20 at room temperature for 2 hours and 1 hour, respectively. Protein signal was detected with an Odyssey infrared imager and software (Li-Cor) or with SuperSignal West Pico Chemiluminescent Substrate (Thermo Fisher Scientific, Inc.) and film. Band intensity was quantified using ImageJ and protein levels were normalized to the loading control α-Tubulin.

The following antibodies were used for immunofluorescence: GAP-43 (1:5,000, EMD Millipore, Billerica, MA), β-III-Tubulin (1:1000, Sigma), hnRNP-Q1 (1:100, Anaspec), 488 Phalloidin (1:1,000, Life Technologies), Goat anti-Mouse Cy3 (1:500, Jackson Immuno Research Laboratories, Inc., West Grove, PA), Donkey anti-Rabbit Cy5 (1:500, Jackson

Immuno Research Laboratories, Inc.). Immunofluorescence was performed as described in the Chapter 1 Materials and Methods section.

Fluorescence *In Situ* Hybridization

Stellaris fluorescence *in situ* hybridization (FISH) probes were used to detect *Gap-43* mRNA and *mCherry* mRNA as a negative control (Biosearch Technologies, Petaluma, CA). FISH was performed using the manufacturer's protocol but with some alterations. Cortical neurons were fixed with 4% paraformaldehyde (Sigma-Aldrich) in 1x PBS for 10 minutes, washed with 1x PBS, incubated in 2x SSC and then equilibrated in warm 10% formamide in 2x SSC. The neurons were then blocked with hybridization buffer (10% dextran sulfate, 2× SSC, 4 mg/ml BSA, 20 mM ribonucleoside vanadyl complex, 10 mM sodium phosphate buffer, pH 7.0, 10% formamide, 10 μg *E. coli* tRNA and 10 μg salmon sperm DNA) for 1.5 hours at 37° C and then hybridized with 1:400 of each stellaris probe in hybridization buffer overnight at 37° C. The neurons were washed with warm 10% formamide in 2x SSC followed by extensive washing with 2x SSC. Coverslips were mounted with prolong gold anti-fade reagent with 4′,6-diamidino-2-phenylindole (DAPI, Life Technologies).

Fluorescence Microscopy

Cells were imaged as described in the Chapter 1 Materials and Methods section. GAP-43 and hnRNP-Q1 signal intensity in the cell body and longest neurite of cortical neurons were quantified by thresholding the volume of either cell area with the GFP signal and calculating the mean gray area. The mean gray areas of three in focus stacks were averaged. Immunofluorescence images were prepared by creating easy 3D images with

constant look-up table values across all conditions in Imaris (Bitplane).

qRT-PCR Experiments

RNA was extracted from hnRNP-Q1 #1 or Scrambled siRNA transfected lysates with TRIzol (Ambion/Life Technologies) and total mRNAs were reverse transcribed into cDNA with superscriptIII reverse transcriptase (Life Technologies) and oligo(dT) primers (Life Technologies) according to the manufacture's instructions. Real-time PCR was performed with a LightCycler real-time PCR system and LightCycler SYBR Green I reagent (Roche). Primer sequences are as follows, *Gap-43*: 5'-ACAAGATGGTGTCAAGCC-3' and 5'-CATCGGTAGTAGCAGAGC-3' and *γ-Actin*: 5'-CTGGTGGATCTCTGTGAGCAC-3' and 5'-AAACGTTCCCAACTCAAGGC-3'.

The Dentate Gyrus and the remaining region (Ammon's horn) of the hippocampus were dissected from P30 C57BL/6J mice following a standard protocol[278]. Total RNA from each region was extracted with Trizol (Ambion/Life Technologies) and reverse transcribed using random primers (Promega, Madison, WI) and the Quantitect Reverse Transcription Kit with DNAse treatment (Qiagen, Valencia, CA). Real-time PCR was performed using Quanta SYBR Green FastMix for iQ kit (Quanta Biosciences, Gaithersburg, MD) in a iQ5 Multicolor Real-time PCR detection System (Bio-Rad Laboratories, Inc., Hercules, CA). Primer sequences are as follows: *HuD*: 5'-GCAGAGAAAGCCATCAACACTTTA-3' and 5'- GCTTCTTCTGCCTCAATCCTCT-3', *Gap-43*: 5'-AGATGGCTCTGCTACTACCGA-3' and 5'- CCTTGGAGGACGGGGAGTT-3', *hnRNP-Q1*: 5'-GTAGAGCCGGTTATTCACAGAG-3' and 5'- TCATTGTAACAGGTCAGGACCG-3' and *β-Actin*: 5'-TGTTACCAACTGGGACGACA-3' and 5'-

GGGGTGTTGAAGGTCTCAAA-3'. Relative quantification of each mRNA was determined based on the standard curve generated using corresponding primers and all relative concentrations were normalized to β- *Actin* mRNA levels as an internal control.

2.5: Figures

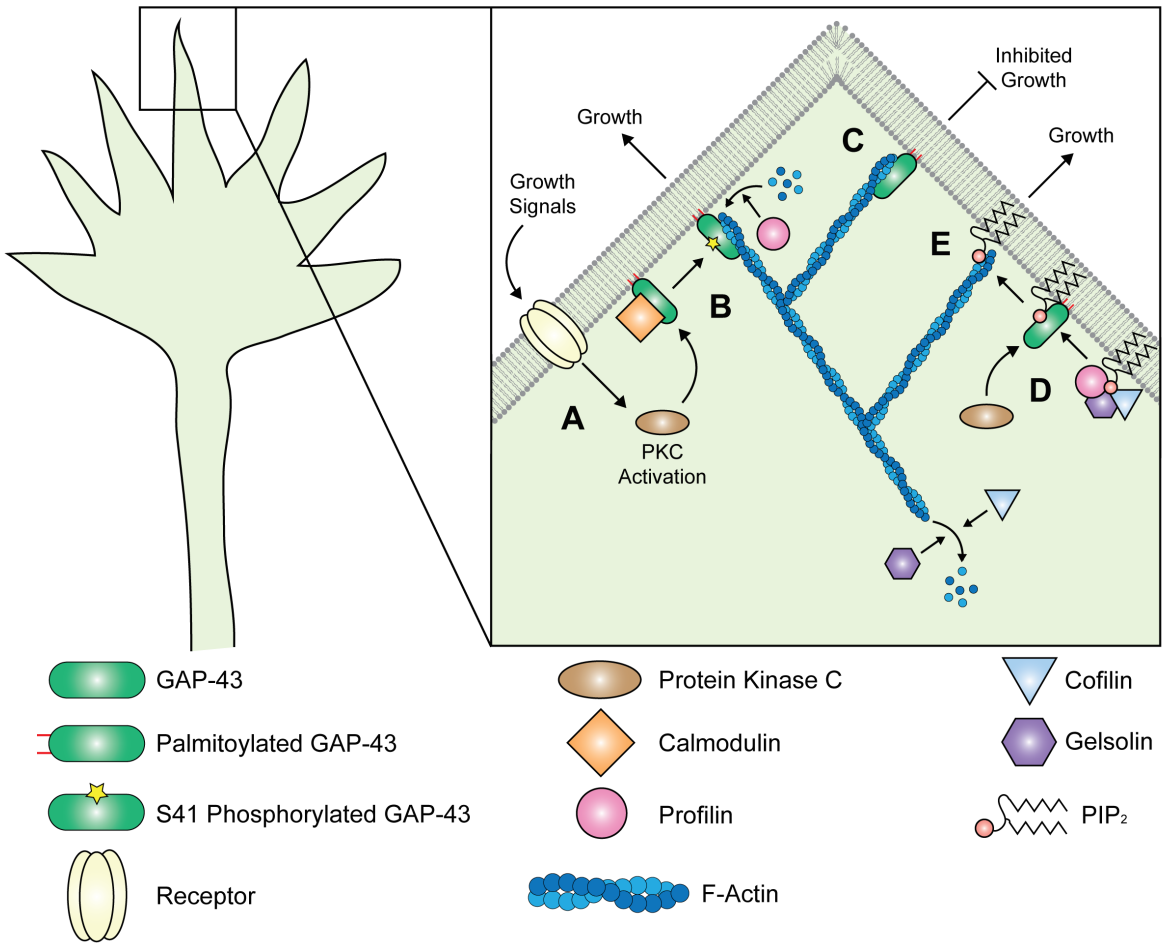

Figure 2-1: GAP-43 Affects Actin Dynamics by Multiple Mechanisms. An enlarged view of a filopodium from an axonal growth cone is shown. (A) Calmodulin binds GAP-43 in resting cells and prevents S41 phosphorylation. Growth signals lead to Protein Kinase C activation and phosphorylation of GAP-43 at S41. (B) Phosphorylated GAP-43 binds F-actin and functions as a lateral stabilizer of actin filaments leading to actin polymerization and filopodial growth. (C) Unphosphorylated GAP-43 functions as an actin filament capping protein leading to attenuated actin polymerization and inhibited filopodial growth. (D) Unphosphorylated GAP-43 also sequesters PIP_2 leading to increased actin dynamics due to the release of profilin, cofilin and gelsolin. (E) Phosphorylated GAP-43 can then stabilize

actin filaments while PIP_2 diffuses in the plasma membrane to promote the interaction between the actin network and the plasma membrane, which enhances filopodial growth.

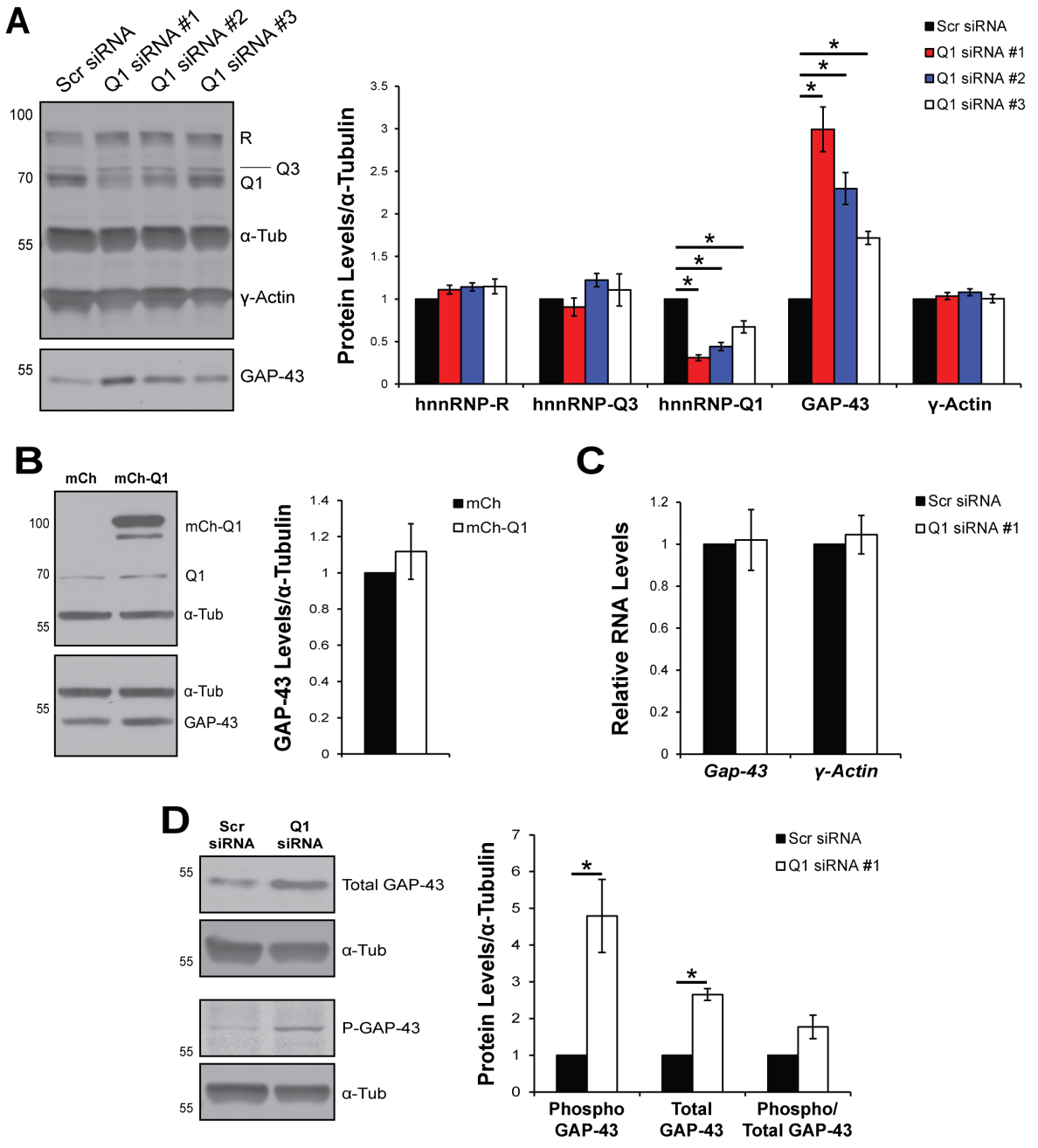

Figure 2-2: Increased GAP-43 Protein Expression Upon hnRNP-Q1 Knockdown in N2a Cells. (A) GAP-43 and γ-Actin protein levels were assessed by immunoblot with the Odyssey infrared imaging system in N2a cell lysates 72 hours after hnRNP-Q1 #1, hnRNP-Q1 #2, hnRNP-Q1 #3 or Scrambled siRNA transfection. n=6, one-way ANOVA, Dunnett's post-hoc, hnRNP-R p-values: Scr vs Q1 #1 p=0.3897, Scr vs Q1 #2 p=0.2057, Scr vs Q1 #3

p=0.1801, hnRNP-Q3 p-values: Scr vs Q1 #1 p=0.8869, Scr vs Q1 #2 p=0.4025, Scr vs Q1 #3 p=0.8486, hnRNP-Q1 p-values: Scr vs Q1 #1 p<0.0001, Scr vs Q1 #2 p<0.0001, Scr vs Q1 #3 p=0.0002, GAP-43 p-values: Scr vs Q1 #1 p<0.0001, Scr vs Q1 #2 p<0.0001, Scr vs Q1 #3 p=0.0163, γ-Actin p-values: Scr vs Q1 #1 p=0.8493, Scr vs Q1 #2 p=0.3335, Scr vs Q1 #3 p=0.9995. (B) GAP-43 protein levels were assessed by immunoblot by chemiluminescence in N2a cell lysates ~16 hours after 3xFlag-mCherry or 3xFlag-mCherry-hnRNP-Q1 transfection. n=7, one-sample t-test, p-value=0.4733. (C) *GAP-43* and *γ-Actin* mRNA levels were assessed by qRT-PCR with cDNA reverse transcribed from N2a cell lysates 72 hours after hnRNP-Q1 #1 or Scrambled siRNA transfection. n=6, one-sample t-test, p-values: *Gap-43* p=0.6415, *γ-Actin* p=0.8956. (D) Total GAP-43 and S41 phosphorylated GAP-43 protein levels were assessed by immunoblot with the Odyssey infrared imaging system in N2a cell lysates 72 hours after hnRNP-Q1 #1 or Scrambled siRNA transfection. n=6, one-sample t-test, p-values: P-GAP-43 p=0.0123, Total GAP-43 p=0.0001, P-GAP-43/Total GAP-43 p=0.0615.

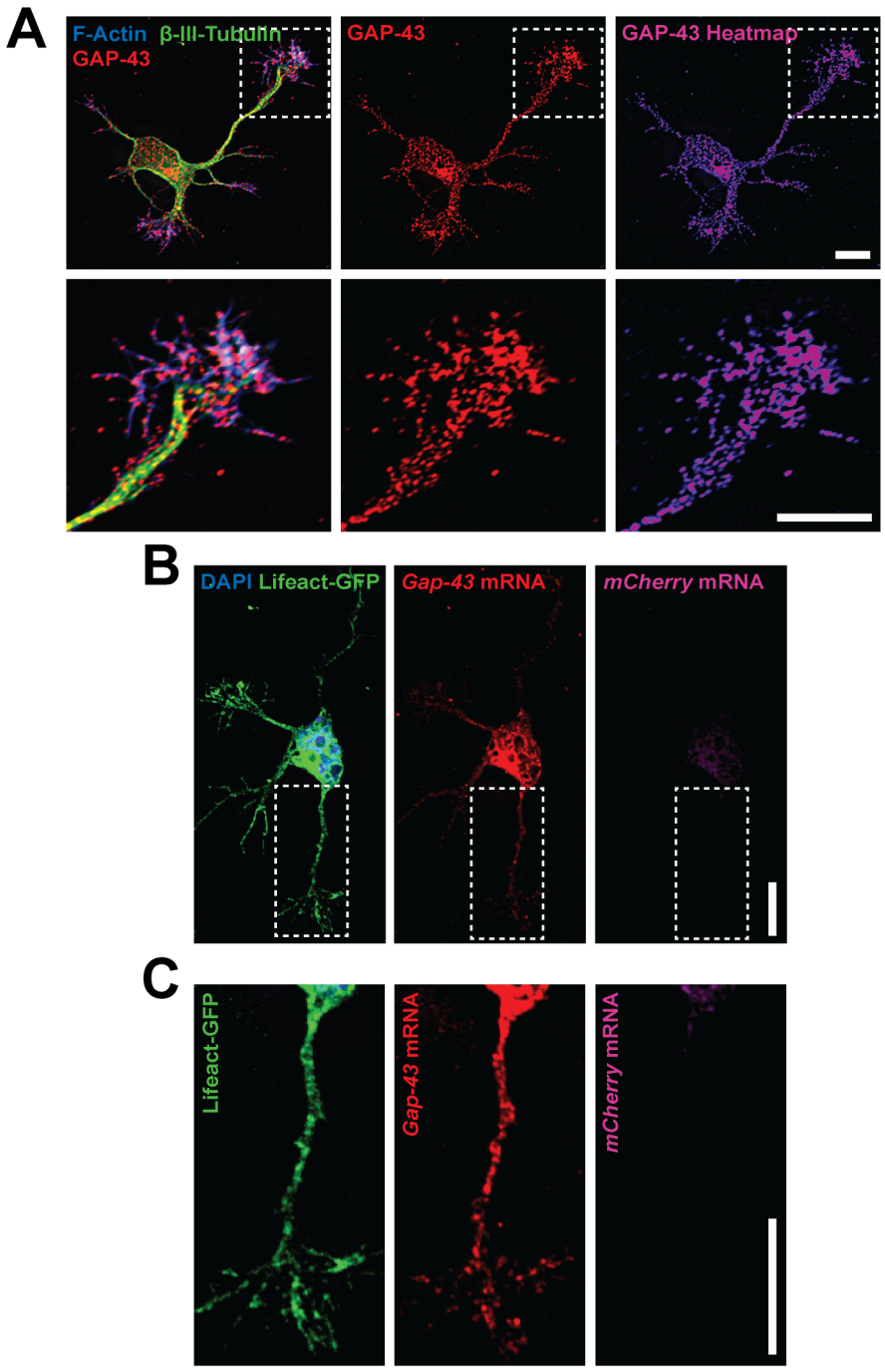

Figure 2-3: GAP-43 Protein and mRNA Localization in Incipient Cortical Neurons. (A) Primary cortical neurons were fixed after 28.5 hours in culture and processed for immunofluorescence with β-III-Tubulin and GAP-43 antibodies. F-actin was detected with fluorescent conjugated phalloidin. (B) Primary cortical neurons were transfected with

Lifeact-GFP by nucleofection and cultured for 28.5 hours. *Gap-43* and *mCherry* mRNAs were detected by fluorescence *in situ* hybridization and GFP positive cells were imaged. (C) Enlarged view of a neurite and growth cone (white box in (B)). Scale bars = 10 μm.

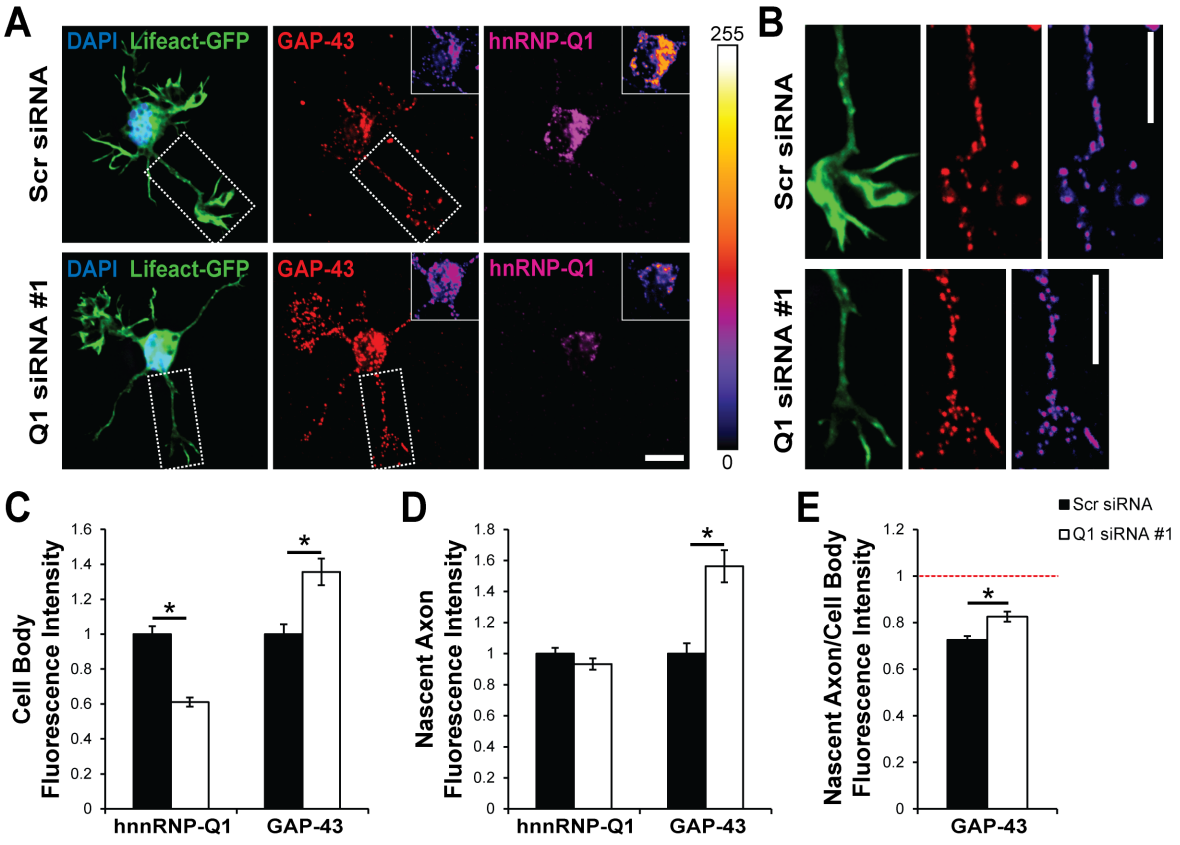

Figure 2-4: Increased GAP-43 Protein Expression Upon hnRNP-Q1 Knockdown in Incipient Cortical Neurons. Primary cortical neurons were transfected with hnRNP-Q1 #1 or Scrambled siRNA + Lifeact-GFP by nucleofection and cultured for 28.5 hours. GAP-43 and hnRNP-Q1 were detected by immunofluorescence and GFP positive cells were imaged. Primary cortical neurons were transfected with hnRNP-Q1 #1 or Scrambled siRNA + Lifeact-GFP by nucleofection and cultured for 28.5 hours. GAP-43 and hnRNP-Q1 were detected by immunofluorescence and GFP positive cells were imaged. (A) Representative images with inset heatmaps and (B) enlarged views of the nascent axon with a GAP-43 heatmap (white box in (A)). Scale bars = 10 μm. Quantification of GAP-43 and hnRNP-Q1 signal intensity in (C) cell bodies and (D) the nascent axon. n=6, Scr: 198 neurons and Q1: 178 neurons from 6 independent experiments, one-sample t-test, cell body p-values: hnRNP-

Q1 p<0.0001, GAP-43 p=0.0002, nascent axon p-values: hnRNP-Q1 p=0.2044, GAP-43 p<0.0001. (E) Ratio of nascent axon/cell body GAP-43 protein levels. n=6, Scr: 198 neurons and Q1: 178 neurons from 6 independent experiments, one-sample t-test, p-value=0.0002.

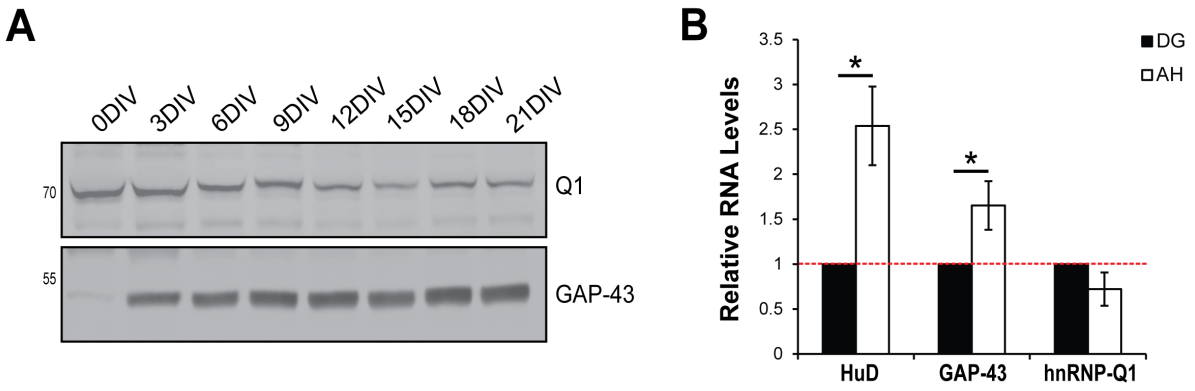

Figure 2-5: Inverse Correlation between hnRNP-Q1 and GAP-43 Expression. (A) Time course of high-density cultured primary cortical neurons immunoblotted for hnRNP- Q1 and GAP-43. (DIV = days *in vitro*) (B) The levels of *HuD*, *Gap-43* and *hnRNP-Q1* mRNAs in Ammon's Horn (AH) and the Dentate Gyrus (DG) were quantified by qRT-PCR. The relative level of each mRNA in Ammon's Horn is shown relative to the Dentate Gyrus. n=4, t-test, p-values: *HuD* p=0.0261, *GAP-43* p=0.0330, *Q1* p=0.1006.

2.6: Supplemental Figures

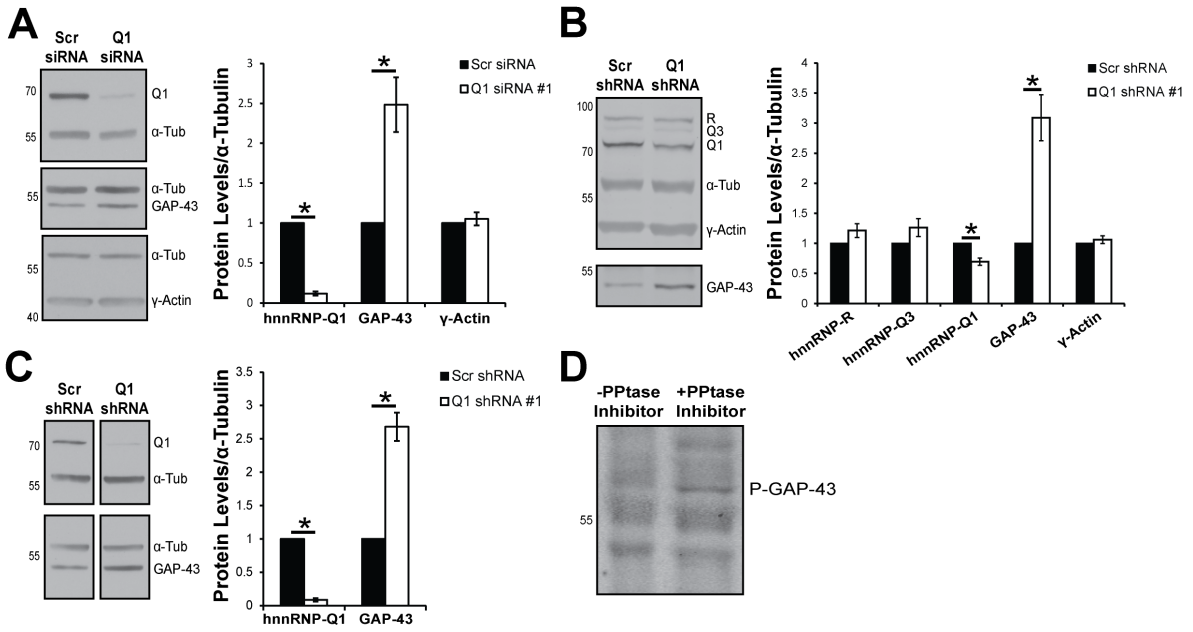

Supplemental Figure 2-1: hnRNP-Q1 Knockdown Efficiency and Phospho-GAP-43 Antibody Specificity. GAP-43 and γ-Actin protein levels were assessed by immunoblot in N2a cell lysates 72 hours after hnRNP-Q1 #1 or Scrambled (A) siRNA or (B, C) shRNA transfection. Protein signal was detected with the (B) Odyssey infrared imaging system or with (A, C) SuperSignal West Pico Chemiluminescent Substrate and film. (A) n=8, one-sample t-test, p-values: hnRNP-Q1 $p<0.0001$, GAP-43 $p=0.0035$, γ-Actin $p=0.5436$. (B) n=6, one-sample t-test, p-values: hnRNP-R $p=0.1183$, hnRNP-Q3 $p=0.1391$, hnRNP-Q1 $p=0.0036$, GAP-43 $p=0.0027$, γ-Actin $p=0.3800$. (C) n=6, one-sample t-test, p-values: hnRNP-Q1 $p<0.0001$, GAP-43 $p=0.0005$. (D) S41 phosphorylated GAP-43 protein signal was assessed by immunoblot with the Odyssey infrared imaging system in N2a cell lysates supplemented or not supplemented with phosphatase inhibitor. The phospho-GAP-43 band is shifted to a higher molecular weight (~60 kDa) as compared to the unphosphorylated GAP-43 (~50 kDa).

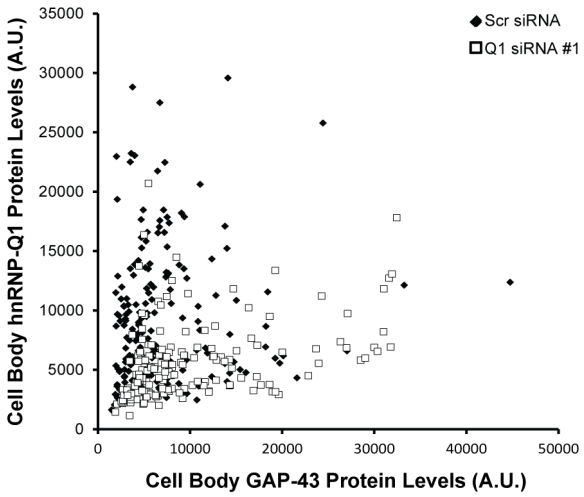

Supplemental Figure 2-2: Single Cell Analysis of hnRNP-Q1 Knockdown in Incipient Cortical Neurons. Plot of cell body hnRNP-Q1 protein levels against cell body GAP-43 protein levels for each cell from Figure 2-4.

Chapter 3

hnRNP-Q1 Regulation of GAP-43 Expression Affects Neuron Morphology

Portions of this chapter were adapted from the following manuscript:

Williams, K.R., Stefanovic, S., McAninch, D.S., Xing, L., Allen, M., Li, W., Feng, Y., Mihailescu, M.R., Bassell, G.J. (2015) hnRNP-Q1 Represses Nascent Axon Growth in Cortical Neurons by Inhibiting *Gap-43* mRNA Translation. *Mol Biol Cell*. Revision Under Review.

3.1: Introduction

GAP-43 regulates axonal growth and growth cone guidance by modulating actin cytoskeleton dynamics[249]. Therefore, we hypothesized that the observed hnRNP-Q1-mediated regulation of GAP-43 expression may affect GAP-43 function and lead to altered axon morphology. This hypothesis suggests that hnRNP-Q1 may contribute to the precise regulation of GAP-43 expression as a means to control GAP-43 function.

3.1.1: Cellular Functions of GAP-43

GAP-43 overexpression is generally associated with increased growth in neurons *in vitro* and *in vivo*. Dorsal root ganglia neurons (DRGs) overexpressing GAP-43 have increased axonal length but not branching[250, 271], GAP-43 transgenic mice that constitutively express GAP-43 demonstrate increased motor nerve and hippocampal mossy fiber sprouting[281] and *D. rerio* overexpressing GAP-43 demonstrate increased complexity of their retinal arbors due to increased length and branching[282]. Interestingly, *M. musculus* and *D. rerio* overexpressing non-phosphorylatable (S41A) GAP-43 do not demonstrate increased growth suggesting a requirement of S41 phosphorylation to promote growth[281, 282]. However, studies with the *H. sapiens* neuroblastoma cell line SH-SY5Y suggest that unphosphorylated GAP-43 also contributes to growth promotion. Differentiated SH-SY5Y cells have longer neurites when wildtype or non-phosphorylatable (S41A) GAP-43 is overexpressed and excess filopodia formation with pseudo-phosphorylated (S41D) GAP-43 overexpressed[283]. These findings suggest that unphosphorylated GAP-43 promotes neurite growth and phosphorylated GAP-43 promotes filopodia formation. Conversely, GAP-43 depletion is generally associated with reduced growth *in vivo*. Reduced axonal growth in GAP-43

knockout mice is demonstrated by a nearly complete loss of serotonergic innervation of the cortex and hippocampus[284]. Additionally, GAP-43 has been demonstrated to play an important role in axonal growth cone pathfinding. GAP-43 heterozygous mice have multiple thalamocortical axon pathfinding defects that lead to an enlarged whisker barrel cortex[285], the retinal axons of GAP-43 knockout mice are delayed in crossing the optic chiasm and are tangled due to aberrant turning[286] and GAP-43 knockout mice also fail to form the anterior commissure, hippocampal commissure and corpus callosum[287]. Interestingly, GAP-43 knockout neurons are able to form growth cones but they are abnormal and have smaller lamellas and reduced levels of F-actin *in vitro*[287, 288].

The growth promoting function of GAP-43 has also been well-established and taken advantage of as a therapeutic strategy in the field of neuronal regeneration. GAP-43 protein and mRNA levels are upregulated in response to axotomy or nerve crush in several neuronal cell types[255, 256, 289-293]. Additionally, the levels of GAP-43 protein correlate with regenerative capability. Increased GAP-43 expression enhances sprouting and regeneration of PC12 cells after axotomy[260] and only DRGs with elevated GAP-43 expression are capable of rapidly regenerating through nerve crush lesion[294]. Conversely, knocking down GAP-43 in cerebellar climbing fibers *in vivo* reduced the ability of these neurons to regenerate following injury[258, 295]. Interestingly, GAP-43 expression can also endow regeneration-incompetent neurons, like Purkinje cells, with the ability to regenerate. Purkinje cells overexpressing GAP-43 and the cell adhesion molecule L1 demonstrate increased sprouting and regeneration and are able to grow into non-permissive environments[261, 296]. These results suggest that GAP-43 is a master regulator of axonal growth that is required for neuronal development and regeneration.

3.1.2: Cellular Functions of hnRNP-Q1

hnRNP-Q1 was first demonstrated to affect cell morphology by repressing *RhoA* mRNA translation[218]. hnRNP-Q1 knockdown reduces dendritic arbor complexity and spine density of 12 *day in vitro* (DIV) primary hippocampal neurons by increasing RhoA expression and signaling[218]. hnRNP-Q1 knockdown also increased cell spreading and the number of focal adhesions in C2C12 mouse myoblast cells[218]. Additionally, several members of the Rho-GTPase signaling pathway were identified as hnRNP-Q1 target mRNAs by microarray analysis including Cdc42, N-Wasp, six Arp2/3 complex components, PAK, Ena/VASP, profilin and cofilin[215]. These findings suggest that hnRNP-Q1 affects cell morphology through the post-transcriptional regulation of actin binding protein expression. In support of this, hnRNP-Q knockdown (siRNA targeting all hnRNP-Q isoforms) increased both axon and dendrite branching and length in 3DIV and 7DIV primary cortical neurons[215]. Furthermore, hnRNP-Q1 knockdown increased neurite length, neruite branching and filopodia formation in differentiated N2a cells by altering the mRNA localization of Cdc42/N-Wasp signaling pathway components[215]. These findings indicate that hnRNP-Q1 may affect neuronal morphology differently depending on the stage of neuronal development; hnRNP-Q1 potentially attenuates growth in incipient neurons and enhances growth in mature neurons.

3.1.3: Chapter 3 Hypothesis and Objectives

Given that GAP-43 is a potent regulator of axonal growth, we assessed whether the hnRNP-Q1-mediated regulation of GAP-43 expression affects neuronal morphology. We hypothesized that hnRNP-Q1 modulates the nascent axon length of incipient cortical neurons

and N2a cell process extension by regulating GAP-43 expression. Our results reveal that hnRNP-Q1 knockdown increased the nascent axon length and also the total neurite length and neurite number of incipient cortical neurons and increase N2a cell process extension by increasing GAP-43 expression. Additionally, the number of focal adhesions is reduced upon hnRNP-Q1 knockdown suggesting that these cells may be more dynamic and/or motile. These results demonstrate that hnRNP-Q1 affects neuronal morphology by regulating GAP-43 expression, which may be a critical for neuronal development.

3.2: Results

3.2.1: Elevated GAP-43 Expression in hnRNP-Q1 Deficient Cortical Neurons Increased Neurite Length and Number

The role of GAP-43 in promoting axon growth has been extensively studied[250, 271, 282, 288]. Therefore, we determined if elevated GAP-43 protein levels due to hnRNP-Q1 knockdown affect neurite length and number. In order to investigate whether hnRNP-Q1 knockdown phenotypes were due to increased GAP-43 protein levels, we performed rescue experiments by knocking down GAP-43. GAP-43 knockdown efficiency was tested by transfecting N2a cells with GAP-43 or Scrambled siRNA or shRNA and performing an immunoblot analysis of cell lysates after 72 hours. GAP-43 protein levels were efficiently knocked down (siRNA: 94% reduction, shRNA: 91% reduction, Supplemental Figure 3-1 A, B). To determine if hnRNP-Q1 knockdown affected primary cortical neuron morphology, neurons were electroporated with hnRNP-Q1 #1 or Scrambled siRNA and Lifeact-GFP but also with GAP-43 or Scrambled siRNA to specifically link any phenotypes to increased GAP-43 protein levels. The neurons were fixed after 28.5 hours in culture, processed for immunofluorescence

with GAP-43 and hnRNP-Q1 antibodies and transfected cells were selected by GFP signal (Figure 3-1 A).

We performed a single cell analysis, which consisted of quantifying cell body hnRNP-Q1 and GAP-43 protein levels and measuring nascent axon length, total neurite length and neurite number. Plotting hnRNP-Q1 protein levels against GAP-43 protein levels for each cell revealed three major expression patterns (Figure 3-1 B): (1) high hnRNP-Q1 and low GAP-43 protein levels, which was most prevalent in Control and GAP-43 knocked down cells (2) low hnRNP-Q1 and high GAP-43 protein levels, which was most prevalent in hnRNP-Q1 knocked down cells and (3) low hnRNP-Q1 and low GAP-43 protein levels, which was a common expression profile in all experimental conditions. The threshold between low and high protein levels for both hnRNP-Q1 and GAP-43 was set at 12,500 A.U. based the expression plot (Figure 3-1 B). Analysis of the percent of cells showing each of the three expression patterns illustrates an inverse relationship between hnRNP-Q1 and GAP-43 expression (Figure 3-1 C). In control cells, the majority (51.4%) of neurons had low hnRNP-Q1 and low GAP-43 protein levels, presumably due to multiple factors regulating each protein (Figure 3-1 C). For example, GAP-43 protein turnover may be dynamically regulated, which is supported by the finding that GAP-43 protein is degraded by the ubiquitin-proteasome system[297]. Therefore, steady state GAP-43 protein levels may not increase in some cells upon hnRNP-Q1 knockdown due to high levels of GAP-43 protein turnover, despite the increased *Gap-43* mRNA translation rate. Additionally, cells may be lacking sufficient levels of other factors that are required to result in increased GAP-43 protein levels (e.g. HuD to stabilize *Gap-43* mRNA). Nonetheless, a substantial percentage of cells (35.8%) showed high hnRNP-Q1 and low GAP-43 protein levels under control

conditions, consistent with the proposed role of hnRNP-Q1 as a negative regulator of GAP-43 expression (Figure 3-1 C). Depletion of hnRNP-Q1 revealed a marked decrease in cells showing high hnRNP-Q1 and low GAP-43 protein levels (from 35.8% to 4.1%), suggesting removal of GAP-43 repression by hnRNP-Q1 knockdown (Figure 3-1 C). Conversely, knockdown of hnRNP-Q1 resulted in a marked increase in cells with low hnRNP-Q1 and high GAP-43 protein levels (from 4.6% to 27.6%), further suggesting that the elevation in GAP-43 protein levels was directly attributed to loss of hnRNP-Q1 (Figure 3-1 C). The phenotype of high GAP-43 protein levels in hnRNP-Q1 depleted cells (27.6%) was abolished by simultaneous knockdown of GAP-43 (1.6%), demonstrating that GAP-43 can be efficiently depleted (Figure 3-1 C). Additionally, knockdown of GAP-43 by itself did not change the negative correlation between hnRNP-Q1 and GAP-43 protein levels, wherein a substantial percentage of cells (32.6%) still showed high hnRNP-Q1 and low GAP-43 protein levels (Figure 3-1 C). Furthermore, a very small percentage of cells had high hnRNP-Q1 and high GAP-43 protein levels (Control: 8.1%, GAP-43: 0.6%, hnRNP-Q1: 7.6% and hnRNP-Q1 & GAP-43: 3.3%).

To determine if elevated GAP-43 protein levels due to hnRNP-Q1 knockdown affect neurite length and number, we specifically analyzed the cells within the population that exhibited the characteristic expression pattern for each condition (highlighted in Figure 3-1 C and the average protein levels and the plot of hnRNP-Q1 vs. GAP-43 protein levels of the selected neurons are displayed in Supplemental Figure 3-2 A, B). Cultured neurons develop lamellipodia shortly after being plated (~6 hours), which transform into distinct processes after ~12 hours[298]. One of these minor processes is specified to become the axon and begins to grow at an accelerated rate as compared to the remaining processes after ~1-2 days in

culture[298]. Therefore, the longest neurite after 28.5 hours in culture will likely develop into the axon and was called the nascent axon in our studies. The total length and number of all neurites was also quantified. Cells with low levels of GAP-43 protein and high levels of hnRNP-Q1 protein were selected in the control conditions (Scr siRNA + Scr siRNA: 35.8% of cells and Scr siRNA + GAP-43 siRNA: 32.6% of cells), cells with low levels of hnRNP-Q1 protein and high levels of GAP-43 protein were selected in the Q1 siRNA + Scr siRNA condition (27.6% of cells, red outline in Figure 3-1 B) and cells with low levels of both proteins were selected in the Q1 siRNA + GAP-43 siRNA condition (78.8% of cells). Neurons with elevated GAP-43 protein levels following hnRNP-Q1 knockdown correlated with an increased length of the nascent axon by 1.44 fold (31.00 μm to 44.76 μm, Figure 3-1 A, D), total length of all the neurites by 1.66 fold (86.11 μm to 143.12 μm, Figure 3-1 B, E) and number of neurites per cell by 1.44 fold (4.84 to 6.96, Figure 3-1 C, F). Simultaneously knocking down GAP-43 rescued all three phenotypes back to control levels, which demonstrates that increased GAP-43 protein levels are responsible for the neuritic and axonal phenotypes in hnRNP-Q1 deficient neurons (Figure 3-1 A-F). Additionally, plotting nascent axon length, total neurite length or neurite number against GAP-43 protein levels for each selected cell supports a positive correlation between these values (Figure 3-2 G-I). The nascent axon length, total neurite length and neurite number of Q1 siRNA + Scr siRNA cells with low levels of hnRNP-Q1 protein and low levels of GAP-43 protein (60.6% of cells) were also quantified to confirm that GAP-43 is driving the increased neurite growth. The average nascent axon length (1.03 fold, p-value=0.9745), total neurite length (0.91 fold, p-value=0.8029) and neurite number (0.83 fold, p-value=0.3102) were not significantly altered as compared to control Scr siRNA + Scr siRNA cells (data not shown).

Additionally, live cell imaging of incipient cortical neurons 28.5 hours after being electoporated with hnRNP-Q1 or Scrambled siRNA and Lifeact-GFP illustrates the increased growth observed upon hnRNP-Q1 knockdown (Figure 3-3). Furthermore, similar results were obtained with non-rescue experiments (selected neurons from Figure 2-4). The single cell analysis is shown in Supplemental Figure 3-3 A-C and the nascent axon length, total neurite length and neurite number averages, frequency distributions and correlation plots are shown in Supplemental Figure 3-4 A-I. Also, the average protein levels and the plot of hnRNP-Q1 vs. GAP-43 protein levels of the selected neurons are shown in Supplemental Figure 3-5 A, B. Taken together, these results support our model that increased axon growth in hnRNP-Q1 depleted cells is attributed to elevated GAP-43 expression.

3.2.2: Increased Focal Adhesions in hnRNP-Q1 Deficient Cortical Neurons

hnRNP-Q1 knockdown was previously demonstrated to increase cell spreading and the number of focal adhesions in C2C12 mouse myoblast cells[218]. Therefore, focal adhesions were also assessed in incipient cortical neurons upon hnRNP-Q1 knockdown. Neurons were electroporated with hnRNP-Q1 #1 or Scrambled siRNA and Lifeact-GFP, fixed after 28.5 hours in culture and processed for immunofluorescence with Paxillin and hnRNP-Q1 antibodies (Figure 3-4 A). Individual focal adhesions could not be quantified due to strong Paxillin signal. Instead average Paxillin signal intensity was quantified as a readout of focal adhesion number. Interestingly, cell body hnRNP-Q1 and Paxillin protein levels are positively correlated suggesting that hnRNP-Q1 knockdown reduces the number of focal adhesions (Figure 3-4 B). These results suggest that hnRNP-Q1 depletion may cause incipient cortical neurons to be more dynamic and/or motile. This phenotype may or may not

be due to increased GAP-43 protein levels.

3.2.3: Elevated GAP-43 Expression in hnRNP-Q1 Deficient N2a Cells Increased Process Extension

We also determined if hnRNP-Q1 knockdown affects the morphology of N2a cells. N2a cells were transfected with hnRNP-Q1 #1 or Scrambled siRNA, GAP-43 or Scrambled siRNA and Lifeact-GFP and fixed after 72 hours. The cells were then processed for immunofluorescence with GAP-43 and hnRNP-Q1 antibodies and transfected cells were selected by GFP signal (Figure 3-5 A). Cells were categorized based on their degree of process extension (Supplemental Figure 3-6 A). hnRNP-Q1 knockdown significantly increased the proportion of cells with processes as compared to control cells (Cat. 2 = 21.7%, Cat. 3 = 12.3%, Cat. 4 = 4.5% and Cat. 2 = 12.7%, Cat. 3 = 2.6%, Cat. 4 = 0.3%, respectively, Figure 3-5 B). Simultaneously knocking down GAP-43 reduced the proportion of cells with processes (Cat. 2 = 21.1%, Cat. 3 = 6.9%, Cat. 4 = 0.8%, Figure 3-5 B) demonstrating that increased GAP-43 protein levels contribute to this phenotype. However, the Q1 siRNA + GAP-43 siRNA treated cells are significantly more differentiated than the Scr siRNA + Scr siRNA treated cells suggesting that additional hnRNP-Q1 mRNA targets are involved in process extension (Figure 3-5 B). Additionally, these results are similar to those obtained with non-rescue experiments with hnRNP-Q1 #1 or Scrambled shRNA (Cat. 2 = 27.71%, Cat. 3 = 35.67%, Cat. 4 = 18.79% and Cat 2. = 28.2%, Cat 3. = 15.7%, Cat. 4 = 3.2%, respectively, Supplemental Figure 3-6 B). However, the increased process extension phenotype observed upon hnRNP-Q1 knockdown is less dramatic with the rescue experiments because the media was changed frequently to remove any secreted growth

factors (Figure 3-5 B and Supplemental Figure 3-6 B). This decision was based on experiments with hnRNP-Q1 shRNA that revealed untransfected cells with increased GAP-43 protein levels and enhanced differentiation (Supplemental Figure 3-6 C). In support of these findings, overexpressing GAP-43 in N2a cells for 72 hours also induces process extension. GAP-43 overexpression increased the proportion of cells with processes as compared to the control cells (Cat. 2 = 41.6%, Cat. 3 = 16.5%, Cat. 4 = 3.9% and Cat 2. = 24.4%, Cat 3. = 11.9%, Cat. 4 = 3.7%, respectively, Supplemental Figure 3-6 D). Taken together, these results support our model that increased N2a cell process extension in hnRNP-Q1 depleted cells is at least partially attributed to elevated GAP-43 expression.

3.3: Discussion

Our results reveal a novel function for hnRNP-Q1 to control nascent axon and neurite growth in incipient neurons by repressing *Gap-43* expression. At 28.5 hours *in vitro* cortical neurons are beginning to polarize but do not demonstrate the stereotypical axonal Tau enrichment and dendritic MAP2 enrichment. These results suggest that hnRNP-Q1 plays an important role in regulating nascent axon outgrowth by modulating GAP-43 expression. Similar phenotypes have been reported upon hnRNP-Q knockdown in primary cortical neurons that have undergone Tau and MAP2 expression polarization (3DIV and 7DIV) due to reduced *Cdc42* and *N-Wasp* mRNA localization[215]. These findings suggest that hnRNP-Q1 attenuates neurite growth and branching at intermediate stages of neuronal development as well. Conversely, hnRNP-Q1 knockdown in 12DIV primary hippocampal neurons leads to reduced dendritic arbor complexity and spine density due to increased *RhoA* mRNA translation suggesting that hnRNP-Q1 enhances growth in mature hippocampal neurons[218].

Therefore, hnRNP-Q1 may regulate different mRNA targets during specific stages of development to affect neuronal morphology.

Our findings also demonstrate that hnRNP-Q1-mediated repression of GAP-43 expression inhibits N2a cell differentiation. Similar N2a cell phenotypes were observed due to reduced *Cdc42* and *N-Wasp* mRNA localization upon hnRNP-Q1 knockdown suggesting that multiple hnRNP-Q1 mRNA targets may contribute to the regulation of cell morphology[215]. In support of this, several actin binding proteins have been identified as hnRNP-Q1 mRNA targets[215]. Additionally, these targets may be components of the same pathway suggesting that hnRNP-Q1 can dramatically alter cell morphology by post-transcriptionally regulating the expression of an entire pathway. Cdc42 and RhoA are both members of the Rho-GTPase family[299]. GTPases cycle between an active GTP-bound state and an inactive GDP-bound state with the help of guanine nucleotide exchange factors and GTPase-activating proteins[299]. Interestingly, GAP-43 has been demonstrated to cooperate with both Cdc42 and RhoA to regulate cell morphology. Overexpressing GAP-43 in Rat-1 fibroblasts leads to the formation of long filopodia, increased F-actin immunoreactivity and reduced cell spreading[300]. Simultaneously expressing dominant negative RhoA blocks these phenotypes suggesting that GAP-43 modulates *R. norvegicus* fibroblast cell morphology by regulating RhoA activity[300]. Additionally, overexpressing the N-terminal 14 residues of GAP-43 induces filopodia formation in COS-7 cells and filopodia formation and neurite branching of 10DIV hippocampal neurons[301]. These phenotypes are blocked by the simultaneous expression of dominant negative Cdc42 suggesting that GAP-43 modulates *C. aethipos* fibroblast and hippocampal neuron morphology by regulating Cdc42 activity[301]. Both studies also demonstrated that N-terminal palmitoylation of GAP-43 is required to induce these

phenotypes demonstrating that GAP-43 also modulates actin cytoskeleton dynamics by activating small GTPases in a palmitoylation-dependent manner[300, 301]. Additionally, the spatial and temporal activation of Rho-GTPases is precisely controlled to dynamically regulate the actin cytoskeleton[299]. For example in migrating fibroblasts, RhoA is most active at the leading edge of the cell while Cdc42 and Rac1, an additional Rho-GTPase, are most active 2 μm behind the leading edge[302]. These findings suggest that hnRNP-Q1 may affect actin cytoskeleton dynamics through the coordinated post-transcriptional regulation of GAP-43, Cdc42 and RhoA expression.

The post-transcriptional regulation of GAP-43 expression by HuD has also been demonstrated to affect cell morphology. Knocking down HuD in PC12 cells reduced *Gap-43* mRNA stability, GAP-43 protein levels and PKC-induced neurite outgrowth by NGF treatment[303]. Conversely, overexpressing HuD in PC12 cells increased Gap-43 mRNA and protein levels and lead to spontaneous neurite outgrowth that was dependent on GAP-43 expression[303]. These findings suggest that HuD stabilization of *Gap-43* mRNA affects cell morphology and indicate that the post-transcriptional regulation of GAP-43 expression likely contributes to GAP-43 function. Our findings suggest that hnRNP-Q1 would antagonize HuD function to stabilize *Gap-43* mRNA and enhance GAP-43 function by repressing GAP-43 expression and function.

We revealed that hnRNP-Q1 regulates neuronal morphology by repressing GAP-43 expression. hnRNP-Q1 attenuates neurite growth and process extension of incipient cortical neurons and N2a cells, respectively. Additionally, hnRNP-Q1 has been suggested to enhance the number of focal adhesions potentially leading to reduced cell dynamics or motility. These results suggest that the post-transcriptional regulation of GAP-43 expression by hnRNP-Q1

affects GAP-43 function. The specific mechanism of hnRNP-Q1-mediated repression of GAP-43 expression will be discussed in the next chapter.

3.4: Materials and Methods

Plasmids

The 3xFlag-mCherry-rat GAP-43 construct was a generous gift from Dr. Jeff Twiss.

Cell Culture and Transfection

Cortical neurons were cultured as described in the Chapter 1 Materials and Methods section. The neurons were nucleofected as described in the Chapter 1 Materials and Methods except with 150pmol of each siRNA and 2.5 μg of Lifeact-GFP.

N2a cells were cultured and transfected as described in the Chapter 2 Materials and Methods section. N2a cells for immunofluoresnce experiments were plated on coverslips that were coated with 1mg/ml poly-L-lysine (Sigma Aldrich) in Borate Buffer (40 mM boric acid, 10 mM sodium tetraborate, pH 8.5) for 2 hours followed by vigorous washing with H^2O. The following conditions were used for transfection: 40 pmol of each siRNA and 500 ng Lifeact-GFP for process extension rescue experiments, 800 ng shRNA for process extension non-resuce experiments and 600 ng pcDNA3.1 and 5 ng 3xFlag-mCherry or 100 ng 3xFlag-mCherry-rt GAP-43 for GAP-43 overexpression experiments. Cells were fixed 72 hours after transfection and processed for immunofluorescence. The media was changed twice per day for rescue experiments to remove any secreted growth factors.

Antibodies and Immunofluorescence

The following antibodies were used for immunofluorescence: GAP-43 (1:5,000, EMD Millipore), hnRNP-Q1 (1:100, Anaspec), Paxillin (1:150, BD Biosciences, San Jose, CA), 488 Phalloidin (1:1000, Life Technologies), Rhodamine Phalloidin (1:1000, Life Technologies), Goat anti-Mouse Cy3 (1:500, Jackson Immuno Research Laboratories, Inc., West Grove, PA), Donkey anti-Rabbit Cy5 (1:500, Jackson Immuno Research Laboratories, Inc.). Immunofluorescence was performed as described in the Chapter 1 Materials and Methods section.

Fluorescence Microscopy

Fixed cells were imaged as described in the Chapter 1 Materials and Methods section. GAP-43 and hnRNP-Q1 signal intensity in the cell body and longest neurite of cortical neurons were quantified by thresholding the volume of either cell area with the GFP signal and calculating the mean gray area. The mean gray areas of three in focus stacks were averaged. Neurites were traced and neurite number and length was quantified using the NeuronJ plug-in for ImageJ. Neurites were defined as any protrusion longer than 6.4 μm and the longest neurite was called the nascent axon. Immunofluorescence images were prepared by creating easy 3D images with constant look-up table values across all conditions in Imaris (Bitplane).

Live cells were visualized with a 60x oil objective on a Nikon A1R laser scanning confocal microscope with an environment chamber for temperature and CO_2 control. Images were acquired with Nikon Elements software every minute for two hours. Cells were plated on poly-L-lysine (Sigma-Aldrich) coated 2-well Lab-Tek chambered coverglass (Thermo Fisher Scientific, Inc.) as described in the Chapter 1 Materials and Methods section.

3.5: Figures

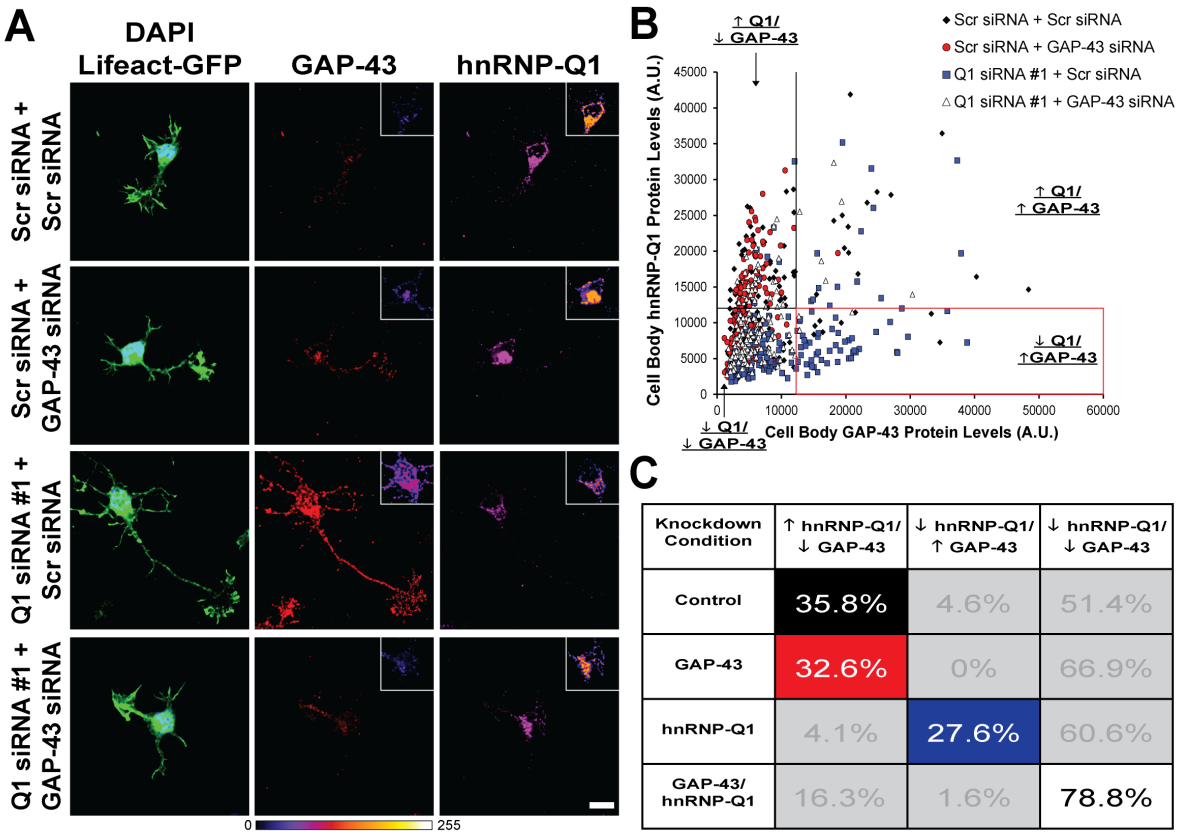

Knockdown Condition	↑ hnRNP-Q1/ ↓ GAP-43	↓ hnRNP-Q1/ ↑ GAP-43	↓ hnRNP-Q1/ ↓ GAP-43
Control	35.8%	4.6%	51.4%
GAP-43	32.6%	0%	66.9%
hnRNP-Q1	4.1%	27.6%	60.6%
GAP-43/ hnRNP-Q1	16.3%	1.6%	78.8%

Figure 3-1: Double Knockdown of hnRNP-Q1 and GAP-43 in Cortical Neurons.

Primary cortical neurons were transfected with hnRNP-Q1 #1 or Scrambled siRNA, GAP-43 or Scrambled siRNA and Lifeact-GFP by nucleofection and processed for immunofluorescence with GAP-43 and hnRNP-Q1 antibodies after 28.5 hours. (A) Representative images with inset heatmaps. Scale bar = 10 μm. (B) Plot of cell body hnRNP-Q1 protein levels against cell body GAP-43 protein levels for each neuron. The threshold between low and high levels of each protein was set at 12,500 A.U. as depicted by the black lines. The red outline indicates the cell population with low levels of hnRNP-Q1 and high levels of GAP-43 that were assessed for increased neurite length and number in Figure 3-2 (Q1 siRNA + Scr siRNA cells only). (C) Table showing the correlation between hnRNP-Q1

and GAP-43 protein levels. The percentage of total cells in each category is listed and the highlighted populations (corresponding to the bar graphs in Figure 3-2 A-C) were analyzed for neurite length and number.

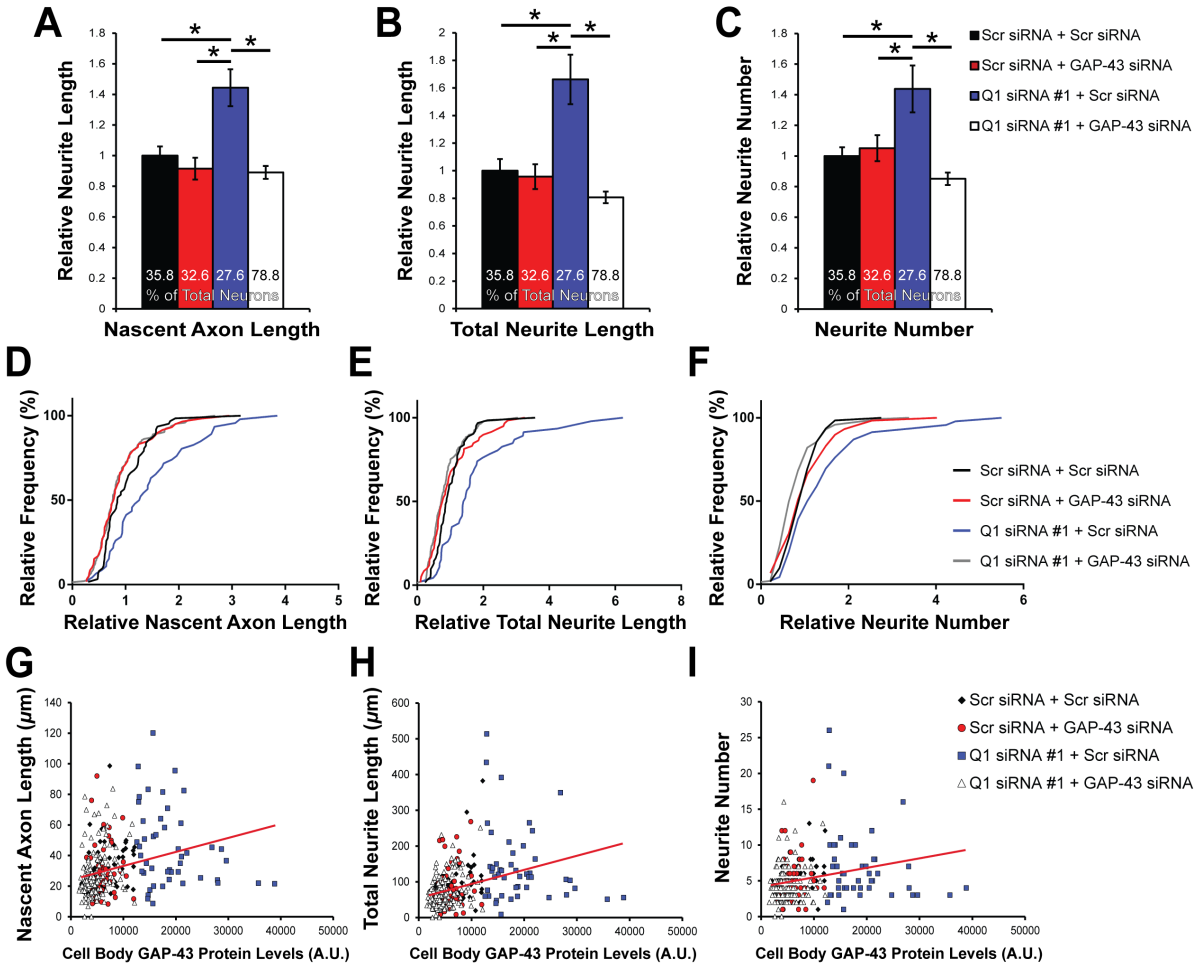

Figure 3-2: Increased Cortical Neuron Nascent Axon Length, Total Neurite Length and Neurite Number due to Increased GAP-43 Protein Expression upon hnRNP-Q1 Knockdown. Average (A) nascent axon length, (B) total neurite length and (C) neurite number of selected neurons from Figure 3-1 were quantified. n=7, Scr + Scr: 62 out of 173 cells, Scr + GAP-43: 59 out of 181 cells, Q1 + Scr: 47 out of 170 cells and Q1 + GAP-43: 145 out of 184 cells from 7 independent experiments, one-way ANOVA, Tukey's post-hoc, nascent axon length p-values: Scr + Scr vs. Scr + GAP-43 p=0.8423, Scr + Scr vs Q1 + Scr p=0.0004, Scr + Scr vs Q1 + GAP-43 p=0.5784, Scr + GAP-43 vs Q1 + Scr p<0.0001, Scr + GAP-43 vs Q1 + GAP-43 p=0.9921, Q1 + Scr vs Q1 + GAP-43 p<0.0001, total neurite length p-values: Scr + Scr vs. Scr + GAP-43 p=0.9884, Scr + Scr vs Q1 + Scr p<0.0001, Scr

+ Scr vs Q1 + GAP-43 p=0.2956, Scr + GAP-43 vs Q1 + Scr p<0.0001, Scr + GAP-43 vs Q1 + GAP-43 p=0.5334, Q1 + Scr vs Q1 + GAP-43 p<0.0001, neurite number p-values: Scr + Scr vs. Scr + GAP-43 p=0.9707, Scr + Scr vs Q1 + Scr p=0.0021, Scr + Scr vs Q1 + GAP-43 p=0.4028, Scr + GAP-43 vs Q1 + Scr p=0.0098, Scr + GAP-43 vs Q1 + GAP-43 p=0.1699, Q1 + Scr vs Q1 + GAP-43 p<0.0001. (D-F) Cumulative distribution plots for each measurement of selected neurons from Figure 3-1. (G-I) Plots demonstrating a positive correlation between nascent axon length, total neurite length and neurite number and GAP-43 protein levels of selected neurons from Figure 3-1. Red lines = trend lines.

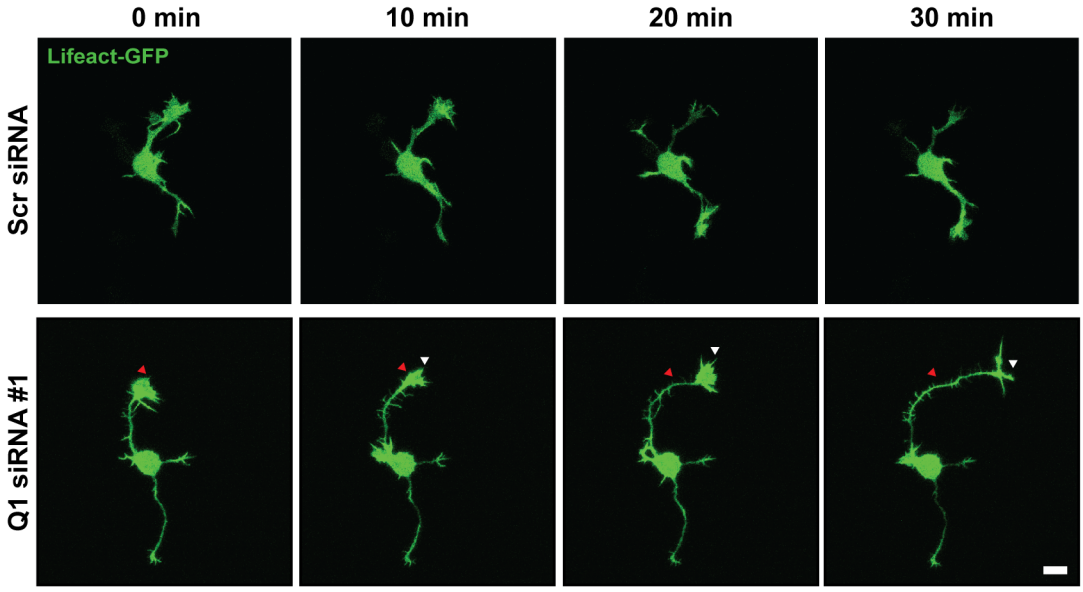

Figure 3-3: Live Cell Imaging of Increased Neurite Growth upon hnRNP-Q1 Knockdown. Primary cortical neurons were transfected with hnRNP-Q1 #1 or Scrambled siRNA and Lifeact-GFP by nucleofection and imaged on a Nikon A1R confocal microscope every minute for 2 hours. Images from every 10 minutes for the first 30 minutes are shown and arrow heads demonstrate the neurite growth. Scale bar = 10 μm.

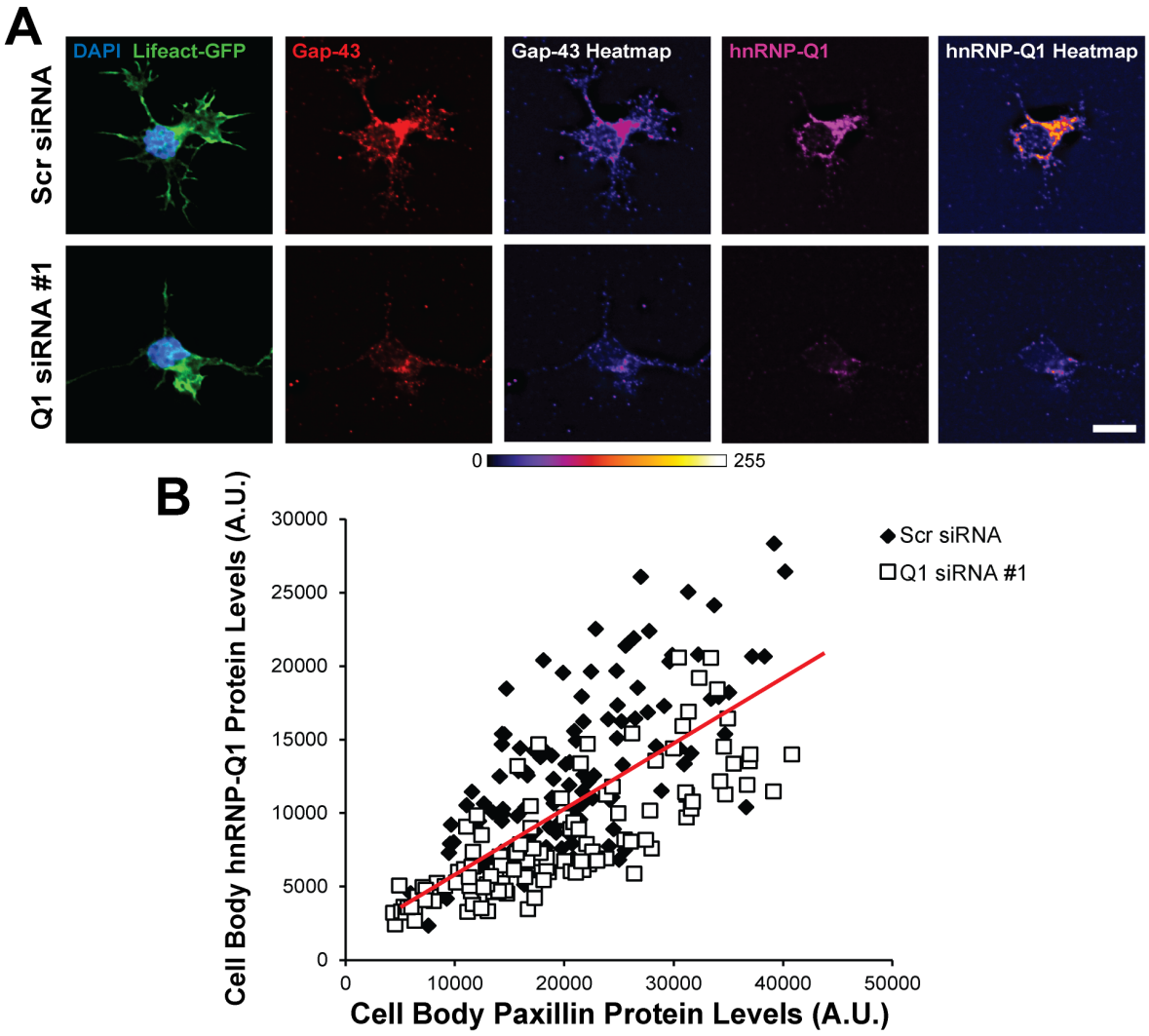

Figure 3-4: Increased Cortical Neuron Focal Adhesions upon hnRNP-Q1 Knockdown. Primary cortical neurons were transfected with hnRNP-Q1 #1 or Scrambled siRNA and Lifeact-GFP by nucleofection and processed for immunofluorescence with Paxillin and hnRNP-Q1 antibodies after 28.5 hours. (A) Representative images with corresponding heatmaps. Scale bar = 10 μm. (B) Plot of cell body hnRNP-Q1 protein levels against cell body Paxillin protein levels for each neuron. Red line = trend line.

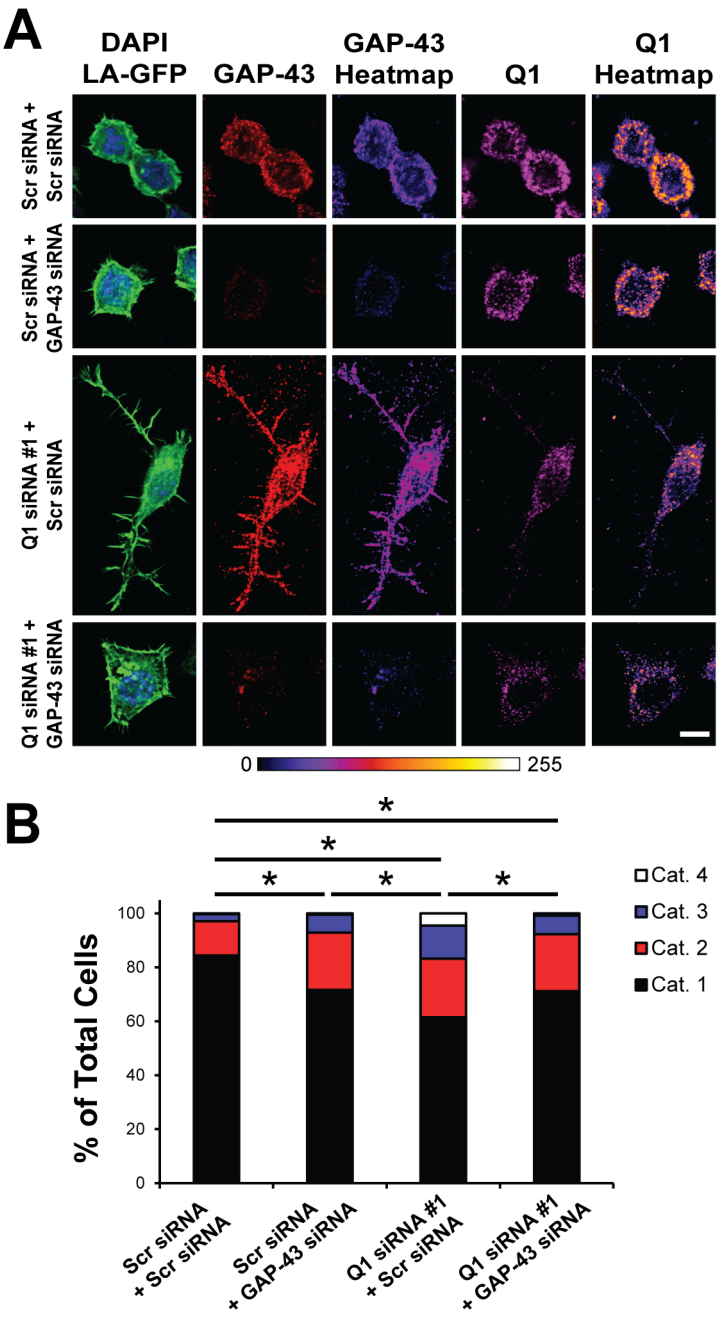

Figure 3-5: Increased N2a Cell Process Extension due to Increased GAP-43 Protein Expression upon hnRNP-Q1 Knockdown. N2a cells were transfected with hnRNP-Q1 #1 or Scrambled siRNA, GAP-43 or Scrambled siRNA and Lifeact-GFP and processed for immunofluorescence with GAP-43 and hnRNP-Q1 antibodies after 72 hours. Cells were then imaged and categorized based on their degree of process extension (see Supplemental Figure

3-6 A). (A) Representative images. Scale bar = 10 μm. (B) Quantification of the results. Percent of cells in each category: Scr + Scr: Cat. 1 = 84.4%, Cat 2. = 12.7%, Cat 3. = 2.6%, Cat. 4 = 0.3%, Scr + GAP-43: Cat. 1 = 71.6%, Cat 2. = 21.3%, Cat 3. = 6.7%, Cat. 4 = 0.4%, Q1 + Scr: Cat. 1 = 61.5%, Cat 2. = 21.7%, Cat 3. = 12.3%, Cat. 4 = 4.5%, Q1 + GAP-43: Cat. 1 = 71.2%, Cat 2. = 21.1%, Cat 3. = 6.9%, Cat. 4 = 0.8%. n=4, Scr + Scr: 379 cells, Scr + GAP-43: 239 cells, Q1 + Scr: 286 cells and Q1 + GAP-43: 261 cells from 4 independent experiments, Kruskal-Wallis test, Dunn's post-hoc, p-values: Scr + Scr vs. Scr + GAP-43 $p=0.0029$, Scr + Scr vs Q1 + Scr $p<0.0001$, Scr + Scr vs Q1 + GAP-43 $p=0.0013$, Scr + GAP-43 vs Q1 + Scr $p=0.0137$, Scr + GAP-43 vs Q1 + GAP-43 $p>0.9999$, Q1 + Scr vs Q1 + GAP-43 $p=0.0156$.

3.6: Supplemental Figures

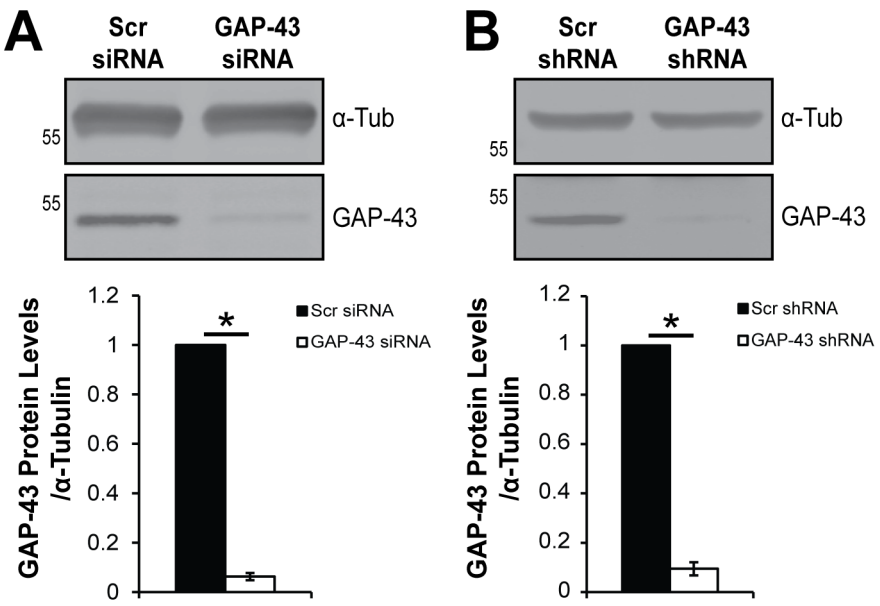

Supplemental Figure 3-1: GAP-43 Knockdown Efficiency. GAP-43 protein levels were assessed by immunoblot with the Odyssey infrared imaging system in N2a cell lysates 72 hours after GAP-43 or Scrambled (A) siRNA or (B) shRNA transfection. (A) n=7, one-sample t-test, p-value<0.0001. (B) n=6, one-sample t-test, p-value<0.0001.

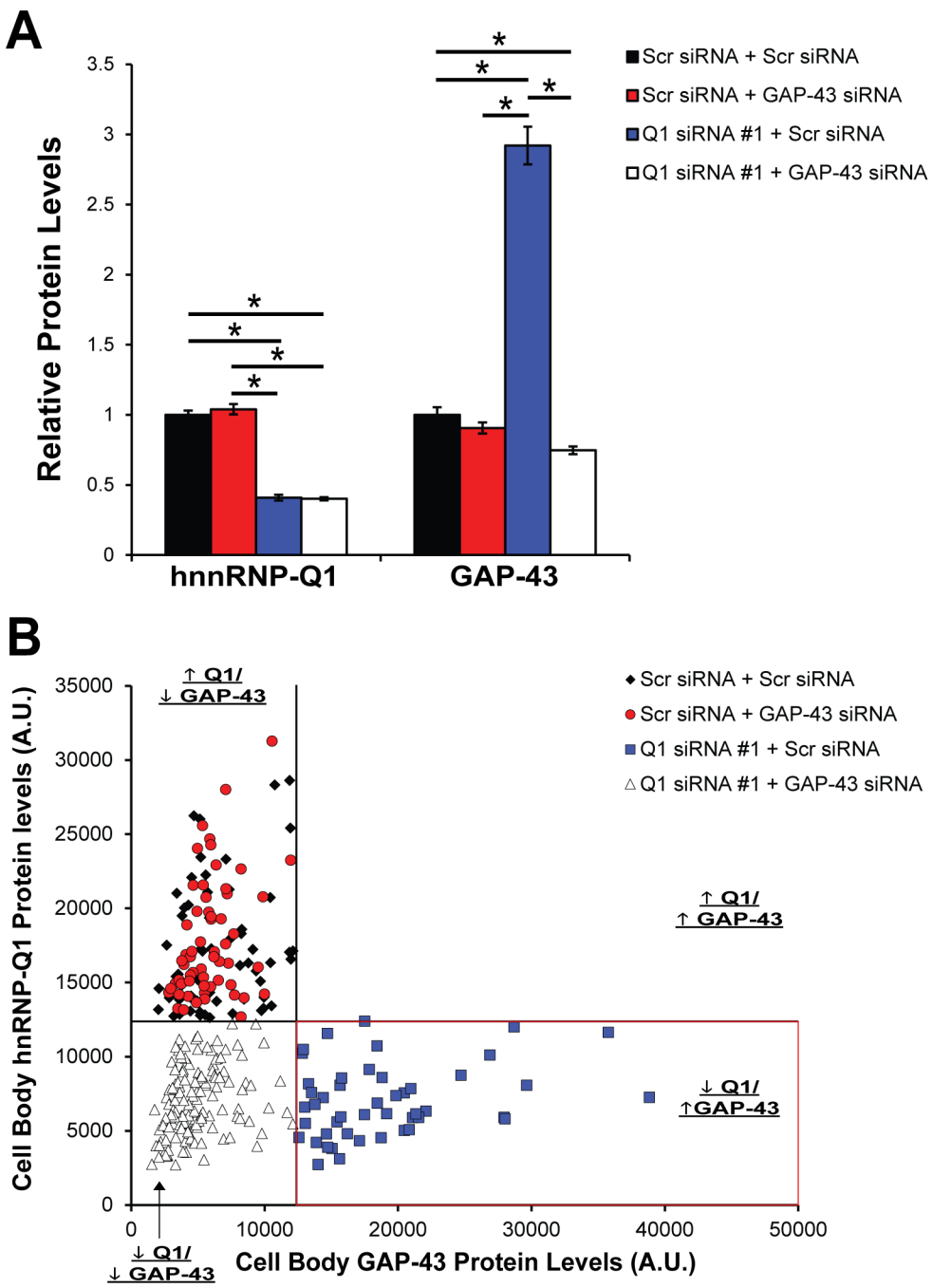

Supplemental Figure 3-2: Characterization of Selected Neuron GAP-43 and hnRNP-Q1 Expression from Rescue Experiments. (A) Average cell body hnRNP-Q1 and GAP-43 signal intensity of the selected neurons from Figures 3-1 and 3-2. n=7, Scr + Scr: 62 out of 173 cells, Scr + GAP-43: 59 out of 181 cells, Q1 + Scr: 47 out of 170 cells and Q1 + GAP-

43: 145 out of 184 cells from 7 independent experiments, one-way ANOVA, Tukey's post-hoc, hnRNP-Q1 p-values: Scr + Scr vs. Scr + GAP-43 p=0.6221, Scr + Scr vs Q1 + Scr p<0.0001, Scr + Scr vs Q1 + GAP-43 p<0.0001, Scr + GAP-43 vs Q1 + Scr p<0.0001, Scr + GAP-43 vs Q1 + GAP-43 p<0.0001, Q1 + Scr vs Q1 + GAP-43 p=0.9958, GAP-43 p-values: Scr + Scr vs. Scr + GAP-43 p=0.716, Scr + Scr vs Q1 + Scr p<0.0001, Scr + Scr vs Q1 + GAP-43 p=0.0037, Scr + GAP-43 vs Q1 + Scr p<0.0001, Scr + GAP-43 vs Q1 + GAP-43 p=0.1436, Q1 + Scr vs Q1 + GAP-43 p<0.0001. (B) Plot of cell body hnRNP-Q1 protein levels against cell body GAP-43 protein levels for each selected neuron from Figures 3-1 and 3-2. The threshold between low and high levels of each protein was set at 12,500 A.U. as depicted by the black lines. Red outline indicates the cell population with low levels of hnRNP-Q1 and high levels of GAP-43 that were assessed for increased neurite length and number in Figure 3-2.

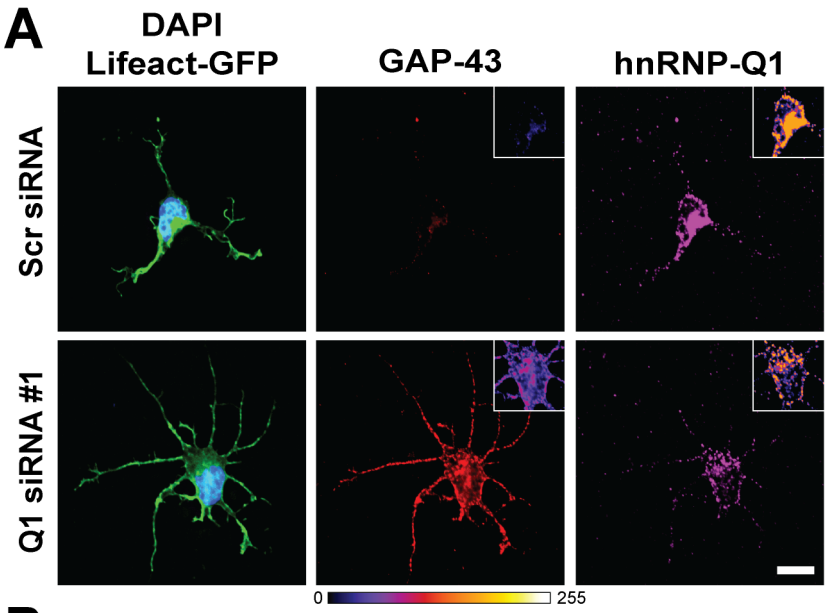

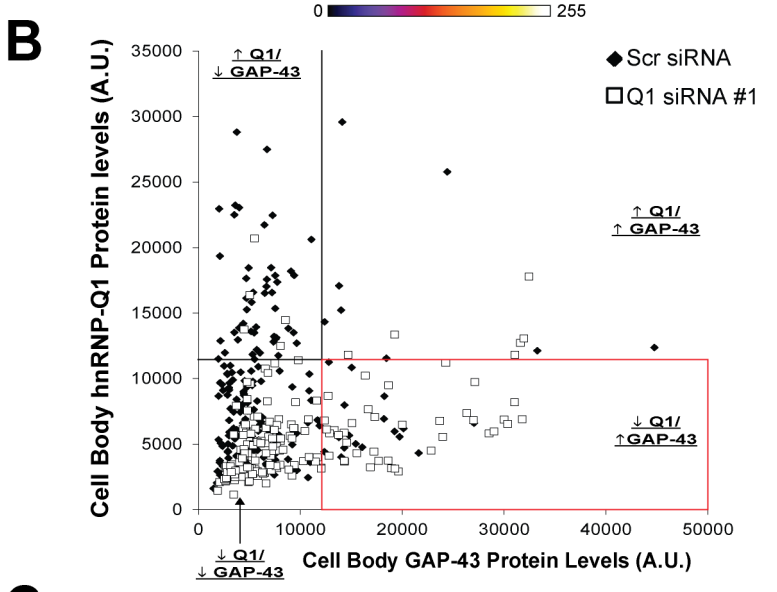

C

Knockdown Condition	↑ hnRNP-Q1/ ↓ GAP-43	↓ hnRNP-Q1/ ↑ GAP-43	↓ hnRNP-Q1/ ↓ GAP-43
Control	21.2%	10.1%	66.7%
hnRNP-Q1	5.0%	17.3%	75.4%

Supplemental Figure 3-3: Knockdown of hnRNP-Q1 in Cortical Neurons. Primary cortical neurons were transfected with hnRNP-Q1 #1 or Scrambled siRNA and Lifeact-GFP

by nucleofection and processed for immunofluorescence with GAP-43 and hnRNP-Q1 antibodies after 28.5 hours. (A) Representative images with inset heatmaps. Scale bar = 10 μm. (B) Plot of cell body hnRNP-Q1 protein levels against cell body GAP-43 protein levels for each neuron. The threshold between low and high levels of each protein was set at 12,500 A.U. as depicted by the black lines. Red outline indicates the cell population with low levels of hnRNP-Q1 and high levels of GAP-43 that were assessed for increased neurite length and number in Supplemental Figure 3-4 (Q1 siRNA + Scr siRNA cells only). (C) Table showing the correlation between hnRNP-Q1 and GAP-43 protein levels. The percentage of total cells in each category is listed and the highlighted populations (corresponding to the bar graphs in Supplemental Figure 3-4 A-C) were analyzed for neurite length and number.

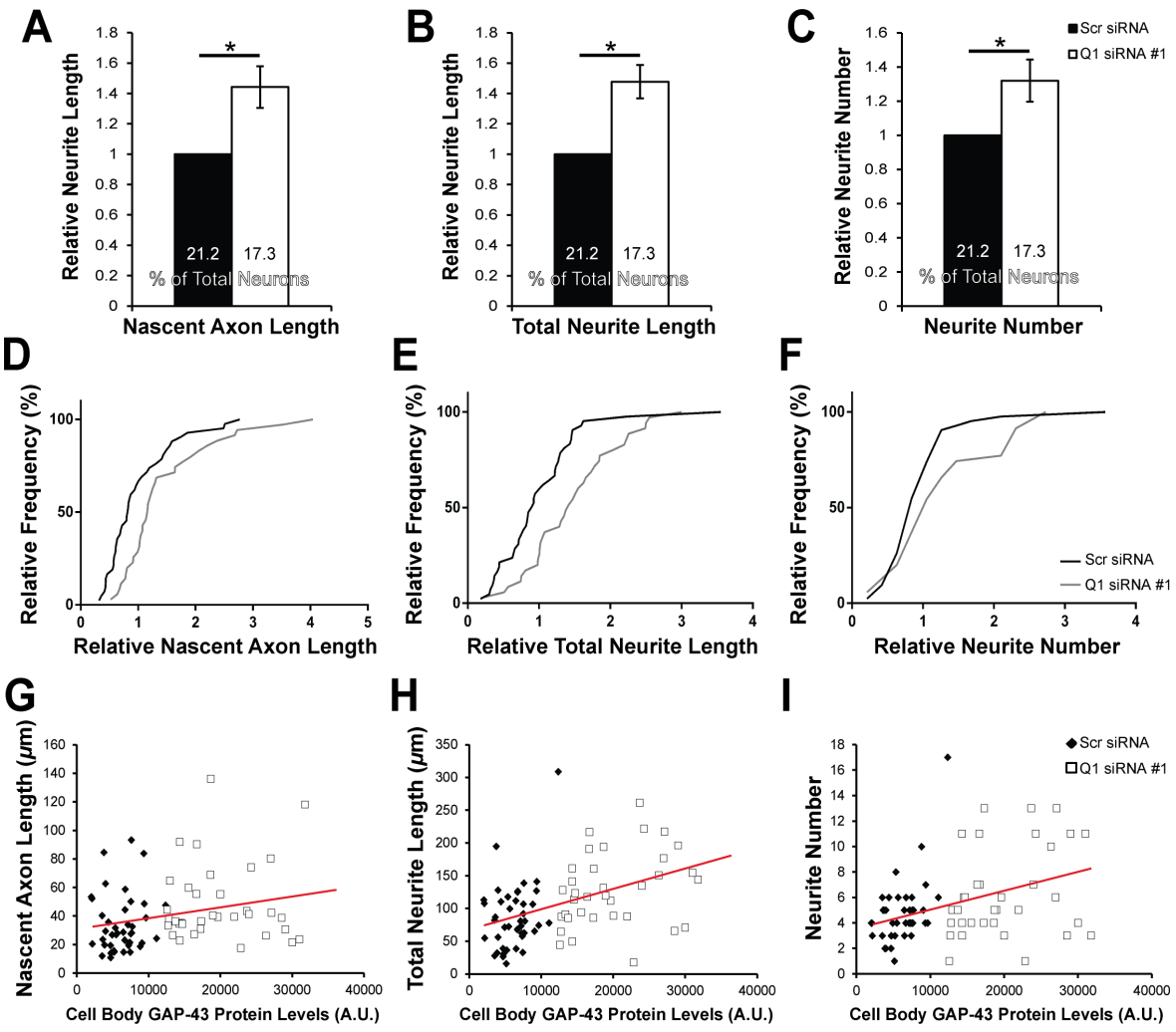

Supplemental Figure 3-4: Increased Cortical Neuron Nascent Axon Length, Total Neurite Length and Neurite Number upon hnRNP-Q1 Knockdown. Average (A) nascent axon length, (B) total neurite length and (C) neurite number of selected neurons from Supplemental Figure 3-3 were quantified. n=6, Scr: 42 out of 198 cells and Q1: 35 out of 178 cells from 6 independent experiments, one-sample t-test, p-values: nascent axon length $p<0.0001$, total neurite length $p<0.0001$ and neurite number $p=0.0142$. (D-F) Cumulative distribution plots for each measurement of selected neurons from Supplemental Figure 3-3. (G-I) Plots demonstrating a positive correlation between nascent axon length, total neurite length and neurite number and GAP-43 protein levels of selected neurons from Supplemental

Figure 3-3. Red lines = trend lines.

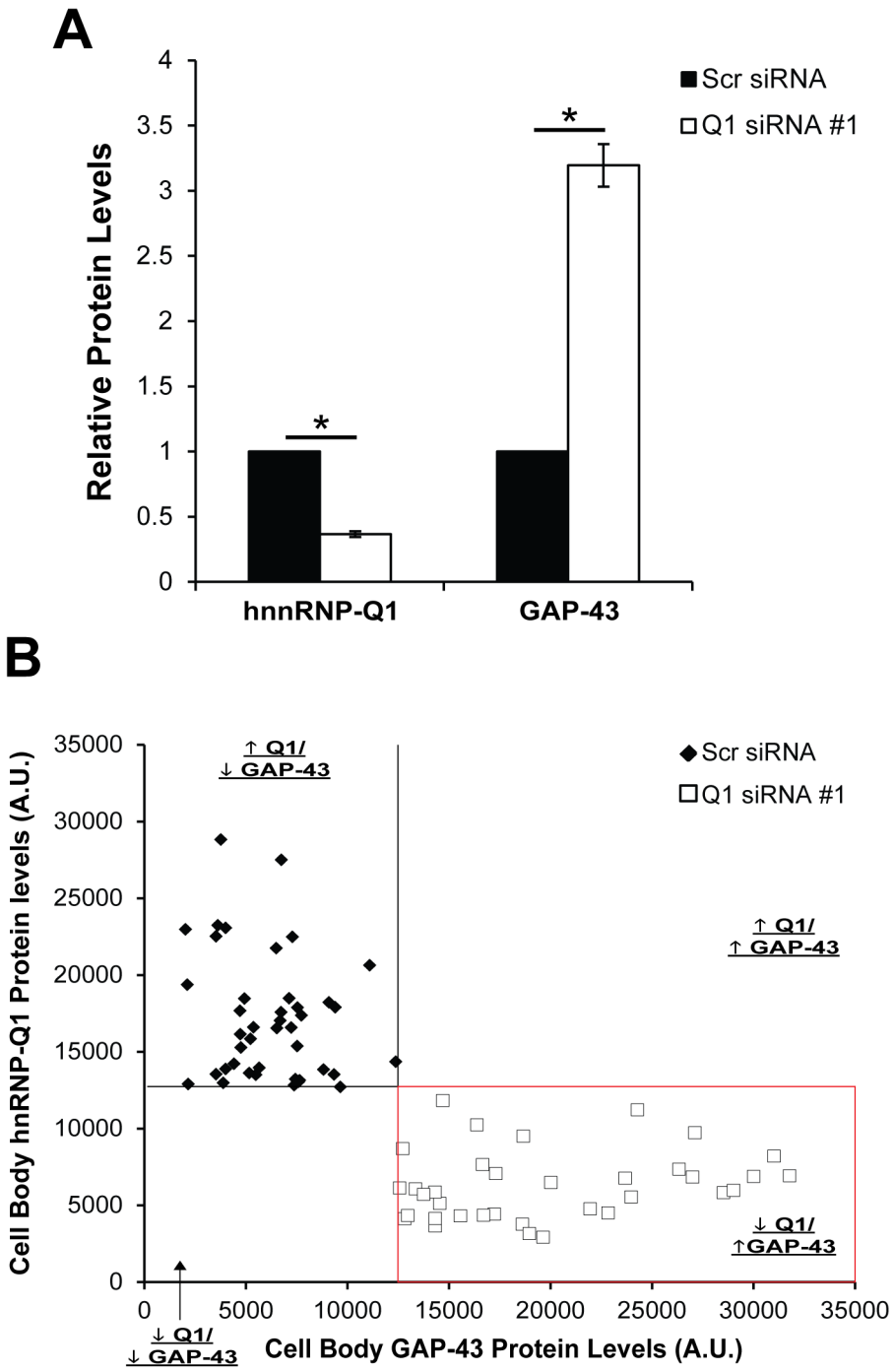

Supplemental Figure 3-5: Characterization of Selected Neuron GAP-43 and hnRNP-Q1 Expression from Non-rescue Experiments. Average cell body hnRNP-Q1 and GAP-43 signal intensity of the selected neurons from Supplemental Figures 3-3 and 3-4. (A) n=6, Scr: 42 out of 198 cells and Q1: 35 out of 178 cells from 6 independent experiments, one-sample

t-test, p-values: hnRNP-Q1 $p < 0.0001$, GAP-43 $p < 0.0001$. (B) Plot of cell body hnRNP-Q1 protein levels against cell body GAP-43 protein levels for each selected neuron from Supplemental Figures 3-3 and 3-4. The threshold between low and high levels of each protein was set at 12,500 A.U. as depicted by the black lines. Red outline indicates the cell population with low levels of hnRNP-Q1 and high levels of GAP-43 that were assessed for increased neurite length and number in Supplemental Figure 3-4.

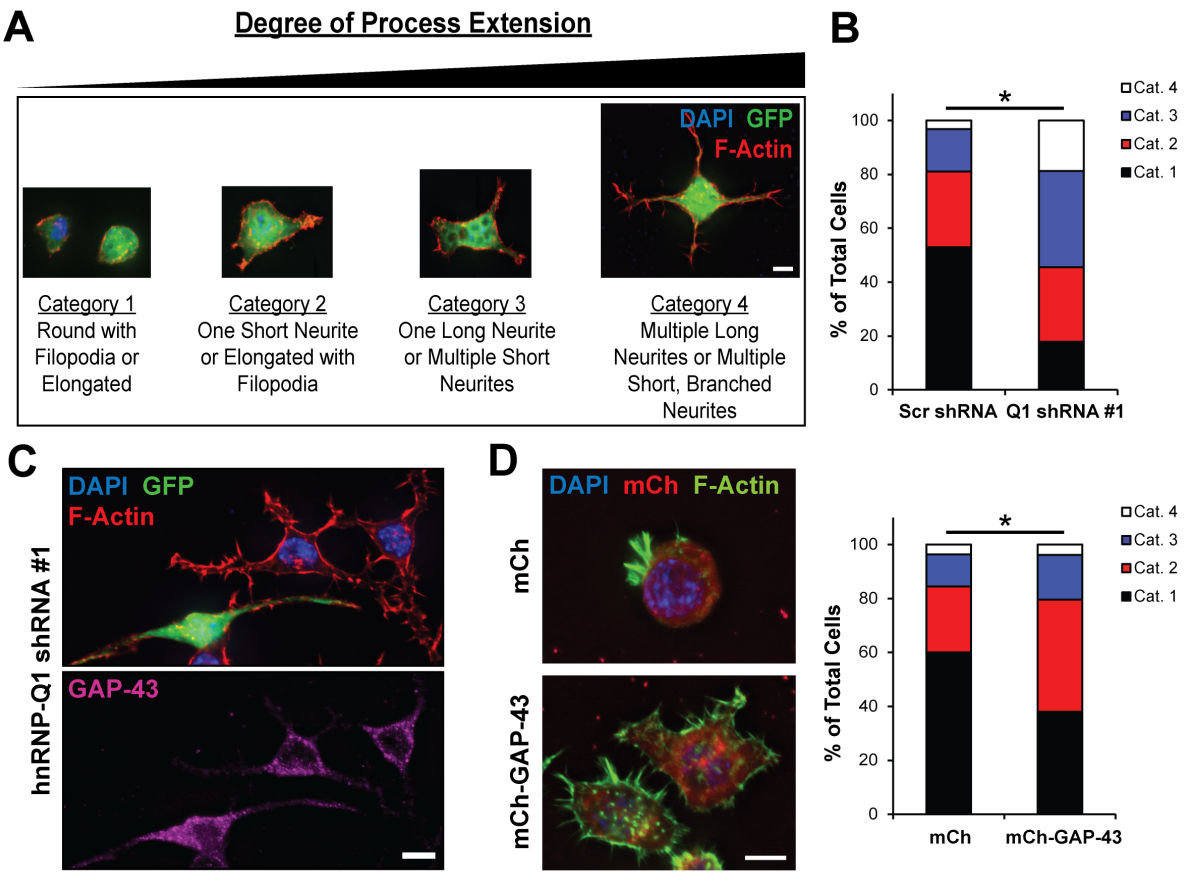

Supplemental Figure 3-6: Increased N2a Cell Process Extension upon hnRNP-Q1 Knockdown. (A) N2a cells were transfected with hnRNP-Q1 #1 or Scrambled shRNA, which co-expresses GFP. The cells were fixed after 72 hours and processed for immunofluorescence with fluorescently conjugated phalloidin to label F-actin. Transfected cells were selected by GFP signal and representative images from each category were assembled. Scale bar = 10 μm. (B) N2a cells were transfected with hnRNP-Q1 #1 or Scrambled shRNA and processed for immunofluorescence with GAP-43 and hnRNP-Q1 antibodies after 72 hours. Cells were then imaged and categorized based on their degree of process extension. Percent of cells in each category: Scr: Cat. 1 = 52.9%, Cat 2. = 28.2%, Cat 3. = 15.7%, Cat. 4 = 3.2%, Q1: Cat. 1 = 17.8%, Cat 2. = 27.7%, Cat 3. = 35.7%, Cat. 4 = 18.8%, n=4, Scr: 433 cells and Q1: 314 cells from 4 independent experiments, Mann-

Whitney test, p-value<0.0001. (C) Representative image of N2a cells transfected with hnRNP-Q1 #1 shRNA. Some untransfected cells also demonstrate increased GAP-43 signal intensity and increased process extension. (D) N2a cells were transfected with 3x-Flag-mCherry or 3x-Flag-mCherry-GAP-43 and processed for immunofluorescence with fluorescently conjugated phalloidin after 72 hours. Percent of cells in each category: mCh: Cat. 1 = 60.1%, Cat. 2 = 24.4%, Cat. 3 = 11.9%, Cat. 4 = 3.7%, mCh-GAP-43: Cat. 1 = 38.0%, Cat. 2 = 41.6%, Cat. 3 = 16.5%, Cat. 4 = 3.9%. n=4, mCh: 328 cells and mCh-GAP-43: 363 cells from 4 independent experiments, Mann-Whitney test, p-value<0.0001.

Chapter 4

Mechanism of hnRNP-Q1-Mediated Regulation of GAP-43 Expression

Portions of this chapter were adapted from the following publication and manuscript:

Wigington, C.P.*, Williams, K.R.*, Meers, M.P., Bassell, G.J., Corbett, A.H. (2013) Poly(A) RNA binding proteins and polyadenosine RNA: new members and novel functions. Wiley Interdiscip Rev RNA. 5(5): 601-22. PMID: 24789627. * indicates equal contribution

Williams, K.R., Stefanovic, S., McAninch, D.S., Xing, L., Allen, M., Li, W., Feng, Y., Mihailescu, M.R., Bassell, G.J. (2015) hnRNP-Q1 Represses Nascent Axon Growth in Cortical Neurons by Inhibiting *Gap-43* mRNA Translation. *Mol Biol Cell*. Revision Under Review.

4.1: Introduction

Here we investigate whether hnRNP-Q1-mediated post-transcriptional repression of GAP-43 expression is due to a translational mechanism given the previously identified functions of hnRNP-Q1. This mechanism may contribute to the known post-transcriptional mechanisms of GAP-43 expression regulation to spatially and temporally control GAP-43 expression.

4.1.1: Potential Gap-43 mRNA Cis-Regulatory Elements

Studies that identified hnRNP-Q1 as a polyA binding protein[208, 219] and demonstrated that hnRNP-Q1 binds to polyA RNA through its RRM domains[226] provided insight into potential *Gap-43* mRNA cis-regulatory elements. hnRNP-Q1 does not regulate the expression of γ-Actin and hnRNP-Q1 only interacts with about 10% of total mRNAs suggesting that hnRNP-Q1 regulates a specific subset of mRNAs. Therefore, internal polyA stretches may be a cis-regulatory element that binds hnRNP-Q1. *M. musculus Gap-43* mRNA contains two 11 nucleotide polyA stretches in the 3'-UTR and *H. sapiens Gap-43* mRNA isoforms 1 and 2 contain a single 17 nucleotide polyA stretch in the 3'-UTR. Internal polyA stretches have previously been identified as cis-regulatory elements in the 5'-UTR of *PABPC1* mRNA and the 3'-UTR of *YB-1* mRNA, which are bound by PABPC1 to negatively and positively regulate translation, respectively[83]. Additionally, there are 2,464 instances of ≥12 nucleotide polyA stretches that occur in exons in the *H. sapiens* transcriptome and 82% on these stretches occur in the UTRs of mRNA transcripts[83]. These findings support internal polyA stretches serving as cis-regulatory elements.

The 2,250 mRNA targets that were identified as hnRNP-Q1 targets by microarray

analysis were analyzed for potential hnRNP-Q1 consensus sequences. This analysis identified two 6 nucleotide consensus sequences in the 3'-UTRs of hnRNP-Q1 mRNA targets: AYAAYY and UAUYRR where Y = C/U and R = A/G[215]. *M. musculus Gap-43* mRNA contains two of these consensus sequences, one in the coding region (ATAACT) and one in the 3'-UTR (TATTAA) and *H. sapiens Gap-43* mRNA isoforms 1 and 2 contain seven of these consensus sequences, three in the 5'-UTR (ACAAUU, ACAACC and UAUUGG), two in the coding region (AUAACU and UAUCAA) and two in the 3'-UTR (UAUCGA and UAUUAA). Additionally, hnRNP-Q1 has been suggested to bind these consensus sequences in the *Cdc42* mRNA through the RGG box domain[215].

Another potential *Gap-43* mRNA cis-regulatory element is the G-Quadruplex (GQ) due to presence of an RGG box domain in hnRNP-Q1. The best-established example of the RGG box/GQ interaction is between FMRP and its target mRNAs[32-35]. *M. musculus Gap-43* mRNA contains several predicted GQ sequences and the sequence with the highest G-score is in the 5'-UTR (G-Score = 42, QGRS Mapper[304], Supplemental Figure 4-1 A, D). *H. sapiens Gap-43* mRNA isoforms 1 and 2 also contain several predicted GQ sequences and the sequence with the highest G-score is also in the 5'-UTR (G-Score = 36, QGRS Mapper[304], Supplemental Figure 4-1 B, C, E). Therefore, hnRNP-Q1 may bind to one or more of these potential cis-regulatory elements to repress GAP-43 expression.

4.1.2: G-Quadruplexes and Translation Regulation

Four guanine DNA or RNA nucleotides can interact in a planar configuration by Hoogsteen-type hydrogen bonds to form a G-Quartet and two or more G-Qaurtets can stack to form a GQ[305]. GQs are stabilized by K^+ and Na^+ ions binding the central channel but RNA

GQs can fold in the absence of cations[306]. DNA GQs have been demonstrated to serve a capping function at the end of single-stranded telomeres and to repress transcription when present in promoter regions[307, 308]. RNA GQs affect gene expression by regulating mRNA localization and translation. GQs in the 3'-UTRs of *Psd-95* and *CamKIIα* mRNAs are required for their dendritic localization[37]. Additionally, GQs present in the 5'-UTRs and 3'-UTRs of mRNAs regulate translation. More specifically, GQs proximal to the 5' cap tend to inhibit translation by blocking ribosome assembly or scanning while GQs near an IRES tend to enhance ribosome recruitment[309]. Several examples of 5'-UTR GQs modulating translation have been reported and ~3000 *H. sapiens* 5'-UTRs contain at least one predicted GQ sequence[309]. These findings suggest that this mechanism of translation regulation may be widespread. 3'-UTR GQs have also been demonstrated to repress translation[36, 310] suggesting that GQs likely modulate mRNA translation by multiple mechanisms.

4.1.3: Mechanisms of mRNA Binding Protein Translation Regulation

As discussed previously, two well-characterized trans-regulatory factors are IMP1/ZBP1 and FMRP. IMP1/ZBP1 binds to the zipcode cis-regulatory element in *β-Actin* mRNA and holds the mRNA in a translationally silent state by preventing 60S ribosomal subunit recruitment while it is trafficked to the leading edge of motile fibroblasts or axonal growth cones[47]. Upon arrival, guidance cues like BDNF or netrin-1 lead to activation of Src kinase, which phosphorylates IMP1/ZBP1[47, 49, 50]. Phospohorylated IMP1/ZBP1 releases *β-Actin* mRNA allowing it to undergo local translation[47]. FMRP is also regulated by phosphorylation. The FMRP binding site in the 3'-UTR of *Psd-95* mRNA folds into two tandem G-Quadruplex structures suggesting that FMRP binds to GQs to repress *Psd-95*

mRNA translation[36]. Phosphorylated FMRP recruits RISC and facilitates miRNA-125a binding to *Psd-95* mRNA, which has been suggested to block translation by stalling actively translating ribosomes[51, 52]. Activation of group 1 metabotropic glutamate receptors leads to activation of PP2a, which deposphorylates FMRP[52, 53]. Unphosphorylated FMRP causes the RISC complex to dissociate from *Psd-95* mRNA allowing it to undergo local translation[52, 54].

The mechanisms of IMP1/ZBP1 and FMRP translation repression demonstrate that phosphorylation and miRNAs can regulate the function of trans-regulatory factors and contribute to translation repression, respectively. Interestingly, *M. musculus* hnRNP-Q1 contains multiple phosphorylated residues that were identified by mass spectrometry (PhosphoSitePlus[311]). The phosphosites that are conserved in *H. sapiens* include S249 (beginning of RRM 2), Y373 (middle of RRM3), Y432 (linker region before RGG box), Y485 (middle of RGG box) and Y488 (middle of RGG box, Supplemental Figure 4-7 A)[311]. The presence of conserved phospho-residues in the RNA binding domains suggests that hnRNP-Q1 mRNA binding may be regulated by phosphorylation. However, little is known about hnRNP-Q1 phosphorylation regulation other than it is tyrosine phosphorylated by the insulin receptor[235, 237, 238] and dephosphorylated by SH2 domain-containing phosphatase 2 (SHP2)[239]. Additionally, *M. musculus* and *H. sapiens* (isoforms 1 and 2) *Gap-43* mRNA contains multiple predicted miRNA binding sites (3 in the 5'-UTR, 3 in the coding region and 1 in the 3'-UTR and 1 in the 5'-UTR, 1 in the coding region and 3 in the 3'-UTR, respectively, miRBase[312]). These findings suggest hnRNP-Q1-mediatied inhibition of *Gap-43* mRNA translation may be involve miRNAs and be regulated by phosphorylation.

4.1.4: Chapter 4 Hypothesis and Objectives

Given that hnRNP-Q1 post-transcriptionally represses GAP-43 expression and that hnRNP-Q1 has previously been demonstrated to modulate translation, we assessed whether hnRNP-Q1 inhibits *Gap-43* mRNA translation. We hypothesized that hnRNP-Q1 binds to specific sequences or secondary structures in *Gap-43* mRNA to inhibit translation. Our results reveal that hnRNP-Q1 binds to multiple regions of *Gap-43* mRNA but binds to 5'-UTR with the highest affinity. A predicted GQ sequence in the 5'-UTR is necessary and sufficient for hnRNP-Q1 to bind this region and this GQ sequence is able to fold into a stable intramolecular GQ structure. Additionally, hnRNP-Q1 binds to the *Gap-43* 5'-UTR GQ (5'GQ) through the RGG box domain. Furthermore, hnRNP-Q1 repressed endogenous *Gap-43* mRNA translation, deleting the 5'GQ relieved hnRNP-Q1-mediated translation repression and the 5'GQ was sufficient to mediate hnRNP-Q1-dependent translation repression. These results reveal a novel molecular interaction between hnRNP-Q1 and the *Gap-43* 5'GQ, demonstrate that hnRNP-Q1 specifically represses *Gap-43* mRNA translation and indicate that the 5'GQ contributes to the mechanism.

4.2: Results

4.2.1: hnRNP-Q1 Directly Binds a G-Quadruplex Sequence in the 5'-UTR of Gap-43 mRNA

To investigate a possible translational mechanism for how hnRNP-Q1 represses GAP-43 expression, we first determined if hnRNP-Q1 directly interacts with *Gap-43* mRNA and identified *Gap-43* mRNA sequences that are involved in hnRNP-Q1 binding. Biotinylated probes corresponding to the *Gap-43* 5'-UTR, coding region and 3'-UTR were *in vitro* transcribed along with the *γ-Actin* 3'-UTR as a negative control (Figure 4-1 A). Equimolar concentrations of the RNA probes were incubated with recombinant GST or GST-

hnRNP-Q1 protein and the probes were precipitated with NeutrAvidin agarose beads. Co-purifying protein was assessed by GST immunoblot. GST-hnRNP-Q1 but not GST was precipitated with probes corresponding to all three regions of the *Gap-43* mRNA but not with the *γ-Actin* 3'-UTR probe (Figure 4-1 B) demonstrating that hnRNP-Q1 directly interacts with *Gap-43* mRNA. Interestingly, we noticed that the 5'- UTR precipitated the most GST-hnRNP-Q1 followed by the coding region and then the 3'-UTR (Figure 4-1 B). Thus, we focused our analysis on a predicted G-Quadruplex (GQ) sequence in the 5'-UTR region of *Gap-43* mRNA because these structures have previously been demonstrated to repress translation[309]. The predicted GQ sequence that we assessed had the highest G-Score of all predicted GQs in the *Gap-43* mRNA (#14 GQ G-Score = 42, QGRS Mapper[304], Supplemental Figure 4-1 A, D). *H. sapiens Gap-43* mRNA isoforms 1 and 2 also have a predicted GQ with a high G-Score in the 5'-UTR suggesting a conserved mechanism (#239 G-Score = 36, QGRS Mapper[304], Supplemental Figure 4-1 B, C, E). We found that deleting the *Gap-43* 5'-UTR GQ sequence (5'GQ) (5'-GGGAGGGAGGGAGGGA-3') almost completely abolished GST-hnRNP-Q1 binding to the 5'-UTR (reduced by 88%, Figure 4-1 B).

Since hnRNP-Q1 appears to bind multiple regions of *Gap-43* mRNA, we next determined if deleting the 5'GQ affects hnRNP-Q1 binding to full-length *Gap-43* mRNA. Biotinylated probes corresponding to full-length *Gap-43* mRNA with and without the 5'GQ were *in vitro* transcribed (Figure 4-1 C) and used for biotin pull-down experiments. Deleting the 5'GQ reduced GST-hnRNP-Q1 binding to full-length *Gap-43* mRNA by 41% suggesting that this sequence is a major site for hnRNP-Q1 binding (Figure 4-1 D). Additional predicted GQ sequences in *Gap-43* mRNA were assessed for their ability to bind hnRNP-Q1 (#88 G-

Score = 21 (5'-UTR) and #338 G-Score = 21 (coding region), QGRS Mapper[304], Supplemental Figure 4-1 A, D). GST-hnRNP-Q1 binding was not reduced by deleting either GQ #88 or #338 suggesting that additional hnRNP-Q1 binding sites in *Gap-43* mRNA may not be GQs (Supplemental Figure 4-2 A, B). However, hnRNP-Q1 does bind GQs in other mRNAs demonstrating that hnRNP-Q1 is a bona fide GQ-binding protein (Supplemental Figure 4-3 A, B). In support of this, several previously identified hnRNP-Q1 target mRNAs also contain predicted GQ sequences with relatively high G-scores (QGRS Mapper[304], Table 4-1). Furthermore, GST-hnRNP-Q1 and endogenous hnRNP-Q1 bind the 5'GQ better than either a 12 nucleotide or 30 nucleotide poly(A) probe (Figure 4-1 E-G). These results suggest that the 5'GQ is a major hnRNP-Q1 binding site and that the 5'GQ and not the poly(A) tail are involved in hnRNP-Q1-mediated GAP-43 regulation as predicted by the results from Svitkin et al. 2013.

4.2.2: hnRNP-Q1 Directly Binds PolyA Stretches and a Consensus Sequence in the 3'-UTR of Gap-43 mRNA

The interaction between hnRNP-Q1 and the *Gap-43* 3'-UTR was also assessed in more detail. The *Gap-43* 3'-UTR was *in vitro* transcribed with ^{32}P-UTP and samples were prepared with an equal concentration of 3'-UTR RNA probe and increasing concentrations of GST or GST-hnRNP-Q1 (0-0.4 pmol). Electrophoretic mobility shift assays (EMSAs) were performed by running the samples on a 5% non-denaturing gel and radioactive signal was detected by exposing the gel to film. Binding was visualized by a shift of the unbound 3'-UTR probe to a higher molecular weight position in the gel. Increasing concentrations of GST-hnRNP-Q1 shifted the 3'-UTR probe to a higher molecular weight but GST did not

(Supplemental Figure 4-4 A). These findings demonstrate that hnRNP-Q1 directly interacts with the *Gap-43* 3'-UTR, which is consistent with the biotin pulldown data in Figure 4-1 B.

Biotin pulldown experiments were also performed to potentially identify *Gap-43* 3'-UTR sequences that bind hnRNP-Q1. As discussed in the introduction, the 3'-UTR contains two 11 nucleotide polyA stretches and an hnRNP-Q1 consensus sequence. Therefore, biotinylated probes corresponding to the *Gap-43* 3'-UTR, the 3'-UTR with the polyA stretches deleted and the 3'-UTR with the consensus sequence deleted were *in vitro* transcribed along with the *γ-Actin* 3'-UTR as a negative control (Supplemental Figure 4-4 B). Equimolar concentrations of the RNA probes were incubated with recombinant GST or GST-hnRNP-Q1 protein and the probes were precipitated with NeutrAvidin agarose beads. Co-purifying protein was assessed by GST immunoblot. GST-hnRNP-Q1 but not GST was precipitated with the 3'-UTR probe and this interaction was completely abolished by deleting the polyA stretches or the consensus sequence (0.05 fold and 0.28 fold, respectively, Supplemental Figure 4-4 C). These findings suggest that hnRNP-Q1 directly interacts with both polyA stretches and the consensus sequence in the 3'-UTR of *Gap-43* mRNA. However, since the 5'-UTR binds hnRNP-Q1 with the highest affinity, this region and specifically the 5'GQ was pursued as a potential cis-regulatory sequence that is bound by hnRNP-Q1 to modulate Gap-43 mRNA translation.

4.2.3: hnRNP-Q1 Binds the Gap-43 5'-UTR G-Quadruplex Sequence through the RGG Box

Given that RGG box domains have been demonstrated to specifically bind GQ forming mRNA sequences[33-35, 313], we next determined if hnRNP-Q1 interacts with the 5'GQ through the RGG box domain. 3x-Flag-mCherry, 3x-Flag-mCherry/hnRNP-Q1, 3x-Flag-

mCherry/hnRNP-Q1 ΔRGG Box and 3x-Flag-mCherry/hnRNP-Q1 RGG Box were overexpressed in N2a cells for ~16 hours. Biotin pulldown experiments were then performed with the 5'GQ probe and the N2a cell lysates. Co-purifying protein was assessed by Flag immunoblot. 3x-Flag-mCherry/hnRNP-Q1 and 3x-Flag-mCherry/hnRNP-Q1 RGG Box bind to the 5'GQ probe while 3x-Flag-mCherry/hnRNP-Q1 ΔRGG Box does not (Figure 4-2 A). These results demonstrate that the hnRNP-Q1 RGG box is necessary and sufficient to bind the *Gap-43* 5'GQ. We also employed fluorescence spectroscopy to determine the binding affinity. We designed a fluorescently labeled *Gap-43* 5'GQ probe in which the adenine at position four was replaced with 2-aminopurine (2AP). 2AP is a highly fluorescent analog of adenine whose steady-state fluorescence is sensitive to changes in the microenvironment[314, 315]. A sample of 150 nM 2AP-labeled *Gap-43* 5'GQ mRNA was prepared in 10 mM cacodylic acid buffer pH 6.5 and 50 nM increments of the hnRNP-Q1 RGG box peptide were titrated while monitoring the changes in the steady-state 2AP fluorescence (Figure 4-2 B). The resulting binding curves were fit with Equation 1 (Materials and Methods) to reveal a dissociation constant (K_d) of 131 ± 14 nM for the complex formed between the *Gap-43* 5'GQ RNA probe and the hnRNP-Q1 RGG box (Figure 4-2 B). These experiments were performed in triplicate and the reported error represents the standard deviation of the K_d from the three independent measurements.

4.2.4: The Gap-43 5'-UTR G-Quadruplex Sequence Folds into a G-Quadruplex Structure

We next determined if the *Gap-43* 5'GQ folds into a GQ structure, as predicted by the GQ prediction software QGRS Mapper[304]. The *Gap-43* 5'GQ probe (with a linker, 5'-GGGAGGGAGGGAGGGA+GAGC-3') was *in vitro* transcribed, purified by electrophoresis

and run on a denaturing polyacrylamide gel to verify probe purity (Supplemental Figure 4-5 A). We first analyzed 5'GQ probe folding by 20% non-denaturing polyacrylamide gel with varied KCl concentrations (0-150 mM). A single band was observed at all KCl concentrations investigated, indicating that a single GQ conformation was adopted (Supplemental Figure 4-5 B). However, there was a small shift in the band position after KCl was added, which supports potassium driven stability of the GQ structure (Supplemental Figure 4-5 B).

1D ^{1}H NMR spectroscopy was then used to analyze the imino proton resonance region. Imino proton resonances in the 10-12 ppm region have been assigned to guanine imino protons engaged in Hoogsteen base pairs within individual G-Quartets and are considered signatures of GQ structure formation[33, 316, 317]. As discussed previously, RNA GQs can fold in the absence of these ions, but have low stability[306]. Resonances are present in the 10-12 ppm region, even in the absence of KCl (Figure 4-3 A), indicating GQ formation within the 5'GQ probe. The intensity of these resonances increased upon the addition of KCl, demonstrating that the structure was stabilized by K^{+} ions (Figure 4-3 A). A mutant *Gap-43* 5'GQ probe (with a linker, 5'-GCGAGCGAGCGAGCGA+GAGC-3') was also synthesized in which guanine nucleotides predicted to be engaged in GQ formation were replaced with cytosine nucleotides and the secondary structure was analyzed by 1D ^{1}H NMR spectroscopy. As expected, the GQ imino proton resonances are no longer present in the 10-12 ppm region in the absence and presence of 150 mM KCl (Supplemental Figure 4-5 C). However, resonances are present in the region 12.6-13.4 ppm region, which correspond to imino protons involved in G-C Watson-Crick base pairs, consistent with the predicted hairpin structure of the *Gap-43* 5'GQ mutant RNA probe (Supplemental figure 4-5 C, D). This result

confirms that mutation of the guanine nucleotides abolishes GQ structure formation suggesting that *Gap-43* 5'GQ structure formation is required for hnRNP-Q1 binding.

GQ folding within the 5'GQ RNA probe was also analyzed by acquiring CD spectra in the presence of increasing KCl concentrations (5-150 mM). Parallel GQ structures exhibit a positive band at ~265 nm and a negative band at ~240 nm whereas antiparallel GQ structures exhibit a negative band at ~260 nm and a positive band at ~295 nm[318-322]. The 5'GQ RNA probe exhibited the signature of a parallel GQ structure, even in the absence of K^+ ions (Figure 4-3 B). As KCl levels increased, the intensities of these bands increased, indicating the K^+ ions drive GQ stability (Figure 4-3 B), consistent with the ^{1}H NMR spectroscopy results. However, minimal changes were observed in the spectra upon the increase in salt concentration from 5 mM to 150 mM implying that 5'GQ RNA probe required low ionic strength to achieve a fully stable GQ structure (Figure 4-3 B).

To obtain information about the stability of the 5'GQ structure, we performed UV spectroscopy thermal denaturation experiments. A main hypochromic transition with a melting temperature (T_m) of 78°C is present in the UV thermal denaturation profile of the 5'GQ RNA probe at 295 nm, corresponding to the GQ dissociation (Figure 4-3 C). The beginning of a second transition is visible above 90°C at high RNA concentrations, likely due to the formation of an alternate intermolecular conformation promoted by high RNA concentrations. To determine if the 5'GQ RNA probe adopts an *intramolecular* or *intermolecular* structure we performed thermal denaturation experiments at a fixed KCl concentration and variable RNA probe concentrations. The melting temperature does not depend on the RNA concentration (Figure 4-3 D), indicating that the 5'GQ RNA probe adopts an intramolecular structure (Equation 3, Materials and Methods). Upon establishing

that the GQ conformation giving rise to the main hypochromic transition in the UV thermal denaturation curve of the 5'GQ RNA probe is intramolecular, we fitted it with Equation 4 (Materials and Methods), which assumes a two state model, to determine the thermodynamic parameters of GQ formation in the presence of 5 mM KCl (Figure 4-3, C inset graph). The enthalpy of formation of a single G-Quartet plane has been reported to range between -18 kcal/mol and -25 kcal/mol[323]. Thus, the value obtained for the enthalpy of GQ formation in the 5'GQ RNA probe for the main transition (ΔH^0 =-64.3±0.1 kcal/mol) is consistent with the presence of three G-Quartet planes. Taken together, these results suggest that the 5'GQ, which is a main hnRNP-Q1 binding site, folds into a stable parallel, intramolecular GQ structure containing three G-Quartet planes (Figure 4-3 E).

4.2.5: hnRNP-Q1 Co-localizes with Gap-43 mRNA in Incipient Cortical Neurons

To determine is hnRNP-Q1 interacts with *Gap-43* mRNA in incipient cortical neurons, FISH experiments were performed. Cortical neurons were electroporated with pEGFP/hnRNP-Q1 immediately after dissection, fixed after 28.5 hours in culture and processed for Stellaris FISH with *Gap-43* cy3 probes and *β-Actin* cy5 probes (Figure 4-4 A). Several *Gap-43* mRNA granules contain GFP-hnRNP-Q1 suggesting that hnRNP-Q1 interacts with *Gap-43* mRNA in the neurites of cortical neurons (Figure 4-4 A). Additionally, *β-Actin* mRNA is also present in some of the *Gap-43* mRNA-GFP-hnRNP-Q1 granules suggesting that these mRNAs may be trafficked together (Figure 4-4 A). FISH experiments were also performed to determine if the 5'GQ affects the neuritic localization of the mRNA. The 3'-UTR ARE cis-regulatory sequence has previously been demonstrated to be necessary and sufficient for Gap-43 mRNA localization so deleting the 5'GQ was not expected to affect

mRNA localization. We generated a construct with the following cassette: *Gap-43* 5'-UTR (with or without the 5'GQ)-3xFlag-mCherry-*Gap-43* Coding Region-*Gap- 43* 3'-UTR (FL or Δ5'GQ reporters) to perform these experiments. Cortical neurons were electroporated with the FL or Δ5'GQ reporters immediately after dissection, fixed after 28.5 hours in culture and processed for Stellaris FISH with *mCherry* cy5 probes (Figure 4-4 B). As expected, the Δ5'GQ reporter mRNA is localized to both the cell body and neurites similar to FL reporter mRNA as detected by mCherry FISH signal. These findings demonstrate that hnRNP-Q1 interacts with *Gap-43* mRNA in the neurites of cortical neurons and suggest that the 5'GQ is involved in translation modulation and not mRNA localization.

4.2.6: hnRNP-Q1 Represses Endogenous Gap-43 mRNA Translation

To determine if hnRNP-Q1 specifically represses endogenous *Gap-43* mRNA translation, L-Azidohomoalanine (AHA) pulse labeling experiments were performed[324]. N2a cells were transfected with hnRNP-Q1 #1 or Scrambled siRNA and 72 hours later the cells were starved of methionine for 1 hour and then pulsed with the methionine analog AHA for 2 hours. AHA combined with the protein synthesis inhibitor anisomycin was used as a control. Excess AHA was washed away, cell lysates were collected and the click-it chemistry reaction was performed to covalently link biotin to AHA that was incorporated into newly synthesized proteins. Endogenous GAP-43 protein was then immunoprecipitated (efficiency shown in Supplemental Figure 4-6 A) and newly synthesized GAP-43 protein was visualized by immunoblot with streptavidin and anti-GAP-43 (Figure 4-5 A). hnRNP-Q1 depletion increased AHA GAP-43 protein levels by 2.80 fold and anisomycin treatment reduced AHA GAP-43 protein levels (Scr: 0.22 fold, Q1: 0.13 fold, Figure 4-5 B). Total AHA labeled

protein levels also increase upon hnRNP-Q1 knockdown (1.62 fold, quantified from 1% input, Figure 4-5 C) suggesting that hnRNP-Q1 regulates a large subset of mRNA transcripts. hnRNP-Q1 knockdown was quantified in Supplemental Figure 4-6 B.

Proximity ligation assays were also performed to confirm that hnRNP-Q1 represses endogenous *Gap-43* mRNA translation[324, 325]. N2a cells were transfected with hnRNP-Q1 #1 or Scrambled siRNA and Lifeact-GFP and 72 hours later the cells were pulsed with puromycin for 5 minutes. Media without puromycin was used as a control. Excess puromycin was extracted, the cells were fixed and proximity ligation reactions were performed with GAP-43 and puromycin antibodies. α-Tubulin and puromycin antibodies were used as a control. The GAP-43 or α-Tubulin and puromycin antibodies were bound by secondary antibodies conjugated to oligonucleotides. If a GAP-43 or α-Tubulin antibody was within 30-40 nM of the puromycin antibody, which occurs when puromycin was incorporated into a GAP-43 or α-Tubulin peptide chain undergoing translation, the oligonucleotides from each secondary antibody were ligated together to form a closed loop. The oligonucleotide loop was then amplified by rolling circle amplification and fluorescently labeled oligonucleotides were hybridized to the product. Transfected cells were selected by GFP signal (Figure 4-5 D). hnRNP-Q1 knockdown significantly increased both the volume and intensity of GAP-43 proximity ligation puncta (5.30 fold and 5.13 fold, respectively, Figure 4-5 E, F) and the no puromycin controls demonstrated reduced signal (volume: Scr: 0.18 fold, Q1: 0.42 fold, intensity: Scr: 0.19 fold, Q1: 0.45 fold, Figure 4-5 E, F). However, hnRNP-Q1 knockdown did not affect the volume or intensity of α-Tubulin proximity ligation puncta (0.95 fold and 0.93 fold, respectively, Figure 4-5 E, F) and the no puromycin controls demonstrated reduced signal (volume – Scr: 0.19 fold, Q1: 0.22 fold, intensity – Scr: 0.19 fold, Q1: 0.23 fold,

Figure 4-5 E, F). These results further suggest that hnRNP-Q1 represses *Gap-43* mRNA translation but not global translation.

4.2.7: hnRNP-Q1 Represses Gap-43 mRNA Translation Through the 5'-UTR G-Quadruplex

AHA pulse labeling experiments were also performed to determine if the 5'GQ is involved in hnRNP-Q1-mediated inhibition of *Gap-43* mRNA translation. N2a cells were transfected with the FL or Δ5'GQ reporter constructs (described above) ~56 hours after hnRNP-Q1 #1 or Scrambled siRNA transfection. After ~16 hours, the cells where starved of methionine for 1 hour and labeled with the methionine analog AHA for 2 hours. AHA incorporated into newly synthesized proteins was labeled with biotin, 3xFlag-mCherry-tagged GAP-43 was immunoprecipitated with anti-Flag and newly synthesized 3xFlag-mCherry-tagged GAP-43 was visualized by immunoblot with streptavidin and anti-Flag (Figure 4-6 A). The results revealed that hnRNP-Q1 depletion increased translation of the FL reporter by 1.50 fold (Figure 4-6 B). Additionally, the Δ5'GQ reporter was less sensitive to hnRNP-Q1 repression but hnRNP-Q1 knockdown did significantly increase Δ5'GQ reporter translation (Scr: 2.64 fold, Q1: 3.39 fold, Figure 4-6 B). These findings suggest that hnRNP-Q1 represses *Gap-43* mRNA translation in a 5'GQ dependent manner but indicate that additional *Gap-43* mRNA sequences may also contribute to this process. hnRNP-Q1 knockdown was quantified in Supplemental Figure 4-6 C and a representative example of construct overexpression is shown in Supplemental Figure 4-6 D. In support of the AHA pulse labeling results, the Δ5'GQ reporter is expressed at a higher rate in N2a cells than FL reporter (1.28 fold, Figure 4-6 C).

Luciferase assays were also performed to support the AHA pulse labeling findings. The *Gap-43* 5'-UTR with or without the 5'GQ was inserted upstream of the firefly luciferase coding region (5' or 5'ΔGQ constructs). N2a cells were transfected with hnRNP-Q1 #1 or Scrambled siRNA, the 5' or 5'ΔGQ firefly luciferase reporter constructs and a renilla luciferase construct. Luciferase assays were performed after 72 hours. The results revealed that hnRNP-Q1 depletion increased expression of the 5' reporter as demonstrated by a 1.57 fold increase in luminescence (Figure 4-6 D). Additionally, the 5'ΔGQ reporter was less sensitive to hnRNP-Q1 repression but hnRNP-Q1 knockdown did significantly increase 5'ΔGQ reporter expression (Scr: 2.61 fold, Q1: 3.05 fold, Figure 4-6 D). These findings support the AHA pulse labeling results, which suggest that additional *Gap-43* mRNA sequences contribute to this mechanism. Additionally, luciferase assays were performed with a construct that had just the 5'GQ inserted upstream of the firefly luciferase coding region. N2a cells were transfected with hnRNP-Q1 #1 or Scrambled siRNA, the 5'GQ or empty vector firefly luciferase reporter constructs and a renilla luciferase construct. Luciferase assays were performed after 72 hours. The results demonstrate that inserting the 5'GQ represses luciferase expression as compared to the empty vector (0.56 fold) and knocking down hnRNP-Q1 relieves this repression (0.81 fold, Figure 4-6 E). Additionally, expression of the empty vector showed a non-significant trend toward being slightly increased upon hnRNP-Q1 knockdown (1.23 fold, Figure 4-6 E) suggesting that they polyA tail may contribute to this mechanism but the effect of the endogenous *Gap-43* demonstrate that the 5'GQ is involved in hnRNP-Q1-mediated inhibition of *Gap-43* mRNA translation.

4.2.8: A Potential Role for Phosphorylation and miRNA in hnRNP-Q1-mediated Gap-43

mRNA Translation Inhibition

To gain insights into the role of hnRNP-Q1 in repressing translation, the interaction between hnRNP-Q1 and translation factors was assessed by immunofluorescence. eIF4E is the cytoplasmic cap binding protein, eIF3η is a component of the eIF3 complex which binds to the 40S ribosome and facilitates initiation factor recruitment and the Y10b antibody recognizes the 5.8s ribosomal RNA, which is a component of the 60S ribosomal subunit. N2a cells were lysed and incubated with eIF4E, eIF3η, Y10b of IgG control antibodies. The antibodies were immunoprecipitated with protein G agarose beads and co-purifying hnRNP-Q1 was assessed by immunoblot. hnRNP-Q1 does not interact with eIF4E, eIF3η or the ribosome, which may suggest that hnRNP-Q1 inhibits mRNA translation at an early stage (Supplementary Figure 4-7 B).

hnRNP-Q1 may be regulated by a phosphorylation mechanism and miRNA may contribute to hnRNP-Q1-mediated translation repression. hnRNP-Q1 contains three phospho-residues near or in the RGG box suggesting that phosphorylation may regulate hnRNP-Q1 binding to the 5'GQ (Supplemental Figure 4-7 A). Additionally, three miRNAs are predicted to target the *M. musculus Gap-43* 5'-UTR and one miRNA is predicted to target the *H. sapiens Gap-43* 5'-UTR (Supplemental Figure 4-7 C). These findings suggest that miRNA may contribute to hnRNP-Q1-mediated inhibition of *Gap-43* mRNA through the 5'GQ. In support of this, hnRNP-Q1 was demonstrated to interact with AGO1, the catalytic component of the RISC complex, by co-immunoprecipitation (Supplemetal Figure 4-7 D). *M. musculus* myoblast C2C12 cells were lysed and incubated with rat AGO1, rabbit AGO1 or IgG control antibodies. The antibodies were immunoprecipitated with protein G agarose beads and co-purifying hnRNP-Q1 was assessed by immunoblot (Supplemental Figure 4-7 D). These

findings suggest that miRNA may cooperate with hnRNP-Q1 to repress *Gap-43* mRNA translation.

4.3: Discussion

Our results demonstrate that *Gap-43* mRNA is a novel target that is translationally repressed by the mRNA binding protein hnRNP-Q1. These findings contribute to the growing literature about the role of hnRNP-Q1 in regulating translation. hnRNP-Q1 has previously been demonstrated to repress cap-dependent translation of *RhoA* and *YB-1* mRNAs[217, 218]. However, the specific mechanism of hnRNP-Q1 binding and translation regulation has yet to be uncovered. Here we identified a predicted GQ sequence in the 5'-UTR of *Gap-43* mRNA, determined that it folds into a stable parallel, intramolecular GQ structure and demonstrated that it directly binds the hnRNP-Q1 RGG box. Additionally, the 5'GQ is involved in hnRNP-Q1-mediated translation repression of *Gap-43* mRNA as demonstrated by AHA pulse labeling and luciferase assay experiments. Furthermore, hnRNP-Q1 appears to bind the 5'GQ with higher affinity than poly(A) sequences and luciferase assays reveal that the polyA tail represses expression to a lesser extent that the 5'GQ suggesting a novel mechanism to that described by Svitkin et al., 2013. In support of this, we have previously demonstrated that hnRNP-Q1 represses RhoA mRNA translation by binding to non-poly(A) sequences[218]. These results suggest that hnRNP-Q1 is a novel GQ binding protein and point to a potential mechanism for hnRNP-Q1-mediated translational regulation. GQ structures proximal to the 5' cap tend to inhibit translation by blocking ribosome assembly or scanning[309]. Therefore, hnRNP-Q1 may bind to the *Gap-43* 5'GQ to prevent ribosome assembly or scanning. hnRNP-Q1 may repress the cap-dependent

translation of *YB-1* by a similar mechanism. *YB-1* mRNA is predicted to contain a GQ with a moderately high G-Score in its 5'-UTR region (G-Score = 20, QGRS Mapper)[304]. In contrast, *RhoA* mRNA translation appears to be regulated in a slightly different manner because the 3'-UTR is sufficient for hnRNP- Q1-mediated translation repression. However, the 3'-UTR of *RhoA* mRNA also contains a predicted GQ with a high G-Score (G-Score = 41, QGRS Mapper)[304] and 3'-UTR GQs have also been demonstrated to regulate translation[36, 310]. Additionally, multiple hnRNP-Q1 target mRNAs contain predicted GQs and the predicted GQ with the highest G-score is present in the same mRNA region (5'-UTR, coding region or 3'-UTR) in both *M. musculus* and *H. sapiens* mRNAs in several of these targets. Interestingly, mRNA targets that are translationally enhanced by hnRNP-Q1 tend to have predicted GQs with the highest G-score in the coding region and the mRNA target that is localized by hnRNP-Q1 (*Cdc42*) has a predicted GQ with the highest G-score in the 3'-UTR. These findings suggest that GQ structures may be the primary interacting motifs for hnRNP-Q1 and that the position of the GQ may determine if hnRNP-Q1 translationally inhibits (5'-UTR or 3'-UTR), translationally enhances (coding region) or localizes (3'-UTR) the mRNA target.

hnRNP-Q1 binds to multiple regions of *Gap-43* mRNA suggesting that the additional binding events may also influence translation or affect mRNA processing. Interestingly, the coding region contains a predicted GQ sequence with a moderately high G-Score (G-Score = 21, QGRS Mapper)[304] suggesting that hnRNP-Q1 may also interact with this region of the mRNA through a GQ structure. However, deleting this GQ sequence did not reduce hnRNP-Q1 binding indicating that hnRNP-Q1 interacts with a different cis-regulatory element in this region, potentially a consensus sequence. The *Gap-43* 3'-UTR does not contain any predicted

GQ sequences suggesting that this interaction is also mediated by an alternative cis-regulatory element. In support of this, deleting two 11 nucleotide polyA stretches and the consensus sequence separately abolished binding indicating that hnRNP-Q1 can also interact with polyA sequences, as supported by Mizutani et al. 2000 and Svitkin et al. 2013, and the consensus sequences identified by Chen et al. 2012 in *Gap-43* mRNA. Future studies may address whether the 3'-UTR polyA sequences and/or the consensus sequences are involved in *Gap-43* mRNA processing and post-transcriptional regulation events.

hnRNP-Q1 function may be modulated by phosphorylation which is supported by the findings that the insulin receptor tyrosine phosphorylates[235, 237, 238] and SHP2 dephosphorylates hnRNP-Q1[239]. Interestingly, there are three conserved phosphosites that are near or in the RGG box domain, Y432, Y485 and Y488, suggesting that hnRNP-Q1 binding the *Gap-43* 5'GQ and potentially additional GQ structures may be modulated by phosphorylation[311]. Additionally, miRNA may contribute to hnRNP-Q1-mediated inhibition of *Gap-43* mRNA translation. Interestingly, three *M. musculus* miRNAs target the 5'-UTR, miR-7011-5p, miR-7088-5p and miR-7665-5p, while only one *H. sapiens* miRNA targets the 5'-UTR, miR-6847-5p. Furthermore, hnRNP-Q1 interacts with AGO1 by co-immunoprecipitation. These findings suggest that hnRNP-Q1 may recruit RISC to *Gap-43* mRNA to silence translation. A similar mechanism has been reported for FMRP where phosphorylated FMRP binds GQs in the 3'-UTR of *Psd-95* mRNA and recruits RISC to facilitate miRNA-125a binding, which has been suggested to block translation by stalling actively translating ribosomes[51, 52]. FMRP is dephosphorylated by PP2a in response to group 1 metabotropic glutamate receptor activation, which causes the RISC complex to dissociate from *Psd-95* mRNA to relieve the translation inhibition[52, 53]. Alternatively, miRNA may

contribute to hnRNP-Q1-mediated inhibition of Gap-43 *mRNA* translation by other mechanisms (i.e. hnRNP-Q1 may regulate miRNA expression). Additionally, hnRNP-Q1-mediated inhibition of *Gap-43* mRNA translation may occur locally in axons and growth cones as a mechanism to enrich GAP-43 protein in axonal growth cones. In support of this, *Gap-43* mRNA has been demonstrate to be locally translated in axons[250] and Gap-43 mRNA co-localizes with GFP-hnRNP-Q1 in the axons of cortical neurons. Taken together, these preliminary studies suggest that phosphorylation of hnRNP-Q1 and miRNAs may play a role in hnRNP-Q1-mediated translation inhibition of *Gap-43* mRNA and that this mechanism may occur locally in axons and growth cones.

4.4: Materials and Methods

Antibodies, Immunoprecipitation and Immunoblotting

The following antibodies were used for immunoprecipitation and/or immunoblotting: GST (1:1000, Covance, Princeton, NJ), hnRNP-Q/R (1:100, Sigma-Aldrich), Flag (Ms, Sigma), Gap43 (1:5000, Abcam), A-Tubulin (1:50,000, Sigma-Alrich), eIF4E (1 μg, 1:200, Santa Cruz), eIF3η (1 μg, 1:200, Santa Cruz), Y10b (1 μg, Santa Cruz), rat AGO1 (5 μg, Sigma-Aldrich), rabbit AGO1 (5 μg, 1:1000, EMD Millipore), Mouse IgG (5 μg, EMD Millipore), Rabbit IgG (5 μg, EMD Millipore), Rat IgG (5 μg, Affymetrix eBioscience, San Diego, CA), TrueBlot Anti-Mouse HRP (1:3000, Rockland Immunochemicals Inc.) and TrueBlot Anti-Rabbit HRP (1:3000, Rockland Immunochemicals Inc.), IRDye 680LT Streptavidin (1:1000, Li-Cor), IRDdye 680LT Donkey Anti-Mouse (1:20,000, Li-Cor), IRDye 800CW Donkey Anti-Mouse (1:20,000, Li-Cor) and IRDye 800CW Donkey Anti-Rabbit (1:20,000, Li-Cor). Immunoprecipitations were performed with N2a cells or mouse

myoblast C2C12 cells, which were both cultured as described in the Chapter 2 Materials and Methods section. The cells were lysed with Co-IP buffer (150 mM NaCl, 50 mM Tris-HCl, pH 8.0, 5 mM $MgCl_2$, 0.5 mM Dithiothreitol, 1% NP-40 supplemented with 1x protease inhibitor (Roche), 1x RNase inhibitor (Ambion/Life Technologies)) and insoluble material was pelleted by centrifugation. 1 μg or 5 μg of each antibody was added to each tube and they were rotated at 4°C for 2 hours. Protein G agarose beads (Roche) were re-suspended in Co-IP buffer, added to each tube and rotated at 4°C for 1 hour. After washing, the pellets and 5% input were prepared for immunoblotting. Immunoblotting was performed as described in the Chapter 2 Materials and Methods section.

Fluorescence *In Situ* Hybridization

Full-length mouse *Gap-43* cDNA with and without the 5'GQ sequence was subcloned into 3xFlag-mCherry in the following order: *Gap-43* 5'-UTR-3xFlag-mCherry-*Gap-43* coding region-*Gap-43* 3'-UTR (FL or Δ5'GQ reporters). Cortical neurons were cultured as described in the Chapter 1 Materials and Methods section. The neurons were nucleofected with as described in the Chapter 1 Materials and Methods section except with 2.5 μg of pEGFP-hnRNP-Q1 or 2 μg pEGFP-hnRNP-Q1 and 2 μg FL or Δ5GQ reporters. FISH with Stellaris probes was performed ~120 hours after transfection as described in the Chapter 2 Materials and Methods section except for the addition of a β-*Actin* mRNA probe (Biosearch Technologies).

Fluorescence Microscopy

Cells were imaged as described in the Chapter 1 Materials and Methods section.

Biotin Pulldown Assays

Gap-43 and *γ-Actin* sequences were amplified from mouse brain cDNA and the *Gap-43* 5'-UTR, coding region and 3'-UTR were pieced together by overlap extension PCR. The *Gap43* 5'-UTR G-Quadruplex (5'GQ) sequence was deleted by ordering a forward primer lacking the sequence. All sequences of interest were subcloned into pGEM T-easy (Promega). The constructs were linearized and used as a template for *in vitro* transcription with T7 or Sp6 Maxiscript kits (Ambion/Life Technologies). Biotin-11-cytidine-5′-triphosphate (biotin-11-CTP, Roche) was used in a ratio of 1:4 with unlabeled CTP to produce biotinylated sense RNA probes. Unincorporated nucleotides were removed with G-25 spin columns (GE Healthcare Bio-Sciences, Piscataway, NJ) and the RNA probes were concentrated by ethanol precipitation. RNA probe concentration was analyzed by A260 absorption and probe quality was assessed by formaldehyde gel electrophoresis. *In vitro* transcribed probes or commercially synthesized RNA oligos with a 5'-end biotin label (GE Dharmacon, Lafayette, CO) were then used for biotin pull-down assays. Recombinant GST or GST-hnRNP-Q1 (~10 ng, as described in Xing et al. 2012) was incubated with equimolar concentrations of RNA probes in IP buffer (RIPA buffer supplemented with 1x protease inhibitor (Roche) and 1x RNase inhibitor (Ambion/Life Technologies)) containing 100 ng/μL *S. cerevisiae* tRNA for 20 minutes at room temperature. NeutrAvidin agarose (Thermo Fisher Scientific, Inc., Waltham, MA) preblocked with 20 μg DNase-, RNase-free BSA (Roche) was used to precipitate the biotinylated RNA probes. After extensive washing with IP buffer, co-purifying protein was assessed by immunoblotting for GST.

Additional Gap-43 mRNA deletion constructs were generated by overlap extension

PCR followed by subcloning into pGEM T-easy (Promega). Biotin pulldown assays were also performed with stage E17 mouse embryonic brains that were flash frozen in liquid nitrogen and stored at -80°C. The brains were lysed by pipetting with IP buffer and insoluble material was pelleted by centrifugation. Co-purifying protein was assessed by immunoblotting for hnRNP-Q/R. Commercially synthesized RNA oligos with a 5'-end biotin label were also ordered for sequences corresponding to the following mRNAs: *NR2B*, *p250gap*, *Psd-95*, *Shank1a*, *Shank1b* and *Smndc1* (GE Dharmacon). 12 nucleotide polyA and 30 nucleotide polyA RNA oligos with a 5'-end biotin label were also ordered (GE Dharmacon).

3x-Flag-mCherry/hu hnRNP-Q1 ΔRGG Box and 3x-Flag-mCherry/hu hnRNP-Q1 RGG Box constructs were generated by amplifying hnRNP-Q1 from 3x-Flag-mCherry/hu hnRNP-Q1 and inserting them into the 3x-Flag-mCherry vector. Sequences for the amplification primers are as follows, ΔRGG Box: 5'-CCGGCTCGAGCTATGGCTACA GAACATGTTAATGG-3' and 5'-CCGGGGTACCTGGAGGGGGCATATGAGG-3' and RGG Box: 5'-CCGGCTCGAGCTACAAGAGGTCGAGGGCG-3' and 5'-CCGGGGTAC CTCATTGTAACAGGTCAGGACCG-3'. N2a cells were cultured and transfected as described in the Materials and Methods sections of Chapters 2 and 3. 2 μg of each 3x-Flag-mCherry construct was overexpressed in N2a cells and the cell lysates were used for biotin pulldown assays after ~16 hours. Co-purifying protein was assessed by immunoblotting for Flag.

Electrophoretic Mobility Shift Assays

Linearized pGEMTeasy/*Gap-43* 3'-UTR construct was used as a template for *in vitro*

transcription with the T7 Maxiscript kit (Ambion/Life Technologies). ^{32}P UTP (PerkinElmer, Waltham, MA) was used in a ratio of 1:10 with unlabeled UTP to produce radioactive sense 3'-UTR RNA probes. Unincorporated nucleotides were removed with G-25 spin columns (GE Healthcare Bio-Sciences). Increasing concentrations of recombinant GST or GST-hnRNP-Q1 protein (0-0.4 pmol) were incubated with a fixed concentration of radioactive 3'-UTR RNA probe in binding buffer (25 mM NaCl, 20 mM Tris-HCl, pH 7.5, 0.125 mM EDTA, 0.05% Dithiothreitol and 10% Glycerol) at room temperature for 30 minutes. The samples were run on a 5% native gel at 25 mA for 2 hours in 1x Tris/Borate/EDTA Buffer. The gel was transferred to 3MM Whatman Chromatography paper (GE Healthcare Bio-Sciences) and dried using a gel dryer. Radioactive signal was detected by exposing the gel to film in an autoradiography cassette containing an intensifying screen.

Fluorescence Spectroscopy Experiments

Steady-state fluorescence spectroscopy experiments with the 2AP *Gap-43* 5'GQ RNA probe (5'-GGG2APGGGAGGGAGGGA+GAGC-3') were performed on a Horiba Scientific Fluoromax-4 and accompanying software fitted with a 150 W ozone-free xenon arclamp. Experiments were performed in a 150 μL sample volume, 3 mm path-length quartz cuvette (Starna Cells, Atascadero, CA). The excitation wavelength was set to 310 nm, the emission spectrum was recorded in the range of 330-450 nm, and the bandpass for excitation and emission monochromators were both set to 5 nm. Recombinant hnRNP-Q1 RGG box peptide was synthesized by inserting residues 406-561 into pGEX-2T (GE Healthcare Biosciences), inducing protein synthesis in Rosetta2(DE3)pLysS bacteria (Novagen, Madison, WI), purifying the protein by glutathione affinity and cleaving off the GST tag with

PreScission Protease (GE Healthcare Biosciences). hnRNP-Q1 RGG box peptide was titrated (50 nM) into a fixed concentration of 2AP *Gap-43* 5'GQ RNA (150 nM) and quenching of the fluorescence signal was recorded as a result of the RGG peptide interacting with the RNA probe (each point was corrected for fluorescence contributions originating from the peptide). 1 μM of a synthetic peptide derived from the Hepatitis C virus core protein was added to the RNA sample prior to hnRNP-Q1 RGG box peptide titration to prevent non-specific binding. The binding dissociation constant (K_d) was determined by fitting the binding curves to the equation:

$$F = 1 + \left(\frac{I_B}{I_F} - 1\right)\frac{(K_d+[P]_t+[RNA]_t)-\sqrt{(K_d+[P]_t+[RNA]_t)^2-4[P]_t\,[RNA]_t}}{2[RNA]_t} \qquad [1]$$

where $\frac{I_B}{I_F}$ represents the ratio of the steady state fluorescence intensity of the bound and free mRNA, $[RNA]_t$ is the total concentration of mRNA, and $[P]_t$ is the total peptide concentration.

G-Quadruplex Folding Assays

The *Gap-43* 5'GQ RNA probe (5'-GGGAGGGAGGGAGGGA+GAGC-3') and the mutated *Gap-43* 5'GQ RNA probe (5'-GCGAGCGAGCGAGCGA+GAGC-3') were *in vitro* transcribed by T7 RNA polymerase driven transcription of synthetic DNA templates (TriLink BioTechnologies, Inc., San Diego, CA). The RNA probes were purified by 20% polyacrylamide, 8 M urea gel electrophoresis and electroelution. Subsequently, the probes were dialyzed against 10 mM cacodylic acid, pH 6.5. The *Gap-43* 5'GQ RNA probe and its mutant version were run on a denaturing polyacrylamide gel with previously purified *Psd-95* RNA probe (15 nucleotides) to evaluate the purity.

KCl was added to 15 μM of the *Gap-43* 5'GQ RNA probe in the range 0-150 mM. The samples were annealed by boiling for 5 minutes followed by incubation at room temperature for 10 minutes. 20% native gels in 0.5x Tris/Borate/EDTA buffer were ran at 100V for 3 hours at 4º C. Probe conformations were visualized by UV shadowing at 254 nm using an AlphaImager (Alpha Innotech, Inc., San Leandro, CA).

G-Quadruplex (GQ) formation in the *Gap-43* 5'GQ RNA probe was monitored by 1D ^{1}H NMR spectroscopy at 25º C on a 500 MHz Bruker AVANCE spectrometer. 350 μM RNA samples were prepared in 10 mM cacodylic acid buffer, pH 6.5 in a 90% H_2O/10% D_2O ratio and KCl was titrated in the range 0-150 mM. The water suppression was accomplished using the Watergate pulse sequence[326]. Similar experiments were performed for the mutated *Gap-43* 5'GQ RNA probe, in the presence and absence of 150 mM KCl to demonstrate that when guanine nucleotides predicted to be engaged in GQ formation were mutated the structure no longer formed.

CD spectra were acquired on a Jasco J-810 spectropolarimeter at 25ºC, using a 1 mm path-length quartz cuvette (Starna Cells). A sample of 10 μM *Gap-43* 5'GQ RNA probe in 10 mM cacodylic acid buffer, pH 6.5 was prepared in a volume of 200 μL. GQ formation was monitored between 200-350 nm by titrating KCl in the range 5-150 mM, and averaging a series of 7 scans with a 1 second response time and a 2 nm bandwidth. The spectra were corrected by subtracting the contributions of the cacodylic acid buffer.

UV spectroscopy thermal denaturation experiments were performed on a Cary 3E UV-VIS Spectrophotometer (Varian, Inc.) equipped with a peltier cell. 200 μL samples containing variable *Gap-43* 5'GQ RNA probe concentrations in 10 mM cacodylic acid buffer pH 6.5 and in the presence of 5 mM KCl were annealed as described above and thermally

denatured by varying the temperature in the range 20ºC–95ºC, at a rate of 0.2 °C/minute and monitoring the absorbance changes at 295 nm, wavelength sensitive to GQ denaturation[327]. In order to prevent sample evaporation, a layer of mineral oil was added to the cuvettes.

To study if an *intermolecular* or *intramolecular* GQ is formed within *Gap-43* 5'GQ RNA probe, UV spectroscopy thermal denaturation experiments were performed at variable RNA concentrations ranging from 5–50 μM and a fixed KCl concentration of 5 mM in 10 mM cacodylic acid buffer, pH 6.5. In case of GQ structure formation between *n* number of RNA strands, the melting temperature (T_m) depends on the total RNA concentration (Equation 2) whereas the melting temperature of an intramolecular GQ structure (*n*=1) is independent of the RNA concentration (Equation 3)[323]:

$$\frac{1}{Tm} = \frac{R(n-1)}{\Delta H^\circ_{vH}} \ln C_T + \frac{\Delta S^\circ_{vH} - (n-1)R\ln 2 + R\ln n}{\Delta H^\circ_{vH}} \qquad [2]$$

$$\frac{1}{Tm} = \frac{\Delta S^\circ_{vH}}{\Delta H^\circ_{vH}} \qquad [3]$$

where *R* is the gas constant and ΔH°_{vH} and ΔS°_{vH} are the Van't Hoff thermodynamic parameters.

The thermodynamic parameters of the GQ structure were obtained by fitting the UV thermal denaturation curve to Equation 4, which assumes a two-state model:

$$A(T) = \frac{A_U + A_F e^{-\Delta H^O/RT} e^{\Delta S^O/R}}{e^{-\Delta H^O/RT} e^{\Delta S^O/RT} + 1} \qquad [4]$$

where A_U and A_F represent the absorbance of the unfolded and native GQ RNA structure, respectively, and R is the universal gas constant.

AHA Pulse Labeling

Cells were transfected with hnRNP-Q1 #1 or Scrambled siRNA 72 hours prior to labeling. The cells were washed with room temperature 1x PBS, incubated with DMEM without methionine (DMEM-Met, Life Technologies) for 1 hour at 37º C followed by incubation with 30 μg AHA (Life Technologies) or 100 μg AHA + 40 μM Anisomycin (Sigma-Aldrich) in DMEM-Met for 2 hours are 37º C. The cells were then washed with cold 1x PBS and lysed in 200 μL of click-it lysis buffer (50mM Tris-HCl, pH 8.0, 0.1% Sodium Dodecyl Sulfate) with 1x protease inhibitor (Roche) on ice. The lysates were sconicated and ~30 μg of protein from each condition was used in the click-it reaction. The click-it protein reaction buffer kit (Life Technologies) and 40 μM biotin alkyne (Life Technologies) were used according to the manufacture's instructions for the click-it reaction. After the click-it reaction, 180 μL of each condition was diluted with 820 μL IP buffer (RIPA buffer containing 1x protease inhibitor (Roche)) to stop to click-it reaction. 20 μl of GAP-43 antibody (1:50, Abcam) was added to each and the tubes were rotated at 4º C for 2 hours. Protein G agarose beads (Roche) were re-suspended in IP buffer, added to each tube and rotated at 4º C for 1 hour. After washing, the pellets, 1% input and 5% input were prepared for immunoblotting. Newly translated proteins and total GAP-43 protein were detected with IRDye 680LT Streptavidin (1:1,000, Li-Cor), anti-GAP-43 (1:5000, Abcam) and IRDye 800CW Donkey Anti-Mouse (1:20,000, Li-Cor). α-Tubulin (1:5,000, Sigma-Aldrich) was also detected as a loading control.

The 3x-Flag-mCherry-FL Gap43 or 3x-Flag-mCherry-Gap43 ΔGQ reporters were used for AHA labelling experiments as described above except for the following. The 3xFlag-mCherry-GAP-43 constructs were transfected ~56 hours after siRNA transfection and ~16 hours prior to AHA labelling and 100 μg of protein from each condition was used in the click-it reaction. Anti-Flag agarose beads (Sigma-Aldrich) were resuspended in IP buffer, added to the each condition and the tubes were rotated at 4º C for 2 hours. Newly translated proteins and total 3xFlag-mCherry-GAP-43 protein were detected with IRDye 680LT Streptavidin (1:1,000, Li-Cor), anti-Flag (1:5000, Sigma-Aldrich) and IRDye 800CW Donkey Anti-Mouse (1:20,000, Li-Cor). α-Tubulin (1:5,000, Sigma-Aldrich) was also detected as a loading control. N2a cells were transfected with 500ng of the 3xFlag-mCherry-GAP-43 constructs for ~16 hours to determine if the deleting the 5'GQ sequence causes GAP-43 to have increased expression as detected by immunoblot with anti-Flag (1:5000, Sigma-Aldrich).

Proximity Ligation

Cells were transfected with 40 pmol hnRNP-Q1 #1 or Scrambled siRNA 72 hours prior to labeling. The cells were washed with warm DMEM and incubated with DMEM with or without 91 μM Puromycin (Sigma-Aldrich) for 5 minutes at 37º C. Excess Puromycin was removed by incubating with cold extraction buffer (50 mM Tris-HCl, pH 7.5, 5 mM $MgCl_2$, 25 mM KCl, 0.015% Digitonin) for 2 minutes followed by wash buffer (50 mM Tris-HCl, pH 7.5, 5 mM $MgCl_2$, 25 mM KCl) for 2 minutes. Cells were fixed with 4% paraformaldehyde (Sigma-Aldrich) in 1x PBS for 10 minutes, washed with 1x PBS, permeabilized with 0.2% Triton X-100 in 1x PBS and washed with Tris-Glycine buffer. Cells

were blocked in 5% BSA for 1 hour at room temperature and incubated with primary antibody in 5% BSA for 1 hour at room temperature (1:1000 GAP-43 (Abcam) + 1:200 Puromycin (Developmental Studies Hybridoma Bank, Iowa City, IA) or 1:6000 α-Tubulin (Abcam) + 1:300 Puromycin (Developmental Studies Hybridoma Bank)). Cells were then washed with 1x PBS and the Duolink proximity ligations were performed according to the manufacturer's protocol (Sigma-Aldrich). Images were analyzed with Imaris (Bitplane). Cell volume was measured by creating a contour surface and puncta were selected and their volume and intensity was measured by setting a threshold.

Luciferase Assays

The mouse *Gap-43* 5'-UTR with and without the 5'GQ sequence or the just 5'GQ sequence (by annealing primers, forward: 5'-AGCTTTCAATCT TGGGAGGGAGGGAGGGATCAATCTTC-3' and reverse: 5'-CATGGAAGATTGATCCCTCCCTCCCTCCCAAGATTGAA-3') were subcloned into pGL3 (Promega) upstream of the firefly luciferase coding region with the HindIII and NcoI sites. Cells were transfected with 40 pmol hnRNP-Q1 #1 or Scrambled siRNA, 500 ng firefly luciferase construct and 25 ng renilla luciferase construct (pRL-CMV, Promega). After 72 hours, cells were trypsinized and resuspended in fresh DMEM. 50 μl of cell lysate in triplicate was processed for luciferase activity with the Dual-Glo luciferase assay system (Promega) according to the manufacturer's protocol and a Veritas microplate luminometer (Turner BioSystems/Promega). Renilla luminescence was used as an internal control.

4.5: Figures

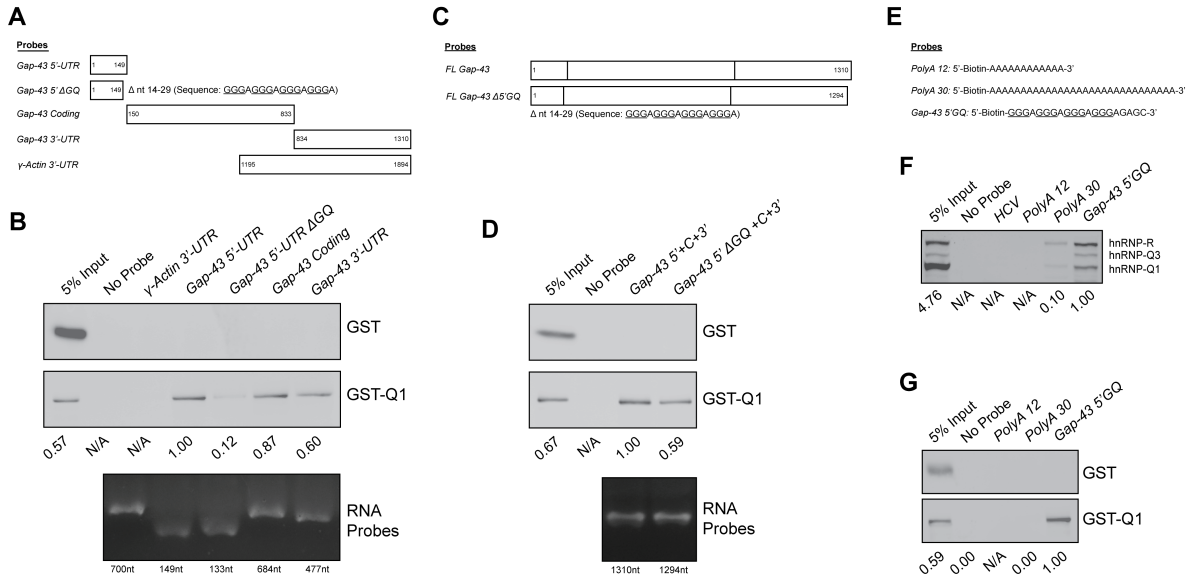

Figure 4-1: hnRNP-Q1 Directly Binds a *Gap-43* 5'-UTR G-Quadruplex Sequence. Biotinylated RNA probes corresponding to (A) specific *Gap-43* mRNA sequences and/or deletions, (A) the *γ-Actin* 3'-UTR or (C) full-length *Gap-43* mRNA, were *in vitro* transcribed (see (B, D) for RNA probe purity). Underlined nucleotides are predicted to be involved in GQ structure formation. The (C) sub-region or (D) full-length RNA probes were incubated with recombinant GST or GST-hnRNP-Q1 protein and precipitated with NeutrAvidin beads. Co-purified protein was assessed by GST immunoblot. (E) 5' biotin end labeled *Gap-43* 5'GQ, 12 nucleotide poly(A) and 30 nucleotide poly(A) RNA probes were incubated with (F) E17 *M. musculus* embryonic brain lysate or (G) recombinant GST or GST- hnRNP-Q1 protein and precipitated with NeutrAvidin beads. Co-purified protein was assessed by hnRNP-Q/R or GST immunoblot, respectively. Relative band intensity is listed below the immunoblots and RNA probe integrity is shown by formaldehyde gel electrophoresis.

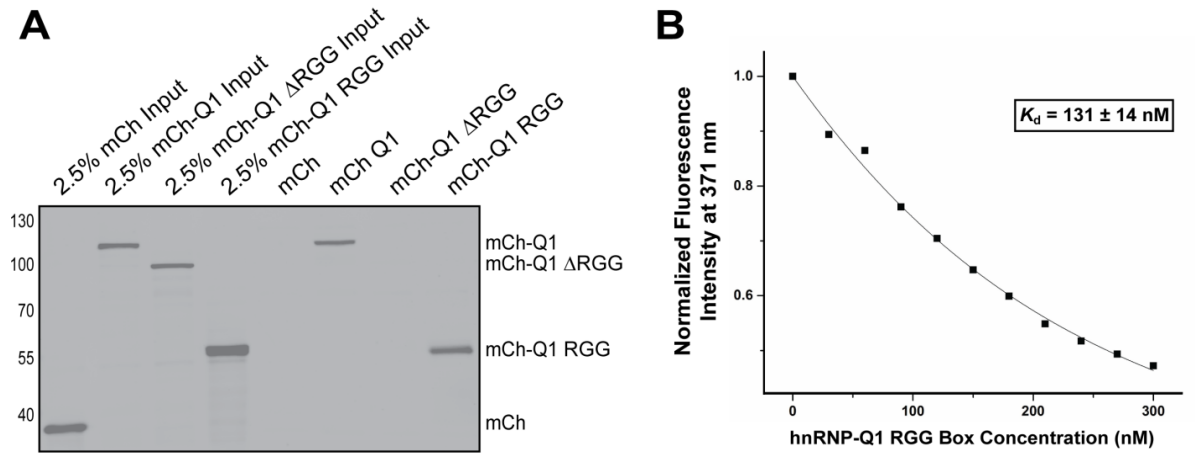

Figure 4-2: hnRNP-Q1 Binds the *Gap-43* 5'-UTR G-Quadruplex Sequence through the RGG Box. (A) 5' biotin end labeled *Gap-43* 5'GQ RNA probe was incubated with N2a cell lysates that were transfected with 3x-Flag-mCherry, 3x-Flag-mCherry-hnRNP-Q1, 3x-Flag-mCherry-hnRNP-Q1 ΔRGG Box or 3x-Flag-mCherry-hnRNP-Q1 RGG Box ~16 hours prior to lysing. The 5' GQ probe was precipitated with NeutrAvidin beads and co-purified protein was assessed by Flag immunoblot. (B) Representative fluorescence spectroscopy binding curve of the hnRNP-Q1 RGG box peptide and 2AP labeled *Gap-43* 5'GQ RNA probe complex in 150 mM KCl and in the presence of a 5-fold excess of the HCV core peptide. The K_d value determined from triplicate experiments was 131 ± 14 nM.

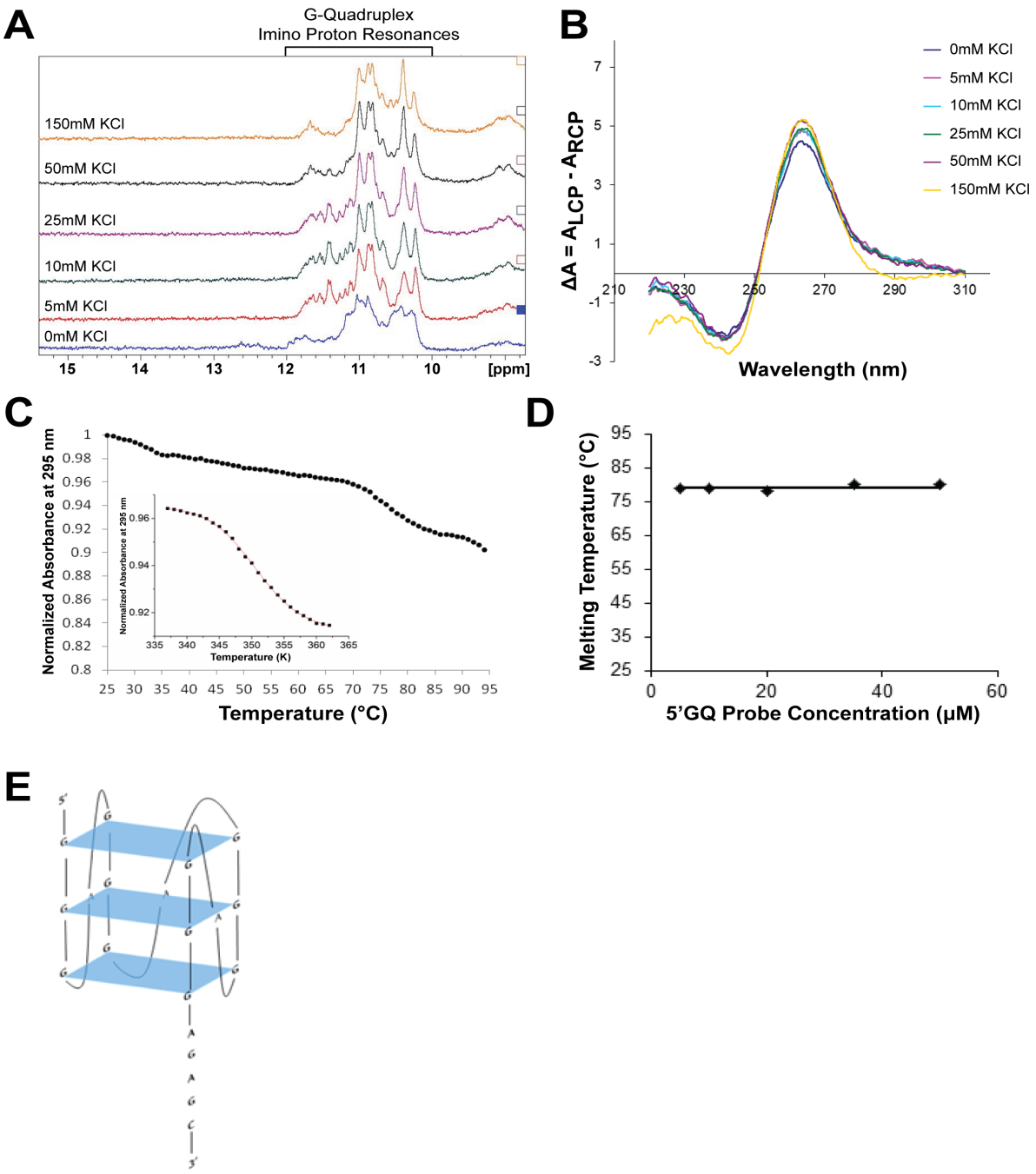

Figure 4-3: The *Gap-43* 5'-UTR G-Quadruplex Sequence Folds into a Stable Parallel, Intramolecular G-Quadruplex Structure. (A) 1D ^{1}H NMR spectroscopy with the *Gap-43* 5'GQ RNA probe reveals that imino proton resonances are present in the 10-12 ppm region even in the absence of KCl. (B) CD spectra of the *Gap-43* 5'GQ RNA probe in the presence of increasing KCl concentrations were acquired and the results fit the signature parallel GQ

curve (negative peak at ~240nm and a positive peak at ~265 nm). (C) UV spectroscopy thermal denaturation of the *Gap-43* 5'GQ RNA probe. Inset: Fit of the main hypochromic transition present in the UV thermal denaturation profile of the *Gap-43* 5'GQ RNA probe with Equation 4 (Materials and Methods) from which the following thermodynamic parameters were determined: ΔH^0 = -64.3±0.1 kcal/mol, ΔS^0 = -183.2±0.1 cal/mol K and ΔG^0 = -9.6±0.1 kcal/mol. (D) *Gap-43* 5'GQ RNA probe melting temperature at 5 mM KCl as a function of the RNA concentration. (E) Arrangement of the predicted GQ structure within the *Gap-43* 5'GQ RNA probe. QGRS Mapper software was used for the prediction[304].

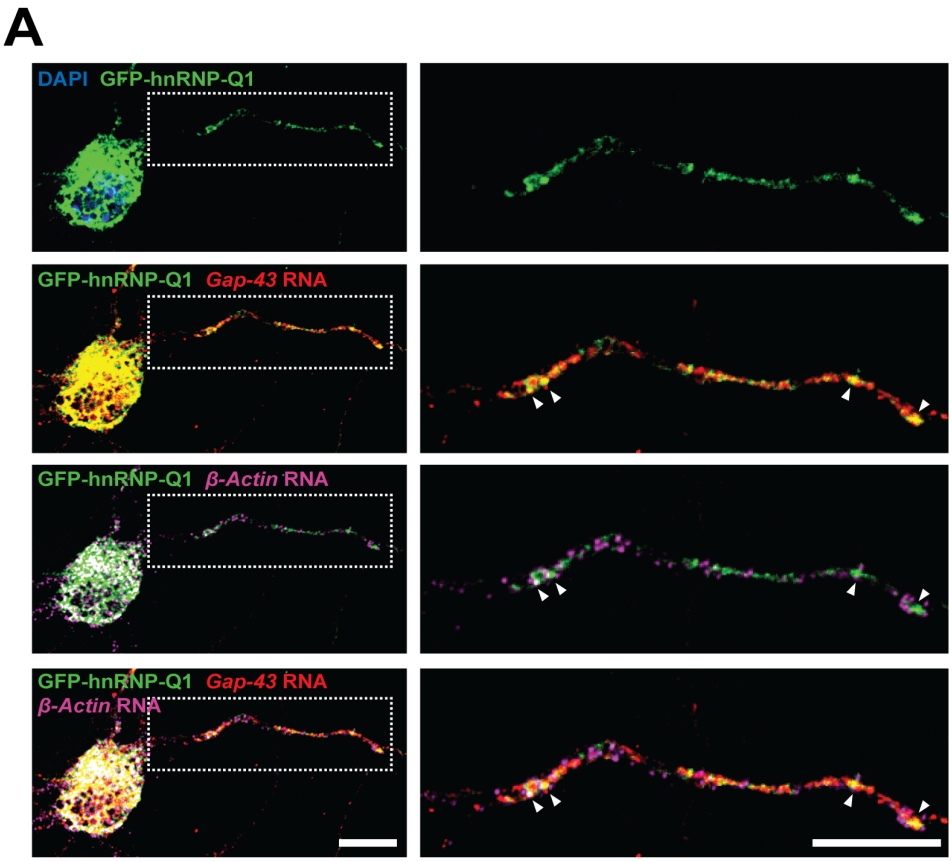
A
DAPI GFP-hnRNP-Q1
GFP-hnRNP-Q1 Gap-43 RNA
GFP-hnRNP-Q1 β-Actin RNA
GFP-hnRNP-Q1 Gap-43 RNA
β-Actin RNA
B
DAPI mCherry-GAP-43 FL
DAPI mCherry-GAP-43 Δ5'GQ
mCherry-GAP-43 FL RNA
mCherry-GAP-43 Δ5'GQ RNA

Figure 4-4: hnRNP-Q1 Co-localizes with *Gap-43* mRNA in the Neurites of Cortical Neurons. Primary cortical neurons were transfected with (A) pEGFP/hnRNP-Q1 or (B) the Gap-43 FL or Δ5'GQ reporters by nucleofection and cultured for ~120 hours. (A) *Gap-43* and *β-Actin* or (B) *mCherry* mRNAs were detected by fluorescence *in situ* hybridization and GFP positive cells were imaged. Scale bars = 10 μm

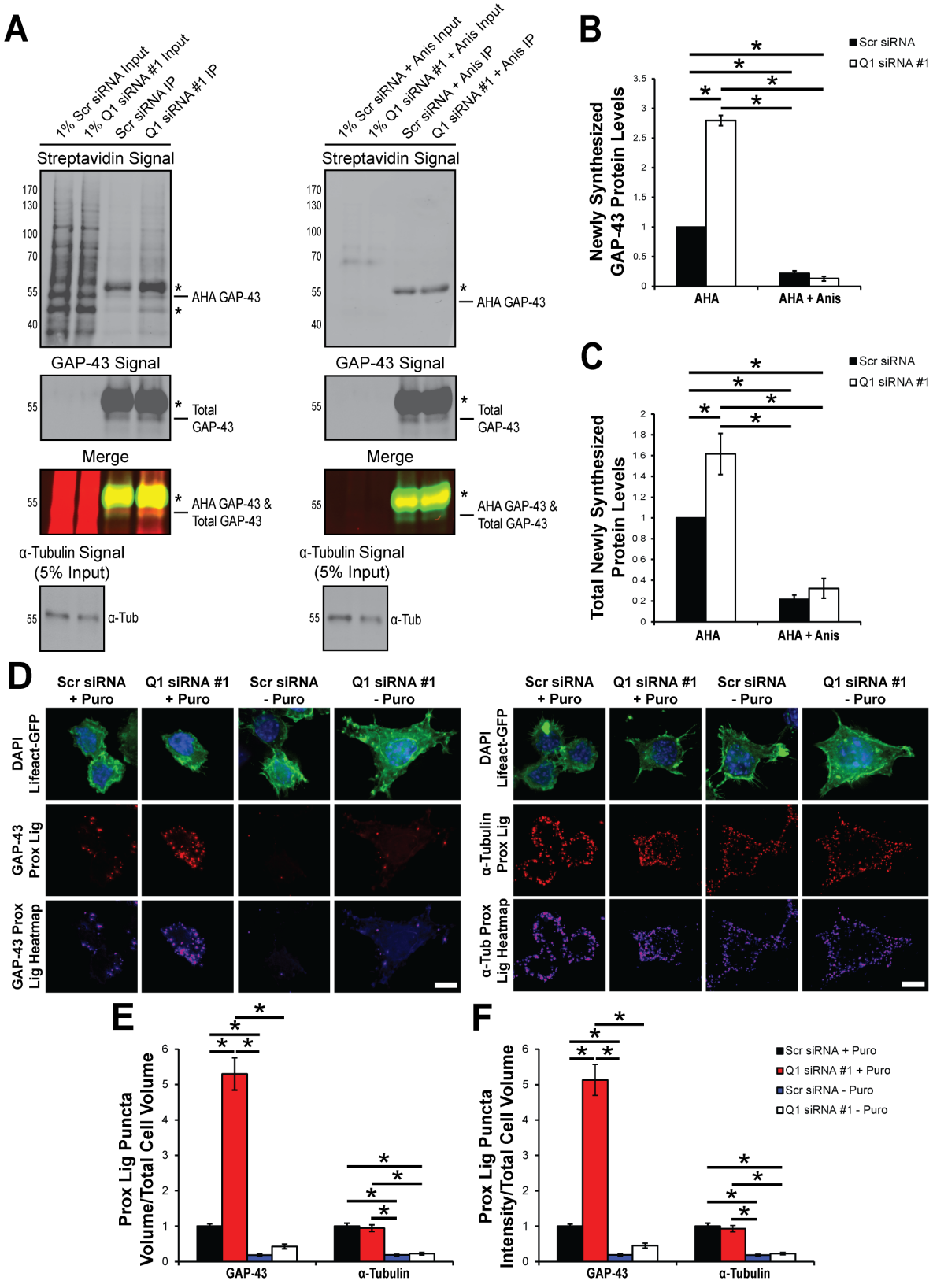
A
1% Scr siRNA Input
1% Q1 siRNA #1 Input
Scr siRNA IP
Q1 siRNA #1 IP
Streptavidin Signal
AHA GAP-43
GAP-43 Signal
Total GAP-43
Merge
AHA GAP-43 & Total GAP-43
α-Tubulin Signal (5% Input)
α-Tub
1% Scr siRNA + Anis Input
1% Q1 siRNA #1 + Anis Input
Scr siRNA + Anis IP
Q1 siRNA #1 + Anis IP
B
Scr siRNA
Q1 siRNA #1
Newly Synthesized GAP-43 Protein Levels
AHA
AHA + Anis
C
Total Newly Synthesized Protein Levels
D
Scr siRNA + Puro
Q1 siRNA #1 + Puro
Scr siRNA - Puro
Q1 siRNA #1 - Puro
DAPI Lifeact-GFP
GAP-43 Prox Lig
GAP-43 Prox Lig Heatmap
α-Tubulin Prox Lig
α-Tub Prox Lig Heatmap
E
Prox Lig Puncta Volume/Total Cell Volume
GAP-43
α-Tubulin
F
Prox Lig Puncta Intensity/Total Cell Volume

Figure 4-5: hnRNP-Q1 Represses Endogenous *Gap-43* mRNA Translation. N2a cells were transfected with hnRNP-Q1 #1 or Scrambled siRNA for 72 hours, starved of methionine for 1 hour and labeled with the methionine analog AHA or AHA + anisomycin for 2 hours. AHA incorporated into newly synthesized proteins was labeled with biotin, endogenous GAP-43 protein was immunoprecipitated and newly synthesized GAP-43 protein was visualized by immunoblot with streptavidin and anti-GAP-43. (A) Representative images. Top panels show the streptavidin signal, middle panels show total GAP-43 and AHA GAP-43/total GAP-43 merged signals and bottom panels show α-Tubulin signal from 5% input. * = non-specific bands. Quantification of (B) AHA GAP-43 protein levels normalized to total α-Tubulin protein levels from 1% or 5% input and (C) total AHA protein levels from 1% input normalized to total α-Tubulin protein levels from 1% or 5% input. n=3, two-way ANOVA, Tukey's post-hoc, GAP-43 p-values: Scr + AHA vs Scr + Anis $p<0.0001$, Scr + AHA vs Q1 + AHA $p<0.0001$, Scr + AHA vs Q1 + Anis $p<0.0001$, Scr + Anis vs Q1 + AHA $p<0.0001$, Scr + Anis vs Q1 + Anis $p=0.6392$, Q1 + AHA vs Q1 + Anis $p<0.0001$, Total p-values: Scr + AHA vs Scr + Anis $p=0.0048$, Scr + AHA vs Q1 + AHA $p=0.0188$, Scr + AHA vs Q1 + Anis $p=0.0111$, Scr + Anis vs Q1 + AHA $p<0.0001$, Scr + Anis vs Q1 + Anis $p=0.9069$, Q1 + AHA vs Q1 + Anis $p=0.0002$. (D) N2a cells were transfected with hnRNP-Q1 #1 or Scrambled siRNA for 72 hours and incubated with or without Puromycin for 5 minutes. The cells were fixed and actively translating GAP-43 and α-Tubulin was detected by proximity ligation. Representative images with corresponding heatmaps are shown. Scale bar = 10 μm. Quantification of (E) proximity ligation puncta volume/total cell volume and (F) proximity ligation puncta signal intensity/total cell volume. n=3, GAP-43: Scr + Puro: 126 cells, Q1 + Puro: 105 cells, Scr - Puro: 107, cells, Q1 - Puro:

109 cells, α-Tubulin: Scr + Puro: 107 cells, Q1 + Puro: 109 cells, Scr - Puro: 113, cells, Q1 - Puro: 118 cells from 3 independent experiments, two-way ANOVA, Tukey's post-hoc, GAP-43 Volume p-values: Scr + Puro vs Scr - Puro p=0.0419, Scr + Puro vs Q1 + Puro p<0.0001, Scr + Puro vs Q1 - Puro p=0.2397, Scr - Puro vs Q1 + Puro p<0.0001, Scr - Puro vs Q1 - Puro p=0.8760, Q1 + Puro vs Q1 - Puro p<0.0001, α-Tubulin Volume p-values: Scr + Puro vs Scr - Puro p<0.0001, Scr + Puro vs Q1 + Puro p=0.9408, Scr + Puro vs Q1 - Puro p<0.0001, Scr - Puro vs Q1 + Puro p<0.0001, Scr - Puro vs Q1 - Puro p=0.9826, Q1 + Puro vs Q1 - Puro p<0.0001, GAP-43 Intensity p-values: Scr + Puro vs Scr - Puro p=0.0318, Scr + Puro vs Q1 + Puro p<0.0001, Scr + Puro vs Q1 - Puro p=0.2403, Scr - Puro vs Q1 + Puro p<0.0001, Scr - Puro vs Q1 - Puro p=0.8303, Q1 + Puro vs Q1 - Puro p<0.0001, α-Tubulin Intensity p-values: Scr + Puro vs Scr - Puro p<0.0001, Scr + Puro vs Q1 + Puro p=0.8904, Scr + Puro vs Q1 - Puro p<0.0001, Scr - Puro vs Q1 + Puro p<0.0001, Scr - Puro vs Q1 - Puro p=0.9753, Q1 + Puro vs Q1 - Puro p<0.0001.

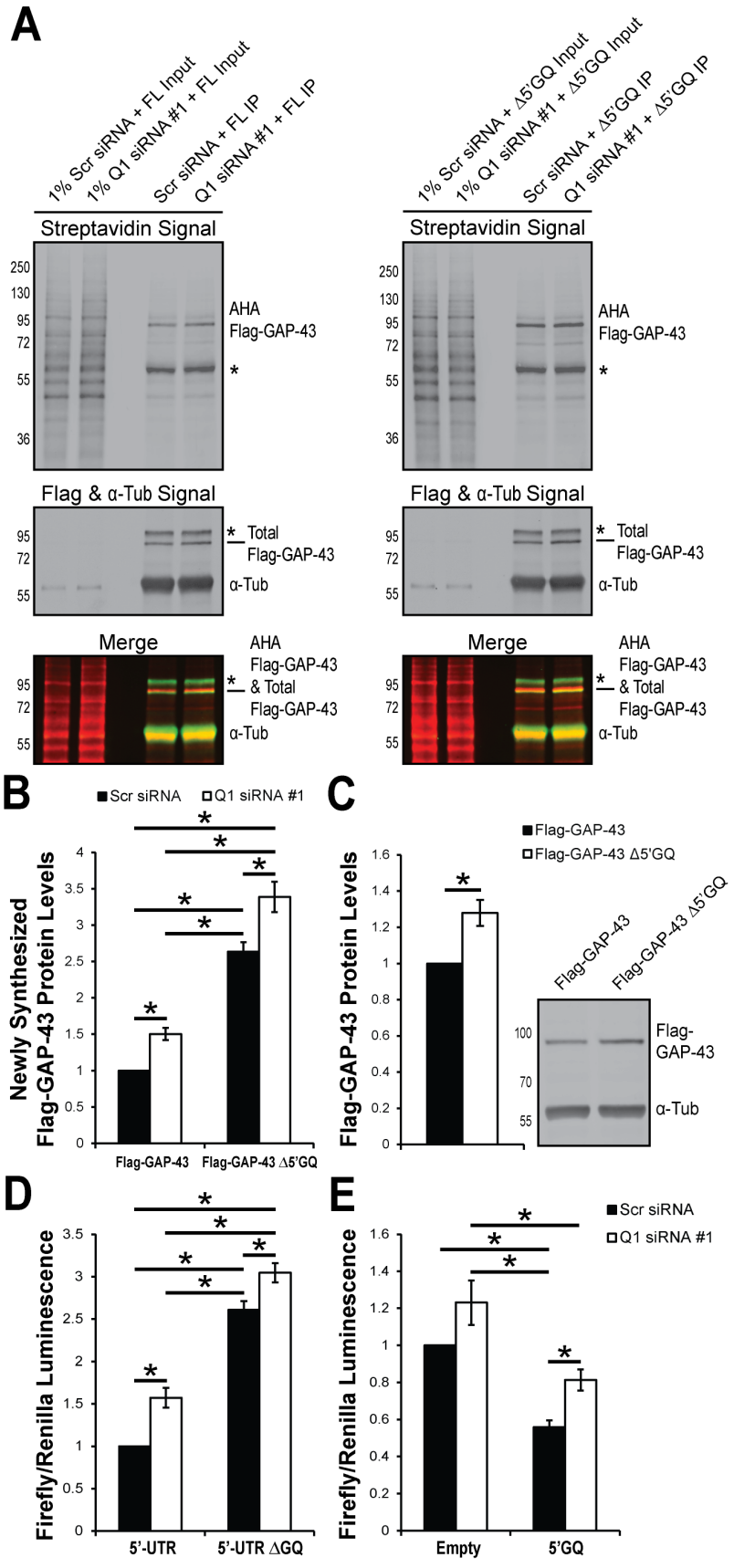
A
1% Scr siRNA + FL Input
1% Q1 siRNA #1 + FL Input
Scr siRNA + FL IP
Q1 siRNA #1 + FL IP
1% Scr siRNA + Δ5'GQ Input
1% Q1 siRNA #1 + Δ5'GQ Input
Scr siRNA + Δ5'GQ IP
Q1 siRNA #1 + Δ5'GQ IP
Streptavidin Signal
250
130
95
72
55
36
AHA
Flag-GAP-43
*
Flag & α-Tub Signal
Total
Flag-GAP-43
α-Tub
Merge
AHA
Flag-GAP-43
& Total
Flag-GAP-43
α-Tub
B
Scr siRNA
Q1 siRNA #1
Newly Synthesized Flag-GAP-43 Protein Levels
Flag-GAP-43
Flag-GAP-43 Δ5'GQ
C
Flag-GAP-43
Flag-GAP-43 Δ5'GQ
Flag-GAP-43 Protein Levels
100
70
55
Flag-GAP-43
α-Tub
D
Firefly/Renilla Luminescence
5'-UTR
5'-UTR ΔGQ
E
Scr siRNA
Q1 siRNA #1
Firefly/Renilla Luminescence
Empty
5'GQ

Figure 4-6: hnRNP-Q1 Represses *Gap-43* Translation through the 5'-UTR G-Quadruplex Sequence. N2a cells were transfected with 3xFlag-mCherry-tagged GAP-43 reporters with (FL) and without (ΔGQ) the 5'GQ ~56 hours after hnRNP-Q1 #1 or Scrambled siRNA transfection. After ~16 hours, the cells where starved of methionine for 1 hour and labeled with the methionine analog AHA for 2 hours. AHA incorporated into newly synthesized proteins was labeled with biotin, 3xFlag-mCherry-tagged GAP-43 was immunoprecipitated and newly synthesized 3xFlag-mCherry-tagged GAP-43 (predicted to be ~75 kDa) was visualized by immunoblot with streptavidin and anti-Flag. (A) Representative images. Top panels show the streptavidin signal and bottom panels show total Flag and α-Tubulin signal and AHA Flag-GAP- 43/Total Flag-GAP-43 merged signals. * = non-specific bands. (B) Quantification of AHA Flag-GAP-43 protein levels normalized to total α-Tubulin protein levels from 1% or 5% input. n=6, two-way ANOVA, Holm Sidak's post-hoc, p-values: Scr + FL vs Scr + ΔGQ $p<0.0001$, Scr + FL vs Q1 + FL $p=0.0127$, Scr + FL vs Q1 + ΔGQ $p<0.0001$, Scr + ΔGQ vs Q1 + FL $p<0.0001$, Scr + ΔGQ vs Q1 + ΔGQ $p=0.0011$, Q1 + FL vs Q1 + ΔGQ $p<0.0001$. (C) The 3xFlag-mCherry tagged GAP-43 reporter constructs were overexpressed in N2a cells for ~16 hours and reporter expression was visualized by Flag immunoblot. n=5, one-sample t-test, p-value=0.0177. (D) N2a cells were transfected with hnRNP-Q1 #1 or Scrambled siRNA, the 5' or 5'ΔGQ firefly luciferase construct and a renilla luciferase construct for normalization. After 72 hours, the cells were trypsinized and processed for luciferase activity. n=5, two-way ANOVA, Tukey's post-hoc, p-values: Scr + 5' vs Scr + ΔGQ $p<0.0001$, Scr + 5' vs Q1 + 5' $p=0.0035$, Scr + 5' vs Q1 + ΔGQ $p<0.0001$, Scr + ΔGQ vs Q1 + 5' $p<0.0001$, Scr + ΔGQ vs Q1 + ΔGQ $p=0.0248$, Q1 + 5' vs Q1 + ΔGQ $p<0.0001$. (E) N2a cells were transfected with hnRNP-Q1 #1 or Scrambled siRNA, the

5’GQ or empty vector firefly luciferase construct and a renilla luciferase construct for normalization. After 72 hours, the cells were trypsinized and processed for luciferase activity. n=6, two-way ANOVA, Holm Sidak’s post-hoc, p-values: Scr + E vs Scr + 5’GQ p=0.0010, Scr + E vs Q1 + E p=0.0543, Scr + E vs Q1 + 5’GQ p=0.0694, Scr + 5’GQ vs Q1 + E p<0.0001, Scr + 5’GQ vs Q1 + 5’GQ p=0.0492, Q1 + E vs Q1 + 5’GQ p=0.0014.

4.6: Supplemental Figures

A Ms *Gap-43* mRNA

```
1 agagggaggg agagggaggg agggaggg ag agcgcgctag cgcgagagag cgagtgagca
61 agcgagcaga aaagaggtgg agagggggg aataaggaag agaggaggaa aggagagaag
121 gcaggaagaa ggcaggggaa gataccacc A TGCTGTGCTG TATGAGAAGA ACCAAACAGG
181 TTGAAAAGAA TGATGAGGAC CAAAAGATTG AACAAGATGG TGTCAAGCCG GAAGATAAGG
241 CTCATAAGGC TGCGACCAAA ATTCAGGCTA GCTTCCGTGG ACACATAACA AGGAAAAAGC
301 TCAAAGGCGA GAAGAAGGGT GATGCACCAG CTGCTGAGGC CGAGGCCAAG GAGAAGGATG
361 ATGCTCCCGT TGCTGATGGT GTGGAGAAGA AGGAGGGAGA TGGCTCTGCT ACTACCGATG
421 CAGCCCCAGC CACCAGCCCC AAGGCTGAGG AGCCCAGCAA GGCAGGAGAT GCACCTTCTG
481 AGGAGAAGAA GGGTGAAGGG GATGCGGCCC CCTCCGAGGA AAAGGCCGGC TCAGCGGAGA
541 CAGAAAGTGC TGCTAAAGCT ACCACTGATA ACTCCCCGTC CTCCAAGGCT GAAGATGGCC
601 CAGCCAAGGA GGAGCCTAAA CAAGCCGATG TGCCTGCTGC TGTCACTGAT GCTGCTGCCA
661 CCACCCCTGC TGCAGAGGAT GCTGCCACCA AGGCAGCGCA GCCTCCAACG GAGACTGCAG
721 AAAGCAGCCA AGCTGAGGAG GAGAAAGACG CTGTAGACGA AGCCAAACCT AAGGAAAGTG
781 CCCGACAGGA TGAGGGTAAA GAAGACCCCG AGGCTGACCA AGAACATGCC TGAactttaa
841 gaaatggctt tccacgttgc ccccacctga accctgtctc tcctgccctt ctcagctcca
901 ctctgaagtt tcctctcctg tcctgctcac gtgtgtgagc ctgtcctctc ctacctatga
961 gccctctctc tctgtgtggc aaacatttaa agaaaaaaaa aaagcaggaa agatcccaag
1021 tccaacagtg tggcttaaac atttgtttct tggtgttgtt atggcgagtt tttggtaatg
1081 atgatgcagt catcttggga aattcttgca ctgtaccccg gttttttgat ctggtgcgtg
1141 tggccctgtg ggagtccact ttcctctcta tttctctctg ttccaagtgt gtgtgtgcaa
1201 tgttccgttc tgaggagtcc aaaatattaa gtgaattcaa aaaccatttc tgtttcctca
1261 ttttcaatgt gatggaatga acaaaaaggt taaaaaatta aaaaaaaaaa
```

B Hu *Gap-43* mRNA Isoform 1

```
1 actgaaggct agagaacaat tccgagaaag agacggagag agagggaaga aaaagacaga
61 tagatagata ttgggggaa ggagaaaaaa ggagaagaga ggaagagag gacagcggag
121 agagagcacc agagagagag ggagagagag agagagcgct agagagaggg agcgagcatg
181 tgcgatgagc aatagctgtg gaccttacag ttgctgctaa ctgccctggt gtgtgtgagg
241 gagagagagg gagggaggga gagagagcgc gctagcgcga gagagcgagt gagcaagcga
301 gcagaaaaga ggtggagagg ggggaataa gaaagagaga gaaggaaagg agagaaggca
361 ggaagaaggc aaggg acgag acaaccATGC TGTGCTGTAT GAGAAGAACC AAACAGGTTG
421 AAAAAAATGA TGACGACCAA AAGATTGAAC AAGATGGTAT CAAACCAGAA GATAAAGCTC
481 ATAAGGCCGC AACCAAAATT CAGGCTAGCT TCCGTGGACA CATAACAAGG AAAAAGCTCA
541 AAGGAGAGAA GAAGGATGAT GTCCAAGCTG CTGAGGCTGA AGCTAATAAG AAGGATGAAG
601 CCCCTGTTGC CGATGGGGTG GAGAAGAAGG GAGAAGGCAC CACTACTGCC GAAGCAGCCC
661 CAGCCACTGG CTCCAAGCCT GATGAGCCCG GCAAAGCAGG AGAAACTCCT TCCGAGGAGA
721 AGAAGGGGGA GGGTGATGCT GCCACAGAGC AGGCAGCCCC CCAGGCTCCT GCATCCTCAG
781 AGGAGAAGGC CGGCTCAGCT GAGACAGAAA GTGCCACTAA AGCTTCCACT GATAACTCGC
841 CGTCCTCCAA GGCTGAAGAT GCCCCAGCCA AGGAGGAGCC TAAACAAGCC GATGTGCCTG
901 CTGCTGTCAC TGCTGCTGCT GCCACCACCC CTGCCGCAGA GGATGCTGCT GCCAAGGCAA
961 CAGCCCAGCC TCCAACGGAG ACTGGGGAGA GCAGCCAAGC TGAAGAGAAC ATAGAAGCTG
1021 TAGATGAAAC CAAACCTAAG GAAAGTGCCC GGCAGGACGA GGGTAAAGAA GAGGAACCTG
1081 AGGCTGACCA AGAACATGCC TGAactctaa gaaatggctt tccacatccc caccctcccc
1141 tctcctgagc ctgtctctcc ctaccctctt ctcagctcca ctctgaagtc ccttcctgtc
1201 ctgctcacgt ctgtgagtct gtcctttccc acccactagc cctctttctc tctgtgtggc
1261 aaacatttaa aaaaaaaaaa aaaaagcagg aaagatccca agtcaaacag tgtggcttaa
1321 acatttttg tttcttggtg ttgttatggc aagtttttgg taatgatgat tcaatcattt
1381 tgggaaattc ttgcactgta tccaagttat ttgatctggt gcgtgtggcc ctgtgggagt
1441 ccactttcct ctctctctct ctctctgttc caagtgtgtg tgcaatgttc cgttcatctg
1501 aggagtccaa aatatcgagt gaattcaaaa tcatttttgt tttcctcctt ttcaatgtga
1561 tggaatgaac aaaaaggaaa aaattcaaaa aacccagttt gttttaaaaa taaataaata
1621 aagcaaatgt gccaattagc gtaaacttgc ggctctaagg ctcctttttc aacccgaata
1681 ttaataaatc atgagagtaa tcaaggtc
```

C Hu *Gap-43* mRNA Isoform 2

```
1 actgaaggct agagaacaat tccgagaaag agacggagag agagggaaga aaaagacaga
61 tagatagata ttgggggaa ggagaaaaaa ggagaagaga ggaagagag gacagcggag
121 agagagcacc agagagagag ggagagagag agagagcgct agagagaggg agcgagcatg
181 tgcgatgagc aatagctgtg gaccttacag ttgctgctaa ctgccctggt gtgtgtgagg
241 gagagagagg gagggaggga gagagagcgc gctagcgcga gagagcgagt gagcaagcga
301 gcagaaaaga ggtggagagg ggggaataa gaaagagaga gaaggaaagg agagaaggca
361 ggaagaaggc aaggg acgag acaaccATGC TGTGCTGTAT GAGAAGAACC AAACAGGTTG
421 AAAAAAATGA TGACGACCAA AAGATTGAAC AAGATGGTAT CAAACCAGAA GATAAAGCTC
481 ATAAGGCCGC AACCAAAATT CAGGCTAGCT TCCGTGGACA CATAACAAGG AAAAAGCTCA
541 AAGGAGAGAA GAAGGATGAT GTCCAAGCTG CTGAGGCTGA AGCTAATAAG AAGGATGAAG
601 CCCCTGTTGC CGATGGGGTG GAGAAGAAGG GAGAAGGCAC CACTACTGCC GAAGCAGCCC
661 CAGCCACTGG CTCCAAGCCT GATGAGCCCG GCAAAGCAGG AGAAACTCCT TCCGAGGAGA
721 AGAAGGGGGA GGGTGATGCT GCCACAGAGC AGGCAGCCCC CCAGGCTCCT GCATCCTCAG
781 AGGAGAAGGC CGGCTCAGCT GAGACAGAAA GTGCCACTAA AGCTTCCACT GATAACTCGC
841 CGTCCTCCAA GGCTGAAGAT GCCCCAGCCA AGGAGGAGCC TAAACAAGCC GATGTGCCTG
901 CTGCTGTCAC TGCTGCTGCT GCCACCACCC CTGCCGCAGA GGATGCTGCT GCCAAGGCAA
961 CAGCCCAGCC TCCAACGGAG ACTGGGGAGA GCAGCCAAGC TGAAGAGAAC ATAGAAGCTG
1021 TAGATGAAAC CAAACCTAAG GAAAGTGCCC GGCAGGACGA GGGTAAAGAA GAGGAACCTG
1081 AGGCTGACCA AGAACATGCC TGAactctaa gaaatggctt tccacatccc caccctcccc
1141 tctcctgagc ctgtctctcc ctaccctctt ctcagctcca ctctgaagtc ccttcctgtc
1201 ctgctcacgt ctgtgagtct gtcctttccc acccactagc cctctttctc tctgtgtggc
1261 aaacatttaa aaaaaaaaaa aaaaagcagg aaagatccca agtcaaacag tgtggcttaa
1321 acatttttg tttcttggtg ttgttatggc aagtttttgg taatgatgat tcaatcattt
1381 tgggaaattc ttgcactgta tccaagttat ttgatctggt gcgtgtggcc ctgtgggagt
1441 ccactttcct ctctctctct ctctctgttc caagtgtgtg tgcaatgttc cgttcatctg
1501 aggagtccaa aatatcgagt gaattcaaaa tcatttttgt tttcctcctt ttcaatgtga
1561 tggaatgaac aaaaaggaaa aaattcaaaa aacccagttt gttttaaaaa taaataaata
1621 aagcaaatgt gccaattagc gtaaacttgc ggctctaagg ctcctttttc aacccgaata
1681 ttaataaatc atgagagtaa tcaaggtc
```

D Ms *Gap-43* mRNA

Position	Region	Sequence	G-Score
14	5'-UTR	GGGAGGGAGGGAGGG	42
88	5'-UTR	GGGAAUAAGGAAGAGAGGAGGAAAGG	21
338	Coding	GGCCGAGGCCAAGGAGAAGG	21
482	Coding	GGAGAAGAAGGGUGAAGGGAUGCGG	19
76	5'-UTR	GGUGGAGAGGGG	18
120	5'-UTR	GGCAGGAAGAAGGCAGG	18
518	Coding	GGAAAAGGCCGGCUCAGCGG	17
378	Coding	GGUGUGGAGAAGAAGGAGGG	16
443	Coding	GGCUGAGGAGCCCAGCAAGGCAGG	13
587	Coding	GGCUGAAGAUGGCCCAGCCAAGGAGG	13

E Hu *Gap-43* mRNA Isoforms 1/2

Position	Region	Sequence	G-Score
239	5'-UTR	GGGAGAGAGAGGGAGGGAGGG	36
73	5'-UTR	GGGGGGAAGGAGAAAAAAGGAGAAGAGAGG	19
311	5'-UTR	GGUGGAGAGGGGGGG	19
357	5'-UTR	GGCAGGAAGAAGGCAAGGG	18
1011/615	Coding	GGGGUGGAGAAGAAGGGAGAAGG	17
1451/1055	Coding	GGACGAGGGUAAAGAAGAGGAACCUGAGG	17
1112/716	Coding	GGAGAAGAAGGGGGAGG	15
1160/764	Coding	GGCUCCTGCAUCCUCAGAGGAGAAGGCCGG	7

Supplemental Figure 4-1: Predicted G-Quadruplex Sequences in *Gap-43* mRNA.

Predicted GQ sequences in (A) *M. musculus*, (B) *H. sapiens* isoform 1 and (C) *H. sapiens* isoform 2 *Gap-43* mRNA as determined by the QGRS Mapper software[304]. The position, mRNA region, sequence and G-score of each predicted sequence is also listed for (D) *M. musculus* and (E) *H. sapiens* isoform 1/2 *Gap-43* mRNA. Red underlined nucleotides are predicted to be involved in GQ structure formation.

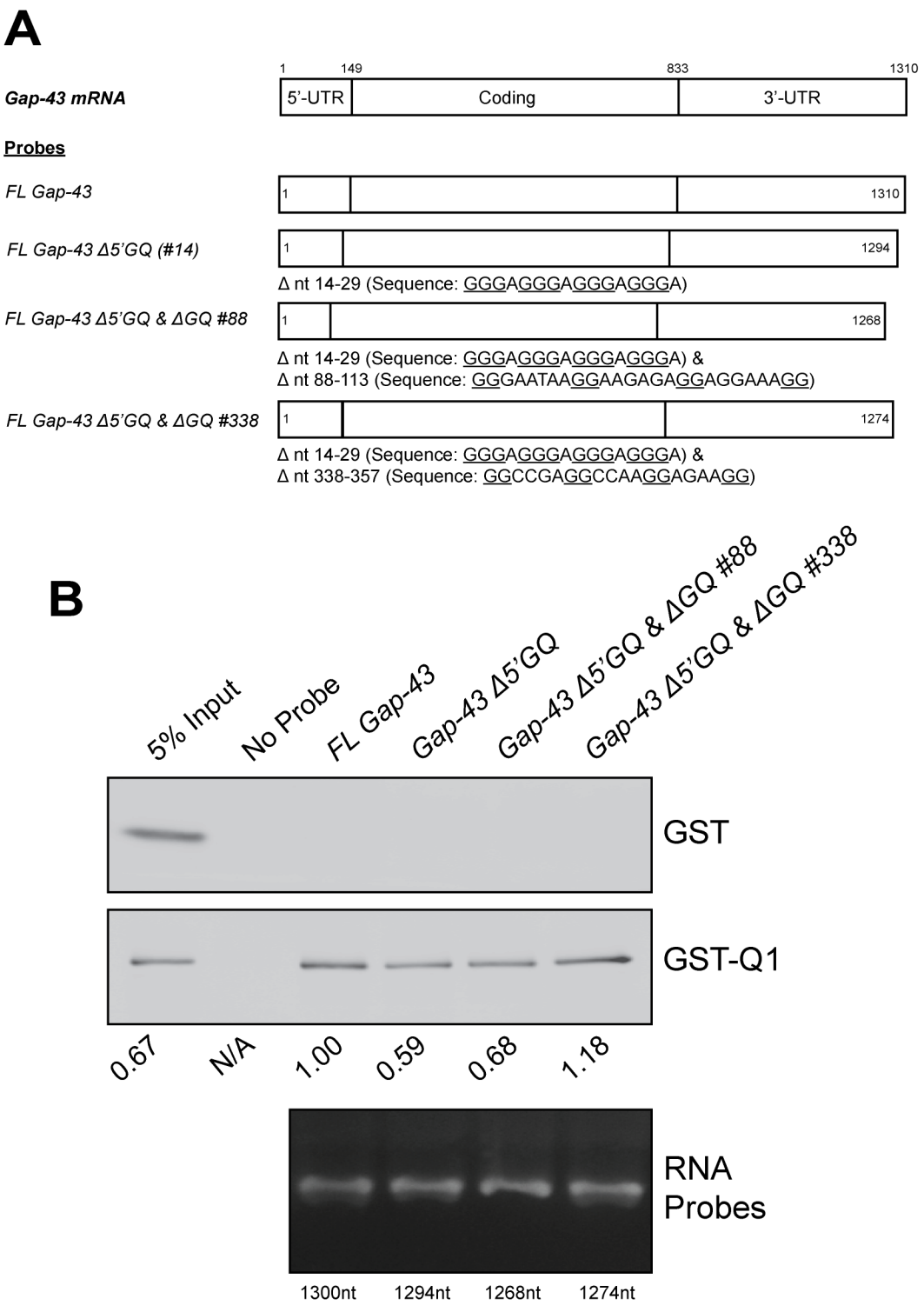

Supplemental Figure 4-2: hnRNP-Q1 does not Bind Additional *Gap-43* G-Quadruplex Sequences. Biotinylated RNA probes corresponding to full-length *Gap-43* mRNA with or

without deletion of GQs #14 (5'GQ), #88 and #338 were *in vitro* transcribed (see (B) for RNA probe purity). Underlined nucleotides are predicted to be involved in GQ structure formation. (B) The RNA probes were incubated with recombinant GST or GST-hnRNP-Q1 protein and precipitated with NeutrAvidin beads. Co-purified protein was assessed by GST immunoblot. Relative band intensity is listed below the immunoblots and RNA probe integrity is shown by formaldehyde gel electrophoresis.

A

RNA Probe Sequences

PolyA 12: 5'-Biotin-AAAAAAAAAAAA-3'

PolyA 30: 5'-Biotin-AAAAAAAAAAAAAAAAAAAAAAAAAAAAAA-3'

Gap-43 5'GQ: 5'-Biotin-GGGAGGGAGGGAGGGAGAGC-3' (G-Score = 42)

Shank1a: 5'-Biotin-GGGGUUGGGGAGGGUGUAGGGGGUGGGG-3' (G-Score = 57)

Shank1b: 5'-Biotin-GGGGAGGAGAGGUCGGGGUGGGGAGUGGGG-3' (G-Score = 54)

NR2B: 5'-Biotin-GGGUACGGGAGGGUAAGGCUGUGGGUCGCGUG-3' (G-Score = 34)

p250gap: 5'-Biotin-GGGUGGGGUGGGGGGUGGCAG-3' (G-Score = 50)

Smndc1: 5'-Biotin-GGGGACCGGGUCGGGUGGGGCUGGG-3' (G-Score = 42)

Psd-95: 5'-Biotin-GGGAAAAGGGAGGGAUGGGUCUAGGGAGUGGGAAAUGGGGAGGGAGGGUGGG-3' (G-Scores = 40 & 42)

B

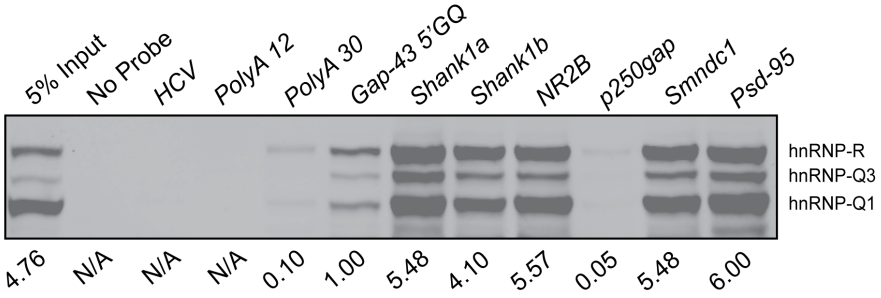

Supplemental Figure 4-3: hnRNP-Q1 Binds to Several G-Quadruplex Sequences but not PolyA RNA. (A) 5' biotin end labeled 12 nucleotide poly(A), 30 nucleotide poly(A), *Gap-43* 5'GQ, *Shank1a*, *Shank1b*, *NR2B*, *p250gap*, *Smndc1* and *Psd-95* RNA probes were used for biotin pulldown experiments. Underlined nucleotides are predicted to be involved in GQ structure formation and the G-scores for each GQ are listed (QGRS Mapper[304]). (B) The RNA probed were incubated with E17 *M. musculus* embryonic brain lysate, precipitated with NeutrAvidin beads and co-purified protein was assessed by hnRNP-Q/R immunoblot. Relative signal intensity is displayed below the blots.

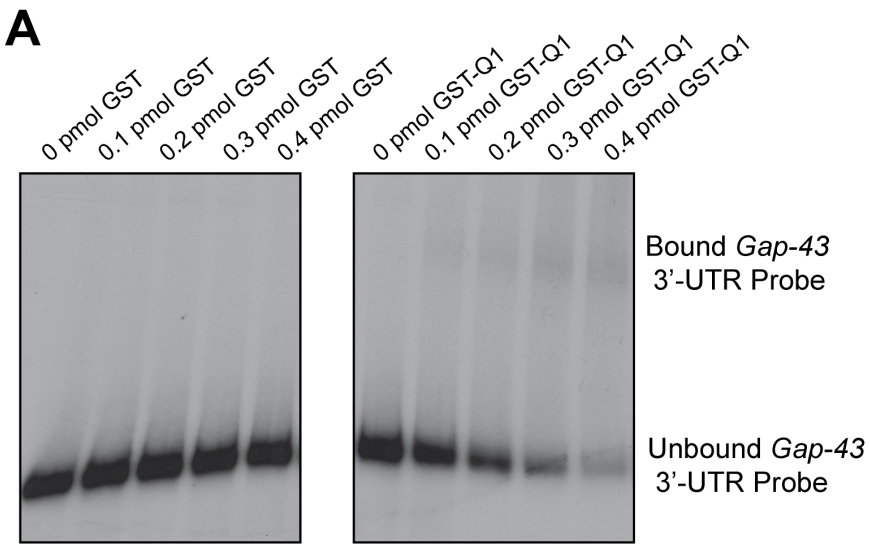
A
0 pmol GST
0.1 pmol GST
0.2 pmol GST
0.3 pmol GST
0.4 pmol GST
0 pmol GST-Q1
0.1 pmol GST-Q1
0.2 pmol GST-Q1
0.3 pmol GST-Q1
0.4 pmol GST-Q1
Bound Gap-43 3'-UTR Probe
Unbound Gap-43 3'-UTR Probe

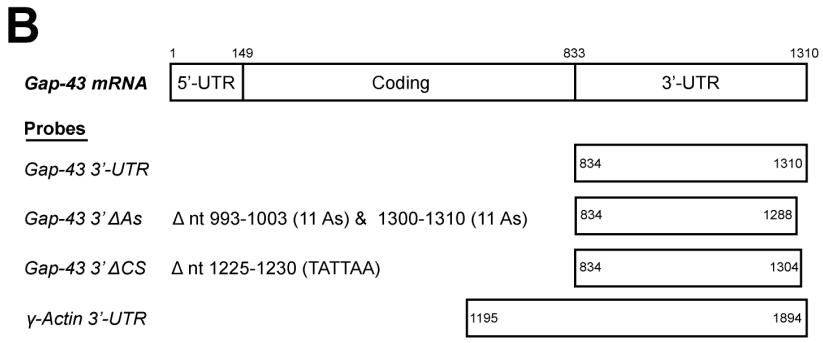
B
1
149
833
1310
Gap-43 mRNA
5'-UTR
Coding
3'-UTR
Probes
Gap-43 3'-UTR
834
1310
Gap-43 3'ΔAs
Δ nt 993-1003 (11 As) & 1300-1310 (11 As)
834
1288
Gap-43 3'ΔCS
Δ nt 1225-1230 (TATTAA)
834
1304
γ-Actin 3'-UTR
1195
1894

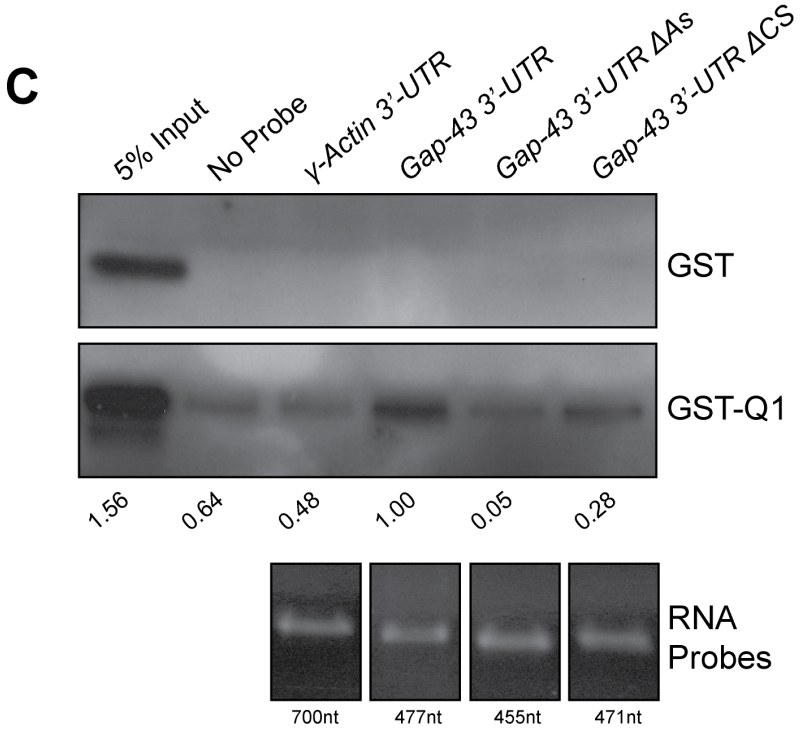
C
5% Input
No Probe
γ-Actin 3'-UTR
Gap-43 3'-UTR
Gap-43 3'-UTR ΔAs
Gap-43 3'-UTR ΔCS
GST
GST-Q1
1.56
0.64
0.48
1.00
0.05
0.28
RNA Probes
700nt
477nt
455nt
471nt

Supplemental Figure 4-4: hnRNP-Q1 Directly Binds *Gap-43* 3'-UTR PolyA Stretches and a Consensus Sequence. (A) Radioactive RNA probes corresponding to the *Gap-43* 3'-UTR were *in vitro* transcribed. The RNA probes were incubated with increasing concentrations of GST or GST-hnRNP-Q1 and binding was assessed by 5% native gel electrophoresis. Radioactive signal was detected by exposing the gel to film. (B) Biotinylated RNA probes corresponding to the 3'-UTR of *Gap-43* mRNA with or without deletion of two 11 nucleotide polyA stretches and the consensus sequence (TATTAA) were *in vitro* transcribed (see (C) for RNA probe purity). (C) The RNA probes were incubated with recombinant GST or GST-hnRNP-Q1 protein and precipitated with NeutrAvidin beads. Co-purified protein was assessed by GST immunoblot. Relative band intensity is listed below the immunoblots and RNA probe integrity is shown by formaldehyde gel electrophoresis.

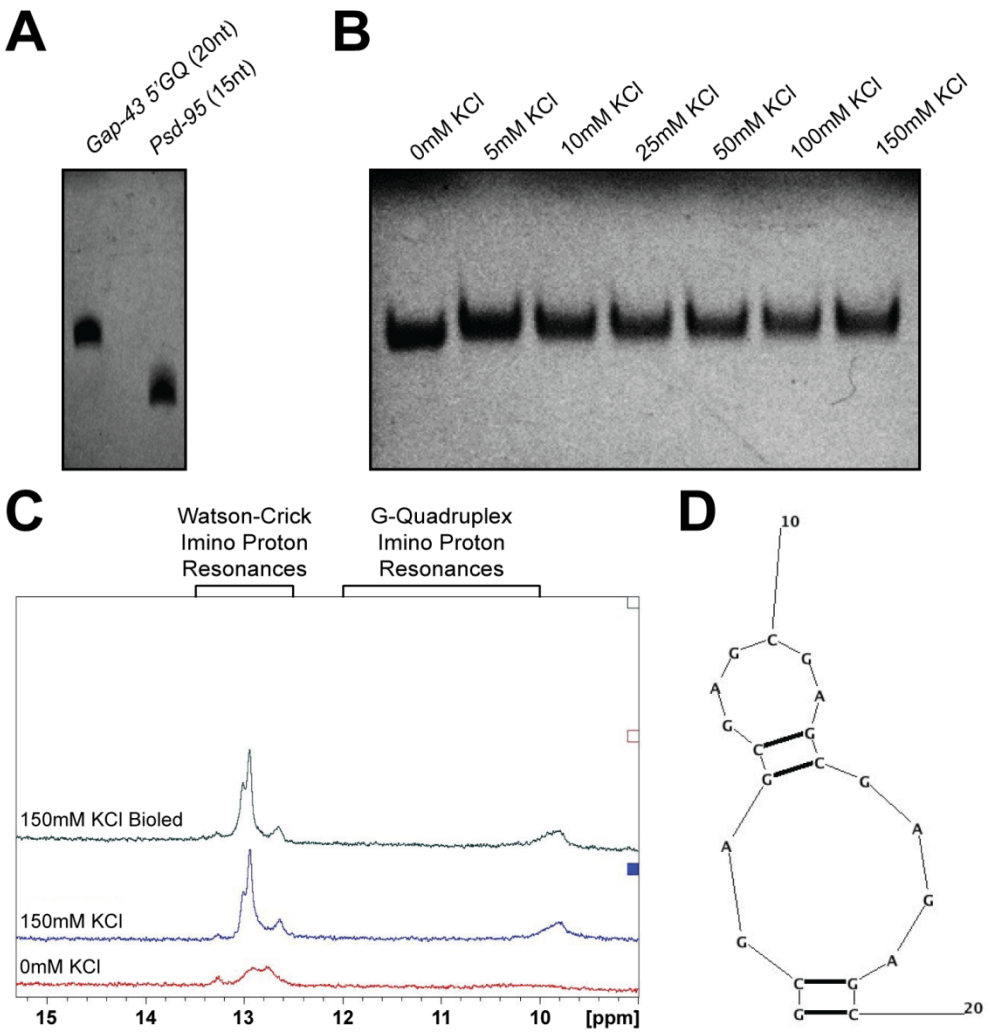

Supplemental Figure 4-5: Additional *Gap-43* 5'-UTR G-Quadruplex Sequence Folding Experiments. (A) The purity of the *Gap-43* 5'GQ RNA probe was assessed by denaturing polyacrylamide gel electrophoresis. A PSD-95 RNA probe was run for comparison. (B) The *Gap-43* 5'GQ RNA probe was annealed in increasing KCl concentrations and GQ conformation was assessed by native gel electrophoresis. (C) 1D ^{1}H NMR spectroscopy with the mutant *Gap-43* 5'GQ RNA probe revealed that imino proton resonances are not present in the 10-12 ppm region demonstrating that mutation of guanine residues that are involved in GQ formation prevents the structure from forming. Imino proton resonances are present in the 12.6-13.4 ppm region, which correspond to Watson-Crick G-C base pairs. (D) The

mutant *Gap-43* 5'GQ RNA probe is predicted to form a hairpin structure, which is supported by the 1D ^{1}H NMR spectroscopy results.

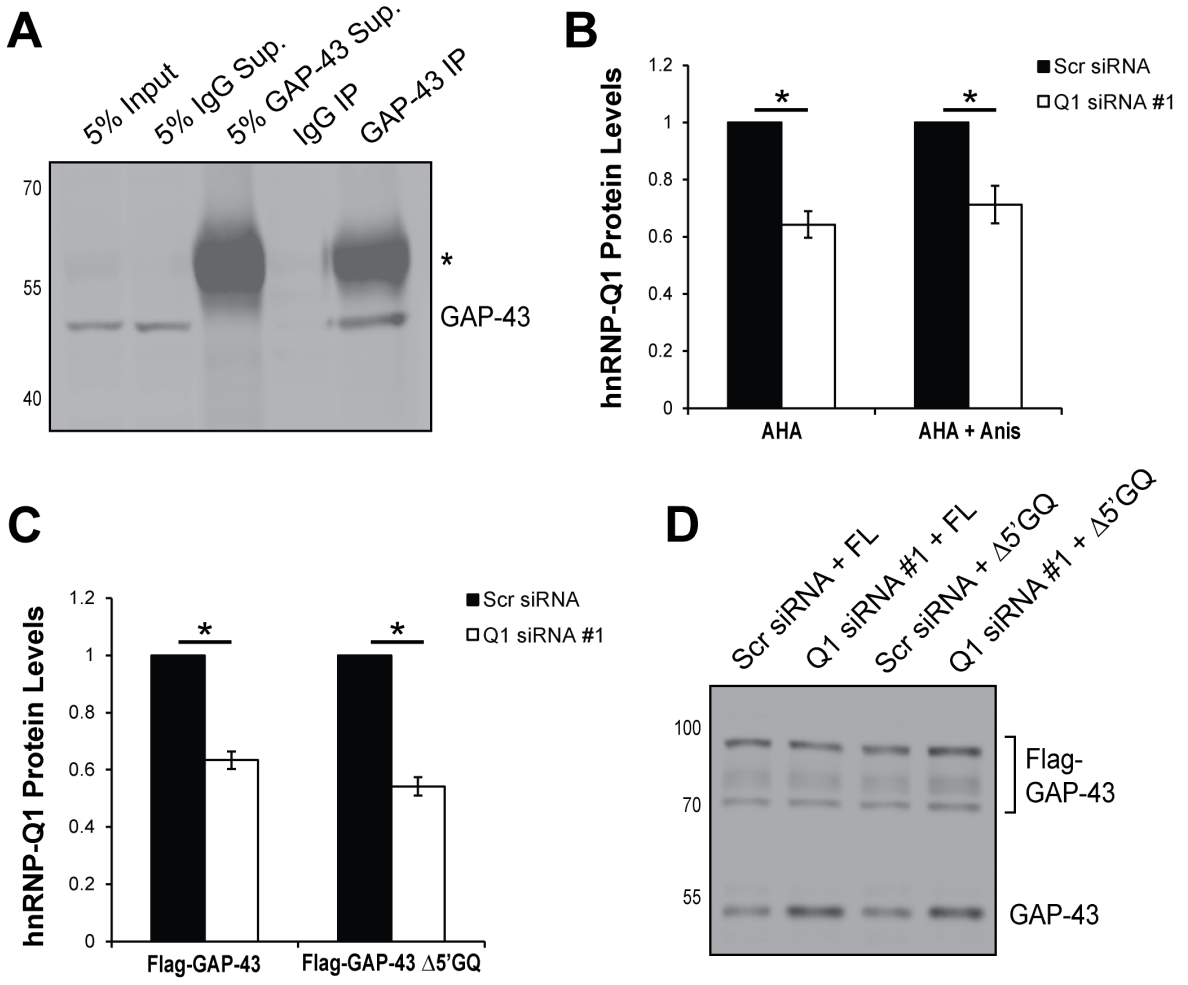

Supplemental Figure 4-6: Controls for AHA Pulse Labeling Experiments. (A) Endogenous GAP-43 protein was immunoprecipitated from N2a cell lysates and immunoprecipitation efficiency was assessed by immunoblot for GAP-43. Sup. = supernatant, * = non-specific bands. (B) hnRNP-Q1 knockdown efficiency for endogenous AHA experiments in Figure 7, A-C. n=3, one-sample t-test, p-values: AHA p=0.0161, AHA + Anis p=0.0489. (C) hnRNP-Q1 knockdown efficiency for reporter AHA experiments in Figure 8, A and B. n=6, one-sample t-test, p-values: Flag-GAP-43 p<0.0001, Flag-GAP-43 ΔGQ p<0.0001. (D) Representative example of Flag-GAP-43 and Flag-GAP-43 ΔGQ

construct overexpression for reporter AHA experiments (3xFlag-mCherry-GAP-43 predicted to be ~75 kDa).

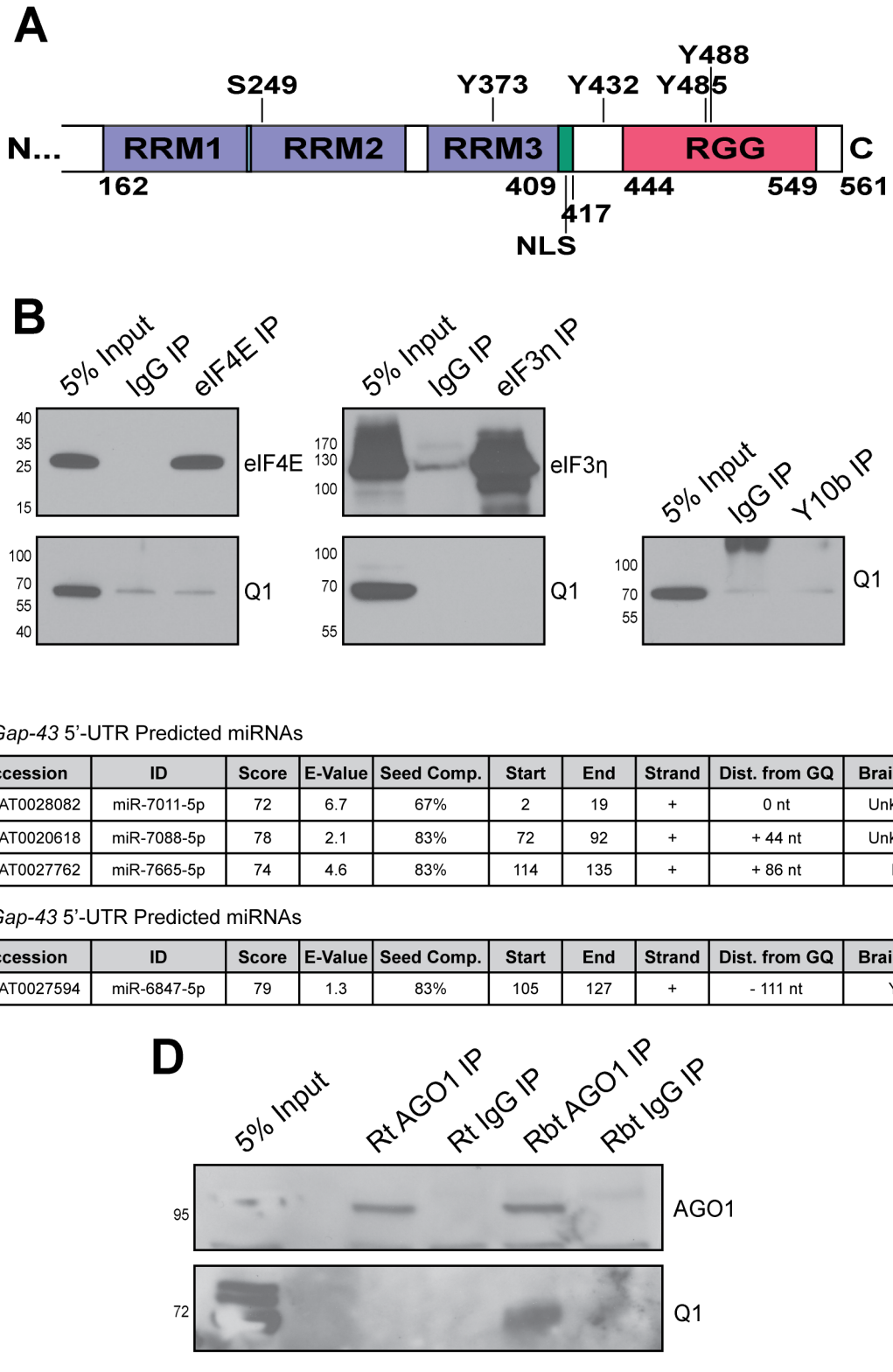

Accession	ID	Score	E-Value	Seed Comp.	Start	End	Strand	Dist. from GQ	Brain Exp.
MIMAT0028082	miR-7011-5p	72	6.7	67%	2	19	+	0 nt	Unknown
MIMAT0020618	miR-7088-5p	78	2.1	83%	72	92	+	+ 44 nt	Unknown
MIMAT0027762	miR-7665-5p	74	4.6	83%	114	135	+	+ 86 nt	No

Accession	ID	Score	E-Value	Seed Comp.	Start	End	Strand	Dist. from GQ	Brain Exp.
MIMAT0027594	miR-6847-5p	79	1.3	83%	105	127	+	- 111 nt	Yes

Supplemental Figure 4-7: A Potential Role for Phosphorylation and miRNA in hnRNP-

Q1-mediated *Gap-43* mRNA Translation Inhibition. (A) hnRNP-Q1 phosphoresidues were identified near or in the RGG box by mass spectrometry[311]. (B) eIF4E, eIF3η, Y10b and control IgGs were immunoprecipitated from N2a cell lysates and co-purifying hnRNP-Q1 was assessed by immunoblot. (C) miRNAs that are predicted to target the *M. musculus* and *H. sapiens* 5'-UTR of *Gap-43* mRNA by miRBase[312]. The name, score (confidence level), E-value (the number of hits expected based on chance, lower values are more significant), seed sequence complementarity (nucleotides 2-7 from the miRNA 5' end), position, strand, distance from the Gap-43 5'GQ and brain expression from miRIAD[328] are listed. (D) AGO1 (rt = rat antibody and rbt = rabbit antibody) and control IgGs were immunoprecipitated from C2C12 cell lysates and co-purifying hnRNP-Q1 was assessed by immunoblot.

4.7: Tables

Q1 mRNA Target	Proposed Q1 Function	Ms GQ Position	Ms GQ Rgion	Ms GQ Sequence	Ms GQ G-Score	Hu GQ Position	Hu GQ Rgion	Hu GQ Sequence	Hu GQ G-Score
Gap-43	Translation Repressor	14	5'-UTR	GGGAGGGAGGGAGGG	42	239	5'-UTR	GGGAGAGAGAGGG-AGGGAGGG	36
YB-1	Translation Repressor	235	Code	GGCAGCGGCGCGGG-UAGUGG	21	262	Code	GGCAGCGGCG-CAGGGAGCGG	21
p53	Translation Enhancer	1472	Code	GGUUCCUGGCCCAAGU-UGGGGAAUAGG	18	1265	Code	GGGAAGGAGCCAGG-GGGGAGCAGGG	33
Cdc42	mRNA Localization	1251	3'-UTR	GGGGAGGAGG	20	1822	3'-UTR	GGGTAGGGTGGGG-GTGGG	42
RhoA	Translation Repressor	2026	3'-UTR	GGGUGGGGGUGGGG-GGG	41	424	Code	GGAAAGCAGGUAGAG-UUGGCUUUGUGG	20
Period3	Translation Enhancer	494	Code	GGGCUCCAGGGGGCG-UCUGGCCAGGAGGG	21	275	Code	GGGAAGCUCCUGGCCC-CGGGAGAGGGGGG	28
Period1	Translation Enhancer	1780	Code	GGGGGGGGACGCUGA-GGGGCCUGGG	36	3563	Code	GGGGCUGCUCGGGGC-GGGGCUGAGCCUGGG	37
Rev-erb α	Translation Enhancer	106, 1031 & 2150	5'-UTR & Code	GGGAAAGGCUC-GGGCAAAAGG, GGUGU-GUGGGGACGUGGCCU-CAGG & GGAGCUCGG-UGCCAUGGGCAUGGG	20	102 & 2149	5'-UTR & Code	GGGAAAGGCUC-GGGCAAAGG & GGAGCUUGGUGC-CAUGGGCAUGGG	20
c-Myc	mRNA Stabilizer	142	5'-UTR	GGGAAAAAGAAGGGA-GGGGAGGG	35	832	Code	GGCGGUGGCGG	21
BiP	Translation Enhancer	168 & 198	Code	GGUGGCGGCGG & GGUGCGGGCCGAGGAG-GAGG	21	306	Code	GGCGCGGGCCGAGGA-GGAGG	21
Aanat	Translation Enhancer	784 & 1170	3'-UTR	GGCCAUGGC-GAGGGUGGG & GGAUGAGGGGCAGC-CAGGAGCCGGG	20	47	5'-UTR	GGGAGCGAGAAGGGGC-GGGGACCCGGG	37
c-Fos	mRNA Stabilizer	603	Code	GGAAUCGGAGGAGGG	18	1351	3'-UTR	GGGCAGGGAAGGGGA-GG	21

Table 4-1: Predicted G-Quadruplexes in hnRNP-Q1 Target mRNAs. The GQ sequence with the highest G-score in each hnRNP-Q1 target mRNA as determined by the QGRS Mapper software are listed[304]. The target mRNA name, hnRNP-Q1 regulated mRNA processing or post-transcriptional regulatory event, GQ sequence postion, GQ sequence mRNA region and GQ sequence are listed for the *M. musculus* and *H. sapiens* mRNA orthologs. Underlined nucleotides are predicted to be involved in GQ structure formation. Several of the mRNA targets have the highest G-score GQ sequence located in the same mRNA region in both *M. musculus* and *H. sapiens* suggesting a conserved mechanism for regulation.

Chapter 5

Summary and Future Directions

Portions of this chapter were adapted from the following manuscript:

Williams, K.R., Stefanovic, S., McAninch, D.S., Xing, L., Allen, M., Li, W., Feng, Y., Mihailescu, M.R., Bassell, G.J. (2015) hnRNP-Q1 Represses Nascent Axon Growth in Cortical Neurons by Inhibiting *Gap-43* mRNA Translation. *Mol Biol Cell*. Revision Under Review.

5.1: Summary

Here we identified *Gap-43* mRNA as a novel hnRNP-Q1 target and demonstrate that GAP-43 expression is repressed by hnRNP-Q1 in N2a cells and primary cortical neurons. hnRNP-Q1 knockdown increased total GAP-43 and phosphorylated GAP-43 protein levels in N2a cells but did not affect *Gap-43* mRNA levels or the ratio of phosphorylated GAP-43/total GAP-43. In support of an inverse relationship, endogenous hnRNP-Q1 and GAP-43 demonstrate opposite expression profiles in cultured cortical neurons and enrichment in hippocampal regions. These findings suggest that hnRNP-Q1 post-transcriptionally inhibits GAP-43 expression.

hnRNP-Q1-mediated repression of GAP-43 expression affects GAP-43 function as demonstrated by a GAP-43-dependent increase in nascent axon length, total neurite length and neurite number of incipient cortical neurons and N2a cell process extension upon hnRNP-Q1 knockdown. Overexpressing GAP-43 in N2a cells also increases process extension and hnRNP-Q1 knockdown in incipient cortical neurons also reduces focal adhesions. These results suggest that hnRNP-Q1 affects GAP-43 function by repressing GAP-43 expression.

hnRNP-Q1 binds to multiple regions of *Gap-43* mRNA but shows high affinity for a predicted GQ sequence in the 5'-UTR. The RGG box of hnRNP-Q1 is necessary and sufficient to bind the 5'GQ sequence, which we demonstrate folds into a stable parallel, intramolecular GQ structure. Additionally, hnRNP-Q1 represses GAP-43 expression by inhibiting *Gap-43* mRNA translation and the 5'GQ is involved in this process. Taken together, these findings suggest that hnRNP-Q1 inhibits *Gap-43* mRNA translation by binding to the 5'GQ and that this mechanism affects the function of GAP-43 to regulate axon

growth.

5.2: Future Directions

Several key questions arise based on our findings, including (1) do multiple cis-regulatory elements contribute to hnRNP-Q1-mediated translation inhibition, (2) what types of GQs does hnRNP-Q1 bind, (3) do other hnRNP-Q1 target mRNAs also contain predicted GQs, (4) do differences in GQ structure and/or position in the mRNA determine the function of bound hnRNP-Q1, (5) does hnRNP-Q1 block translation initiation and if so, (6) at what stage, (7) does hnRNP-Q1 cooperate with the *Gap-43* trans-regulatory factors HuD and IMP1/ZBP1 to regulate GAP-43 expression and (8) does this regulation occur locally in axons and growth cones.

5.2.1: hnRNP-Q1 Interacts with Multiple Cis-regulatory Elements

Our results demonstrate that hnRNP-Q1 inhibits cap-dependent translation of *M. musculus Gap-43* mRNA by binding a 5'-UTR GQ, which contributes to the growing literature about the role of hnRNP-Q1 in regulating translation. hnRNP-Q1 has previously been demonstrated to inhibit cap-dependent translation of *RhoA* and *YB-1* mRNAs [217, 218]. hnRNP-Q1 directly binds the 3'-UTRs of both *M. musculus RhoA* and *H. sapiens YB-1* mRNAs; it binds both the proximal and distal halves of the *RhoA* 3'-UTR[218] and 78 nucleotide proximal region of the *YB-1* 3'-UTR[217]. hnRNP-Q1 does not bind the 5'-UTR and coding region of *RhoA* mRNA[218] but additional regions of *YB-1* mRNA have not been tested[215]. Taken together, these findings suggest that hnRNP-Q1 may bind to multiple regions of an mRNA transcript to suppress translation. In support of this, we demonstrated that

hnRNP-Q1 binds the 5'-UTR, coding region and 3'-UTR of *Gap-43* mRNA and deleting the 5'GQ sequence only reduces hnRNP-Q1 binding to full-length *Gap-43* mRNA by ~40%. The coding region also contains predicted GQs but the 3'-UTR does not indicating that additional *M. musculus Gap-43* cis-regulatory element(s) bind hnRNP-Q1. hnRNP-Q1 has previously been demonstrated to bind polyA RNA[208, 219] and the 3'-UTRs of its target mRNAs are enriched for two six nucleotide consensus sequences: AYAAYY and UAUYRR where Y = C/U and R = A/G[215]. Deleting the predicted GQ with the highest G-score in the coding region of *M. musculus Gap-43* mRNA does not affect hnRNP-Q1 binding (G-score: 21, QGRS Mapper[304]) but deleting either the two 11 nucleotide polyA stretches or the consensus sequence in the 3'-UTR abolishes hnRNP-Q1 binding to this region. These additional cis-regulatory elements may contribute to hnRNP-Q1-mediated inhibition of G*ap-43* mRNA translation or may be involved in mRNA processing events.

RhoA and *YB-1* mRNAs were also characterized to determine if they contain similar cis-regulatory elements to *Gap-43* mRNA. The 3'-UTR of *M. musculus RhoA* mRNA contains a predicted GQ with a high G-score (G-Score = 41, QGRS Mapper[304]) but *H. sapiens RhoA* mRNA does not. However, the 3'-UTR of *M. musculus RhoA* mRNA contains a 6 nucleotide polyA stretch and several consensus sequences including one copy of ATAACT and two copies of both ATAATT and TATTAA, all of which are conserved in *H. sapiens RhoA* mRNA. The 3'-UTR of *M. musculus YB-1* mRNA contains two predicted GQs with moderately high G-scores (G-Scores = 19, QGRS Mapper[304]) but *H. sapiens YB-1* mRNA does not. Additionally, the 3'-UTR of *M. musculus YB-1* mRNA contains a 14 nucleotide polyA stretch and *H. sapiens YB-1* mRNA contains two 6 nucleotide polyA stretches. The 3'-UTR of *M. musculus YB-1* also contains three consensus sequences, one of

which is conserved in *H. sapiens YB-1* mRNA (ACAACT). However, the 3'-UTR of YB-1 mRNA has not been demonstrated to be sufficient for hnRNP-Q1-mediated inhibition suggesting that additional regions may contribute to this regulation. Interestingly, the 5'-UTR and coding region of *M. musculus YB-1* mRNA each contain a predicted GQ with moderately high G-score (G-Scores = 20 and 21, respectively, QGRS Mapper[304]) and the coding region contains three consensus sequences, all of which are conserved in *H. sapiens YB-1* mRNA. These findings suggest that hnRNP-Q1 recognizes at least three cis-regulatory elements, which may function cooperatively to regulate translation or mRNA processing events. GQ structures have previously been implicated in translation inhibition[309], which is consistent with our findings that hnRNP-Q1 inhibits *Gap-43* mRNA translation by binding the 5'GQ through the RGG box. Interestingly, hnRNP-Q1 also enhances IRES translation by binding to 5'-UTR A-rich sequences[220, 222] and hnRNP-Q1 has been demonstrated to bind polyA RNA through the RRM domains[226]. However, several of these targets also have predicted GQ sequences in the coding region. These findings suggest that hnRNP-Q1 may enhance IRES translation by binding 5'-UTR A-rich sequences through the RRMs and/or by binding coding region GQs through the RGG box. Additionally, hnRNP-Q1 localizes *Cdc42* to neurites likely by binding a proximal region of the *Cdc42* 3'-UTR that contains several consensus sequences[215] and the RGG box has been implicated in binding these sequences[215]. Therefore, the type and position of the cis-regulaotry element and potentially neighboring sequences likely dictates the function of hnRNP-Q1 when bound. Future studies may decipher the precise functions of the different cis-regulatory elements that bind hnRNP-Q1, determine if hnRNP-Q1 interacts with multiple elements on a single mRNA transcript and determine whether the elements function cooperatively to regulate mRNA processing and post-

transcriptional regulatory events. An interesting idea would be to determine if hnRNP-Q1 interacts with cis-regulatory elements in both the 5'-UTR ad 3'-UTR simultaneously while the mRNA in held in the closed loop structure.

5.2.2: Potential Mechanism of hnRNP-Q1-mediated Translation Inhibition

Our findings demonstrate that hnRNP-Q1 can inhibit translation by binding to GQ structures in the 5'-UTR. Future studies may address this mechanism in more detail including whether hnRNP-Q1 mRNA targets are enriched for GQ sequences and if the GQ sequences share similar features. It would be interesting to perform a proteomics study to identify targets that have altered expression upon hnRNP-Q1 depletion, which would narrow down the target mRNAs discovered by Chen et al. 2012 to only include targets that are potentially translationally regulated by hnRNP-Q1. The presence and position of GQ sequences in translationally regulated versus non-translationally regulated hnRNP-Q1 target mRNAs could then be assessed to provide clues about GQs that are involved in translation modulation and potentially mRNA processing events. The types of mRNAs in each category can also be characterized to provide insights into the global functions of hnRNP-Q1. Interestingly, we have preliminary results demonstrating that hnRNP-Q1 binds to diverse types of GQ structures. hnRNP-Q1 binds GQ sequences from *NR2B*, *Smndc1* and *Psd-95* mRNAs, which are all expected to form GQ structures with three G-Quartet planes like the *Gap-43* 5'GQ[36, 313], and from *Shank1a* and *Shank1b* mRNAs, which are expected to form GQ structures with four G-Quartet planes[329]. However, hnRNP-Q1 does not bind a GQ sequence from *p250gap* mRNA that is expected to form a GQ structure with three G-Quartet planes (5'-GGGUGGGGUGGGGGG-3'). This sequence has a high G-score but there is no loop present

between the third and fourth G-runs, suggesting that hnRNP-Q1 requires a loop length of at least one nucleotide to bind (G-score = 50, QGRS Mapper[304]). These non-stringent parameters for binding suggest that hnRNP-Q1 may be involved in regulating many mRNAs that contain GQ structures and indicate that GQs may be an important cis-regulatory element for mediating hnRNP-Q1 translation regulation.

Additional aspects of this mechanism to be addressed include how hnRNP-Q1 binding to GQ structures is regulated and how this binding inhibits translation. As discussed in Chapter 4, hnRNP-Q1 is a phosphoprotein that is tyrosine phosphorylated by the insulin receptor[235, 237, 238] and dephosphorylated by SHP2[239]. Phosphorylation has previously been shown to regulate the function of mRBPs, like IMP1/ZBP1[47] and FMRP[52, 330]. Phosphorylation of IMP1/ZBP1 near the third KH domain relieves mRNA binding and translation inhibition[47] while dephosphorylation of FMRP near the RGG box causes the RISC complex to dissociate from the mRNA to relieve the translation inhibition[52, 330]. Since we show here that the hnRNP-Q1 RGG box is necessary and sufficient for *Gap-43* 5'GQ binding, it is likely that phosphorylation near or in the RGG box regulates hnRNP-Q1 binding and/or function. Interestingly, there are three conserved phosphosites near or in the hnRNP-Q1 RGG box domain, Y432, Y485 and Y488[311], suggesting that phosphorylation of one or more of these residues may affect hnRNP-Q1 by a similar mechanism to IMP1/ZBP1 or FMRP. Additionally, hnRNP-Q1 interacts with AGO1 and three *M. musculus* and one *H. sapiens* miRNAs are predicted to target the *Gap-43* 5'-UTR, miR-7011-5p, miR-7088-5p, miR-76651-5p and miR-6847-5p[312], respectively, suggesting that miRNA may contribute to the mechanism similar to FMRP. Furthermore, preliminary studies demonstrate that hnRNP-Q1 does not interact with the translation factors eIF4E, eIF3η or Y10b suggesting that hnRNP-

Q1 inhibits mRNA translation at an early stage. These findings are consistent with 5'-UTR GQs proximal to the 5' cap inhibiting translation by blocking ribosome assembly or scanning[309]. These observations provide hints about the specific mechanism of hnRNP-Q1-mediated inhibition of *Gap-43* mRNA and potentially other mRNAs but more studies need to be performed to reveal specifics of the mechanism. Additionally, identifying other mRBPs that compete with hnRNP-Q1 to bind the 5'GQ sequence, similar to how HuD and KSRP compete to bind the *Gap-43* 3'-UTR ARE to regulate mRNA stability, may provide clues about the mechanism. Potential candidates include hnRNP-F, -H and -M, which bind G-rich sequences[137, 138].

5.2.3: Coordinated Regulation by hnRNP-Q1 and Additional mRNA Binding Proteins

As discussed in Chapter 2, GAP-43 expression is regulated by several mRBPs. HuD stabilizes *Gap-43* mRNA by binding to an AU-rich element (ARE) in the 3'-UTR[80, 331] and KSRP destabilizes the mRNA by competing to bind the same site[82]. Also, *Gap-43* mRNA localization to axons is regulated by IMP1/ZBP1 and the ARE is also necessary and sufficient for this process to occur[271, 332]. These findings suggest that GAP-43 expression is regulated by the coordinated function of multiple proteins. Our results identified hnRNP-Q1 as a novel factor that regulates GAP-43 expression and suggest that HuD, IMP1/ZBP1 and hnRNP-Q1 may form a complex with *Gap-43* mRNA allowing for precise control of GAP-43 expression. hnRNP-Q1 also interacts with SMN[202, 209], which is the protein implicated in SMA as discussed in Chapter 1. SMN functions as a chaperone protein that assembles ribonucleoprotein complexes[106, 333] suggesting that SMN may help assemble the *Gap-43* mRNA-HuD-IMP1/ZBP1-hnRNP-Q1 complex and that this complex may be disrupted in

SMA. Additionally, GAP-43 is required for netrin-1 induced outgrowth and guidance in neocortical callosal axons[334] suggesting that netrin-1 modulates GAP-43 function and may also increase GAP-43 expression. Interestingly, netrin-1 induces the local translation of *β-Actin* mRNA in an IMP1/ZBP1-dependent manner[49] implying that netrin-1 may also play a role in regulating the *Gap-43* mRNA-HuD-IMP1/ZBP1-hnRNP-Q1 complex. Future studies may address the interplay between HuD, IMP1/ZBP1 and hnRNP-Q1, determine whether these factors regulate GAP-43 expression locally in axonal growth cones and investigate the roles of SMN and netrin-1 on this complex.

To gain a global perspective on regulation by the HuD-IMP1/ZBP1-hnRNP-Q1 complex, the mRNA interactomes of these three proteins and potentially additional mRBPs may be compared. As discussed in Chapter 1, mRNAs are decorated with mRBPs throughout their lifecycle and these proteins are responsible for regulating the many mRNA processing and post-transcriptional regulatory events[1, 4]. It is likely that HuD, IMP1/ZBP1 and hnRNP-Q1 have several common mRNA targets, which may be regulated similar to *Gap-43* mRNA. These studies would provide clues about the coordinated functions of HuD, IMP1/ZBP1 and hnRNP-Q1. Identifying the molecular motor involved in localizing this mRBP complex to the axons and growth cones of neurons is another potential future direction. As discussed in Chapter 1, the kinesin KIF11 is involved in transporting the *β-Actin* mRNA-IMP1/ZBP1 complex[31], which suggests that this motor may also transport the *Gap-43* mRNA-HuD-IMP1/ZBP1-hnRNP-Q1 complex. This hypothesis is supported by the finding that *Gap-43* and *β-Actin* mRNAs are able to be trafficked together in neurons. These studies would provide insight into the types of mRNAs regulated by this complex and reveal clues about a common mechanism of regulation.

5.2.4: Systemic Functions on hnRNP-Q1-Mediated Post-Transcriptional Regulation

In order to better appreciate hnRNP-Q1 function, future studies may involve the generation of an hnRNP-Q1 knockout mouse. GAP-43 is enriched in axonal growth cones after polarity is established and also accumulates along nascent axons in cultured hippocampal neurons, suggesting an important early role for GAP-43 in axon outgrowth[280]. Additionally, GAP-43 overexpression mice demonstrate ectopic growth phenotypes *in vivo*, including increased sprouting of mossy fibers in the hippocampus and of motor nerves at the neuromuscular junction[281]. Furthermore, our cultured cortical neuron time course reveals that GAP-43 protein levels remain elevated in mature neurons suggesting that GAP-43 may play an important role in neuronal functions other than axon growth and guidance. Therefore, an hnRNP-Q1 knockout mouse would likely demonstrate increased GAP-43 expression and corresponding ectopic growth phenotypes. Additionally, mice overexpressing GAP-43 demonstrate enhanced spatial learning and memory[253] but excessive overexpression leads to impaired spatial learning and memory[254]. Therefore, behavioral phenotypes of the hnRNP-Q1 knockout mouse would also provide clues about hnRNP-Q1 function.

hnRNP-Q1 has been demonstrated to interact with 2,250 mRNAs so it is likely that several hnRNP-Q1 target mRNAs contribute to neuronal morphology regulation[215]. In support of this, the hnRNP-Q1 target mRNAs *RhoA* and *Cdc42* have both been demonstrated to affect neuronal morphology upon hnRNP-Q1 depletion[215, 218]. However, our results demonstrate that hnRNP-Q1 depletion leads to a GAP-43 dependent increase in neurite length and number. Interestingly, GAP-43 has been demonstrated to function upstream of both RhoA and Cdc42 to regulate cell morphology[300, 301]. Therefore, hnRNP-Q1 may control

neuron morphology by regulating the expression of multiple components of the same pathway. The interplay between *Gap-43*, *RhoA*, *Cdc42* and other hnRNP-Q1 target mRNAs and how their altered expression affects gross morphology is an important future direction that will help decipher the global function of hnRNP-Q1.

5.3: Concluding Remarks

Our results have uncovered a novel mechanism for hnRNP-Q1 to regulate GAP-43 translation and function. We revealed that hnRNP-Q1 represses endogenous *Gap-43* mRNA translation, that hnRNP-Q1 is a novel GQ binding protein and that the *Gap-43* 5'GQ is involved in hnRNP-Q1-mediated translation repression (Figure 5-1). Additionally, we demonstrate that hnRNP-Q1-mediated repression of GAP-43 expression affects its function to regulate neuronal growth, which suggests that this mode of regulation may be critical for neuronal development (Figure 5-1). These findings advance our understanding of how the important neuronal protein GAP-43 is regulated and have identified a potential conserved mechanism for hnRNP-Q1-mediated translation inhibition.

5.4: Figures

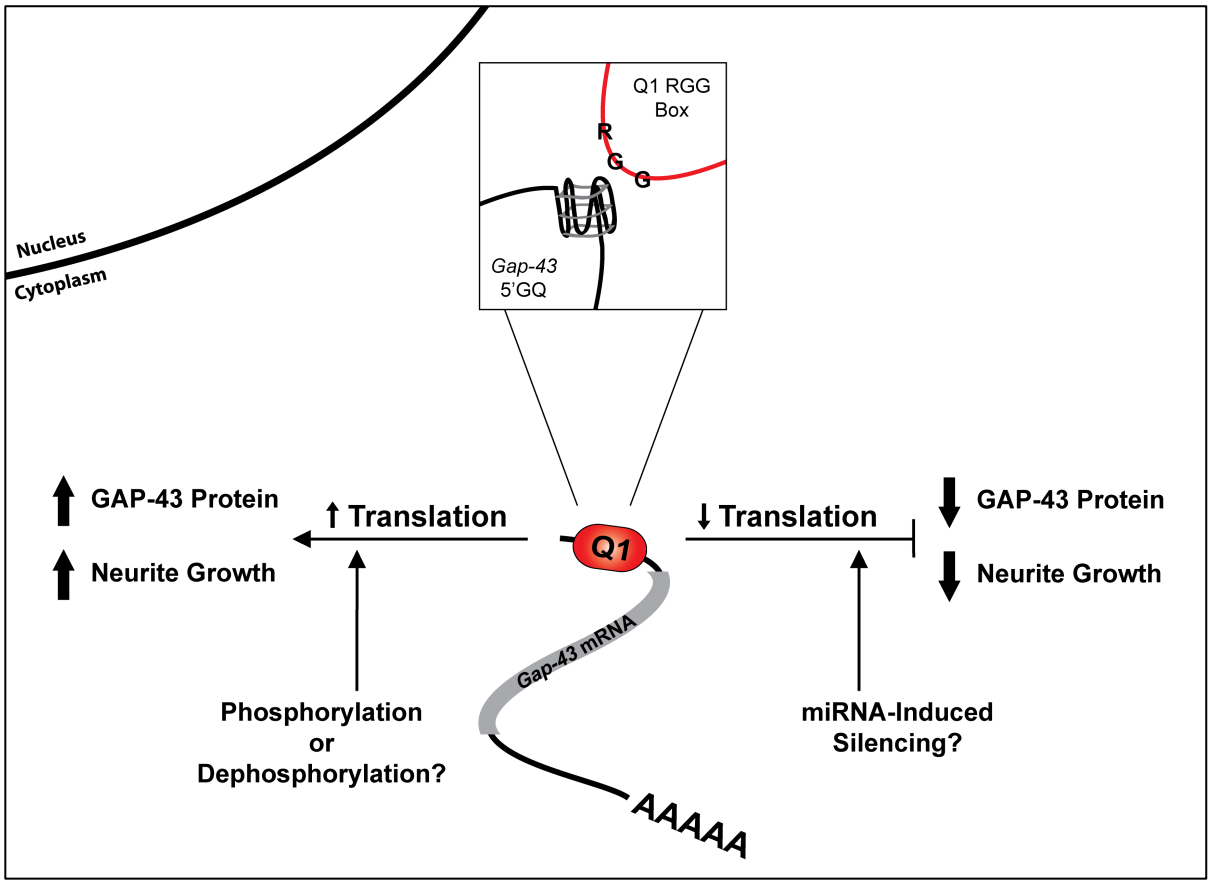

Figure 5-1: Model for hnRNP-Q1-Mediated Inhibition of Gap-43 mRNA Translation. hnRNP-Q1 binds to a G-quadruplex structure in the 5'-UTR of *Gap-43* mRNA through the RGG domain. This interaction inhibits *Gap-43* mRNA translation potentially by inhibiting ribosome assembly or scanning and with the involvement of miRNA, which leads to reduced GAP-43 protein levels and neurite growth. By some unknown mechanism, possibly a phosphorylation event, hnRNP-Q1 likely releases *Gap-43* mRNA and allows it to be translated. This process would lead to increased GAP-43 protein levels and increased neurite growth.

References

1. Glisovic T., Bachorik J.L., Yong J., Dreyfuss G. (2008) RNA-binding proteins and post-transcriptional gene regulation. *FEBS letters* **582**:1977-1986.
2. Castello A., Fischer B., Hentze M.W., Preiss T. (2013) RNA-binding proteins in Mendelian disease. *Trends in genetics : TIG* **29**:318-327.
3. Lukong K.E., Chang K.W., Khandjian E.W., Richard S. (2008) RNA-binding proteins in human genetic disease. *Trends in genetics : TIG* **24**:416-425.
4. Moore M.J. (2005) From birth to death: the complex lives of eukaryotic mRNAs. *Science* **309**:1514-1518.
5. Bentley D.L. (2014) Coupling mRNA processing with transcription in time and space. *Nature reviews Genetics* **15**:163-175.
6. Cho E.J., Takagi T., Moore C.R., Buratowski S. (1997) mRNA capping enzyme is recruited to the transcription complex by phosphorylation of the RNA polymerase II carboxy-terminal domain. *Genes & development* **11**:3319-3326.
7. McCracken S., Fong N., Rosonina E., Yankulov K., Brothers G., Siderovski D., Hessel A., Foster S., Shuman S., Bentley D.L. (1997) 5'-Capping enzymes are targeted to pre-mRNA by binding to the phosphorylated carboxy-terminal domain of RNA polymerase II. *Genes & development* **11**:3306-3318.
8. Gonatopoulos-Pournatzis T., Cowling V.H. (2014) Cap-binding complex (CBC). *The Biochemical journal* **457**:231-242.
9. Eberle A.B., Visa N. (2014) Quality control of mRNP biogenesis: networking at the transcription site. *Seminars in cell & developmental biology* **32**:37-46.

10. Tomaselli S., Locatelli F., Gallo A. (2014) The RNA editing enzymes ADARs: mechanism of action and human disease. *Cell and tissue research* **356**:527-532.

11. Will C.L., Luhrmann R. (2011) Spliceosome structure and function. *Cold Spring Harbor perspectives in biology* **3**:

12. Hirose Y., Tacke R., Manley J.L. (1999) Phosphorylated RNA polymerase II stimulates pre-mRNA splicing. *Genes & development* **13**:1234-1239.

13. Burghes A.H., Beattie C.E. (2009) Spinal muscular atrophy: why do low levels of survival motor neuron protein make motor neurons sick? *Nature reviews Neuroscience* **10**:597-609.

14. Lagier-Tourenne C., Polymenidou M., Cleveland D.W. (2010) TDP-43 and FUS/TLS: emerging roles in RNA processing and neurodegeneration. *Human molecular genetics* **19**:R46-64.

15. Konieczny P., Stepniak-Konieczna E., Sobczak K. (2014) MBNL proteins and their target RNAs, interaction and splicing regulation. *Nucleic acids research* **42**:10873-10887.

16. Le Hir H., Andersen G.R. (2008) Structural insights into the exon junction complex. *Current opinion in structural biology* **18**:112-119.

17. Chan S., Choi E.A., Shi Y. (2011) Pre-mRNA 3'-end processing complex assembly and function. *Wiley interdisciplinary reviews RNA* **2**:321-335.

18. Hirose Y., Manley J.L. (1998) RNA polymerase II is an essential mRNA polyadenylation factor. *Nature* **395**:93-96.

19. Bienroth S., Keller W., Wahle E. (1993) Assembly of a processive messenger RNA polyadenylation complex. *The EMBO journal* **12**:585-594.

20. Wahle E. (1991) A novel poly(A)-binding protein acts as a specificity factor in the second phase of messenger RNA polyadenylation. *Cell* **66**:759-768.

21. Kerwitz Y., Kuhn U., Lilie H., Knoth A., Scheuermann T., Friedrich H., Schwarz E., Wahle E. (2003) Stimulation of poly(A) polymerase through a direct interaction with the nuclear poly(A) binding protein allosterically regulated by RNA. *The EMBO journal* **22**:3705-3714.

22. Kuhn U., Gundel M., Knoth A., Kerwitz Y., Rudel S., Wahle E. (2009) Poly(A) tail length is controlled by the nuclear poly(A)-binding protein regulating the interaction between poly(A) polymerase and the cleavage and polyadenylation specificity factor. *The Journal of biological chemistry* **284**:22803-22814.

23. West S., Gromak N., Proudfoot N.J. (2004) Human 5' --> 3' exonuclease Xrn2 promotes transcription termination at co-transcriptional cleavage sites. *Nature* **432**:522-525.

24. Katahira J. (2015) Nuclear export of messenger RNA. *Genes* **6**:163-184.

25. Meinel D.M., Burkert-Kautzsch C., Kieser A., O'Duibhir E., Siebert M., Mayer A., Cramer P., Soding J., Holstege F.C., Strasser K. (2013) Recruitment of TREX to the transcription machinery by its direct binding to the phospho-CTD of RNA polymerase II. *PLoS genetics* **9**:e1003914.

26. Long J.C., Caceres J.F. (2009) The SR protein family of splicing factors: master regulators of gene expression. *The Biochemical journal* **417**:15-27.

27. Martin K.C., Ephrussi A. (2009) mRNA localization: gene expression in the spatial dimension. *Cell* **136**:719-730.

28. Kislauskis E.H., Zhu X., Singer R.H. (1994) Sequences responsible for intracellular localization of beta-actin messenger RNA also affect cell phenotype. *The Journal of cell biology* **127**:441-451.

29. Ross A.F., Oleynikov Y., Kislauskis E.H., Taneja K.L., Singer R.H. (1997) Characterization of a beta-actin mRNA zipcode-binding protein. *Molecular and cellular biology* **17**:2158-2165.

30. Farina K.L., Huttelmaier S., Musunuru K., Darnell R., Singer R.H. (2003) Two ZBP1 KH domains facilitate beta-actin mRNA localization, granule formation, and cytoskeletal attachment. *The Journal of cell biology* **160**:77-87.

31. Song T., Zheng Y., Wang Y., Katz Z., Liu X., Chen S., Singer R.H., Gu W. (2015) Specific interaction of KIF11 with ZBP1 regulates the transport of beta-actin mRNA and cell motility. *Journal of cell science* **128**:1001-1010.

32. Darnell J.C., Jensen K.B., Jin P., Brown V., Warren S.T., Darnell R.B. (2001) Fragile X mental retardation protein targets G quartet mRNAs important for neuronal function. *Cell* **107**:489-499.

33. Menon L., Mader S.A., Mihailescu M.R. (2008) Fragile X mental retardation protein interactions with the microtubule associated protein 1B RNA. *Rna* **14**:1644-1655.

34. Menon L., Mihailescu M.R. (2007) Interactions of the G quartet forming semaphorin 3F RNA with the RGG box domain of the fragile X protein family. *Nucleic acids research* **35**:5379-5392.

35. Schaeffer C., Bardoni B., Mandel J.L., Ehresmann B., Ehresmann C., Moine H. (2001) The fragile X mental retardation protein binds specifically to its mRNA via a purine quartet motif. *The EMBO journal* **20**:4803-4813.

36. Stefanovic S., Bassell G.J., Mihailescu M.R. (2015) G quadruplex RNA structures in PSD-95 mRNA: potential regulators of miR-125a seed binding site accessibility. *Rna* **21**:48-60.

37. Subramanian M., Rage F., Tabet R., Flatter E., Mandel J.L., Moine H. (2011) G-quadruplex RNA structure as a signal for neurite mRNA targeting. *EMBO reports* **12**:697-704.

38. Muddashetty R.S., Kelic S., Gross C., Xu M., Bassell G.J. (2007) Dysregulated metabotropic glutamate receptor-dependent translation of AMPA receptor and postsynaptic density-95 mRNAs at synapses in a mouse model of fragile X syndrome. *The Journal of neuroscience : the official journal of the Society for Neuroscience* **27**:5338-5348.

39. Dictenberg J.B., Swanger S.A., Antar L.N., Singer R.H., Bassell G.J. (2008) A direct role for FMRP in activity-dependent dendritic mRNA transport links filopodial-spine morphogenesis to fragile X syndrome. *Developmental cell* **14**:926-939.

40. Davidovic L., Jaglin X.H., Lepagnol-Bestel A.M., Tremblay S., Simonneau M., Bardoni B., Khandjian E.W. (2007) The fragile X mental retardation protein is a molecular adaptor between the neurospecific KIF3C kinesin and dendritic RNA granules. *Human molecular genetics* **16**:3047-3058.

41. Lejeune F., Ranganathan A.C., Maquat L.E. (2004) eIF4G is required for the pioneer round of translation in mammalian cells. *Nature structural & molecular biology* **11**:992-1000.

42. Maquat L.E., Tarn W.Y., Isken O. (2010) The pioneer round of translation: features and functions. *Cell* **142**:368-374.

43. Hinnebusch A.G. (2014) The scanning mechanism of eukaryotic translation initiation. *Annual review of biochemistry* **83**:779-812.

44. Lodish H., Berk A., Kaiser C.A., Krieger M., Scott M.P., Bretscher A., Ploegh H., Matsudaira P. (2007) *Molecular Cell Biology, 6th Edition*. W. H. Freeman

45. Jackson R.J., Hellen C.U., Pestova T.V. (2012) Termination and post-termination events in eukaryotic translation. *Advances in protein chemistry and structural biology* **86**:45-93.

46. Sato H., Maquat L.E. (2009) Remodeling of the pioneer translation initiation complex involves translation and the karyopherin importin beta. *Genes & development* **23**:2537-2550.

47. Huttelmaier S., Zenklusen D., Lederer M., Dictenberg J., Lorenz M., Meng X., Bassell G.J., Condeelis J., Singer R.H. (2005) Spatial regulation of beta-actin translation by Src-dependent phosphorylation of ZBP1. *Nature* **438**:512-515.

48. Buxbaum A.R., Wu B., Singer R.H. (2014) Single beta-actin mRNA detection in neurons reveals a mechanism for regulating its translatability. *Science* **343**:419-422.

49. Welshhans K., Bassell G.J. (2011) Netrin-1-induced local beta-actin synthesis and growth cone guidance requires zipcode binding protein 1. *The Journal of neuroscience : the official journal of the Society for Neuroscience* **31**:9800-9813.

50. Sasaki Y., Welshhans K., Wen Z., Yao J., Xu M., Goshima Y., Zheng J.Q., Bassell G.J. (2010) Phosphorylation of zipcode binding protein 1 is required for brain-derived neurotrophic factor signaling of local beta-actin synthesis and growth cone turning. *The Journal of neuroscience : the official journal of the Society for Neuroscience* **30**:9349-9358.

51. Darnell J.C., Van Driesche S.J., Zhang C., Hung K.Y., Mele A., Fraser C.E., Stone E.F., Chen C., Fak J.J., Chi S.W., Licatalosi D.D., Richter J.D., Darnell R.B. (2011) FMRP stalls ribosomal translocation on mRNAs linked to synaptic function and autism. *Cell* **146**:247-261.

52. Muddashetty R.S., Nalavadi V.C., Gross C., Yao X., Xing L., Laur O., Warren S.T., Bassell G.J. (2011) Reversible inhibition of PSD-95 mRNA translation by miR-125a, FMRP phosphorylation, and mGluR signaling. *Molecular cell* **42**:673-688.

53. Narayanan U., Nalavadi V., Nakamoto M., Pallas D.C., Ceman S., Bassell G.J., Warren S.T. (2007) FMRP phosphorylation reveals an immediate-early signaling pathway triggered by group I mGluR and mediated by PP2A. *The Journal of neuroscience : the official journal of the Society for Neuroscience* **27**:14349-14357.

54. Ifrim M.F., Williams K.R., Bassell G.J. (2015) Single-Molecule Imaging of PSD-95 mRNA Translation in Dendrites and Its Dysregulation in a Mouse Model of Fragile X Syndrome. *The Journal of neuroscience : the official journal of the Society for Neuroscience* **35**:7116-7130.

55. Gross C., Yao X., Pong D.L., Jeromin A., Bassell G.J. (2011) Fragile X mental retardation protein regulates protein expression and mRNA translation of the potassium channel Kv4.2. *The Journal of neuroscience : the official journal of the Society for Neuroscience* **31**:5693-5698.

56. Charlesworth A., Meijer H.A., de Moor C.H. (2013) Specificity factors in cytoplasmic polyadenylation. *Wiley interdisciplinary reviews RNA* **4**:437-461.

57. Hessle V., Bjork P., Sokolowski M., Gonzalez de Valdivia E., Silverstein R., Artemenko K., Tyagi A., Maddalo G., Ilag L., Helbig R., Zubarev R.A., Visa N.

(2009) The exosome associates cotranscriptionally with the nascent pre-mRNP through interactions with heterogeneous nuclear ribonucleoproteins. *Molecular biology of the cell* **20**:3459-3470.

58. Jiao X., Chang J.H., Kilic T., Tong L., Kiledjian M. (2013) A mammalian pre-mRNA 5' end capping quality control mechanism and an unexpected link of capping to pre-mRNA processing. *Molecular cell* **50**:104-115.

59. Nagarajan V.K., Jones C.I., Newbury S.F., Green P.J. (2013) XRN 5'-->3' exoribonucleases: structure, mechanisms and functions. *Biochimica et biophysica acta* **1829**:590-603.

60. Iglesias N., Stutz F. (2008) Regulation of mRNP dynamics along the export pathway. *FEBS letters* **582**:1987-1996.

61. Brannan K., Kim H., Erickson B., Glover-Cutter K., Kim S., Fong N., Kiemele L., Hansen K., Davis R., Lykke-Andersen J., Bentley D.L. (2012) mRNA decapping factors and the exonuclease Xrn2 function in widespread premature termination of RNA polymerase II transcription. *Molecular cell* **46**:311-324.

62. Davidson L., Kerr A., West S. (2012) Co-transcriptional degradation of aberrant pre-mRNA by Xrn2. *The EMBO journal* **31**:2566-2578.

63. West S., Proudfoot N.J. (2009) Transcriptional termination enhances protein expression in human cells. *Molecular cell* **33**:354-364.

64. Milligan L., Torchet C., Allmang C., Shipman T., Tollervey D. (2005) A nuclear surveillance pathway for mRNAs with defective polyadenylation. *Molecular and cellular biology* **25**:9996-10004.

65. Libri D., Dower K., Boulay J., Thomsen R., Rosbash M., Jensen T.H. (2002) Interactions between mRNA export commitment, 3'-end quality control, and nuclear degradation. *Molecular and cellular biology* **22**:8254-8266.

66. Burkard K.T., Butler J.S. (2000) A nuclear 3'-5' exonuclease involved in mRNA degradation interacts with Poly(A) polymerase and the hnRNA protein Npl3p. *Molecular and cellular biology* **20**:604-616.

67. Schmid M., Poulsen M.B., Olszewski P., Pelechano V., Saguez C., Gupta I., Steinmetz L.M., Moore C., Jensen T.H. (2012) Rrp6p controls mRNA poly(A) tail length and its decoration with poly(A) binding proteins. *Molecular cell* **47**:267-280.

68. Grenier St-Sauveur V., Soucek S., Corbett A.H., Bachand F. (2013) Poly(A) tail-mediated gene regulation by opposing roles of Nab2 and Pab2 nuclear poly(A)-binding proteins in pre-mRNA decay. *Molecular and cellular biology* **33**:4718-4731.

69. St-Andre O., Lemieux C., Perreault A., Lackner D.H., Bahler J., Bachand F. (2010) Negative regulation of meiotic gene expression by the nuclear poly(a)-binding protein in fission yeast. *The Journal of biological chemistry* **285**:27859-27868.

70. Lemay J.F., D'Amours A., Lemieux C., Lackner D.H., St-Sauveur V.G., Bahler J., Bachand F. (2010) The nuclear poly(A)-binding protein interacts with the exosome to promote synthesis of noncoding small nucleolar RNAs. *Molecular cell* **37**:34-45.

71. Czaplinski K., Ruiz-Echevarria M.J., Paushkin S.V., Han X., Weng Y., Perlick H.A., Dietz H.C., Ter-Avanesyan M.D., Peltz S.W. (1998) The surveillance complex interacts with the translation release factors to enhance termination and degrade aberrant mRNAs. *Genes & development* **12**:1665-1677.

72. Kashima I., Yamashita A., Izumi N., Kataoka N., Morishita R., Hoshino S., Ohno M., Dreyfuss G., Ohno S. (2006) Binding of a novel SMG-1-Upf1-eRF1-eRF3 complex (SURF) to the exon junction complex triggers Upf1 phosphorylation and nonsense-mediated mRNA decay. *Genes & development* **20**:355-367.

73. Yamashita A., Ohnishi T., Kashima I., Taya Y., Ohno S. (2001) Human SMG-1, a novel phosphatidylinositol 3-kinase-related protein kinase, associates with components of the mRNA surveillance complex and is involved in the regulation of nonsense-mediated mRNA decay. *Genes & development* **15**:2215-2228.

74. Ohnishi T., Yamashita A., Kashima I., Schell T., Anders K.R., Grimson A., Hachiya T., Hentze M.W., Anderson P., Ohno S. (2003) Phosphorylation of hUPF1 induces formation of mRNA surveillance complexes containing hSMG-5 and hSMG-7. *Molecular cell* **12**:1187-1200.

75. Fukuhara N., Ebert J., Unterholzner L., Lindner D., Izaurralde E., Conti E. (2005) SMG7 is a 14-3-3-like adaptor in the nonsense-mediated mRNA decay pathway. *Molecular cell* **17**:537-547.

76. Chiu S.Y., Serin G., Ohara O., Maquat L.E. (2003) Characterization of human Smg5/7a: a protein with similarities to Caenorhabditis elegans SMG5 and SMG7 that functions in the dephosphorylation of Upf1. *Rna* **9**:77-87.

77. Anders K.R., Grimson A., Anderson P. (2003) SMG-5, required for C.elegans nonsense-mediated mRNA decay, associates with SMG-2 and protein phosphatase 2A. *The EMBO journal* **22**:641-650.

78. Yamashita A., Chang T.C., Yamashita Y., Zhu W., Zhong Z., Chen C.Y., Shyu A.B. (2005) Concerted action of poly(A) nucleases and decapping enzyme in mammalian mRNA turnover. *Nature structural & molecular biology* **12**:1054-1063.

79. Wu X., Brewer G. (2012) The regulation of mRNA stability in mammalian cells: 2.0. *Gene* **500**:10-21.

80. Chung S., Eckrich M., Perrone-Bizzozero N., Kohn D.T., Furneaux H. (1997) The Elav-like proteins bind to a conserved regulatory element in the 3'-untranslated region of GAP-43 mRNA. *The Journal of biological chemistry* **272**:6593-6598.

81. Beckel-Mitchener A.C., Miera A., Keller R., Perrone-Bizzozero N.I. (2002) Poly(A) tail length-dependent stabilization of GAP-43 mRNA by the RNA-binding protein HuD. *The Journal of biological chemistry* **277**:27996-28002.

82. Bird C.W., Gardiner A.S., Bolognani F., Tanner D.C., Chen C.Y., Lin W.J., Yoo S., Twiss J.L., Perrone-Bizzozero N. (2013) KSRP modulation of GAP-43 mRNA stability restricts axonal outgrowth in embryonic hippocampal neurons. *PloS one* **8**:e79255.

83. Wigington C.P., Williams K.R., Meers M.P., Bassell G.J., Corbett A.H. (2014) Poly(A) RNA-binding proteins and polyadenosine RNA: new members and novel functions. *Wiley interdisciplinary reviews RNA* **5**:601-622.

84. Campbell K. (2005) Cortical neuron specification: it has its time and place. *Neuron* **46**:373-376.

85. Metin C., Deleglise D., Serafini T., Kennedy T.E., Tessier-Lavigne M. (1997) A role for netrin-1 in the guidance of cortical efferents. *Development* **124**:5063-5074.

86. Richards L.J., Koester S.E., Tuttle R., O'Leary D.D. (1997) Directed growth of early cortical axons is influenced by a chemoattractant released from an intermediate target. *The Journal of neuroscience : the official journal of the Society for Neuroscience* **17**:2445-2458.

87. Polleux F., Giger R.J., Ginty D.D., Kolodkin A.L., Ghosh A. (1998) Patterning of cortical efferent projections by semaphorin-neuropilin interactions. *Science* **282**:1904-1906.

88. Polleux F., Morrow T., Ghosh A. (2000) Semaphorin 3A is a chemoattractant for cortical apical dendrites. *Nature* **404**:567-573.

89. Goldman J.S., Ashour M.A., Magdesian M.H., Tritsch N.X., Harris S.N., Christofi N., Chemali R., Stern Y.E., Thompson-Steckel G., Gris P., Glasgow S.D., Grutter P., Bouchard J.F., Ruthazer E.S., Stellwagen D., Kennedy T.E. (2013) Netrin-1 promotes excitatory synaptogenesis between cortical neurons by initiating synapse assembly. *The Journal of neuroscience : the official journal of the Society for Neuroscience* **33**:17278-17289.

90. Faravelli I., Nizzardo M., Comi G.P., Corti S. (2015) Spinal muscular atrophy--recent therapeutic advances for an old challenge. *Nature reviews Neurology* **11**:351-359.

91. Gabanella F., Butchbach M.E., Saieva L., Carissimi C., Burghes A.H., Pellizzoni L. (2007) Ribonucleoprotein assembly defects correlate with spinal muscular atrophy severity and preferentially affect a subset of spliceosomal snRNPs. *PloS one* **2**:e921.

92. Zhang Z., Lotti F., Dittmar K., Younis I., Wan L., Kasim M., Dreyfuss G. (2008) SMN deficiency causes tissue-specific perturbations in the repertoire of snRNAs and widespread defects in splicing. *Cell* **133**:585-600.

93. Huo Q., Kayikci M., Odermatt P., Meyer K., Michels O., Saxena S., Ule J., Schumperli D. (2014) Splicing changes in SMA mouse motoneurons and SMN-depleted neuroblastoma cells: evidence for involvement of splicing regulatory proteins. *RNA biology* **11**:1430-1446.

94. Zhang H.L., Pan F., Hong D., Shenoy S.M., Singer R.H., Bassell G.J. (2003) Active transport of the survival motor neuron protein and the role of exon-7 in cytoplasmic localization. *The Journal of neuroscience : the official journal of the Society for Neuroscience* **23**:6627-6637.

95. Giavazzi A., Setola V., Simonati A., Battaglia G. (2006) Neuronal-specific roles of the survival motor neuron protein: evidence from survival motor neuron expression patterns in the developing human central nervous system. *Journal of neuropathology and experimental neurology* **65**:267-277.

96. Jablonka S., Bandilla M., Wiese S., Buhler D., Wirth B., Sendtner M., Fischer U. (2001) Co-regulation of survival of motor neuron (SMN) protein and its interactor SIP1 during development and in spinal muscular atrophy. *Human molecular genetics* **10**:497-505.

97. Fallini C., Bassell G.J., Rossoll W. (2010) High-efficiency transfection of cultured primary motor neurons to study protein localization, trafficking, and function. *Molecular neurodegeneration* **5**:17.

98. Todd A.G., Morse R., Shaw D.J., Stebbings H., Young P.J. (2010) Analysis of SMN-neurite granules: Core Cajal body components are absent from SMN-cytoplasmic complexes. *Biochemical and biophysical research communications* **397**:479-485.

99. Fallini C., Zhang H., Su Y., Silani V., Singer R.H., Rossoll W., Bassell G.J. (2011) The survival of motor neuron (SMN) protein interacts with the mRNA-binding protein HuD and regulates localization of poly(A) mRNA in primary motor neuron axons. *The Journal of neuroscience : the official journal of the Society for Neuroscience* **31**:3914-3925.

100. Zhang H., Xing L., Rossoll W., Wichterle H., Singer R.H., Bassell G.J. (2006) Multiprotein complexes of the survival of motor neuron protein SMN with Gemins traffic to neuronal processes and growth cones of motor neurons. *The Journal of neuroscience : the official journal of the Society for Neuroscience* **26**:8622-8632.

101. Kanai Y., Dohmae N., Hirokawa N. (2004) Kinesin transports RNA: isolation and characterization of an RNA-transporting granule. *Neuron* **43**:513-525.

102. Tadesse H., Deschenes-Furry J., Boisvenue S., Cote J. (2008) KH-type splicing regulatory protein interacts with survival motor neuron protein and is misregulated in spinal muscular atrophy. *Human molecular genetics* **17**:506-524.

103. Hubers L., Valderrama-Carvajal H., Laframboise J., Timbers J., Sanchez G., Cote J. (2011) HuD interacts with survival motor neuron protein and can rescue spinal muscular atrophy-like neuronal defects. *Human molecular genetics* **20**:553-579.

104. Fallini C., Rouanet J.P., Donlin-Asp P.G., Guo P., Zhang H., Singer R.H., Rossoll W., Bassell G.J. (2014) Dynamics of survival of motor neuron (SMN) protein interaction with the mRNA-binding protein IMP1 facilitates its trafficking into motor neuron axons. *Developmental neurobiology* **74**:319-332.

105. Rossoll W., Jablonka S., Andreassi C., Kroning A.K., Karle K., Monani U.R., Sendtner M. (2003) Smn, the spinal muscular atrophy-determining gene product,

modulates axon growth and localization of beta-actin mRNA in growth cones of motoneurons. *The Journal of cell biology* **163**:801-812.

106. Fallini C., Bassell G.J., Rossoll W. (2012) Spinal muscular atrophy: the role of SMN in axonal mRNA regulation. *Brain research* **1462**:81-92.

107. Timchenko L. (2013) Molecular mechanisms of muscle atrophy in myotonic dystrophies. *The international journal of biochemistry & cell biology* **45**:2280-2287.

108. Dalton J.C., Ranum, L.P.W., Day, J.W. (2013) *Myotonic Dystrophy Type 2*. University of Washington, Seattle

109. Bird T. (2013) *Myotonic Dystrophy Type 1*. University of Washington, Seattle

110. Kino Y., Mori D., Oma Y., Takeshita Y., Sasagawa N., Ishiura S. (2004) Muscleblind protein, MBNL1/EXP, binds specifically to CHHG repeats. *Human molecular genetics* **13**:495-507.

111. Goers E.S., Purcell J., Voelker R.B., Gates D.P., Berglund J.A. (2010) MBNL1 binds GC motifs embedded in pyrimidines to regulate alternative splicing. *Nucleic acids research* **38**:2467-2484.

112. Masuda A., Andersen H.S., Doktor T.K., Okamoto T., Ito M., Andresen B.S., Ohno K. (2012) CUGBP1 and MBNL1 preferentially bind to 3' UTRs and facilitate mRNA decay. *Scientific reports* **2**:209.

113. Rau F., Freyermuth F., Fugier C., Villemin J.P., Fischer M.C., Jost B., Dembele D., Gourdon G., Nicole A., Duboc D., Wahbi K., Day J.W., Fujimura H., Takahashi M.P., Auboeuf D., Dreumont N., Furling D., Charlet-Berguerand N. (2011) Misregulation of miR-1 processing is associated with heart defects in myotonic dystrophy. *Nature structural & molecular biology* **18**:840-845.

114. Wang E.T., Cody N.A., Jog S., Biancolella M., Wang T.T., Treacy D.J., Luo S., Schroth G.P., Housman D.E., Reddy S., Lecuyer E., Burge C.B. (2012) Transcriptome-wide regulation of pre-mRNA splicing and mRNA localization by muscleblind proteins. *Cell* **150**:710-724.

115. Peters O.M., Ghasemi M., Brown R.H., Jr. (2015) Emerging mechanisms of molecular pathology in ALS. *The Journal of clinical investigation* **125**:1767-1779.

116. Dammer E.B., Fallini C., Gozal Y.M., Duong D.M., Rossoll W., Xu P., Lah J.J., Levey A.I., Peng J., Bassell G.J., Seyfried N.T. (2012) Coaggregation of RNA-binding proteins in a model of TDP-43 proteinopathy with selective RGG motif methylation and a role for RRM1 ubiquitination. *PloS one* **7**:e38658.

117. Fallini C., Bassell G.J., Rossoll W. (2012) The ALS disease protein TDP-43 is actively transported in motor neuron axons and regulates axon outgrowth. *Human molecular genetics* **21**:3703-3718.

118. Gendron T.F., Rademakers R., Petrucelli L. (2013) TARDBP mutation analysis in TDP-43 proteinopathies and deciphering the toxicity of mutant TDP-43. *Journal of Alzheimer's disease : JAD* **33 Suppl 1**:S35-45.

119. Xu Z.S. (2012) Does a loss of TDP-43 function cause neurodegeneration? *Molecular neurodegeneration* **7**:27.

120. Chou C.C., Alexeeva O.M., Yamada S., Pribadi A., Zhang Y., Mo B., Williams K.R., Zarnescu D.C., Rossoll W. (2015) PABPN1 suppresses TDP-43 toxicity in ALS disease models. *Human molecular genetics*

121. Raz Y., Raz V. (2014) Oculopharyngeal muscular dystrophy as a paradigm for muscle aging. *Frontiers in aging neuroscience* **6**:317.

122. Banerjee A., Apponi L.H., Pavlath G.K., Corbett A.H. (2013) PABPN1: molecular function and muscle disease. *The FEBS journal* **280**:4230-4250.

123. Apponi L.H., Leung S.W., Williams K.R., Valentini S.R., Corbett A.H., Pavlath G.K. (2010) Loss of nuclear poly(A)-binding protein 1 causes defects in myogenesis and mRNA biogenesis. *Human molecular genetics* **19**:1058-1065.

124. Jenal M., Elkon R., Loayza-Puch F., van Haaften G., Kuhn U., Menzies F.M., Oude Vrielink J.A., Bos A.J., Drost J., Rooijers K., Rubinsztein D.C., Agami R. (2012) The poly(A)-binding protein nuclear 1 suppresses alternative cleavage and polyadenylation sites. *Cell* **149**:538-553.

125. de Klerk E., Venema A., Anvar S.Y., Goeman J.J., Hu O., Trollet C., Dickson G., den Dunnen J.T., van der Maarel S.M., Raz V., t Hoen P.A. (2012) Poly(A) binding protein nuclear 1 levels affect alternative polyadenylation. *Nucleic acids research* **40**:9089-9101.

126. Apponi L.H., Corbett A.H., Pavlath G.K. (2013) Control of mRNA stability contributes to low levels of nuclear poly(A) binding protein 1 (PABPN1) in skeletal muscle. *Skeletal muscle* **3**:23.

127. Pak C., Garshasbi M., Kahrizi K., Gross C., Apponi L.H., Noto J.J., Kelly S.M., Leung S.W., Tzschach A., Behjati F., Abedini S.S., Mohseni M., Jensen L.R., Hu H., Huang B., Stahley S.N., Liu G., Williams K.R., Burdick S., Feng Y., Sanyal S., Bassell G.J., Ropers H.H., Najmabadi H., Corbett A.H., Moberg K.H., Kuss A.W. (2011) Mutation of the conserved polyadenosine RNA binding protein, ZC3H14/dNab2, impairs neural function in Drosophila and humans. *Proceedings of the National Academy of Sciences of the United States of America* **108**:12390-12395.

128. Soucek S., Corbett A.H., Fasken M.B. (2012) The long and the short of it: the role of the zinc finger polyadenosine RNA binding protein, Nab2, in control of poly(A) tail length. *Biochimica et biophysica acta* **1819**:546-554.

129. Sethna F., Moon C., Wang H. (2014) From FMRP function to potential therapies for fragile X syndrome. *Neurochemical research* **39**:1016-1031.

130. Darnell J.C., Klann E. (2013) The translation of translational control by FMRP: therapeutic targets for FXS. *Nature neuroscience* **16**:1530-1536.

131. Suhl J.A., Chopra P., Anderson B.R., Bassell G.J., Warren S.T. (2014) Analysis of FMRP mRNA target datasets reveals highly associated mRNAs mediated by G-quadruplex structures formed via clustered WGGA sequences. *Human molecular genetics* **23**:5479-5491.

132. Klann E., Dever T.E. (2004) Biochemical mechanisms for translational regulation in synaptic plasticity. *Nature reviews Neuroscience* **5**:931-942.

133. Pfeiffer B.E., Huber K.M. (2009) The state of synapses in fragile X syndrome. *The Neuroscientist : a review journal bringing neurobiology, neurology and psychiatry* **15**:549-567.

134. Zhang J., Saur T., Duke A.N., Grant S.G., Platt D.M., Rowlett J.K., Isacson O., Yao W.D. (2014) Motor impairments, striatal degeneration, and altered dopamine-glutamate interplay in mice lacking PSD-95. *Journal of neurogenetics* **28**:98-111.

135. Westmark C.J., Malter J.S. (2007) FMRP mediates mGluR5-dependent translation of amyloid precursor protein. *PLoS biology* **5**:e52.

136. Dreyfuss G., Matunis M.J., Pinol-Roma S., Burd C.G. (1993) hnRNP proteins and the biogenesis of mRNA. *Annual review of biochemistry* **62**:289-321.

137. Han S.P., Tang Y.H., Smith R. (2010) Functional diversity of the hnRNPs: past, present and perspectives. *The Biochemical journal* **430**:379-392.

138. Chaudhury A., Chander P., Howe P.H. (2010) Heterogeneous nuclear ribonucleoproteins (hnRNPs) in cellular processes: Focus on hnRNP E1's multifunctional regulatory roles. *Rna* **16**:1449-1462.

139. Thandapani P., O'Connor T.R., Bailey T.L., Richard S. (2013) Defining the RGG/RG motif. *Molecular cell* **50**:613-623.

140. Valverde R., Edwards L., Regan L. (2008) Structure and function of KH domains. *The FEBS journal* **275**:2712-2726.

141. Busch A., Hertel K.J. (2012) Evolution of SR protein and hnRNP splicing regulatory factors. *Wiley interdisciplinary reviews RNA* **3**:1-12.

142. Jean-Philippe J., Paz S., Caputi M. (2013) hnRNP A1: the Swiss army knife of gene expression. *International journal of molecular sciences* **14**:18999-19024.

143. Izaurralde E., Jarmolowski A., Beisel C., Mattaj I.W., Dreyfuss G., Fischer U. (1997) A role for the M9 transport signal of hnRNP A1 in mRNA nuclear export. *The Journal of cell biology* **137**:27-35.

144. Roy R., Durie D., Li H., Liu B.Q., Skehel J.M., Mauri F., Cuorvo L.V., Barbareschi M., Guo L., Holcik M., Seckl M.J., Pardo O.E. (2014) hnRNPA1 couples nuclear export and translation of specific mRNAs downstream of FGF-2/S6K2 signalling. *Nucleic acids research* **42**:12483-12497.

145. Ma A.S., Moran-Jones K., Shan J., Munro T.P., Snee M.J., Hoek K.S., Smith R. (2002) Heterogeneous nuclear ribonucleoprotein A3, a novel RNA trafficking

response element-binding protein. *The Journal of biological chemistry* **277**:18010-18020.

146. Kosturko L.D., Maggipinto M.J., Korza G., Lee J.W., Carson J.H., Barbarese E. (2006) Heterogeneous nuclear ribonucleoprotein (hnRNP) E1 binds to hnRNP A2 and inhibits translation of A2 response element mRNAs. *Molecular biology of the cell* **17**:3521-3533.

147. Hamilton B.J., Nichols R.C., Tsukamoto H., Boado R.J., Pardridge W.M., Rigby W.F. (1999) hnRNP A2 and hnRNP L bind the 3'UTR of glucose transporter 1 mRNA and exist as a complex in vivo. *Biochemical and biophysical research communications* **261**:646-651.

148. Lee K.H., Kim S.H., Kim H.J., Kim W., Lee H.R., Jung Y., Choi J.H., Hong K.Y., Jang S.K., Kim K.T. (2014) AUF1 contributes to Cryptochrome1 mRNA degradation and rhythmic translation. *Nucleic acids research* **42**:3590-3606.

149. Paek K.Y., Kim C.S., Park S.M., Kim J.H., Jang S.K. (2008) RNA-binding protein hnRNP D modulates internal ribosome entry site-dependent translation of hepatitis C virus RNA. *Journal of virology* **82**:12082-12093.

150. Zhao T.T., Graber T.E., Jordan L.E., Cloutier M., Lewis S.M., Goulet I., Cote J., Holcik M. (2009) hnRNP A1 regulates UV-induced NF-kappaB signalling through destabilization of cIAP1 mRNA. *Cell death and differentiation* **16**:244-252.

151. Fahling M., Mrowka R., Steege A., Martinka P., Persson P.B., Thiele B.J. (2006) Heterogeneous nuclear ribonucleoprotein-A2/B1 modulate collagen prolyl 4-hydroxylase, alpha (I) mRNA stability. *The Journal of biological chemistry* **281**:9279-9286.

152. Pautz A., Linker K., Altenhofer S., Heil S., Schmidt N., Art J., Knauer S., Stauber R., Sadri N., Pont A., Schneider R.J., Kleinert H. (2009) Similar regulation of human inducible nitric-oxide synthase expression by different isoforms of the RNA-binding protein AUF1. *The Journal of biological chemistry* **284**:2755-2766.

153. Zhou R., Chun R.F., Lisse T.S., Garcia A.J., Xu J., Adams J.S., Hewison M. (2015) Vitamin D and alternative splicing of RNA. *The Journal of steroid biochemistry and molecular biology* **148**:310-317.

154. Schepens B., Tinton S.A., Bruynooghe Y., Parthoens E., Haegman M., Beyaert R., Cornelis S. (2007) A role for hnRNP C1/C2 and Unr in internal initiation of translation during mitosis. *The EMBO journal* **26**:158-169.

155. Kim J.H., Paek K.Y., Choi K., Kim T.D., Hahm B., Kim K.T., Jang S.K. (2003) Heterogeneous nuclear ribonucleoprotein C modulates translation of c-myc mRNA in a cell cycle phase-dependent manner. *Molecular and cellular biology* **23**:708-720.

156. Shetty S. (2005) Regulation of urokinase receptor mRNA stability by hnRNP C in lung epithelial cells. *Molecular and cellular biochemistry* **272**:107-118.

157. Meng Q., Rayala S.K., Gururaj A.E., Talukder A.H., O'Malley B.W., Kumar R. (2007) Signaling-dependent and coordinated regulation of transcription, splicing, and translation resides in a single coregulator, PCBP1. *Proceedings of the National Academy of Sciences of the United States of America* **104**:5866-5871.

158. Wang Y., Gao L., Tse S.W., Andreadis A. (2010) Heterogeneous nuclear ribonucleoprotein E3 modestly activates splicing of tau exon 10 via its proximal downstream intron, a hotspot for frontotemporal dementia mutations. *Gene* **451**:23-31.

159. Revil T., Pelletier J., Toutant J., Cloutier A., Chabot B. (2009) Heterogeneous nuclear ribonucleoprotein K represses the production of pro-apoptotic Bcl-xS splice isoform. *The Journal of biological chemistry* **284**:21458-21467.

160. Bomsztyk K., Denisenko O., Ostrowski J. (2004) hnRNP K: one protein multiple processes. *BioEssays : news and reviews in molecular, cellular and developmental biology* **26**:629-638.

161. Mikula M., Bomsztyk K., Goryca K., Chojnowski K., Ostrowski J. (2013) Heterogeneous nuclear ribonucleoprotein (HnRNP) K genome-wide binding survey reveals its role in regulating 3'-end RNA processing and transcription termination at the early growth response 1 (EGR1) gene through XRN2 exonuclease. *The Journal of biological chemistry* **288**:24788-24798.

162. Wang H., Vardy L.A., Tan C.P., Loo J.M., Guo K., Li J., Lim S.G., Zhou J., Chng W.J., Ng S.B., Li H.X., Zeng Q. (2010) PCBP1 suppresses the translation of metastasis-associated PRL-3 phosphatase. *Cancer cell* **18**:52-62.

163. Laursen L.S., Chan C.W., Ffrench-Constant C. (2011) Translation of myelin basic protein mRNA in oligodendrocytes is regulated by integrin activation and hnRNP-K. *The Journal of cell biology* **192**:797-811.

164. Mukhopadhyay N.K., Kim J., Cinar B., Ramachandran A., Hager M.H., Di Vizio D., Adam R.M., Rubin M.A., Raychaudhuri P., De Benedetti A., Freeman M.R. (2009) Heterogeneous nuclear ribonucleoprotein K is a novel regulator of androgen receptor translation. *Cancer research* **69**:2210-2218.

165. Scoumanne A., Cho S.J., Zhang J., Chen X. (2011) The cyclin-dependent kinase inhibitor p21 is regulated by RNA-binding protein PCBP4 via mRNA stability. *Nucleic acids research* **39**:213-224.

166. Yano M., Okano H.J., Okano H. (2005) Involvement of Hu and heterogeneous nuclear ribonucleoprotein K in neuronal differentiation through p21 mRNA post-transcriptional regulation. *The Journal of biological chemistry* **280**:12690-12699.

167. Waggoner S.A., Johannes G.J., Liebhaber S.A. (2009) Depletion of the poly(C)-binding proteins alphaCP1 and alphaCP2 from K562 cells leads to p53-independent induction of cyclin-dependent kinase inhibitor (CDKN1A) and G1 arrest. *The Journal of biological chemistry* **284**:9039-9049.

168. Turunen J.J., Verma B., Nyman T.A., Frilander M.J. (2013) HnRNPH1/H2, U1 snRNP, and U11 snRNP cooperate to regulate the stability of the U11-48K pre-mRNA. *Rna* **19**:380-389.

169. Fisette J.F., Toutant J., Dugre-Brisson S., Desgroseillers L., Chabot B. (2010) hnRNP A1 and hnRNP H can collaborate to modulate 5' splice site selection. *Rna* **16**:228-238.

170. Martinez-Contreras R., Fisette J.F., Nasim F.U., Madden R., Cordeau M., Chabot B. (2006) Intronic binding sites for hnRNP A/B and hnRNP F/H proteins stimulate pre-mRNA splicing. *PLoS biology* **4**:e21.

171. Chou M.Y., Rooke N., Turck C.W., Black D.L. (1999) hnRNP H is a component of a splicing enhancer complex that activates a c-src alternative exon in neuronal cells. *Molecular and cellular biology* **19**:69-77.

172. Alkan S.A., Martincic K., Milcarek C. (2006) The hnRNPs F and H2 bind to similar sequences to influence gene expression. *The Biochemical journal* **393**:361-371.

173. Arhin G.K., Boots M., Bagga P.S., Milcarek C., Wilusz J. (2002) Downstream sequence elements with different affinities for the hnRNP H/H' protein influence the processing efficiency of mammalian polyadenylation signals. *Nucleic acids research* **30**:1842-1850.

174. Bagga P.S., Ford L.P., Chen F., Wilusz J. (1995) The G-rich auxiliary downstream element has distinct sequence and position requirements and mediates efficient 3' end pre-mRNA processing through a trans-acting factor. *Nucleic acids research* **23**:1625-1631.

175. Veraldi K.L., Arhin G.K., Martincic K., Chung-Ganster L.H., Wilusz J., Milcarek C. (2001) hnRNP F influences binding of a 64-kilodalton subunit of cleavage stimulation factor to mRNA precursors in mouse B cells. *Molecular and cellular biology* **21**:1228-1238.

176. White R., Gonsior C., Bauer N.M., Kramer-Albers E.M., Luhmann H.J., Trotter J. (2012) Heterogeneous nuclear ribonucleoprotein (hnRNP) F is a novel component of oligodendroglial RNA transport granules contributing to regulation of myelin basic protein (MBP) synthesis. *The Journal of biological chemistry* **287**:1742-1754.

177. Reznik B., Clement S.L., Lykke-Andersen J. (2014) hnRNP F complexes with tristetraprolin and stimulates ARE-mRNA decay. *PloS one* **9**:e100992.

178. Moursy A., Allain F.H., Clery A. (2014) Characterization of the RNA recognition mode of hnRNP G extends its role in SMN2 splicing regulation. *Nucleic acids research* **42**:6659-6672.

179. Hofmann Y., Wirth B. (2002) hnRNP-G promotes exon 7 inclusion of survival motor neuron (SMN) via direct interaction with Htra2-beta1. *Human molecular genetics* **11**:2037-2049.

180. Sawicka K., Bushell M., Spriggs K.A., Willis A.E. (2008) Polypyrimidine-tract-binding protein: a multifunctional RNA-binding protein. *Biochemical Society transactions* **36**:641-647.

181. Preussner M., Schreiner S., Hung L.H., Porstner M., Jack H.M., Benes V., Ratsch G., Bindereif A. (2012) HnRNP L and L-like cooperate in multiple-exon regulation of CD45 alternative splicing. *Nucleic acids research* **40**:5666-5678.

182. Romanelli M.G., Diani E., Lievens P.M. (2013) New insights into functional roles of the polypyrimidine tract-binding protein. *International journal of molecular sciences* **14**:22906-22932.

183. Rahman M.A., Masuda A., Ohe K., Ito M., Hutchinson D.O., Mayeda A., Engel A.G., Ohno K. (2013) HnRNP L and hnRNP LL antagonistically modulate PTB-mediated splicing suppression of CHRNA1 pre-mRNA. *Scientific reports* **3**:2931.

184. Loh T.J., Cho S., Moon H., Jang H.N., Williams D.R., Jung D.W., Kim I.C., Ghigna C., Biamonti G., Zheng X., Shen H. (2015) hnRNP L inhibits CD44 V10 exon splicing through interacting with its upstream intron. *Biochimica et biophysica acta* **1849**:743-750.

185. Chiou N.T., Shankarling G., Lynch K.W. (2013) hnRNP L and hnRNP A1 induce extended U1 snRNA interactions with an exon to repress spliceosome assembly. *Molecular cell* **49**:972-982.

186. Hung L.H., Heiner M., Hui J., Schreiner S., Benes V., Bindereif A. (2008) Diverse roles of hnRNP L in mammalian mRNA processing: a combined microarray and RNAi analysis. *Rna* **14**:284-296.

187. Guang S., Felthauser A.M., Mertz J.E. (2005) Binding of hnRNP L to the pre-mRNA processing enhancer of the herpes simplex virus thymidine kinase gene enhances both polyadenylation and nucleocytoplasmic export of intronless mRNAs. *Molecular and cellular biology* **25**:6303-6313.

188. Hwang B., Lim J.H., Hahm B., Jang S.K., Lee S.W. (2009) hnRNP L is required for the translation mediated by HCV IRES. *Biochemical and biophysical research communications* **378**:584-588.

189. Hui J., Reither G., Bindereif A. (2003) Novel functional role of CA repeats and hnRNP L in RNA stability. *Rna* **9**:931-936.

190. Brazao T.F., Demmers J., van I.W., Strouboulis J., Fornerod M., Romao L., Grosveld F.G. (2012) A new function of ROD1 in nonsense-mediated mRNA decay. *FEBS letters* **586**:1101-1110.

191. Lleres D., Denegri M., Biggiogera M., Ajuh P., Lamond A.I. (2010) Direct interaction between hnRNP-M and CDC5L/PLRG1 proteins affects alternative splice site choice. *EMBO reports* **11**:445-451.

192. Dery K.J., Gaur S., Gencheva M., Yen Y., Shively J.E., Gaur R.K. (2011) Mechanistic control of carcinoembryonic antigen-related cell adhesion molecule-1 (CEACAM1) splice isoforms by the heterogeneous nuclear ribonuclear proteins hnRNP L, hnRNP A1, and hnRNP M. *The Journal of biological chemistry* **286**:16039-16051.

193. Cho S., Moon H., Loh T.J., Oh H.K., Cho S., Choy H.E., Song W.K., Chun J.S., Zheng X., Shen H. (2014) hnRNP M facilitates exon 7 inclusion of SMN2 pre-mRNA in spinal muscular atrophy by targeting an enhancer on exon 7. *Biochimica et biophysica acta* **1839**:306-315.

194. Jain R.A., Gavis E.R. (2008) The Drosophila hnRNP M homolog Rumpelstiltskin regulates nanos mRNA localization. *Development* **135**:973-982.

195. Ron D. (1997) TLS-CHOP and the role of RNA-binding proteins in oncogenic transformation. *Current topics in microbiology and immunology* **220**:131-142.

196. Calvio C., Neubauer G., Mann M., Lamond A.I. (1995) Identification of hnRNP P2 as TLS/FUS using electrospray mass spectrometry. *Rna* **1**:724-733.

197. Tan A.Y., Manley J.L. (2009) The TET family of proteins: functions and roles in disease. *Journal of molecular cell biology* **1**:82-92.

198. Xiao R., Tang P., Yang B., Huang J., Zhou Y., Shao C., Li H., Sun H., Zhang Y., Fu X.D. (2012) Nuclear matrix factor hnRNP U/SAF-A exerts a global control of alternative splicing by regulating U2 snRNP maturation. *Molecular cell* **45**:656-668.

199. Vu N.T., Park M.A., Shultz J.C., Goehe R.W., Hoeferlin L.A., Shultz M.D., Smith S.A., Lynch K.W., Chalfant C.E. (2013) hnRNP U enhances caspase-9 splicing and is modulated by AKT-dependent phosphorylation of hnRNP L. *The Journal of biological chemistry* **288**:8575-8584.

200. Yugami M., Kabe Y., Yamaguchi Y., Wada T., Handa H. (2007) hnRNP-U enhances the expression of specific genes by stabilizing mRNA. *FEBS letters* **581**:1-7.

201. Glinka M., Herrmann T., Funk N., Havlicek S., Rossoll W., Winkler C., Sendtner M. (2010) The heterogeneous nuclear ribonucleoprotein-R is necessary for axonal beta-

actin mRNA translocation in spinal motor neurons. *Human molecular genetics* **19**:1951-1966.

202. Rossoll W., Kroning A.K., Ohndorf U.M., Steegborn C., Jablonka S., Sendtner M. (2002) Specific interaction of Smn, the spinal muscular atrophy determining gene product, with hnRNP-R and gry-rbp/hnRNP-Q: a role for Smn in RNA processing in motor axons? *Human molecular genetics* **11**:93-105.

203. Huang J., Li S.J., Chen X.H., Han Y., Xu P. (2008) hnRNP-R regulates the PMA-induced c-fos expression in retinal cells. *Cellular & molecular biology letters* **13**:303-311.

204. Kim T.D., Kim J.S., Kim J.H., Myung J., Chae H.D., Woo K.C., Jang S.K., Koh D.S., Kim K.T. (2005) Rhythmic serotonin N-acetyltransferase mRNA degradation is essential for the maintenance of its circadian oscillation. *Molecular and cellular biology* **25**:3232-3246.

205. Lau P.P., Chang B.H., Chan L. (2001) Two-hybrid cloning identifies an RNA-binding protein, GRY-RBP, as a component of apobec-1 editosome. *Biochemical and biophysical research communications* **282**:977-983.

206. Blanc V., Navaratnam N., Henderson J.O., Anant S., Kennedy S., Jarmuz A., Scott J., Davidson N.O. (2001) Identification of GRY-RBP as an apolipoprotein B RNA-binding protein that interacts with both apobec-1 and apobec-1 complementation factor to modulate C to U editing. *The Journal of biological chemistry* **276**:10272-10283.

207. Harris C.E., Boden R.A., Astell C.R. (1999) A novel heterogeneous nuclear ribonucleoprotein-like protein interacts with NS1 of the minute virus of mice. *Journal of virology* **73**:72-80.

208. Mizutani A., Fukuda M., Ibata K., Shiraishi Y., Mikoshiba K. (2000) SYNCRIP, a cytoplasmic counterpart of heterogeneous nuclear ribonucleoprotein R, interacts with ubiquitous synaptotagmin isoforms. *The Journal of biological chemistry* **275**:9823-9831.

209. Mourelatos Z., Abel L., Yong J., Kataoka N., Dreyfuss G. (2001) SMN interacts with a novel family of hnRNP and spliceosomal proteins. *The EMBO journal* **20**:5443-5452.

210. Quaresma A.J., Oyama S., Jr., Barbosa J.A., Kobarg J. (2006) The acidic domain of hnRNPQ (NSAP1) has structural similarity to Barstar and binds to Apobec1. *Biochemical and biophysical research communications* **350**:288-297.

211. Shimizu Y., Nishitsuji H., Marusawa H., Ujino S., Takaku H., Shimotohno K. (2014) The RNA-editing enzyme APOBEC1 requires heterogeneous nuclear ribonucleoprotein Q isoform 6 for efficient interaction with interleukin-8 mRNA. *The Journal of biological chemistry* **289**:26226-26238.

212. Chen H.H., Chang J.G., Lu R.M., Peng T.Y., Tarn W.Y. (2008) The RNA binding protein hnRNP Q modulates the utilization of exon 7 in the survival motor neuron 2 (SMN2) gene. *Molecular and cellular biology* **28**:6929-6938.

213. Kabat J.L., Barberan-Soler S., Zahler A.M. (2009) HRP-2, the Caenorhabditis elegans homolog of mammalian heterogeneous nuclear ribonucleoproteins Q and R, is an

alternative splicing factor that binds to UCUAUC splicing regulatory elements. *The Journal of biological chemistry* **284**:28490-28497.

214. Bannai H., Fukatsu K., Mizutani A., Natsume T., Iemura S., Ikegami T., Inoue T., Mikoshiba K. (2004) An RNA-interacting protein, SYNCRIP (heterogeneous nuclear ribonuclear protein Q1/NSAP1) is a component of mRNA granule transported with inositol 1,4,5-trisphosphate receptor type 1 mRNA in neuronal dendrites. *The Journal of biological chemistry* **279**:53427-53434.

215. Chen H.H., Yu H.I., Chiang W.C., Lin Y.D., Shia B.C., Tarn W.Y. (2012) hnRNP Q regulates Cdc42-mediated neuronal morphogenesis. *Molecular and cellular biology* **32**:2224-2238.

216. McDermott S.M., Meignin C., Rappsilber J., Davis I. (2012) Drosophila Syncrip binds the gurken mRNA localisation signal and regulates localised transcripts during axis specification. *Biology open* **1**:488-497.

217. Lyabin D.N., Nigmatullina L.F., Doronin A.N., Eliseeva I.A., Ovchinnikov L.P. (2013) Identification of proteins specifically interacting with YB-1 mRNA 3' UTR and the effect of hnRNP Q on YB-1 mRNA translation. *Biochemistry Biokhimiia* **78**:651-659.

218. Xing L., Yao X., Williams K.R., Bassell G.J. (2012) Negative regulation of RhoA translation and signaling by hnRNP-Q1 affects cellular morphogenesis. *Molecular biology of the cell* **23**:1500-1509.

219. Svitkin Y.V., Yanagiya A., Karetnikov A.E., Alain T., Fabian M.R., Khoutorsky A., Perreault S., Topisirovic I., Sonenberg N. (2013) Control of translation and miRNA-

dependent repression by a novel poly(A) binding protein, hnRNP-Q. *PLoS biology* **11**:e1001564.

220. Kim J.H., Paek K.Y., Ha S.H., Cho S., Choi K., Kim C.S., Ryu S.H., Jang S.K. (2004) A cellular RNA-binding protein enhances internal ribosomal entry site-dependent translation through an interaction downstream of the hepatitis C virus polyprotein initiation codon. *Molecular and cellular biology* **24**:7878-7890.

221. Cho S., Park S.M., Kim T.D., Kim J.H., Kim K.T., Jang S.K. (2007) BiP internal ribosomal entry site activity is controlled by heat-induced interaction of NSAP1. *Molecular and cellular biology* **27**:368-383.

222. Kim T.D., Woo K.C., Cho S., Ha D.C., Jang S.K., Kim K.T. (2007) Rhythmic control of AANAT translation by hnRNP Q in circadian melatonin production. *Genes & development* **21**:797-810.

223. Kim D.Y., Woo K.C., Lee K.H., Kim T.D., Kim K.T. (2010) hnRNP Q and PTB modulate the circadian oscillation of mouse Rev-erb alpha via IRES-mediated translation. *Nucleic acids research* **38**:7068-7078.

224. Lee K.H., Woo K.C., Kim D.Y., Kim T.D., Shin J., Park S.M., Jang S.K., Kim K.T. (2012) Rhythmic interaction between Period1 mRNA and hnRNP Q leads to circadian time-dependent translation. *Molecular and cellular biology* **32**:717-728.

225. Kim D.Y., Kim W., Lee K.H., Kim S.H., Lee H.R., Kim H.J., Jung Y., Choi J.H., Kim K.T. (2013) hnRNP Q regulates translation of p53 in normal and stress conditions. *Cell death and differentiation* **20**:226-234.

226. Duning K., Buck F., Barnekow A., Kremerskothen J. (2008) SYNCRIP, a component of dendritically localized mRNPs, binds to the translation regulator BC200 RNA. *Journal of neurochemistry* **105**:351-359.

227. Kondrashov A.V., Kiefmann M., Ebnet K., Khanam T., Muddashetty R.S., Brosius J. (2005) Inhibitory effect of naked neural BC1 RNA or BC200 RNA on eukaryotic in vitro translation systems is reversed by poly(A)-binding protein (PABP). *Journal of molecular biology* **353**:88-103.

228. Mukhopadhyay R., Jia J., Arif A., Ray P.S., Fox P.L. (2009) The GAIT system: a gatekeeper of inflammatory gene expression. *Trends in biochemical sciences* **34**:324-331.

229. Grosset C., Chen C.Y., Xu N., Sonenberg N., Jacquemin-Sablon H., Shyu A.B. (2000) A mechanism for translationally coupled mRNA turnover: interaction between the poly(A) tail and a c-fos RNA coding determinant via a protein complex. *Cell* **103**:29-40.

230. Weidensdorfer D., Stohr N., Baude A., Lederer M., Kohn M., Schierhorn A., Buchmeier S., Wahle E., Huttelmaier S. (2009) Control of c-myc mRNA stability by IGF2BP1-associated cytoplasmic RNPs. *Rna* **15**:104-115.

231. Kuchler L., Giegerich A.K., Sha L.K., Knape T., Wong M.S., Schroder K., Brandes R.P., Heide H., Wittig I., Brune B., von Knethen A. (2014) SYNCRIP-dependent Nox2 mRNA destabilization impairs ROS formation in M2-polarized macrophages. *Antioxidants & redox signaling* **21**:2483-2497.

232. Kim D.Y., Kwak E., Kim S.H., Lee K.H., Woo K.C., Kim K.T. (2011) hnRNP Q mediates a phase-dependent translation-coupled mRNA decay of mouse Period3. *Nucleic acids research* **39**:8901-8914.

233. Yoo B.C., Hong S.H., Ku J.L., Kim Y.H., Shin Y.K., Jang S.G., Kim I.J., Jeong S.Y., Park J.G. (2009) Galectin-3 stabilizes heterogeneous nuclear ribonucleoprotein Q to maintain proliferation of human colon cancer cells. *Cellular and molecular life sciences : CMLS* **66**:350-364.

234. Halstead J.M., Lin Y.Q., Durraine L., Hamilton R.S., Ball G., Neely G.G., Bellen H.J., Davis I. (2014) Syncrip/hnRNP Q influences synaptic transmission and regulates BMP signaling at the Drosophila neuromuscular synapse. *Biology open* **3**:839-849.

235. Iwasaki H. (2008) Involvement of PRMT1 in hnRNPQ activation and internalization of insulin receptor. *Biochemical and biophysical research communications* **372**:314-319.

236. Liu H.M., Aizaki H., Choi K.S., Machida K., Ou J.J., Lai M.M. (2009) SYNCRIP (synaptotagmin-binding, cytoplasmic RNA-interacting protein) is a host factor involved in hepatitis C virus RNA replication. *Virology* **386**:249-256.

237. Hresko R.C., Mueckler M. (2002) Identification of pp68 as the Tyrosine-phosphorylated Form of SYNCRIP/NSAP1. A cytoplasmic RNA-binding protein. *The Journal of biological chemistry* **277**:25233-25238.

238. Hresko R.C., Mueckler M. (2000) A novel 68-kDa adipocyte protein phosphorylated on tyrosine in response to insulin and osmotic shock. *The Journal of biological chemistry* **275**:18114-18120.

239. Watanabe N., Kato T., Fujita H., Kitagawa S. (2013) Heterogeneous nuclear ribonucleoprotein Q is a novel substrate of SH2 domain-containing phosphatase-2. *Journal of biochemistry* **154**:475-480.

240. Passos D.O., Quaresma A.J., Kobarg J. (2006) The methylation of the C-terminal region of hnRNPQ (NSAP1) is important for its nuclear localization. *Biochemical and biophysical research communications* **346**:517-525.

241. Kedersha N., Anderson P. (2007) Mammalian stress granules and processing bodies. *Methods in enzymology* **431**:61-81.

242. Moser J.J., Eystathioy T., Chan E.K., Fritzler M.J. (2007) Markers of mRNA stabilization and degradation, and RNAi within astrocytoma GW bodies. *Journal of neuroscience research* **85**:3619-3631.

243. Quaresma A.J., Bressan G.C., Gava L.M., Lanza D.C., Ramos C.H., Kobarg J. (2009) Human hnRNP Q re-localizes to cytoplasmic granules upon PMA, thapsigargin, arsenite and heat-shock treatments. *Experimental cell research* **315**:968-980.

244. Proud C.G. (2015) Mnks, eIF4E phosphorylation and cancer. *Biochimica et biophysica acta* **1849**:766-773.

245. Dong R., Yang G.D., Luo N.A., Qu Y.Q. (2014) HuR: a promising therapeutic target for angiogenesis. *Gland surgery* **3**:203-206.

246. Kotta-Loizou I., Giaginis C., Theocharis S. (2014) Clinical significance of HuR expression in human malignancy. *Medical oncology* **31**:161.

247. Chenard C.A., Richard S. (2008) New implications for the QUAKING RNA binding protein in human disease. *Journal of neuroscience research* **86**:233-242.

248. Klar J., Sobol M., Melberg A., Mabert K., Ameur A., Johansson A.C., Feuk L., Entesarian M., Orlen H., Casar-Borota O., Dahl N. (2013) Welander distal myopathy caused by an ancient founder mutation in TIA1 associated with perturbed splicing. *Human mutation* **34**:572-577.

249. Denny J.B. (2006) Molecular mechanisms, biological actions, and neuropharmacology of the growth-associated protein GAP-43. *Current neuropharmacology* **4**:293-304.

250. Donnelly C.J., Park M., Spillane M., Yoo S., Pacheco A., Gomes C., Vuppalanchi D., McDonald M., Kim H.H., Merianda T.T., Gallo G., Twiss J.L. (2013) Axonally synthesized beta-actin and GAP-43 proteins support distinct modes of axonal growth. *The Journal of neuroscience : the official journal of the Society for Neuroscience* **33**:3311-3322.

251. Rekart J.L., Meiri K., Routtenberg A. (2005) Hippocampal-dependent memory is impaired in heterozygous GAP-43 knockout mice. *Hippocampus* **15**:1-7.

252. Holahan M., Routtenberg A. (2008) The protein kinase C phosphorylation site on GAP-43 differentially regulates information storage. *Hippocampus* **18**:1099-1102.

253. Routtenberg A., Cantallops I., Zaffuto S., Serrano P., Namgung U. (2000) Enhanced learning after genetic overexpression of a brain growth protein. *Proceedings of the National Academy of Sciences of the United States of America* **97**:7657-7662.

254. Holahan M.R., Honegger K.S., Tabatadze N., Routtenberg A. (2007) GAP-43 gene expression regulates information storage. *Learning & memory* **14**:407-415.

255. Erzurumlu R.S., Jhaveri S., Moya K.L., Benowitz L.I. (1989) Peripheral nerve regeneration induces elevated expression of GAP-43 in the brainstem trigeminal complex of adult hamsters. *Brain research* **498**:135-139.

256. Van der Zee C.E., Nielander H.B., Vos J.P., Lopes da Silva S., Verhaagen J., Oestreicher A.B., Schrama L.H., Schotman P., Gispen W.H. (1989) Expression of growth-associated protein B-50 (GAP43) in dorsal root ganglia and sciatic nerve during regenerative sprouting. *The Journal of neuroscience : the official journal of the Society for Neuroscience* **9**:3505-3512.

257. Campbell G., Anderson P.N., Turmaine M., Lieberman A.R. (1991) GAP-43 in the axons of mammalian CNS neurons regenerating into peripheral nerve grafts. *Experimental brain research* **87**:67-74.

258. Grasselli G., Mandolesi G., Strata P., Cesare P. (2011) Impaired sprouting and axonal atrophy in cerebellar climbing fibres following in vivo silencing of the growth-associated protein GAP-43. *PloS one* **6**:e20791.

259. Schreyer D.J., Skene J.H. (1991) Fate of GAP-43 in ascending spinal axons of DRG neurons after peripheral nerve injury: delayed accumulation and correlation with regenerative potential. *The Journal of neuroscience : the official journal of the Society for Neuroscience* **11**:3738-3751.

260. Yankner B.A., Benowitz L.I., Villa-Komaroff L., Neve R.L. (1990) Transfection of PC12 cells with the human GAP-43 gene: effects on neurite outgrowth and regeneration. *Brain research Molecular brain research* **7**:39-44.

261. Zhang Y., Bo X., Schoepfer R., Holtmaat A.J., Verhaagen J., Emson P.C., Lieberman A.R., Anderson P.N. (2005) Growth-associated protein GAP-43 and L1 act

synergistically to promote regenerative growth of Purkinje cell axons in vivo. *Proceedings of the National Academy of Sciences of the United States of America* **102**:14883-14888.

262. Bogdanovic N., Davidsson P., Volkmann I., Winblad B., Blennow K. (2000) Growth-associated protein GAP-43 in the frontal cortex and in the hippocampus in Alzheimer's disease: an immunohistochemical and quantitative study. *Journal of neural transmission* **107**:463-478.

263. de la Monte S.M., Ng S.C., Hsu D.W. (1995) Aberrant GAP-43 gene expression in Alzheimer's disease. *The American journal of pathology* **147**:934-946.

264. Tian S.Y., Wang J.F., Bezchlibnyk Y.B., Young L.T. (2007) Immunoreactivity of 43 kDa growth-associated protein is decreased in post mortem hippocampus of bipolar disorder and schizophrenia. *Neuroscience letters* **411**:123-127.

265. Zaccaria K.J., Lagace D.C., Eisch A.J., McCasland J.S. (2010) Resistance to change and vulnerability to stress: autistic-like features of GAP43-deficient mice. *Genes, brain, and behavior* **9**:985-996.

266. Weber J.R., Skene J.H. (1997) Identification of a novel repressive element that contributes to neuron-specific gene expression. *The Journal of neuroscience : the official journal of the Society for Neuroscience* **17**:7583-7593.

267. Chiaramello A., Neuman T., Peavy D.R., Zuber M.X. (1996) The GAP-43 gene is a direct downstream target of the basic helix-loop-helix transcription factors. *The Journal of biological chemistry* **271**:22035-22043.

268. Diolaiti D., Bernardoni R., Trazzi S., Papa A., Porro A., Bono F., Herbert J.M., Perini G., Della Valle G. (2007) Functional cooperation between TrkA and p75(NTR)

accelerates neuronal differentiation by increased transcription of GAP-43 and p21(CIP/WAF) genes via ERK1/2 and AP-1 activities. *Experimental cell research* **313**:2980-2992.

269. Tedeschi A., Nguyen T., Puttagunta R., Gaub P., Di Giovanni S. (2009) A p53-CBP/p300 transcription module is required for GAP-43 expression, axon outgrowth, and regeneration. *Cell death and differentiation* **16**:543-554.

270. Smith C.L., Afroz R., Bassell G.J., Furneaux H.M., Perrone-Bizzozero N.I., Burry R.W. (2004) GAP-43 mRNA in growth cones is associated with HuD and ribosomes. *Journal of neurobiology* **61**:222-235.

271. Donnelly C.J., Willis D.E., Xu M., Tep C., Jiang C., Yoo S., Schanen N.C., Kirn-Safran C.B., van Minnen J., English A., Yoon S.O., Bassell G.J., Twiss J.L. (2011) Limited availability of ZBP1 restricts axonal mRNA localization and nerve regeneration capacity. *The EMBO journal* **30**:4665-4677.

272. Pascale A., Gusev P.A., Amadio M., Dottorini T., Govoni S., Alkon D.L., Quattrone A. (2004) Increase of the RNA-binding protein HuD and posttranscriptional up-regulation of the GAP-43 gene during spatial memory. *Proceedings of the National Academy of Sciences of the United States of America* **101**:1217-1222.

273. Klebe R.J.R., F.H. (1969) Neuroblastoma: Cell culture analysis of a differentiating stem cell system. *The Journal of cell biology* **43**:

274. Munoz J.P., Alvarez A., Maccioni R.B. (2000) Increase in the expression of the neuronal cyclin-dependent protein kinase cdk-5 during differentiation of N2A neuroblastoma cells. *Neuroreport* **11**:2733-2738.

275. Kosik K.S., Finch E.A. (1987) MAP2 and tau segregate into dendritic and axonal domains after the elaboration of morphologically distinct neurites: an immunocytochemical study of cultured rat cerebrum. *The Journal of neuroscience : the official journal of the Society for Neuroscience* **7**:3142-3153.

276. Clayton G.H., Perez G.M., Smith R.L., Owens G.C. (1998) Expression of mRNA for the elav-like neural-specific RNA binding protein, HuD, during nervous system development. *Brain research Developmental brain research* **109**:271-280.

277. Namgung U., Routtenberg A. (2000) Transcriptional and post-transcriptional regulation of a brain growth protein: regional differentiation and regeneration induction of GAP-43. *The European journal of neuroscience* **12**:3124-3136.

278. Hagihara H., Toyama K., Yamasaki N., Miyakawa T. (2009) Dissection of hippocampal dentate gyrus from adult mouse. *Journal of visualized experiments : JoVE*

279. Dent E.W., Meiri K.F. (1992) GAP-43 phosphorylation is dynamically regulated in individual growth cones. *Journal of neurobiology* **23**:1037-1053.

280. Goslin K., Schreyer D.J., Skene J.H., Banker G. (1990) Changes in the distribution of GAP-43 during the development of neuronal polarity. *The Journal of neuroscience : the official journal of the Society for Neuroscience* **10**:588-602.

281. Aigner L., Arber S., Kapfhammer J.P., Laux T., Schneider C., Botteri F., Brenner H.R., Caroni P. (1995) Overexpression of the neural growth-associated protein GAP-43 induces nerve sprouting in the adult nervous system of transgenic mice. *Cell* **83**:269-278.

282. Leu B., Koch E., Schmidt J.T. (2010) GAP43 phosphorylation is critical for growth and branching of retinotectal arbors in zebrafish. *Developmental neurobiology* **70**:897-911.

283. Nguyen L., He Q., Meiri K.F. (2009) Regulation of GAP-43 at serine 41 acts as a switch to modulate both intrinsic and extrinsic behaviors of growing neurons, via altered membrane distribution. *Molecular and cellular neurosciences* **41**:62-73.

284. Donovan S.L., Mamounas L.A., Andrews A.M., Blue M.E., McCasland J.S. (2002) GAP-43 is critical for normal development of the serotonergic innervation in forebrain. *The Journal of neuroscience : the official journal of the Society for Neuroscience* **22**:3543-3552.

285. McIlvain V.A., Robertson D.R., Maimone M.M., McCasland J.S. (2003) Abnormal thalamocortical pathfinding and terminal arbors lead to enlarged barrels in neonatal GAP-43 heterozygous mice. *The Journal of comparative neurology* **462**:252-264.

286. Strittmatter S.M., Fankhauser C., Huang P.L., Mashimo H., Fishman M.C. (1995) Neuronal pathfinding is abnormal in mice lacking the neuronal growth cone protein GAP-43. *Cell* **80**:445-452.

287. Shen Y., Mani S., Donovan S.L., Schwob J.E., Meiri K.F. (2002) Growth-associated protein-43 is required for commissural axon guidance in the developing vertebrate nervous system. *The Journal of neuroscience : the official journal of the Society for Neuroscience* **22**:239-247.

288. Aigner L., Caroni P. (1995) Absence of persistent spreading, branching, and adhesion in GAP-43-depleted growth cones. *The Journal of cell biology* **128**:647-660.

289. Curtis R., Green D., Lindsay R.M., Wilkin G.P. (1993) Up-regulation of GAP-43 and growth of axons in rat spinal cord after compression injury. *Journal of neurocytology* **22**:51-64.

290. Schmitt A.B., Breuer S., Voell M., Schwaiger F.W., Spitzer C., Pech K., Brook G.A., Noth J., Kreutzberg G.W., Nacimiento W. (1999) GAP-43 (B-50) and C-Jun are up-regulated in axotomized neurons of Clarke's nucleus after spinal cord injury in the adult rat. *Neurobiology of disease* **6**:122-130.

291. Chen L.J., Ren Y.H., Liu L., Zhang X.Q., Zhao Y., Wu W.T., Li F. (2010) Upregulated expression of GAP-43 mRNA and protein in anterior horn motoneurons of the spinal cord after brachial plexus injury. *Archives of medical research* **41**:513-518.

292. Khullar S.M., Fristad I., Brodin P., Kvinnsland I.H. (1998) Upregulation of growth associated protein 43 expression and neuronal co-expression with neuropeptide Y following inferior alveolar nerve axotomy in the rat. *Journal of the peripheral nervous system : JPNS* **3**:79-90.

293. Anderson K.D., Merhege M.A., Morin M., Bolognani F., Perrone-Bizzozero N.I. (2003) Increased expression and localization of the RNA-binding protein HuD and GAP-43 mRNA to cytoplasmic granules in DRG neurons during nerve regeneration. *Experimental neurology* **183**:100-108.

294. Andersen L.B., Schreyer D.J. (1999) Constitutive expression of GAP-43 correlates with rapid, but not slow regrowth of injured dorsal root axons in the adult rat. *Experimental neurology* **155**:157-164.

295. Allegra Mascaro A.L., Cesare P., Sacconi L., Grasselli G., Mandolesi G., Maco B., Knott G.W., Huang L., De Paola V., Strata P., Pavone F.S. (2013) In vivo single branch axotomy induces GAP-43-dependent sprouting and synaptic remodeling in cerebellar cortex. *Proceedings of the National Academy of Sciences of the United States of America* **110**:10824-10829.

296. Gianola S., Rossi F. (2004) GAP-43 overexpression in adult mouse Purkinje cells overrides myelin-derived inhibition of neurite growth. *The European journal of neuroscience* **19**:819-830.

297. De Moliner K.L., Wolfson M.L., Perrone Bizzozero N., Adamo A.M. (2005) Growth-associated protein-43 is degraded via the ubiquitin-proteasome system. *Journal of neuroscience research* **79**:652-660.

298. Dotti C.G., Sullivan C.A., Banker G.A. (1988) The establishment of polarity by hippocampal neurons in culture. *The Journal of neuroscience : the official journal of the Society for Neuroscience* **8**:1454-1468.

299. Duman J.G., Mulherkar S., Tu Y.K., J X.C., Tolias K.F. (2015) Mechanisms for spatiotemporal regulation of Rho-GTPase signaling at synapses. *Neuroscience letters* **601**:4-10.

300. Aarts L.H., Schrama L.H., Hage W.J., Bos J.L., Gispen W.H., Schotman P. (1998) B-50/GAP-43-induced formation of filopodia depends on Rho-GTPase. *Molecular biology of the cell* **9**:1279-1292.

301. Gauthier-Campbell C., Bredt D.S., Murphy T.H., El-Husseini Ael D. (2004) Regulation of dendritic branching and filopodia formation in hippocampal neurons by specific acylated protein motifs. *Molecular biology of the cell* **15**:2205-2217.

302. Machacek M., Hodgson L., Welch C., Elliott H., Pertz O., Nalbant P., Abell A., Johnson G.L., Hahn K.M., Danuser G. (2009) Coordination of Rho GTPase activities during cell protrusion. *Nature* **461**:99-103.

303. Mobarak C.D., Anderson K.D., Morin M., Beckel-Mitchener A., Rogers S.L., Furneaux H., King P., Perrone-Bizzozero N.I. (2000) The RNA-binding protein HuD is required for GAP-43 mRNA stability, GAP-43 gene expression, and PKC-dependent neurite outgrowth in PC12 cells. *Molecular biology of the cell* **11**:3191-3203.

304. Kikin O., D'Antonio L., Bagga P.S. (2006) QGRS Mapper: a web-based server for predicting G-quadruplexes in nucleotide sequences. *Nucleic acids research* **34**:W676-682.

305. Davis J.T. (2004) G-quartets 40 years later: from 5'-GMP to molecular biology and supramolecular chemistry. *Angewandte Chemie* **43**:668-698.

306. Joachimi A., Benz A., Hartig J.S. (2009) A comparison of DNA and RNA quadruplex structures and stabilities. *Bioorganic & medicinal chemistry* **17**:6811-6815.

307. Huppert J.L. (2008) Hunting G-quadruplexes. *Biochimie* **90**:1140-1148.

308. Lipps H.J., Rhodes D. (2009) G-quadruplex structures: in vivo evidence and function. *Trends in cell biology* **19**:414-422.

309. Bugaut A., Balasubramanian S. (2012) 5'-UTR RNA G-quadruplexes: translation regulation and targeting. *Nucleic acids research* **40**:4727-4741.

310. Arora A., Suess B. (2011) An RNA G-quadruplex in the 3' UTR of the proto-oncogene PIM1 represses translation. *RNA biology* **8**:802-805.

311. Hornbeck P.V., Chabra I., Kornhauser J.M., Skrzypek E., Zhang B. (2004) PhosphoSite: A bioinformatics resource dedicated to physiological protein phosphorylation. *Proteomics* **4**:1551-1561.

312. Kozomara A., Griffiths-Jones S. (2014) miRBase: annotating high confidence microRNAs using deep sequencing data. *Nucleic acids research* **42**:D68-73.

313. Stefanovic S., DeMarco B.A., Underwood A., Williams K.R., Bassell G.J., Mihailescu M.R. (2015) Fragile X mental retardation protein interactions with a G quadruplex structure in the 3'-untranslated region of NR2B mRNA. *Molecular bioSystems*

314. Bharill S., Sarkar P., Ballin J.D., Gryczynski I., Wilson G.M., Gryczynski Z. (2008) Fluorescence intensity decays of 2-aminopurine solutions: lifetime distribution approach. *Analytical biochemistry* **377**:141-149.

315. Serrano-Andres L., Merchan M., Borin A.C. (2006) Adenine and 2-aminopurine: paradigms of modern theoretical photochemistry. *Proceedings of the National Academy of Sciences of the United States of America* **103**:8691-8696.

316. Furtig B., Richter C., Wohnert J., Schwalbe H. (2003) NMR spectroscopy of RNA. *Chembiochem : a European journal of chemical biology* **4**:936-962.

317. Nambiar M., Goldsmith G., Moorthy B.T., Lieber M.R., Joshi M.V., Choudhary B., Hosur R.V., Raghavan S.C. (2011) Formation of a G-quadruplex at the BCL2 major breakpoint region of the t(14;18) translocation in follicular lymphoma. *Nucleic acids research* **39**:936-948.

318. Kypr J., Kejnovska I., Renciuk D., Vorlickova M. (2009) Circular dichroism and conformational polymorphism of DNA. *Nucleic acids research* **37**:1713-1725.

319. Miyoshi D., Nakao A., Sugimoto N. (2003) Structural transition from antiparallel to parallel G-quadruplex of d(G4T4G4) induced by Ca2+. *Nucleic acids research* **31**:1156-1163.

320. Paramasivan S., Rujan I., Bolton P.H. (2007) Circular dichroism of quadruplex DNAs: applications to structure, cation effects and ligand binding. *Methods* **43**:324-331.

321. Randazzo A., Spada G.P., da Silva M.W. (2013) Circular dichroism of quadruplex structures. *Topics in current chemistry* **330**:67-86.

322. Vorlickova M., Tomasko M., Sagi A.J., Bednarova K., Sagi J. (2012) 8-oxoguanine in a quadruplex of the human telomere DNA sequence. *The FEBS journal* **279**:29-39.

323. Hardin C.C., Perry A.G., White K. (2000) Thermodynamic and kinetic characterization of the dissociation and assembly of quadruplex nucleic acids. *Biopolymers* **56**:147-194.

324. Tom Dieck S., Muller A., Nehring A., Hinz F.I., Bartnik I., Schuman E.M., Dieterich D.C. (2012) Metabolic labeling with noncanonical amino acids and visualization by chemoselective fluorescent tagging. *Current protocols in cell biology / editorial board, Juan S Bonifacino [et al]* **Chapter 7**:Unit7 11.

325. David A., Dolan B.P., Hickman H.D., Knowlton J.J., Clavarino G., Pierre P., Bennink J.R., Yewdell J.W. (2012) Nuclear translation visualized by ribosome-bound nascent chain puromycylation. *The Journal of cell biology* **197**:45-57.

326. Piotto M., Saudek V., Sklenar V. (1992) Gradient-tailored excitation for single-quantum NMR spectroscopy of aqueous solutions. *Journal of biomolecular NMR* **2**:661-665.

327. Mergny J.L., Phan A.T., Lacroix L. (1998) Following G-quartet formation by UV-spectroscopy. *FEBS letters* **435**:74-78.

328. Hinske L.C., Franca G.S., Torres H.A., Ohara D.T., Lopes-Ramos C.M., Heyn J., Reis L.F., Ohno-Machado L., Kreth S., Galante P.A. (2014) miRIAD-integrating microRNA inter- and intragenic data. *Database : the journal of biological databases and curation* **2014**:

329. Zhang Y., Gaetano C.M., Williams K.R., Bassell G.J., Mihailescu M.R. (2014) FMRP interacts with G-quadruplex structures in the 3'-UTR of its dendritic target Shank1 mRNA. *RNA biology* **11**:1364-1374.

330. Ceman S., O'Donnell W.T., Reed M., Patton S., Pohl J., Warren S.T. (2003) Phosphorylation influences the translation state of FMRP-associated polyribosomes. *Human molecular genetics* **12**:3295-3305.

331. Anderson K.D., Morin M.A., Beckel-Mitchener A., Mobarak C.D., Neve R.L., Furneaux H.M., Burry R., Perrone-Bizzozero N.I. (2000) Overexpression of HuD, but not of its truncated form HuD I+II, promotes GAP-43 gene expression and neurite outgrowth in PC12 cells in the absence of nerve growth factor. *Journal of neurochemistry* **75**:1103-1114.

332. Yoo S., Kim H.H., Kim P., Donnelly C.J., Kalinski A.L., Vuppalanchi D., Park M., Lee S.J., Merianda T.T., Perrone-Bizzozero N.I., Twiss J.L. (2013) A HuD-ZBP1 ribonucleoprotein complex localizes GAP-43 mRNA into axons through its 3' untranslated region AU-rich regulatory element. *Journal of neurochemistry* **126**:792-804.

333. Li D.K., Tisdale S., Lotti F., Pellizzoni L. (2014) SMN control of RNP assembly: from post-transcriptional gene regulation to motor neuron disease. *Seminars in cell & developmental biology* **32**:22-29.

334. Shen Y., Meiri K. (2013) GAP-43 dependency defines distinct effects of netrin-1 on cortical and spinal neurite outgrowth and directional guidance. *International journal of developmental neuroscience : the official journal of the International Society for Developmental Neuroscience* **31**:11-20.